NASA CONTRACTOR REPORT

NASA CR-161293

EXTRATERRESTRIAL PROCESSING AND MANUFACTURING OF LARGE SPACE SYSTEMS, Volume 1

By Space Systems Laboratory
Department of Aeronautics and Astronautics
Massachusetts Institute of Technology
Cambridge, Massachusetts 02139

September 1979

Final Report

Prepared for

NASA - George C. Marshall Space Flight Center
Marshall Space Flight Center, Alabama 35812

TABLE OF CONTENTS

VOLUME 1: CHAPTERS 1-6

TABLE OF CONTENTS

(Continued)

TABLE OF CONTENTS
(Continued)

TABLE OF CONTENTS

(Continued)

REFERENCES

CHAPTER 1

INTRODUCTION

1.1: CONTRACT BACKGROUND

On February 2, 1978 NASA Marshall Space Flight Center awarded a seven month contract (NAS8-32925) to the MIT Department of Aeronautics and Astronautics for a study entitled "Extraterrestrial Processing and Manufacturing of Large Space Systems (Phase 1)". Later negotiations extended the contract to nine months by adding supplemental tasks. Work on the contract began on June 20, 1978, and the expected termination date was March 31, 1979.

Following discussions between MIT and NASA MSFC, a follow-on effort extended the contract to further investigate solar cell production processes, specifically automation requirements and production control tradeoffs. This research also included an experimental section on deposition processes. This follow-on effort extended the contract to July 31, 1979. MIT requested and received a one-month no-cos- extension for the preparation of this detailed final report, making the due date August 31, 1979.

The NASA MSFC Contracting Officer's Representative is Georg F. von Tiesenhausen (205-453-2789). The MIT Principal Investigator is Professor Rene H. Miller (617-253-2263). The MIT Study Manager is David B.S. Smith (617-253-2272).

1.2: CONTRIBUTORS TO THE STUDY

Work on the contract has been performed by the Space Systems Laboratory of the Department of Aeronautics and Astronautics. The members of the study team are listed in Table 1.1. Five

TABLE 1.1: STUDY PARTICIPANTS

Participating Faculty

      Rene H. Miller   Principal Investigator
      James W. Mar
      Leon Trilling
      John F. Elliott
      P. Guenther Werner

Research Staff

      David B.S. Smith   Study Manager
      Alan Bannister
      David L. Akin
      Glen J. Kissel
      David D. Dreyfuss

Part-time Student Researchers

      Sylvia I. Barrett
      Craig R. Carignan
      John T. Dorsey
      D. Scott Eberhardt
      Douglas C. Finch
      Jonathan A. Goldman
      Marc J. Gronet
      Chris K. Johannessen
      John W. Jordan
      Charles A. Lurio
      Carolyn S. Major
      Kent C. Massey
      Laura C. Rodman
      Joel A. Schwartz
      Robert E. Sullivan
      Eric D. Thiel

MIT faculty participated in the study: from the Department of Aeronautics and Astronautics, Professors Miller and Mar (who jointly head the Space Systems Laboratory), and Professor Trilling; from the Department of Materials Science and Engineering, Professor Elliott; and from the Department of Mechanical Engineering, Professor Werner. Professor Miller is the Principal

1.2

Investigator and the study's Systems specialist. Professor Mar has expertise in materials and structures, and served as Principal Investigator during Professor Miller's absence. Professor Trilling is a specialist in gas-surface interactions and deposition processes. Professor Elliott is an expert in material refining and processing. Professor Werner is the manufacturing and industrial operations specialist.

The study also employed five graduate student research assistants: Dave Smith was Study Manager and design integrator; Alan Bannister supervised the design of the Klystron, waveguide, and DC-DC converter manufacturing sections of the SMF; Dave Akin was the study's costing specialist; Glen Kissel was the automation and production control specialist; and David Dreyfuss supervised the experimental research on direct vaporization.

The remaining study personnel were undergraduate researchers who were responsible for the bulk of the research and design work. In a contract stressing space-specific designs ("thinking zero-g") and advanced technologies (assumed technology date: 1990), the undergraduates' fresh approach to problems proved invaluable in generating novel ideas.

The study effort on this contract has been enhanced by other activities within the Department of Aeronautics and Astronautics. Besides this contract with NASA MSFC, the MIT Space Systems Laboratory is conducting research in three related areas: human operations in zero-g, novel structural concepts for large space structures, and modeling and optimization of space industrialization scenarios. This research should

eventually suggest several Shuttle experiments, and should identify critical technologies in the development of space industrial operations.

The zero-g work has concentrated until now on an evaluation of water as a zero-g simulation medium, i.e. under what conditions and how much does water-drag affect the predictions for human EVA operations in space. This has led to development of a mathematical model of human body dynamics underwater, and of an underwater harness and instrumentation. Comparison of theory and underwater test results has indicated constraints within which water is a suitable simulation medium and the mathematical model can produce zero-g predictions by accounting for the water-drag. This work is funded by a NASA HQ grant.

Work on large space structure design has concentrated on the use of environmental forces (i.e. gravity gradient, magnetic, solar pressure, thermal emission) to reduce structural requirements on large floppy structures. The SSL is also investigating the potential of inflatable structures, and preparing a vacuum drop chamber to study the free-fall dynamics of such structures. This research is also being conducted under a NASA HQ grant.

The research on space industrialization scenarios has produced a highly flexible computer program capable of modeling a wide range of options, including earth-based and lunar-material construction of solar power satellites. The program in-

1.4

cludes a detailed line item costing subroutine covering re-
search, development, procurement, and operations costs of
space industrial components, allowing variable spending
patterns during the years of R & D and operations. Optimi-
zation programs using linear and integer programming to min-
imize life cycle costs of space industrialization have also
been developed. This work is done in-house, using depart-
mental funds.

Associated laboratories within the Department of Aero-
nautics and Astronautics include: The Technology Laboratory
for Advanced Composites, which studies the manufacture and
properties of aerospace-structural components made from ad-
vanced composites such as graphite-epoxy or Kevlar-epoxy
(Air Force Contracts); the Man-Vehicle Laboratory, which has
studied posture control in space for several years, and is
preparing experiments on balance, vestibular functions, and
motion sickness for Spacelab I (NASA JSC contract); and the
Gas Turbine and Plasma Dynamics Laboratory, which has worked
on ion engines and plasma thrusters (NASA and Air Force con-
tracts).

The Department of Aeronautics and Astronautics has also
conducted systems studies as a integral part of its curriculum.
Past topics in the graduate level Advanced Systems Engineering
class include "A Systems Design for a Prototype Space Colony"
(1976), "Three Candidate Designs for Satellite Solar Power

1.5

Stations" (1974), "Satellite Solar Power Station -- A Systems Study" (1973), "Space Disposal of Nuclear Wastes" (1972), and "A Proposal For a Humanitarian Earth Resources Satellite" (1970). Undergraduate Space Systems topics in the recent past included optimization of the Space Transportation System, sizing of second generation shuttles, reuseable booster design with air breathing first stages, laser propulsion, and optimized inter-orbital transportation systems. All of this past and on-going work forms a sizable body of experience available to this study effort.

1.3: COMPLEMENTARY STUDIES

During the time of this study, two other NASA studies were in progress, on topics closely related to this contract's. In "Extraterrestrial Materials Processing and Construction" (Contract NAS 09-051-001, for NASA JSC), the Lunar and Planetary Institute reviewed and developed methods for mining, beneficiating, and refining lunar raw materials for a lunar or space manufacturing operation.

At the same time, the Convair Division of General Dynamics was working on "Lunar Resources Utilization for Space Construction" (Contract NAS9-15560, for NASA JSC). This study is a systems evaluation of a number of possible scenarios involving the use of lunar materials to manufacture space products. One important early task of this study was to establish an economic-feasibility threshold for lunar-material use. Other objectives of this JSC-GD study were the modification of the reference earth-baseline Solar Power Satellite design to one using lunar

1.6

material components, and the development of preliminary designs for elements of space industrialization (e.g. lunar bases, transportation systems, processing and manufacturing facilities, habitats).

As mandated by the SOW and by discussions with the MSFC COR, the MIT study received important inputs from both of these studies (these inputs are described throughout this report). A number of discussions were held, both on the phone and in person, and progress reports were circulated between members of all three studies.

1.4: STUDY OBJECTIVES

The purpose of this study, as stated in the NASA Statement of Work, is "to provide NASA with pertinent and readily usable information on extraterrestrial processing of materials and manufacture of components and elements of large space systems." Briefly stated, the objective of this study is to develop requirements, preliminary designs, and costs for a Space Manufacturing Facility (SMF), which would receive raw materials from the Moon and the Earth, personnel and supplies from th Earth, and energy from the Sun, to produce components of la space structures such as communications antennas, space stations, and solar power satellites (SPS). This concept is explained in more detail in the next section.

More specifically, the study objectives were listed as a set of tasks in the SOW:

Task 1: Define space program scenarios for low and

1.7

medium options (no SPS). The high option will use an SPS program scenario provided by NASA.

Task 2: Define the beneficiation, smelting, refining, alloying, and other processes that are required to convert the beneficiated, primary processed lunar material into the required commercial feedstock for the manufacturing processes.

Task 3: For each desired product define the required forming, manufacturing, assembly, and other processes from feedstock to the finished product.

Task 4: Define type, total quantity and annual delivery rate of supplemental terrestrial feedstock material for each of the material quantities and rates based on the product requirements.

Task 5: Define the SMF operations, equipment and facilities required to implement the processes defined in Task 2 for the low, medium and high quantities and rates.

Task 6: Define SMF operations, equipment and facilities required to implement the processes defined in Task 3 for each of the material quantities and rates based on the product requirements and determine the production quantities and rates for each product.

Task 9: Provide conceptual layouts of all major SMF equipments and facilities including material receiving, product storage facilities and energy supply for each rate and total quantity of product material.

Task 10: Determine total SMF masses for each production

1.8

rate. Add mass contigencies for SMF flight mechanical equipment. Determine the number of personnel required and assess the mass of their residential accommodations.

Task 11: Present a preliminary cost analysis and assessment which includes development, acquisition of all SMF elements, initial and operating cost, maintenance and logistics cost, the cost of terrestrial supplementary material and transportation cost for each major element. Define uncertainties and sensitivities for each element.

Task 15: Present all study numerical results in tabulated and graphical form that will permit obtaining values for any intermediate parameters other than those used in the study.

Tasks 7, 8, 12, 13, 14, and 15 (listed below) together form Phase II of the study: the design and costing of a Lunar Manufacturing Facility (LMF) to do the same job as the SMF, but on the lunar surface, and the comparison of the SMF and LMF options.

Task 7: Define the LMF operations, equipment and facilities required to implement the processes defined for the low, medium and high quantities and rates.

Task 8: Define LMF operations, equipment and facilities required to implement the processes defined in Task 2 for each of the material quantities and rates based on the product requirements and determine the production quantities and rates for each product.

1.9

Task 12: Provide conceptional layouts of all major LMF equipments and facilities including material receiving, product storage facilities, and energy supply for each rate and total quantity of product material.

Task 13: Determine total LMF masses for each production rate. Determine the number of personnel required and assess the mass of their residential accommodations.

Task 14: Present a preliminary cost analysis and assessment which includes development, acquisition of all LMF elements, initial and operating cost, maintenance and logistics cost, and the cost of terrestrial supplementary materials and transportation cost for each major element. Define uncertainties and sensitivities for each element.

Task 15: Compare and evaluate the SMF and LMF concept options based on methods and criteria developed by the contractor. Recommend further investigations in support of conclusions drawn in this study and prepare rationale, plans, cost and schedule for the recommended efforts.

During the progress of the study, a number of significant changes were made to these objectives, as issues were clarified by this effort and the two complementary studies. First, the early determination of the economic threshold for lunar materials use done by the JSC-GD study (Ref. 1.1) suggested that a minimum production amount of roughly 570,000 tons of large space structures in 30 years is required to make lunar materials use economically viable. Furthermore, even liberal

1.10

estimates of future satellite requirements do not approach this figure, unless SPS's are included. (Dr. Gerard K. O'Neill suggested at one meeting that a space-based passive anti-collision radar system might be in this mass range, but current estimates on such structures are uncertain.) Therefore a viable lunar-material scenario would include the production of SPS's. MIT's in-house studies (mentioned above) are in agreement with this conclusion.

The immediate result of this finding was that the 'low and medium options' mentioned in Task 1 of the SOW were economically unacceptable. It was therefore decided that this study would disregard those options and concentrate on the high production option (with SPS). Task 1 was therefore reduced to defining the program scenario for the high production option, and several tasks requiring research for low, medium, and high options were narrowed to the high-option effort only.

Second, it was decided that the beneficiation and refining of lunar ores into SMF feedstock was the province of the JSC-LPI study, and that similar research by the MIT team would be an unnecessary duplication. Therefore the characteristics of the lunar material inputs into the MIT SMF designs were developed from the results of the LPI research, and through consultations with the participants in that study. Since the refining schemes proposed by the JSC-LPI study produce highly purified materials, the processing requirements in the MIT SMF designs were reduced to alloying the inputs when terrestrial

1.11

alloying elements were required, and purifying metallurgical grade silicon to semiconductor grade for solar-cell production.

Third, research in this study and the JSC-GD study suggested that certain processes in the overall scenario belong on the Moon, while others should be in space. Specifically, refining lunar ore on the Moon has the advantage that the product launched into space con_ists entirely of the desired material. Thus the launch system need not launch the unwanted constituents in lunar ores. Also, a number of refining processes involving the movement and separation of fluids benefit from being in a gravity field, reinforcing the suggestion that beneficiation and refining should be done on the Moon.

On the other hand, a number of products (most importantly solar cells) appeared too fragile to survive stresses during launch from the Moon, be it by mass-driver or chemical rocket. It was therefore judged that the fabrication proces. ɛ for fragile components (e.g. solar cells, truss members, klystron parts, waveguides) should be in space. Since such processes form the bulk of the SMF, the Lunar Manufacturing Facility became an unlikely option, since many of its products would require redesign to launch-rate them, leading to more complex fabrication and more massive products.

After study of these results and consultations with the GD and MIT research teams, NASA decided that Phase II of this study, the design of the Lunar Manufacturing Facility, was unnecessary, and that the purpose of the studies would be ade-

quately served by the scenario evaluations in the JSC-GD ef-
fort, the lunar processing designs of the JSC-LPI study, and
the SMF design in this MSFC-MIT study.

These developments all contributed to the gradual evolu-
tion of the study objectives. The end product of that evolu-
tion is an updated set of study objectives, presented in
Table 1.2.

TABLE 1.2: UPDATED STUDY OBJECTIVES

1) Define space program scenarios for production
   of large space structures (including SPS's)
   from lunar materials, and define in detail the
   large space structure components to be produced.

2) Define the SMF refining, alloying, and other
   processes required to convert the refined lunar
   material inputs into feedstock for the required
   manufacturing processes.

3) Define the SMF manufacturing, assembly, and
   other processes required to convert the feed-
   stock into components of large space structures.

4) Define types and quantities of Earth materials
   needed in the production of the large space
   structure components.

5) Develop conceptual layouts of all major SMF
   equipment and facilities.

6) Design a "reference SMF", including definition
   of the SMF operations, equipment, and facilities
   required to implement the processes in (2) and (3)
   above, including support equipment, storage faci-
   lities, personnel requirements, and habitation
   facilities.   (continued)

TABLE 1.2 Continued

7) Present a preliminary cost analysis and assess-
   ment which includes development, acquisition of
   all SMF elements, initial and operating cost,
   maintenance and logistics cost, cost of terres-
   trial materials, and transportation cost for each
   major element. Define uncertainties and sen-
   sitivities for each element.

8) Present all study numerical results in tabu-
   lated and graphical form that will permit ob-
   taining values for any intermediate parameters
   other than those used in the study.

1.5: THE SPACE MANUFACTURING FACILITY CONCEPT

Figure 1.1 presents the major elements in an earth-based
large space structure construction scenario. Components of
large space structures, after manufacture on Earth, are launched
to an Earth Orbit Terminal. There they are repackaged (pos-
sibly including subassembly of large space structure components)
and ferried to the Geosynchronous Orbit Complex for final assem-
bly and checkout. Studies have shown that the major costs of
such a scenario is the transportation from the ground to low-
earth orbit (LEO) of 1) the structure components and 2) the
fuel required for the transfer of those components to geosyn-
chronous orbit (GSO).

An alternative scenario, aimed at reducing these costs, is
presented in Fig. 1.2 (adapted from Fig. 1 of the SOW). In
this system, most of the materials required for the large space

1.14

```
GB   - Ground Base
EOT  - Earth Orbit Terminal
GSOC- Geosynchronous Orbit
          Terminal
```
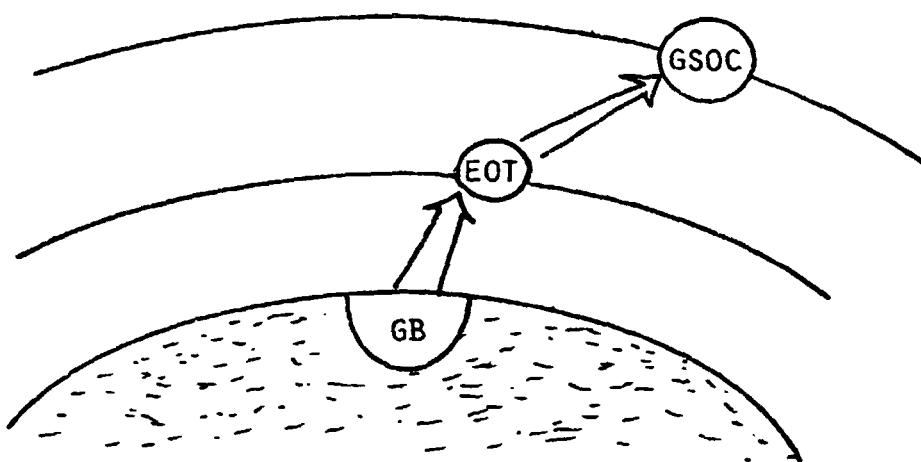

FIGURE 1.1:   MAJOR ELEMENTS OF EARTH-BASED
              CONSTRUCTION SCENARIO

structures would be mined and beneficiated on the Moon, at a
Lunar Resource Complex. These lunar materials would then be
launched into space to a cargo Transition Point, repackaged,
and ferried to a Space Manufacturing Facility. This SMF would
process, manufacture, and assemble the lunar materials into
components of large space structures. These components would
then be shipped to the Geosyrchronous Orbit Complex and assem-
bled (together with some terrestrial components) into the de-
sired large space structures.

    The potential advantage of this scenario over its earth-
based counterpart is that the bulk of the material reouired
comes from the Moon. This material therefore has a far smaller

GB   - Ground Base
EOT - Earth Orbit Terminal
LOT - Lunar Orbit Terminal
LRC - Lunar Resource Complex
TP   - Cargo Transport Point
SMF - Space Manufacturing
       Facility
GSOC - Geosynchronous Orbit
       Complex
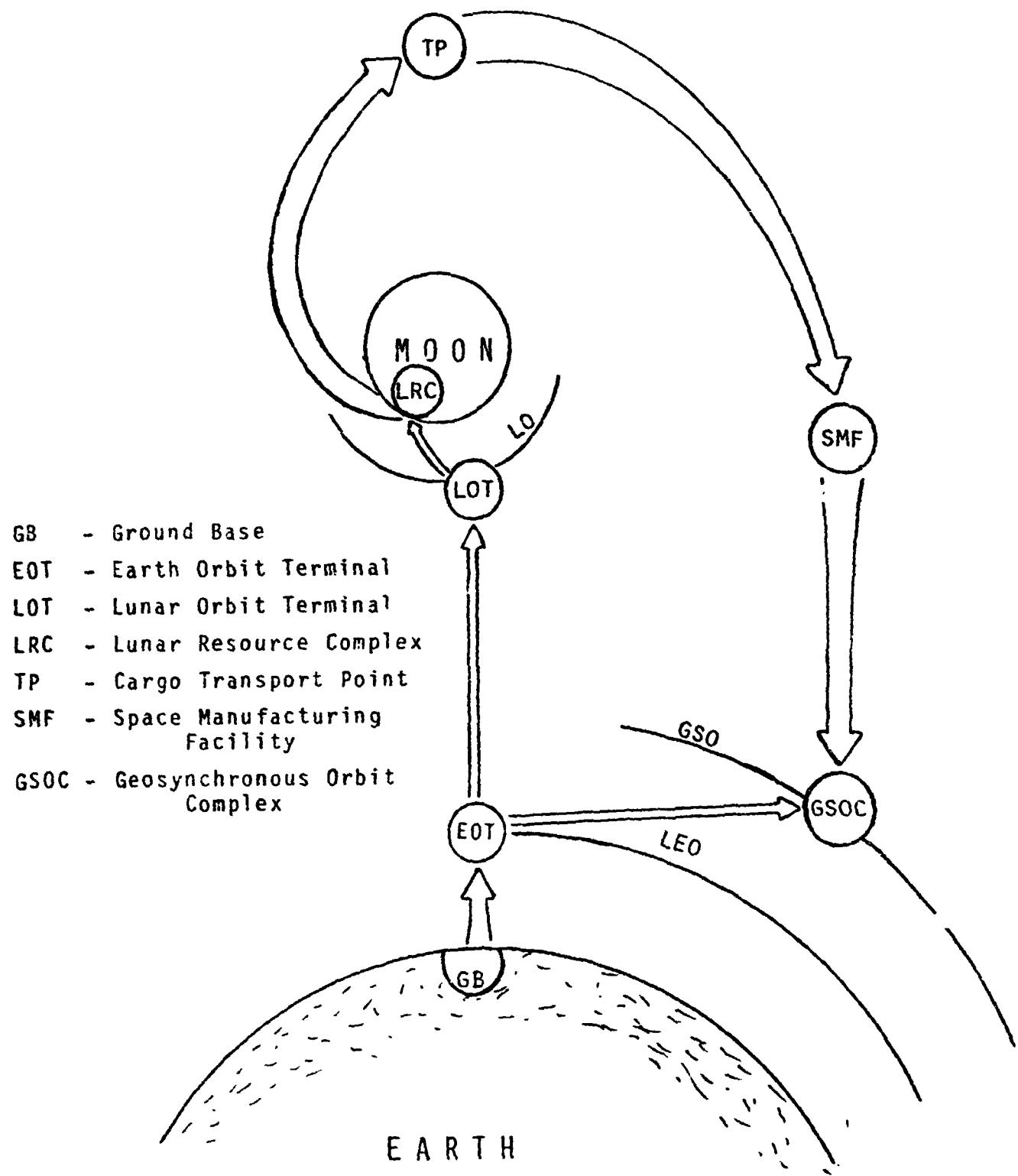
FIGURE 1.2:   MAJOR ELEMENTS OF LUNAR MATERIAL SCENARIO

1.16

gravitational field to overcome than material launched from
Earth: the energy required for lunar escape at the lunar sur-
face is 4.5% of the energy requirement for earth escape at the
Earth's surface. In addition, the lack of lunar atmosphere
makes possible the use of catapults (such as the electromagnetic
mass-driver) to launch payloads without use of propellant.

The lunar surface material can also be refined to yield
propellants for rockets. These propellants can fuel launch
systems from the lunar surface (an alternative to catapults),
and orbital transfer vehicles between various points in the
system, including the transportation legs between LEO and
lunar orbit (LO) and between LEO and GSO. This use of lunar-
derived fuel can therefore reduce transportation costs even
for the required terrestrial inputs.

However, the lunar-material scenario requires a number of
facilities (e.g. lunar base, cargo transition point, SMF) and
devices (e.g. lunar landers, TP-SMF interorbital transports)
not needed by the earth-based construction scenario. Also,
personnel must travel farther from Earth in the lunar material
system, adding to their transportation costs. These financial
advantages and disadvantages must be traded off to determine
the most cost-effective approach to large-scale space indus-
trialization; hence this study, which investigates one of
the key cost elements in the lunar-material scenario: the Space
Manufacturing Facility.

Figure 1.3 presen's a more specific schematic of the SMF concept, showing major inputs and outputs (these are treated in detail in later chapters of this report). As described earlier, the bulk of the input raw materials comes from the Moon; other raw materials come from Earth. The required personnel and logistics supplies travel between Earth and the SMF.

The most likely source of power for the SMF is solar energy; a less likely alternative is nuclear energy. Thus the cost of energy for the SMF operations resembles the cost pattern for SPS's: a large initial outlay for the solar array, followed by a very low operating cost (due to the absence of need for fuel and the low maintenance req'irement). Therefore, for long operating times, the cost of energy in SMF operations can be substantially lower than the cost of energy in earth manufacture; this is another potential cost reduction in the lunar material scenario over the earth-based construction scenario.

The location of the SMF was unspecified in the SOW, and remained open during the contract. A number of locations are possible (e.g. lunar orbit, the Lagrange points, resonant earth-moon orbits, GSO), but the determination of the optimum location depends on tradeoffs involving transportation systems, personnel stay time, and availability of materials and energy, which are beyond the scope of this contract. In any case, location had little effect on the design of the SMF production equipment; the areas affected are pointed out and discussed throughout this report.

MOON

Lunar Raw
Materials

Products ← S M F ← Energy

S U N

Earth Raw
Materials

Crew and
Logistics

1.19

EARTH
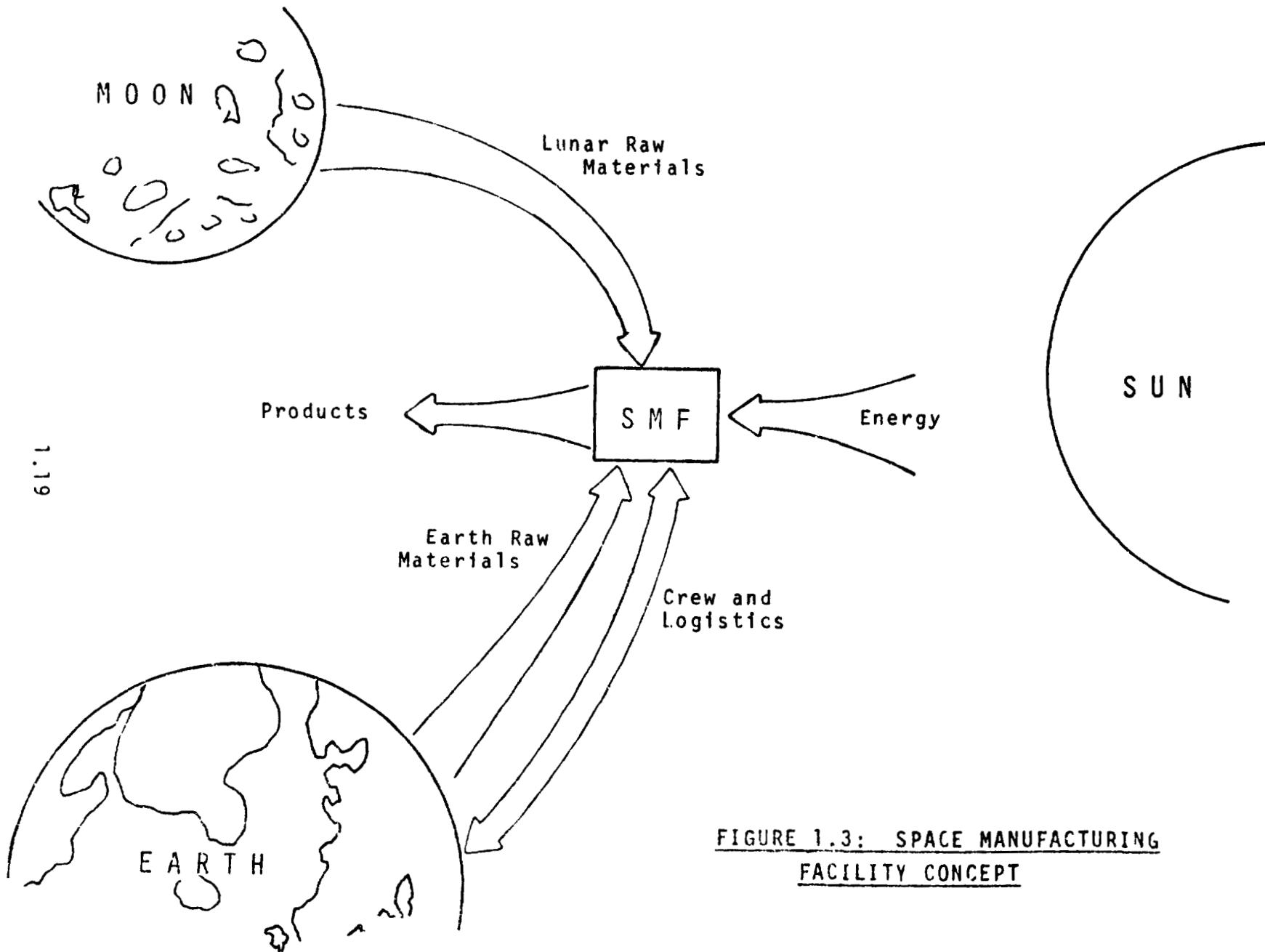
FIGURE 1.3: SPACE MANUFACTURING
FACILITY CONCEPT

CHAPTER 2

ASSUMPTIONS AND GUIDELINES

2.1: GENERAL REMARKS ON ASSUMPTIONS

To keep the research effort within the scope of this pre-
liminary study, a number of assumptions were provided in the
SOW. However, as the study progressed, and as results came in
from the two complementary studies (described above), many of
these assumptions were revised or removed, and other assump-
tions made where appropriate. For example, the progressive
modifications in the study objectives (discussed in Sec. 1.4)
changed the assumptions on SMF production levels and types of
products. These alterations led to an updated set of assump-
tions and guidelines, which are described in the sections be-
low.

Assumptions were also made to resolve certain questions
arising during the SMF design process, since resolution of
these questions would require research effort beyond the scope
of this contract. These assumptions are also listed below,
and discussed throughout this report.

In general, the assumptions and guidelines used in this
study fall into three categories. The first category is one
guideline on the performance of this study: this study makes
maximum use of past and present studies in the fields of
large space systems, lunar resources utilization, and space
processing and manufacturing. This guideline is taken di-
rectly from the SOW. In particular, this study does not do

any specific design of habitation systems, but uses the results of prior studies in this area.

The second category consists of basic assumptions affecting the SMF scenario: production levels, characteristics of outputs and inputs, and technology level. These are discussed in Sec. 2.2, "SMF Scenario Assumptions".

The third category includes general assumptions and guidelines affecting the design of a reference SMF, such as component lifetime and use of automation. These are presented in Sec. 2.3, "General SMF Design Guidelines and Assumptions".

In addition, a number of specific assumptions were made in the design of individual processes and pieces of equipment. These specific machine design assumptions are stated and explained throughout this report, particularly in Chaps. 5 and 7.

2.2: SMF SCENARIO ASSUMPTIONS

2.2.1: Table of Scenario Assumptions: Table 2.1 presents the basic assumptions affecting the SMF scenario. The assumptions are discussed below.

2.2.2: SMF Products: As described in Sec. 1.4, "Study Objectives", early results of the JSC-GD study indicated that production of less than 570,000 tons of material in 30 years would make the lunar-material scenario economically unsatisfactory. Since such a production level cannot be met by satellites without including the SPS, the lunar-material scenario must include production of SPS's (at roughly 100,000 tons per 10-GW SPS), and the SMF outputs must therefore include SPS components.

TABLE 2.1:   GENERAL ASSUMPTIONS

SMF Products:

SMF output includes SPS components.

SPS's produced are the JSC-Boeing
baseline design, modified to use
lunar materials.

Beyond the lunar-material substi-
tutions, there are no major redesigns
of the SPS.

SMF Lunar Inputs:

Possible inputs are silicon, silica,
aluminum, iron, calcium, magnesium,
titanium, oxygen, and slag.

Inputs arrive at the SMF in refined
condition.

Inputs arrive at the SMF in special-
ized shapes, e.g. rods.

Technology Level in SMF Design: the year 1990.

The JSC-GD study (Ref. 2.1) then proceeded to compare the
needs of a 30-year production output of 537,000 tons of SPS's
and 29,000 tons of other satellites (the maximum predicted re-
quirement for non-SPS satellites), with the needs of a 30-year
production output of 570,000 tons of SPS's (each scenarios
adding up to the 570,000-ton minimum).   The various material
requirements vary by at most 2% between the two scenarios.
Therefore the material requirements of an all-SPS scenario
adequately model the needs of a mixed-output scenario.

2.3

The JSC-GD study also pointed out that many of the components of non-SPS satellites were similar to SPS components (e.g. truss structures, antennas, solar-cell arrays, radiators, heat pipes, electrical wire), and that those components not similar to SPS components were not likely to be made from lunar materials (e.g. electronics, thrusters, batteries). Therefore an SPS production scheme can adequately model a mixed-output scenario: the SMF can be designed to produce primarily SPS components, while staying flexible enough to produce variations of those components for use in other space applications.

As mandated by study guidelines in the SOW and discussions with the MSFC COR, the SPS design used in defining the SMF outputs was the Boeing-JSC Recommended Preliminary Baseline Concept (Ref. 2.7). Since this baseline design is an earth-launched SPS, the design had to be modified to substitute lunar materials for the earth materials in the SPS components.

The JSC-GD study performed such modifications, producing a lunar-material SPS design (Ref. 2.3). The MIT study team reviewed the Boeing-JSC baseline and the suggested lunar-material substitutions from the JSC-GD study. Designs and specifications for lunar-material components of the SPS were then developed. As suggested by the JSC-GD study, roughly 8000 tons (without growth margin) of terrestrial components are required for every 10-GW SPS. With the lunar-material substitutions assumed and calculated by this study, each lunar-material

2.4

10-GW SPS masses 96,600 tons, including terrestrial components (but without growth margin). Chapter 3, "Specifications of SMF Outputs", describes the lunar-material SPS components in detail, and lists the expected types and quantities of SMF outputs. While some of these output specifications are partially dependent on the production equipment chosen, the outputs listed in Table 3.1 provide a useful example of typical SMF product requirements.

One assumption clearly stated in early discussions between the study team and the MSFC COR is that there are no major redesigns of the SPS beyond those necessary for lunar-material substitutions. This assumption was essential to keep the research work manageable, since major alterations to the SPS would require design effort well beyond the scope of the study. However, this restriction also has a significant effect on the study direction and on the design of the reference SMF.

The reasons for this effect are the differences between the physical and economic design environments of the earth-baseline and lunar-material scenarios. In the Boeing-JSC baseline scenario, the SPS components are manufactured on Earth with 'conventional' equipment, shipped up Earth's gravity well, and assembled in orbit. This establishes a design environment: availability of a wide variety of materials, relatively low cost of production labor, high cost of production energy, environmental constraints in manufacture, large transportation cost of finished components, high cost of labor in assembly.

2.5

The baseline SPS design is therefore optimized within this design environment, leading to sophisticated components designed for low-mass, labor-intensive production, launch-stress survival, and ease of assembly.

The lunar-material SPS scenario sets up a different design environment. The available lunar materials are limited (as described in Chap. 4, "SMF Inputs"). The cost of production labor is high, since this personnel must be maintained in space. Energy is available from sunlight and therefore cheaper than on Earth for long factory operating times (as discussed in Sec. 1.5). The environmental constraints are different: for example, it is easier to get rid of high-temperature heat than low-temperature heat in space, since it must be radiated away. The reverse is usually true on Earth, since high-temperature waste often puts an unacceptable strain on the natural environment. In the lunar-material scenario, transportation costs for the bulk of the SPS material are far lower than in the earth baseline scenario; this is one of the major potential advantages of the lunar option.

Therefore the lunar-material design environment suggests different SPS design optimizations: simple components designed for energy-intensive automated production. These components need not contend with large launch stresses. Possibly most important, the mass of the components has a far less severe effect on the production and transportation costs than in the earth baseline scenario; however, the effect of SPS mass

2.6

increases on SPS operational cost (e.g. stationkeeping fuel) is at present unknown, and could raise the overall program cost. Both lunar and earth scenarios share ease of assembly as an advantage.

Thus the assumption that there are no major SPS redesigns beyond the lunar-material substitutions limits the extent to which the lunar-material SPS design can approach the optimum suggested by the design environment. The solar cell design presents a specific example. The earth-baseline design environment suggests minimum SPS mass. This leads to high-efficiency (12.5%) low-mass solar cells to minimize SPS area. This in turn leads to complicated production requirements for the solar cells. Restricting the lunar-material SPS to the same area requires 12.5% efficient cells as well, thus exporting the production complexity into space. However, allowing an increase in SPS area and a reduction in solar cell efficiency brings in a number of alternative energy-collection systems with simpler production requirements. The cost tradeoff is between the reduction in in-space production cost and the increase in SPS operating cost. A more subtle tradeoff involves the use of concentrators to focus sunlight into the solar cells. In the earth baseline scenario, the cost tradeoff is between the reduced requirement for solar cells and the increased in-space assembly requirements for the concentrators. Since the earth-based solar-cell production is cheaper than the in-space assembly (the major cost being transportation), the earth

baseline design optimizes without concentrators. In the lunar

material scenario, even though increased assembly requirements

are also expensive, reduction of solar cell production can

lead to greater savings than a similar reduction in the earth

baseline scenario. Therefore the lunar-material SPS design

might optimize with concentrators.

It is not the contention of he study group that the as-

sumption of no major SPS redesign was too restrictive. As

mentioned above, this restriction was essential to keep the

study manageable. However, the study group wishes to point

out the effects of such a restriction, and to suggest that

later studies should develop an optimized lunar-material SPS

and production system. This issue is further discussed in

Chap.13, "Possible System Tradeoffs".

2.2.3: SMF Lunar Inputs: The assumption of the possible

inputs listed in Table 2.1 was taken directly from the SOW.

These lunar inputs are discussed in detail in Chap. 4, "SMF

Inputs".

As mentioned in Sec. 1.4, it was decided during the course

of the study that beneficiation and refining of lunar ores

into raw materials for the SMF was the province of the com-

plementary JSC-LPI study. Examination of that study's output

(Ref. 2.4) and discussions with members of the LPI team in-

dicated that lunar materials could be refined to high purities

on the Moon. It was therefore assumed that lunar inputs

would arrive at the SMF in refined condition, as discussed in

2.8

Chap. 4.

This study assumes that the lunar materials are launched from the Moon by chemical rocket (as discussed in Sec. 4.5). The lunar inputs to the SMF are therefore available in specialized shapes, e.g. rods and slabs. The input shapes to the reference SMF are described in Chap. 4.

2.2.4: <u>Technology Level</u>: The study group chose the year 1990 as the technology cutoff date to allow for 10 years of research from this date (1979). During the years 1990-1995, space hardware for the lunar-material scenario is developed and tested. The first full-scale earth-launched SPS is brought on line in 1995, and during the years 1995-2000 the earth production system is progressively replaced by the lunar-material scenario. Although this full schedule may be shown to be economically unrealistic by later studies, the technology cutoff date should be reasonable even if later timelines are altered.

2.3: <u>GENERAL SMF DESIGN GUIDELINES AND ASSUMPTIONS</u>

The operational lifetime of the SMF components is 20 to 30 years (with maintenance). This assumption is taken directly from the SOW.

The SMF designs make maximum use of automation, except in instances where economic arguments justify the use of human labor. For example, space workers do some repair and supervision of equipment. Further discussion of the issue of human productivity (dependent on the level of automation) appears in Chap.9, "Maintenance and Repair", and Chap. 13,

"Possible System Tradeoffs". This guideline is taken from the SOW.

Equipment for the SMF is not limited to extensions of terrestrial equipment. It is highly desirable that space specific machinery designs be developed. This guideline is from the SOW.

CHAPTER 3

SPECIFICATIONS OF SMF OUTPUTS

3.1: TABULATED OUTPUTS

As mentioned in Sec. 2.2.2, "SMF Products", the expected
products of an SMF (SPS's and other satellites) can be ade-
quately modeled by SPS components. As suggested by the SOW
and MSFC COR the SPS design used in defining those components
was the Boeing-JSC Recommended Preliminary Baseline Concept
(Ref. 3.1), modified by lunar-material substitutions. The
JSC-GD study described such substitutions, producing a lunar-
material SPS design (Ref. 3.2).

The MIT study team closely reviewed the Boeing-JSC base-
line and the lunar-material substitutions suggested by the
JSC-GD study. MIT then developed designs and specifications
for the lunar-material components of the SPS, and computed the
SMF outputs required to produce such SPS's. Table 3.1 presents
this list of outputs (the even-number total is coincidental).
Some of the output specifications in this table are partially
dependent on the production equipment chosen, and therefore
keyed to the reference SMF design. The SPS component designs
used and the rationale for each output level are described in
the next section.

3.2: EXPLANATION OF SMF PRODUCT SPECIFICATIONS

3.2.1: General Remarks: Many of the output levels listed are
based on Boeing SPS design data and the lunar-material substi-
tutions suggested by the JSC-GD study. The Boeing data used

TABLE 3.1: SMF OUTPUTS

(For 1 10-GW SPS, Without Growth Margin)

PRODUCT	QUANTITY/SPS	MASS/SPS (Tons)
Solar Cell Arrays	2.17×10^{10} Cells (10% extra)	4.4×10^4
Structural Member Ribbon	6.5×10^6 Meters (5% extra)	2.3×10^4
Klystron Assemblies	2.04×10^5 Pieces (5% extra)	1.5×10^4
Waveguides	1.8×10^6 Pieces (10% extra)	1.2×10^4
Busbar Strips	1.4×10^6 Meters (1% Extra)	2.8×10^3
DC-DC Converters	461 Pieces (1% extra)	2.1×10^3
Elec. Wire and Cables	1.4×10^8 Meters (5% extra)	6.7×10^2
DC-DC Converter Radiators	461 Pieces (1% extra)	5.6×10^2
End Joints	$\sim 4 \times 10^3$ Pieces	~ 8
Joint Clusters	~ 1500 Pieces	~ 8
	Total Mass	1.0×10^5 Tons

Note: The Quantity/SPS figures include an extra allocation for wastage expected during SPS assembly operations. These extra percentages are indicated in parentheses.

is contained in Table 3.2, taken from the SPS "Recommended Pre-liminary Baseline Concept" produced by NASA JSC (Ref. 3.1). This table also appears in the JSC-GD study (Ref. 3.2, Tab. X-1).

The expected output levels have been modified by a number of factors: 1) modification to the product designs brought on by manufacturing requirements; 2) uncertainties as to the ap-plicability of specified growth margins to various products; 3) contradictions on SPS component masses, dimensions, and numbers, between various sources describing successive iter-ations of SPS design.

The study group first reviewed the 26.6% mass margin listed at the bottom of the table. Boeing developed this margin through uncertainty analyses on the designs of the various SPS components. Therefore the margin does not apply uniformly to all components. Furthermore, the component redesigns required for lunar-material substitution and for in-space manufacture carry their own uncertainties, different from their earth base-line counterparts. The MIT study group therefore felt that the use of this 26.6% growth margin could lead to inaccuracies if applied to an SPS using lunar derived material and manufactured in space.

A more accurate growth margin should be computed by un-certainty analyses on the component designs in the lunar mate-rial SPS. However, such uncertainty analyses would first re-quire the detailed design of a lunar-material SPS. Since this effort is well beyond the scope of the present studies, the

3.3

TABLE 3.2: MASS BREAKDOWN OF EARTH BASELINE 10-GW SPS

	QUANTITY	MASS, KG
SOLAR ARRAY	1	**51.779.200**
PRIMARY STRUCTURE		5.385.000
ROTARY JOINT (MECHANICAL)	2	66.800
FLIGHT CONTROL SYSTEM	4	179.000
THRUSTERS	160	(46.800)
MECHANICAL SYSTEMS	4 SETS	(32.200)
CONDUCTORS	4 SETS	(8.000)
POWER PROCESSORS	12	(88.000)
AVIONICS (INSTR. COMM. COMPUTERS)	4 SETS	4.000
ENERGY CONVERSION SYSTEM		43.750.000
SOLAR CELLS	20×10^9	(11.670.850)
SUBSTRATE AND COVERS	78×10^6 PANELS	(28.313.230)
INTERCONNECTS	78×10^6 (1/PANEL)	(1.150.160)
JOINT/SUPPORT TAPES	256 SETS (1/BAY)	(300.360)
CATENARY	256 SETS (1/BAY)	(258.290)
TOLERANCE & OTHER		(2.057.110)
POWER DISTRIBUTION		2.398.400
POWER BUSSES	3	(2.030.000)
CELL STRING FEEDERS	163.000	(38.800)
DISCONNECTS AND SWITCHGEAR	208	(156.000)
ENERGY STORAGE	—	(20.200)
ROTARY JOINT (ELECTRICAL)	2	(39.200)
SUPPORT STRUCTURE	2	(114.200)
MICROWAVE POWER TRANSMISSION SYSTEM	2	**25.223.200**
ANTENNA STRUCTURE	2	500.000
PRIMARY STRUCTURE	2	(105.000)
SECONDARY STRUCTURE	122 SUBASS'YS	(395.000)
ANTENNA CONTROL SYSTEM	24 UNITS	11.000
MPTS POWER DISTRIBUTION		5.866.200
POWER BUSSES	3	(760.600)
SWITCHGEAR AND DISCONNECTS	912	(273.600)
DC-DC CONVERTERS	456	(2.482.000)
THERMAL CONTROL	456	(1.472.000)
ENERGY STORAGE	—	(598.600)
SUPPORT STRUCTURE	—	(279.400)
SUBARRAYS (6932 x 2)	13.864	18.846.000
WAVEGUIDES	1.663.680	(4.314.000)
KLYSTRONS (97056 x 2)	194.112	(9.316.000)
THERMAL CONTROL	194.112 SETS	(4.174.000)
CONTROL CIRCUITS AND CABLES	194.112 SETS	(1.042.000)

TOTAL SATELLITE MASS (10 GW OUTPUT) -		77.002.400 KG
MARGIN (26.6% BASED ON UNCERTAINTY ANALYSIS) -		20.482.638 KG
PREDICTED ACTUAL MASS	**-**	**97.485.038 KG**

study group feels that the most accurate method to develop SMF output levels is to base them on the Boeing-JSC data **without** growth margin.

The following sections show how the values in Table 3.1 were developed from those in Table 3.2, through the lunar material substitutions suggested by the JSC-GD study, and/or redesigns suggested by in-space manufacturing constraints.

3.2.2: Solar Cells: The total solar cell area in one 10-GW SPS is taken to be 100 km^2 (Ref. 3.1). Lunar material substitutions are made as per JSC-GD suggestion. The resulting solar cell design is shown in Fig. 3.1.

6.4 CM

7.7 CM

Optical Cover
75 μ SiO$_2$

1 μ AL GRID PATTERN (TOP CONTACT)

2 μ AL SHEET (BACK CONTACT)

50 μ SI WAFER (DOPED)

SUBSTRATE: 50 μ SiO$_2$

GRID FINGERS
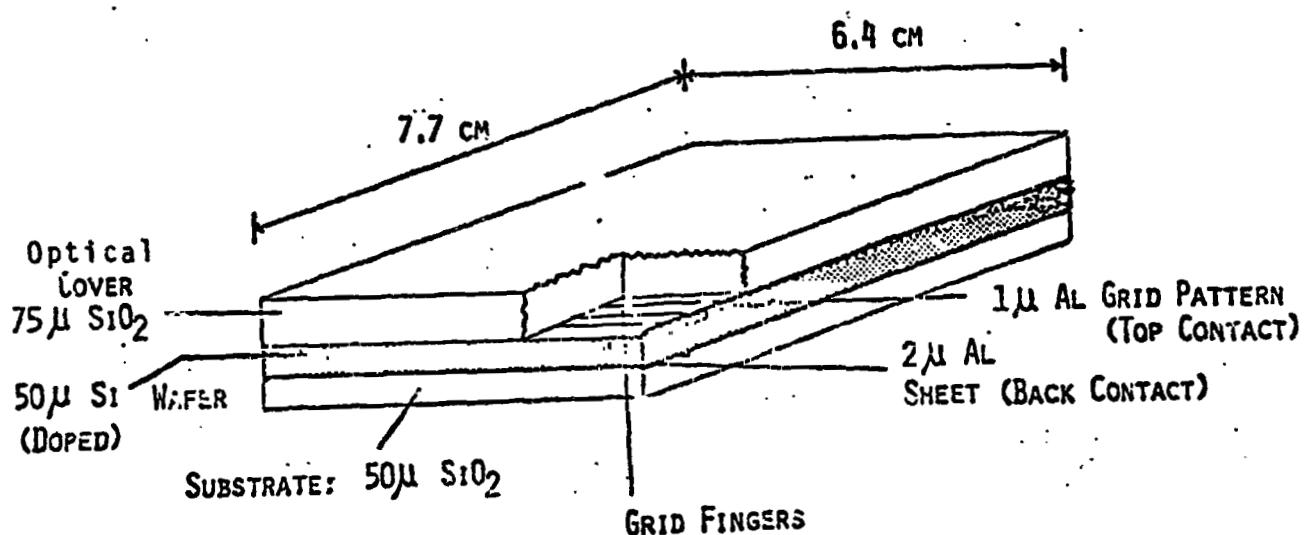
FIGURE 3.1:   VIEW OF LUNAR-MATERIAL SOLAR CELL

3.5

Since the density of SiO_2 is 2.18 tons/m^3, and that of Si is 2.33 tons/m^3, the total solar-cell mass is given by:

$$(100 \times 10^6 m^2)[(125 \times 10^{-6})(2.18) + (50 \times 10^{-6})(2.33)]$$

$$= 3.89 \times 10^4 \text{ tons}$$

In addition, the solar cells require 575 tons of aluminum contacts, and the solar-cell arrays need 610 tons of electrical interconnects and 350 tons of Kapton tape for structural backing (these figures have been calculated from the array designs). The solar cell arrays therefore mass:

$$(3.89 \times 10^4 \text{tons}) + (575 + 610 + 350) = 4.04 \times 10^4 \text{ tons}$$

Adding 10% for estimated breakage during SPS assembly, the required SMF output for one 10-GW SPS (without growth margin) is:

$$(1.1)(4.04 \times 10^4) = 4.4 \times 10^4 \text{ tons}$$

The materials breakdown for the solar cell arrays is as follows (masses in tons):

Aluminum (contacts, interconnects)	1.30×10^3
Silicon (solar cell wafers)	1.26×10^4
Dopants (solar cell wafers)	negligible
Silica (optical covers, substrates)	3.00×10^4
Kapton tape (structural backing)	3.85×10^2
Total	4.4×10^4

3.2.3: Structural Member Ribbon: A number of structural member designs are possible candidates for SPS use. The structural masses for the earth baseline design in Table 3.2 (5385 tons for solar array structure and 500 tons for antenna structure) are apparently for tapered-tube beams. Switching to continuous-chord beams raised the solar array structure estimate to 7155 tons (Ref. 3.3). The dimensions of the Boeing continuous-chord beams are shown in Fig. 3.2. Such continuous-chord beams are relatively simple to manufacture, and devices for their assembly are well under development (such as the Grumman beam-builder). This prompted the

MATERIALS: P-1700 GRAPHITE (POLYSULFONE IMPREG)
S-101 GLASS COVER
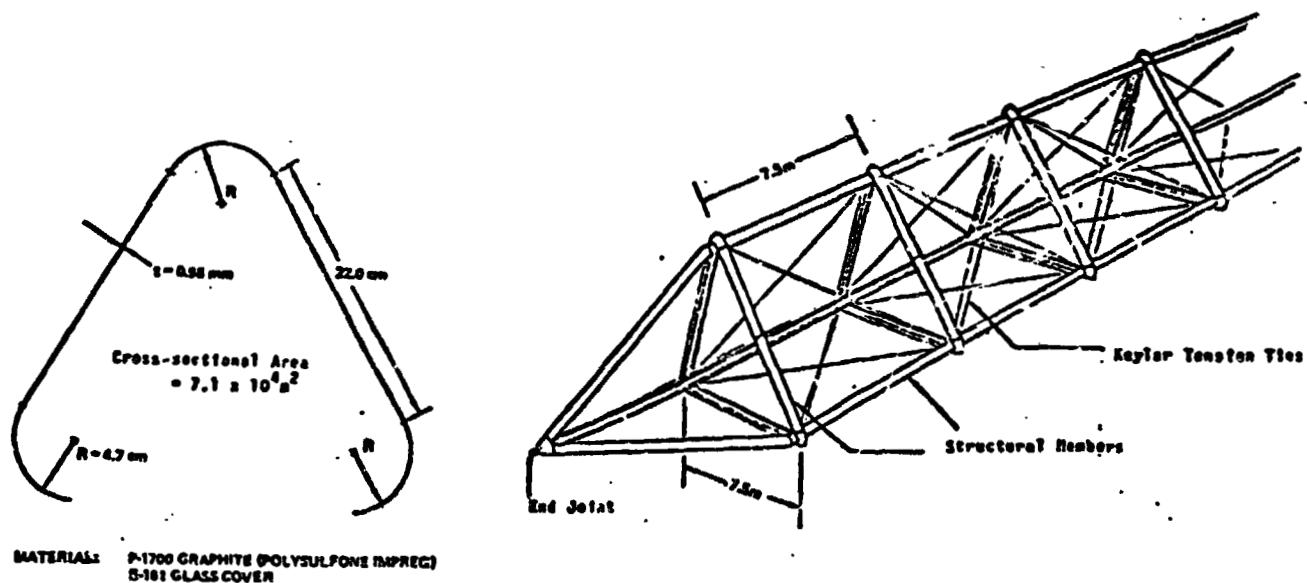
FIGURE 3.2: BOEING-DESIGN CONTINUOUS CHORD BEAM

3.7

study group to include a structural member ribbon production system in its reference SMF design. The ribbon is made of aluminum, .74 m wide, which can then be formed into the cross-section shown in the figure above. A discussion of the various structural member options appears in Chap. 5, "Candidate SMF Processes".

If the antenna structure mass (500 tons) in Table 3.2 is raised to 664 tons to account for switching to continuous-chord beams (using the same percentage as the solar array structure), the earth baseline structural mass is then 7819 tons. If the structure has the configuration shown above, and has material density 1.77 tons/m^3, this corresponds to a total structural member length of 6.2 x 10^6 meters.

The thickness of the aluminum members replacing the graphite/epoxy (G/E) earth baseline members has been calculated by matching the stiffnesses (EI) of the members. For equal cross-sectional shapes, and for members with thicknesses much smaller than cross-sectional dimensions, the moments of inertia can be considered proportional to the cross-sectional areas, and therefore to the thicknesses. Therefore matching the stiffnesses of the G/E and Al members leads to:

$$\frac{E_{G/E}}{E_{Al}} = \frac{t_{Al}}{t_{G/E}}$$

where:

$$E_{G/E} = \text{modulus of elasticity of G/E} \quad = 127 \text{ GPa}$$
(adjusted for the effect of glass fabric layers)

$$E_{Al} = \text{modulus of elasticity of Al} \quad = 59 \text{ GPa}$$

$$t_{G/E} = \text{thickness of G/E members} \quad = .96 \text{ mm}$$

$$t_{Al} = \text{thickness of Al members}$$

Thus $t_{Al} = 1.77$ mm, and the mass of aluminum (density 2.7 tons/m^3) required for the structural members is 2.2×10^4 tons. Adding a 5% allowance for wastage during beam forming and assembly raises the SMF output to 2.3×10^4 tons for one 10-GW SPS without growth margin.

Note: The study group feels that this figure may be unnecessarily large. When aerospace aluminum structures are replaced with graphite-expoxy, mass savings are usually roughly 30%. It is therefore unlikely that the reverse process would multiply the structural mass by 2.8. Furthermore the geometric configuration, e.g. column lengths, node points, etc., optimized for G/E would not be the optimum for an aluminum structure. This suggests that just matching of stiffnesses (EI) is not the proper criterion for switching materials. However, developing more accurate design criteria requires detailed knowledge of the expected load history of the structure. Since this information is at present uncertain, the study group stayed with the matching of stiffnesses which is conservative.

3.9

The materials breakdown for the structural member ribbon
is as follows (masses in tons):

Aluminum (6063 alloy)	2.3×10^4
Magnesium (6063 alloy)	1.6×10^2
Silicon (6063 alloy)	92
Total	2.3×10^4

3.2.4: Klystron Assemblies: The klystron assemblies each
consist of the klystron itself (solenoid cavity, solenoid
poles, solenoid coil windings, and other components), the
solenoid and collector housings, a radiator sheet, and six
heat pipes (between the klystron module and the radiator
sheet). These are shown in Fig. 3.3. The masses of these
components are listed below (in kg/assembly):

Solenoid cavity	5.1
Solenoid poles	3.6
Solenoid coil windings	10.2
Other Compcnents	15.6
Collector housing	4.3
Solenoid housing	9.0
Heat pipes	17.4
Radiator sheet	8.4
Total	73.6

The mass figures for the solenoid cavity, solenoid poles,
solenoid coil windings, and 'other components' are taken from
JSC-GD study's P. R. No. 7 (Ref. 3.4). The collector and so-
lenoid housing masses were calculated by multiplying the JSC-

Figure labels: Collector, Solenoid Housing, Heat Pipes, Radiator Sheet, 144 m, 2.18 m, 1 mm
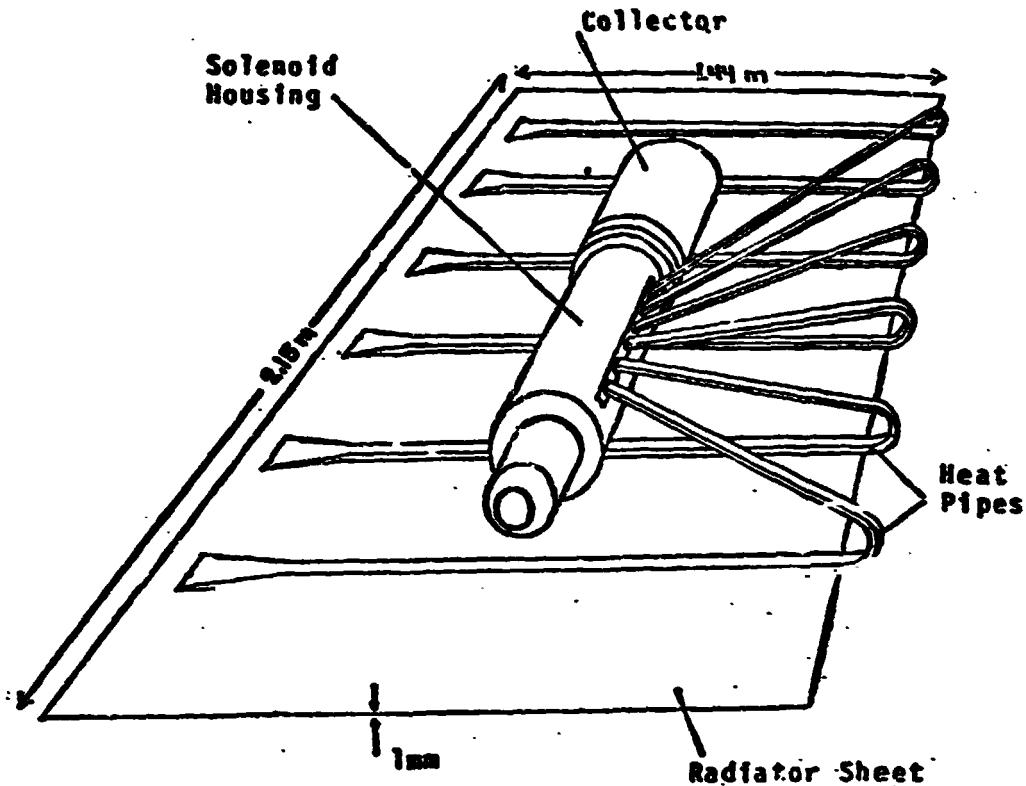
RE 3.3: KLYSTRON ASSEMBLY

GD P.R. 7 mass estimates by a factor of 5, following consul-
tations with Mr. Art Kelly of Raytheon's Power Tube Division
(Waltham, MA), who suggested that microphonic noise problems
would require housing thicknesses several times larger than
the 1 mm in the Boeing design.

The masses for heat pipes and radiator sheet are calcu-
ated from a design based on manufacturing requirements (see
Figs. 3.3 and 3.4 for dimensions). The radiator sheet has
the same area as the klystron radiators in the Boeing design
(Ref. 3.2, Fig. X-7). The aluminum sheet has thickness 1 mm
(considered minimum for handling), and thus masses:

3.11

Heat Pipe Segment
(Formed from ribbon
3.5x.25x.001 m)

Heat Pipe Ribbon
(1.6 x .125 x .001 m)
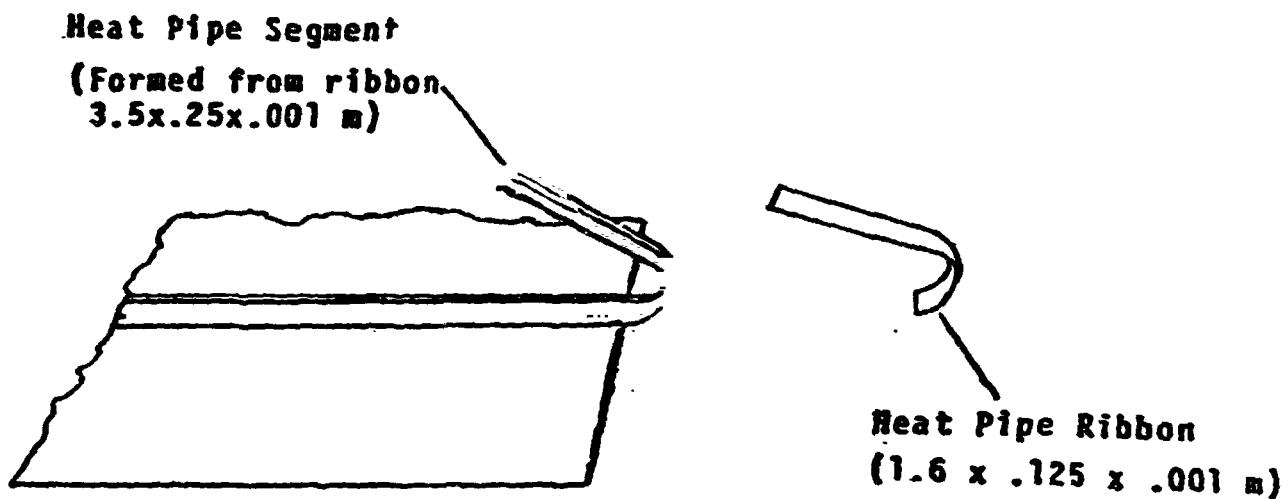
6 Heat Pipes/Assembly
All Aluminum (density 2700 kg/m^3)

FIGURE 3.4: KLYSTRON HEAT PIPE

$$(2.15 \text{ m})(1.44 \text{ m})(.001 \text{ m})(2700 \text{ kg/m}^3) = 8.4 \text{ kg}$$

The heat pipes each mass:

$$(2700 \text{ kg/m}^3)[(3.5)(.25)(.001) + (1.6)(.125)(.001)] = 2.9 \text{ kg}$$

leading to a heat pipe mass (6 heat pipes/assembly) of 17.4 kg per assembly.

As shown in Table 3.2, the baseline design includes 1.94×10^5 klystron assemblies per 10-GW SPS. This leads to a mass of klystron assemblies of 1.4×10^4 tons. Adding a 5%

allocation for wastage during SPS assembly, the SMF output of klystron assemblies is 1.5×10^4 tons for one 10-GW SPS (without growth margin).

The materials breakdown for klystron assemblies is as follows (masses in tons):

Aluminum (radiators, housings, coils, solenoid cores)	1.0×10^4
Iron (solenoid poles)	7.3×10^2
S-Glass (glass cloth insulation)	9.0×10^2
Parts From Earth	3.2×10^3
Total	1.5×10^4

3.2.5: Waveguides: The waveguide output requirements were based on the Boeing-JSC baseline design. The study group first modeled each transmitting antenna as a disc with radius 500 m, made of waveguide boxes placed side-by-side (see Fig. 3.5).

It may be possible to manufacture groups of waveguides together, thus allowing single-thickness partitions between some of the waveguides. However, the study group kept the double walls in the model, to account for the end partitions in the waveguides and for the feeder waveguides between the klystrons and the transmitting waveguides. There is also some uncertainty as to whether foamed glass can be cast from single sheets and then machined to close tolerances, which presents problems for multi-waveguide sections.

Section AA

←——— 1000 m ———→

· Transmitting Antenna
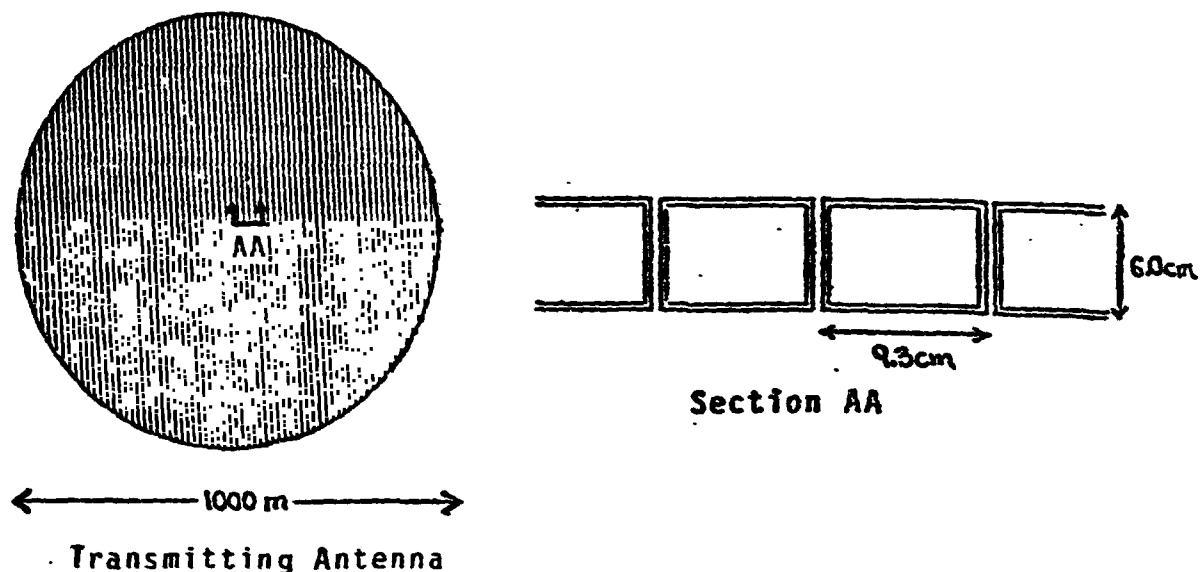
(Dimensions from Boeing Study, Ref. 3.3)

FIGURE 3.5: SIZING MODEL FOR ANTENNA WAVEGUIDES

Given the model above, the area of the side walls is (.65) times the combined area of the top and bottom faces. Therefore, for each antenna, the total area of the waveguide sheet required is:

$$(1 + .65)(2)[\pi(500)^2] = 2.6 \times 10^6 \text{ m}^2$$

For both antennas, the total waveguide sheet area is therefore $5.2 \times 10^6 \text{ m}^2$.

As suggested by the JSC-GD study, the waveguides are made from foamed glass in the SMF reference design. Consultations with Dr. David Rostoker of Corning Glass Co. have indicated that: 1) foamed glass can be produced in sheets as thin as 2.5 mm, but that thinner sheets would be plagued by produc-

3.14

tion and handling problems; 2) foamed glass which could be machined to the required surface tolerances would have a density of .8 tons/m^3.

Taking the waveguide sheet thickness to be 2.5 mm, and the density .8 tons/m^3, the waveguide sheet volume for the two antennas would be 1.3 x $10^4 m^3$, and its mass 1.04 x 10^4 tons. This mass consists of 1.03 x 10^4 tons of natural lunar glass and 135 tons of foaming agents. The foaming agents mass is calculated as 1.3% of the total foamed glass mass (percentage taken from foamed-glass figures on page 4.7-5, Ref. 3.4).

As shown in the JSC-GD P.R. 2, App. X, Fig. X-5 (Ref. 3.2), the required thickness of aluminum coating the inside of the waveguides is 6.67 microns. Since all the waveguide sheet pieces are coated on one side, the total aluminum coating area is therefore 5.2 x $10^6 m^2$, and its mass 94 tons. This brings the total waveguide mass to 1.05 x 10^4 tons. Adding 10% extra for wastage during assembly, the SMF output mass of waveguides for one 10-GW SPS (without growth margin) is 1.2 x 10^4 tons.

Note: The aluminum thickness used (6.67 microns) is based on coating a smooth waveguide surface. This could require a process to fill in the surface imperfections (broken bubbles) in the foamed glass sheets, or the deposition of a thicker layer of aluminum. Both of these options could raise

3.15

the waveguide mass. However, in view of the conservative

sizing assumptions (double-walled partitions and 2.5 mm thick-

ness), the study group kept the figure calculated above as

the waveguide output mass.

The materials breakdown for the waveguides is as follows
(masses in tons):

Natural Lunar Glass	1.13×10^4
Foaming Agents	1.5×10^2
Aluminum (interior coating)	$\underline{1.0 \times 10^2}$
Total	1.2×10^4

3.2.6: Busbar Strips: The busbars in the earth baseline SPS

are aluminum sheets 1 mm thick. The SMF therefore produces

1 mm thick aluminum, and the output mass is thus the same

(2030 tons for the solar array and 760 tons for the antennas).

Adding 1% extra for wastage during assembly, the SMF output

mass for busbar strips is 2.8×10^3 tons for one 10-GW SPS

(without growth margin).

For convenience in manufacturing and handling, the busbars

are produced as strips .74 m wide in the reference SMF design.

Therefore the total busbar strip length (including the 1%

wastage allocation) is 1.4×10^6 meters.

The materials breakdown for the busbar strips is as fol-

lows (masses in tons):

Aluminum	$\underline{2.8 \times 10^3}$
Total	2.8×10^3

<u>3.2.7: DC-DC Converters</u>: The earth baseline DC-DC converters are modified for SMF manufacture as per the JSC-GD study suggestions, i.e. replacing the transformer core with a SENDUST core and the copper coils with aluminum coils. The mass of the required 456 converters (without radiators or growth margin) is the 2049 tons (Ref. 3.4). Adding 1% for wastage during SPS assembly (5 extra converters) raises their number to 461 and their mass to 2.1×10^3 tons for one 10-GW SPS (without growth margin).

The materials breakdown for the DC-DC converters is as follows (masses in tons):

Aluminum (core alloy, coils)	3.0×10^2
Silicon (core alloy)	1.0×10^2
Iron (core alloy)	8.5×10^2
S-Glass (glass cloth insulation)	1.9×10^2
Parts From Earth	6.3×10^2
Total	2.1×10^3

<u>3.2.8: Electrical Wires and Cables</u>: The mass of aluminum cables and electrical wires required (without growth margin) is 633 tons (Ref. 3.4). This includes 267 tons of woven-glass insulation on the wires. Since the aluminum wires and cables are 1.13 mm in diameter, this corresponds to a total length of 1.3×10^8 meters. Adding a 5% allocation for wastage during SPS assembly raises the SMF output of cables and wires to a total length of 1.4×10^8 meters and a mass of 6.7×10^2 tons for one 10-GW SPS (without growth margin).

3.17

The materials breakdown for electrical wires and cables
is as follows (masses in tons):

Aluminum	3.8×10^2
S-Glass (glass cloth insulation)	2.9×10^2
Total	6.7×10^2

3.2.9: DC-DC Converter Radiators: The DC-DC converter radi-
ators were designed for simplicity of manufacture (see
Fig. 3.6). As shown in the figure, the mass of each radiator
is 1220 kg. Since 456 radiators are needed per SPS, the
total required mass is 5.56×10^2 tons. Adding 1% extra
(5 radiators) for wastage during SPS assembly brings the re-
quired SMF output for DC-DC converter radiators to 461 pieces,
of mass 5.6×10^2 tons, for one 10-GW SPS (without growth mar-
gin.)

The materials breakdown for the DC-DC converter radiators
is as follows (masses in tons):

Aluminum	5.6×10^2
Total	5.6×10^2

3.2.10: End Joints and Joint Clusters: The numbers of these
pieces were estimated from the physical layout of the Boeing-
JSC baseline design. In the continuous-chord tribeam struc-
ture, end joints are required only at the ends of the beams,
where the longerons are brought to a point. Joint clusters
join groups of tribeams together by their end joints. Since

Manifold

Radiator Pipe

Aluminum Sheet

10.08 m

36.55 m

.001m

.001m

.125 m

DC-DC Converter Radiator:

Aluminum Sheet Mass/radiator
= 995 kg

Total Radiator Mass
= 1220 kg

Radiator Pipe:

Made from .25 x .001 m
Al Ribbon

Total length/radiator
= 310.5 m

Mass/radiator = 210 kg

Manifold:

35 cm

8.12 m

Manifold cast in 5 pieces
from Al .001 m thick
2 Manifolds/radiator
Mass/radiator = 15 kg (est.)
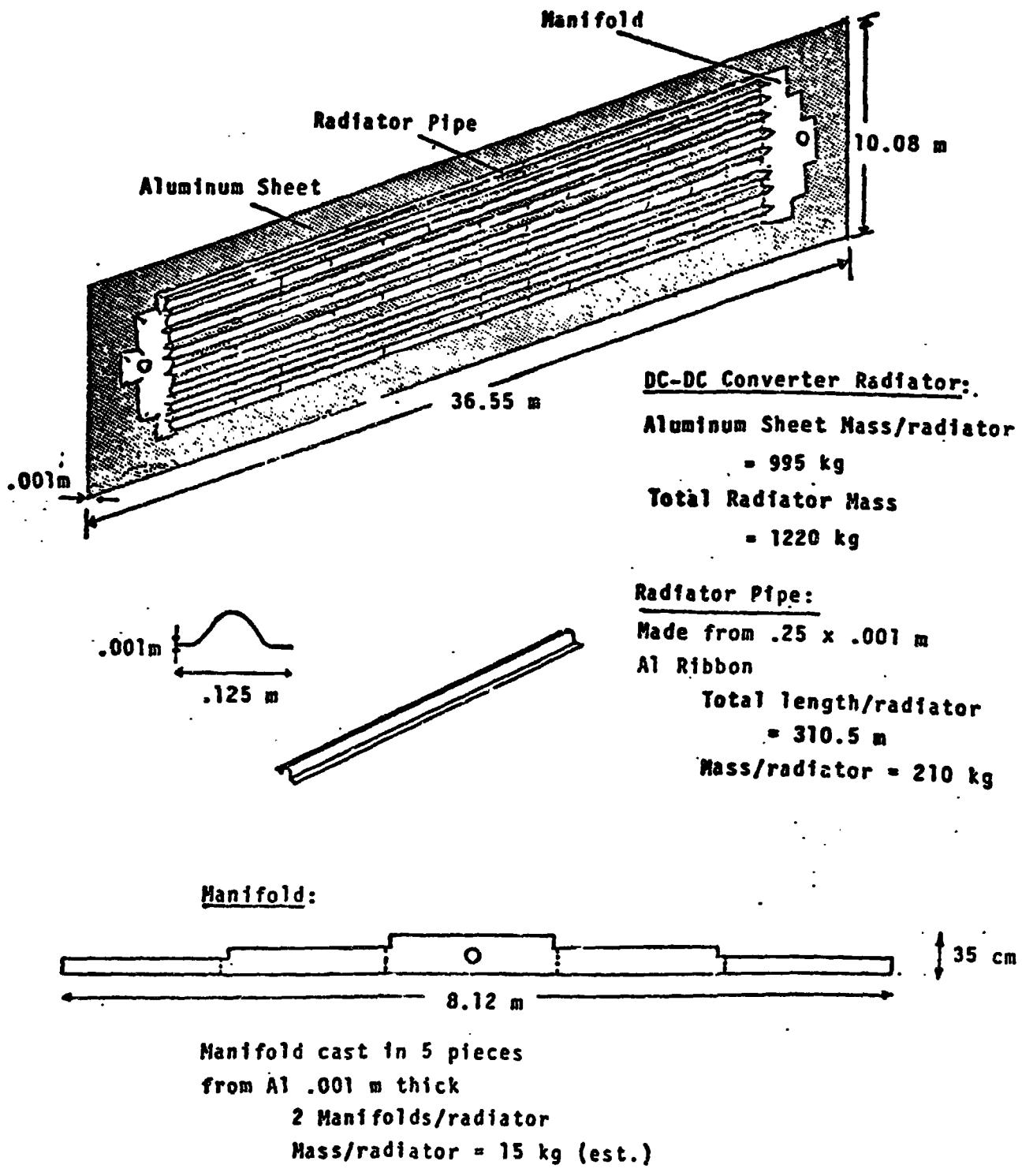
FIGURE 3.6:   DC-DC CONVERTER RADIATOR DESIGN

3.19

no specific designs were available for the end joints and joint clusters, the masses of each piece were estimated at 2 kg and 5.2 kg, respectively; this leads to an estimated total SMF output of 8 tons each for these components for one 10-GW SPS (without growth margin).

These masses are so low that these components could possibly be brought form Earth at a lesser cost. However, since other casting operations are required at the SMF anyway, these products were left in the SMF outputs. The study group felt that they might serve as examples of 'economic border line' outputs.

The materials breakdown for the end joints and joint clusters is as follows (masses in tons):

End Joints:	Aluminum (6063 alloy)	8
	Magnesium (6063 alloy)	negligible
	Silicon (6063 alloy)	negligible
	Total	8
Joint Clusters:	Aluminum (6063 alloy)	8
	Magnesium (6063 alloy)	negligible
	Silicon (6063 alloy)	negligible
	Total	8

3.3: COMPARISON OF EARTH-BASELINE AND LUNAR-MATERIAL SPS'S

In a comparison between Tables 3.1 and 3.2, the relevant total mass figure in Table 3.2 (the earth-baseline) is 77,002 tons (no growth margin), since the total SMF output

3.20

(100,000 tons) has no SPS growth margin in it either. However,
this mass should be raised to 78,940 tons to account for
switching to a continuous-chord beam design (as described in
Sec. 3.2.3, "Structural Member Ribbon", above).

In the lunar-material SPS totals, removing the allowances
for SPS assembly wastage gives a total mass of SMF-produced
components (for one 10-GW SPS without growth margin) of 93,200
tons. The estimated Earth inputs to the SPS assembly are
3,400 tons (reduced for the JSC-GD study estimate of 10,190
tons, to remove the growth margin, and to account for 4,600
tons of earth inputs incorporated into the SMF outputs, i.e.
klystron and DC-DC converter electronics and Kapton tape).
Thus the lunar-material 10-GW SPS mass estimate is 96,600
tons (without growth margin).

The 17,700-ton spread between the earth-baseline (78,900
tons) and lunar-material (96,600 tons) SPS's is accounted for
principally by the larger structural member and waveguide
masses in the lunar-material SPS. Replacement of the earth-
baseline graphite/epoxy structure by aluminum raises the
structural mass by 14,100 tons (from 7,819 tons to 22,000 tons).
However, as described in Sec. 3.2.3, "Structural Member Ribbon",
the study group has some doubts on the applicability of an
equal-stiffness criterion to this replacement. The change
from earth-baseline to lunar-material waveguides raises their
mass by 6,200 tons (from 4,314 tons to 10,500 tons).

However, the substitution of lunar aluminum for earth

3.21

baseline copper removes 400 tons for the DC-DC converters and
500 tons from DC-DC converter radiators. And the lunar-material
solar cells (4.02 x 10^4 tons) are 1,400 tons lighter than their
earth-baseline equivalent (4.14 x 10^4 tons, without 'catenary,
tolerance and other'). These increases and decreases add up
to 18,000 tons, very close to the mass spread (17,700 tons) in
the totals. The remaining discrepancy is due to minor varia-
tions between lunar-mate,,al and earth-baseline component
masses, and round-off errors in the calculations.

3.4: TABULATED MATERIALS BREAKDOWN OF SMF OUTPUTS

Section 3.2 above includes the materials breakdowns of the
various SMF outputs. These listings were examined to deter-
mine which components of the outputs should come from Earth.

In the solar cell arrays, Kapton tape comes from Earth
because it cannot be made from lunar materials. Dopants
come from Earth because they have to be very pure, and the re-
quired mass is low (less than a ton per 10-GW SPS).

In the klystron assemblies, a number of klystron parts
require either complex manufacture or non-lunar materials.
These parts therefore come from Earth.

In the waveguides, the foaming agents (typically carbon,
sulfates, water) are not available on the Moon. Therefore,
they come from Earth.

In the DC-DC converters, a number of parts require com-
plex manufacture or non-lunar materials. These parts there-
fore come from Earth.

Taking these points of origin into account, the materials
breakdowns of the SMF outputs were rearranged, and the types
and quantities of materials in the SMF outputs were tabulated.
This information is presented in Table 3.3. It should be
noted that some of the specifications of these outputs are
dependent on the processes proposed in the reference SMF de-
signed by this study, and therefore keyed to the reference
design.

TABLE 3.3: TYPES AND QUANTITIES OF MATERIALS IN SMF OUTPUTS

(for 1 10-GW SPS without growth margin)

Lunar Inputs	Masses (in tons)
Al (total mass, 3.8×10^4)	
In solar cell arrays	1.3×10^3
In structural member ribbon	2.3×10^4
In klystron assemblies	1.0×10^4
In waveguides	1.0×10^2
In busbar strips	2.8×10^3
In DC-DC converters	3.0×10^2
In electrical wires and cables	3.8×10^2
In DC-DC converter radiators	5.6×10^2
In end joints	8
In joint clusters	8
SiO$_2$	
In solar cells	3.0×10^4
Si (total mass, 1.3×10^4)	
In solar cell arrays	1.3×10^4
In structural member ribbon	92
In DC-DC converters	1.0×10^2
In end joints	negligible
In joint clusters	negligible
(continued)	

TABLE 3.3 Continued

Lunar Inputs	Masses (in tons)
Natural Lunar Glass	
In waveguides	1.1×10^4
Fe (total mass, 1.6×10^3)	
In klystron assemblies	7.3×10^2
In DC-DC converters	8.5×10^2
S-Glass (total mass, 1.4×10^3)	
In klystron assemblies	9.0×10^2
In DC-DC converters	1.9×10^2
In electrical wires and cables	2.9×10^2
Mg (total mass, 1.6×10^2)	
In structural member ribbon	1.6×10^2
In end joints	negligible
In joint clusters	negligible
Earth Inputs	
Klystron Parts	
In klystron assemblies	3.2×10^3
DC-DC Converter Parts	
In DC-DC converters	6.3×10^2
Kapton Tape	
In solar cell arrays	3.9×10^2
Foaming Agents	
In waveguides	1.5×10^2
Dopants	
In solar cell arrays	negligible
Total Mass	1.0×10^5 Tons

CHAPTER 4

SMF INPUTS

4.1: GENERAL REMARKS

4.1.1: Organization: This chapter describes the characteristics of the material inputs to the reference SMF designed by this study. Section 4.2 lists the lunar materials theoretically available to a space manufacturing facility. Section 4.3 presents the types and quantities of the material inputs to the reference SMF. Section 4.4 discusses the desired purities from the lunar refining processes. Section 4.5 presents the physical shapes of the inputs to the reference SMF. The above-mentioned characteristics of the reference SMF material inputs are then collected in Table 4.5 in Sec. 4.6. Section 4.7 discusses the inputs to the reference SMF which do not contribute materials to the outputs (such as lubricants, oxygen, consumables, spare parts) and the personnel input.

4.1.2: Nomenclature: To keep the different types of inputs organized, this report uses a specialized nomenclature. "Material inputs" refers to those inputs which will contribute material to the SMF outputs (after some wastage in production). Inputs to the factories which are not incorporated into products, although used up by production processes (such as machine lubricants and oxygen for pneumatic actuators) are labeled "expendables". A distinction is sometimes made between lunar expendables and earth expendables, indicating the source of the expendables. Spare parts used for equipment repairs

are called "refurbishment parts". Inputs to the SMF for the

life-support of the space workers are called "consumables".

Here again, a distinction is made between earth consumables

(such as food) and lunar consumables (such as breathing oxygen).

Oxygen used in stationkeeping thrusters is labeled "propellant".

4.2: AVAILABLE LUNAR MATERIALS

The elemental abundances in lunar soil are presented in

Table 4.1 (adapted from data in Ref. 4.1). As shown in the

table, these abundances vary between the lunar maria and the

highland regions. However, the variations withing the maria

and within the highlands are small. This is because the

TABLE 4.1: ELEMENTAL ABUNDANCES IN LUNAR REGOLITH

Element	Abundance in Mare (weight %)	Abundance in Highland (weight %)
O	41.3	44.6
Si	20.4	21.0
Ti	3.1	.3
Al	6.8	13.3
Fe	13.2	4.9
Mg	5.8	4.6
Ca	7.9	10.7
Na	.3	.3
Cr	.3	.1
K	.1	.1
Mn	.2	.1
P	.1	.1
S	.1	.1
Totals	99.6	99.9

Moon's geologic history has lacked most of the processes which
have segregated materials on earth (e.g. erosion, sedimentation,
life), hence the Moon tends to be homogeneous. (One theory
suggests that differences between maria and highlands are due
to volcanic action.) Therefore average abundances are accurate
enough to represent the abundances within each type of terrain.

For the purposes of this study, the first seven elements
are available as lunar inputs to the SMF (as discussed in
Sec. 2.2). Beyond the list in the table, Ref. 4.1 also lists
67 other elements present in trace quantities (parts per mil-
lion or parts per billion). Review of literature on lunar re-
sources use and discussions with researchers in the field (par-
ticularly Dr. Robert Waldron at the Lunar and Planetary In-
stitute and Dr. Richard Williams at NASA JSC) suggest that
some of these minority elements (including hydrogen) might be
extracted in usable quantities with complex processing tech-
niques. A discussion of the effect of availability of lunar
materials on the SMF concept appears in Chap. 13, "Possible
System Tradeoffs".

Notably absent from the list of available elements (O, Si,
Ti, Al, Fe, Mg, Ca) are hydrogen, nitrogen, and carbon. There-
fore hydrocarbon materials (including plastics and most fuels)
must be brought from Earth. The same applies to nitrogen for
breathing atmospheres and the hydrogen constituent in water.
Since such transportation is relatively expensive, this pushes
the SMF processes and equipment designs away from the use of

carbon, carbon compounds, and water; this is a radical departure from normal industrial practice on Earth.

Examination of the JSC-LPI study results (Ref. 4.2) and discussions with participants in that study indicated that a variety of compounds are available from the refining processes defined in that study. In particular, silica glass (SiO_2), aluminum oxide (Al_2O_3), and magnesium oxide (MgO) can be produced. Therefore S-glass (65% SiO_2, 25% Al_2O_3, 10% MgO by mass) can be produced. In addition, natural lunar glass can be electrostatically separated from fine (<90 microns) lunar soil particles after these have been crushed down to <5 micron size (Ref. 4.3). Silica, S-glass, and natural lunar glass are requested inputs for solar cell production, glass-fiber production, and foamed-glass production, respectively.

4.3: TYPES AND QUANTITIES OF MATERIAL INPUTS TO REFERENCE SMF

The materials breakdown of the S F outputs (listed in Table 3.3 in Sec. 3.4) is the starting point for the computation of the material inputs of the SMF. The types of material inputs needed are the same as the types of materials required in the SMF outputs.

If there were no wastage in the production processes, the quantities of material inputs would also be the same as the output quantities listed in Table 3.3. This table would then serve as a list of types and quantities of material inputs as well. However, some wastage is likely to occur in every production process, and the inputs must therefore include allow-

ances for this wastage.

Wastage levels are dependent on production equipment design, and therefore the calculation of material input quantities first requires the choice of an SMF design. The reference SMF designed during this study was therefore used to estimate wastage and to calculate quantities of material inputs. The processes and equipment i.i the reference SMF are presented in Chap. 6, "SMF Layouts" and Chap. 7, "Production Equipment Specifications".

The types and quantities of material inputs required by the reference SMF are presented in Table 4.2. The quantity figures are taken from the massflow schematics in Chap. 6. The rationale for the wastage estimates and the calculations of the input quantity figures are given in that chapter.

TABLE 4.2: TYPES AND QUANTITIES OF MATERIAL INPUTS FOR THE REFERENCE SMF

(for 1 10-GW SPS without growth margin)

Lunar Inputs	Masses (in tons)
Al (total mass, 4.4×10^4)	
In solar cell arrays	3.1×10^3 (58% waste)
In structural member ribbon	2.5×10^4 (10% waste)
In klystron assemblies	1.1×10^4 (10% waste)
In waveguides	1.7×10^2 (39% waste)
In busbar strips	3.1×10^3 (10% waste)
In DC-DC Converters	3.3×10^2 (10% waste)
In electrical wires and cables	4.2×10^2 (10% waste)
In DC-DC converter radiators	6.2×10^2 (10% waste)
In end joints	9 (10% waste)
In joint clusters	9 (10% waste)
(continued)	

4.5

TABLE 4.2 Continued

Lunar Inputs	Masses (in tons)
SiO$_2$	
In solar cells	5.0×10^4 (40% waste)
Si (total mass, 2.7×10^4)	
In solar cell arrays	2.7×10^4 (52% waste)
In structural member ribbon	1.0×10^2 (10% waste)
In DC-DC converters	1.1×10^2 (10% waste)
In end joints	negligible
In joint clusters	negligible
Natural Lunar Glass	
In waveguides	1.8×10^4 (37% waste)
Fe (total mass, 1.7×10^3)	
In klystron assemblies	8.0×10^2 (10% waste)
In DC-DC converters	9.4×10^2 (10% waste)
S-Glass (total mass, 1.5×10^3)	
In klystron assemblies	9.9×10^2 (10% waste)
In DC-DC converters	2.1×10^2 (10% waste)
In electrical wires and cables	3.2×10^2 (10% waste)
Mg (total mass, 1.8×10^2)	
In structural member ribbon	1.8×10^2 (10% waste)
In end joints	negligible
In joint clusters	negligible
Earth Inputs	
Klystron Parts	
In klystron assemblies	3.5×10^3 (10% waste)
DC-DC Converter Parts	
In DC-DC converters	7.0×10^2 (10% waste)
Kapton Tape	
In solar cell arrays	4.2×10^2 (10% waste)
Bonding Agents	
In waveguides	2.4×10^2 (37% waste)
Dopants	
In solar cell arrays	negligible
Total Mass	1.5×10^5 Tons

4.4: PURITIES OF SMF INPUTS

4.4.1   General Remarks: In general, the material purities

available from refining processes can be increased by two

methods: running the material through more refining cycles, and switching to a more effective (but more complex) refining process. The purity available from increasing the number of refining cycles is usually limited by the characteristics of the process used; beyond a certain number of cycles, gains in purity are negligible. Therefore increases in purity first increase the quantity of machinery, up to purities of 90 - 95%. Above this figure the complexity of the machinery goes up, as the refiner switches to increasingly more sophisticated processes. The quantity of machinery may go up as well, if the more complex processes have lower yields than the lower-purity refining cycles.

Therefore demands in purity by the SMF designer can significantly increase the quantity and complexity of the lunar refining equipment needed. Thus certain manufacturing processes, though not optimal for the SMF alone, may be optimal for the system as a whole, because their inputs require cheaper refining techniques. Similarly, an optimization of the entire system could suggest modifications to the SPS design, to use lunar materials which require less refining. These considerations are beyond the scope of this study, but should be included in later evaluations of lunar-material space industrialization.

Another problem is that the expected purity of refined materials is one of the most difficult parameters to predict in refinery design. In the design of Earth refining equipment, the output purities are seldom accurately known until

after the construction of a pilot plant.

4.4.2: Tabulated Purities of Reference SMF Material Inputs:

For this study, the input purities required were determined by examination of the required outputs (see Chap. 3) and of the proposed reference SMF processes (see Chaps. 6 and 7). The purities of SMF inputs are listed in Table 4.3. In the explanations that follow, the available lunar-material purities were decided after examination of the output of the JSC-LPI study (Ref. 4.2) and discussions with Dr. Waldron of LPI.

4.4.3: Aluminum: The highest purity aluminum required in the SPS is for electrical applications: solar-cell contacts and interconnects, busbars, wires, coils, waveguide coatings. Alloys such as 1060 (99.6+% Al) and 1100 (99.9+% Al) are used for electrical conductors on Earth. The conductivity drops rapidly with the decrease of aluminum purity. These electrical-grade purities are available from the refining processes

TABLE 4.3: PURITIES OF MATERIAL INPUTS TO REFERENCE SMF

Lunar Inputs	Purity
Aluminum (electrical grade)	99.6+ %
Silica (optical grade)	96
Silicon (metallurgical grade)	99.9
Natural Lunar Glass	as separated from soil
Iron	99.9
S-Glass	glass-fiber grade
Magnesium	99
Earth Inputs	
Klystron Parts	---
DC-DC Converter Parts	---
Kapton Tape	---
Foaming Agents	as needed
Dopants (semiconductor grade)	99.999

suggested by the JSC-LPI study. Another use of aluminum in the reference SMF is in Al 6063 alloy (structural members, end joints, joint clusters). Since the aluminum content of this alloy is 98.9%, close to electrical grade purity, the entire aluminum input to the reference SMF was set at 99.6+% purity.

4.4.4: Silica: The entire requirement for SiO_2 is in solar cells. The solar-cell optical cover is 60% of this glass. Its purity requirement is that of commercial optical glass: 96% silica. For simplicity, the substrate glass (the remaining 40%) was also set at optical purity, though its primary functions are structural integrity and radiation protection. A lower grade of substrate glass could be used in the reference SMF, provided that it were compatible with the proposed manufacturing processes.

4.4.5: Silicon: The most demanding purity requirement in the lunar-material SPS is that of silicon. For the type of solar cells used in the Boeing-JSC baseline, the silicon wafer must be made from semiconductor grade silicon (99.999% silicon). Lunar-material substitutions do not affect this requirement, since silicon is the only lunar material likely to be used to make 12.5% efficient solar cells (according to current knowledge). After examination of the JSC-LPI study reports (Ref. 4.2) and consultation with Dr. Waldron at LPI, this study concluded that the purification of silicon to semiconductor grade was not guaranteed by the proposed lunar processes. The hydrofluoric acid leaching process suggested in that study should produce metallurgical grade (99.9%) silicon, and that is the

4.9

purity set down for the entire SMF silicon input. The silicon used for the solar cells therefore requires additional refining at the SMF. Note: this additional refining could be done on the Moon, after production of the metallurgical grade silicon. However, semiconductor grade silicon can easily be contaminated in handling, and this option would therefore increase the complexity of the Moon-to-SMF transportation system.

4.4.6: Natural Lunar Glass: Natural lunar glass is used in the reference SMF design to produce foamed glass for waveguides. Foamed glass is produced on Earth by Corning Glass Co., and a company in France. It has also been researched in the Soviet Union. Detailed information on the required purity of the glass input is therefore proprietary or otherwise unavailable. It was therefore assumed that, by the year 1990, processes to produce foamed glass from natural lunar glass, beneficiated but not refined, would be available. The natural lunar glass is electrostatically separated from the fine particles in lunar soil, after these particles have been crushed to <5 micron size. The separated glass is shipped to the SMF without further enhancement of purity.

4.4.7: Iron: Iron is needed for two uses in the SMF: solenoid poles for the klystrons are pure iron, and transformer cores for the DC-DC converters are SENDUST alloy (85% Fe). Both of these applications require pure iron (for the SENDUST use, pure iron before alloying). The lunar soil contains .5 to .6 wt.% of metallic iron (Ref. 4.4). The surface iron has been baked to a high purity by the solar wind. It is there-

4.10

fore relatively simple to separate it magnetically from the
soil. The iron can then be electrochemically refined to pu-
rities on the order of 99.9% (refining iron is simpler and
less energy-demanding than many other refining processes, e.g.
aluminum extraction). This purity (99.9%) is adequate for in-
puts to the reference SMF.

4.4.8: S-Glass: S-glass is a mixture of 65% SiO_2, 25% Al_2O_3,
and 10% MgO, relatively insensitive to impurities. It is
used in the SMF to make glass fibers to be woven into glass-
cloth electrical insulation. Since optical quality SiO_2 (see
Sec. 4.4.4 above, electrical-grade Al (see Sec. 4.4.3),
rocket-propellant grade oxygen, and commercial-grade mag-
nesium (see Sec. 4.4.9 bei w) can be produced by the lunar
refining processes, S-glass is available in glass-fiber purity.

4.4.9: Magnesium: Magnesium is used in the SMF as an alloy-
ing element in the Al 6063 alloy (.7% Mg) for structural mem-
bers, end joints, and joint clusters. Its purity requirement
is therefore roughly 98 - 99% (commercial purity is 99.8%).
A consultation with Dr. Waldron at LPI indicated that the pro-
posed lunar refining processes could produce Mg in commercial
purities.

4.4.10: Earth Inputs: For klystron parts, DC-DC converter
parts, and Kapton tape, the concept of 'purity' does not ap-
ply. However, these inputs are of sufficient quality to guar-
antee their proper function. The foaming agents (typically
$NaSO_4$, C, H_2O) are as pure as needed for the production of

4.11

foamed glass. As mentioned in Sec. 4.4.6 above, information
on required purities for foamed-glass ingredients is unavail-
able. Dopants for solar cells (typically boron and phospho-
rous) could be commercial purity (99.8%), since their concen-
tration in solar cells is so low (89 kg of boron and 28 kg of
phosphorus per one 10-GW SPS). However, to maximize the so-
lar cell efficiency, the dopants are input in semiconductor
grade purity (99.999%).

4.5: PHYSICAL SHAPES OF REFERENCE SMF MATERIAL INPUTS

The most significant consideration affecting the physical
shape of the SMF material inputs from the Moon is the
choice of transportation system from the lunar surface into
space. There are two fundamental choices: some sort of cat-
apult (such as the electromagnetic mass-driver); or rocket
launch. In the first case, the lunar escape velocity is im-
parted to the material in a short distance and time, and the
payload then coasts to its initial destination. To withstand
the launch accelerations of 500 - 1000 g's, the lunar material
(which will be the SMF input) must have a stress-tolerant
shape, such as a pellet or block. If a mix of materials is
catapulted to a mass-catcher, the pellets or blocks must be
encapsulated or bagged, to avoid contamination between mater-
ials and vacuum-welding of the pieces.

In rocket launch, the pieces must also be kept apart to
avoid welding and contamination. However, the longer accel-
erations of 1 - 2 g's are far less demanding on the payload,
allowing a range of physical shapes, such as columns, rolls,

slabs, or bags of loose material.

An evaluation of the respective merits of the mass-driver and lunar rocket is beyond the scope of this study, and falls within the province of the JSC-GD study. However, from the point of view of the SMF designer, the rocket launch option offers the advantage that the lunar materials in the payload can be in shapes specifically designed for ease of handling and insertion into SMF processes.

As discussed in Sec. 1.4, it was decided that the lunar input materials are refined in a large processing facility on the Moon. Such a facility can also produce rocket propellant, such as the aluminum powder and liquid oxygen suggested by the JSC-GD study (Ref. 4.5). Producing fuel from lunar materials, both for lunar launch and interorbital transportation, can provide significant cost reductions in lunar-material scenarios when compared to scenarios using propellant brought from Earth. However, the relative costs of catapults and rockets for lunar launch are not yet clearly established.

For the design of the reference SMF in this study, it was assumed that lunar materials are launched from the Moon by rocket (as in the JSC-GD study's Option D) and could therefore arrive at the SMF in shapes convenient for input into the factories. The input shapes are described in Table 4.4.

The study group emphasizes that the decision to assume these shapes is not based on a systems analysis of the alternative scenarios (lunar catapults vs. rocket launch). It is only an assumption which simplifies the input sections of the

4.13

SMF. In any case, should later analyses decide in favor of lunar catapults, the reference SMF can be modified to accomodate pellet inputs. These modifications are described in Sec. 5.10, "Modifications Required for Pellet Inputs".

TABLE 4.4: PHYSICAL SHAPES OF MATERIAL INPUTS
TO THE REFERENCE SMF

Type of Input	Shape and Dimensions
Lunar Inputs	
Aluminum:	
For Al and Al alloy products	Rod, 6.4 cm diameter 10 m length
For SENDUST alloy	Rod, 2.5 cm diameter 3 m length
Silica:	Slab, 1 m x 1 m x .04 m
Silicon:	
For solar cell production	Slab, 1.2 m x .42 m x .04 m
For furnaces	Rod, 3.5 cm diameter 3 m length
Natural Lunar Glass:	<5 micron powder, bagged
Iron:	Rod, 6.4 cm diameter 10 m length
S-Glass:	Rod, 5.4 cm diameter 8 m length
Magnesium:	Rod, 1.7 cm diameter 3 m length
Earth Inputs	
Klystron Parts:	Shaped and/or packaged as required by launch stresses and SMF processes
DC-DC Converter Parts:	
Kapton Tape:	
Foaming Agents:	
Dopants:	

4.6: TA_LATED CHARACTERISTICS OF MATERIAL INPUTS TO THE
REFERENCE SMF

Table 4.5 presents types, quantities, purities, and physical shapes of the material inputs to the reference SMF.

TABLE 4.5: CHARACTERISTICS OF MATERIAL INPUTS TO THE REFERENCE SMF

Type of Input	Quantity (tons) (per 1 10-GW SPS without growth margin)	Purity (percentage of pure material)	Physical Shape
Lunar Inputs:			
Aluminum			
For Al and Al alloy products	4.4×10^4	99.6+ %	Rod, 6.4 cm diameter 10 m length
For SENDUST alloy	55	99.6+	Rod, 2.5 cm diameter 3 m length
Silica	5.0×10^4	96	Slab, 1 m x 1 m x .04 m
Silicon			
For solar cells	2.7×10^4	99.9	Slab, 1.2 m x .42 m x .04 m
For alloys	2.1×10^2	99.9	Rod, 3.5 cm diameter 3 m length
Natural Lunar Glass	1.8×10^4	as separated from lunar soil	<5 micron powder, bagged
Iron	1.7×10^3	99.9	Rod, 6.4 cm diameter 10 m length
S-Glas	1.5×10^3	glass-fiber grade	Rod, 6.4 cm diameter 8 m length
Magnesium	1.8×10^2	99	Rod, 1.7 cm diameter 3 m length
Lunar Mass Subtotal:	1.43×10^5 Tons		
Earth Inputs:			
Klyston Parts	3.5×10^3	---	shaped and/or packaged as required by launch stresses and SMF processes
DC-DC Converter Parts	7.0×10^2	---	
Kapton Tape	4.2×10^2	---	
Foaming Agents	2.4×10^2	as needed	
Dopants (Boron, Phosphorous)	negligible	99.999	
Earth Mass Subtotal:	4.9×10^3 Tons		
Total Mass of Material Inputs:	1.5×10^5 Tons		

4.7: OTHER SMF INPUTS

4.7.1: Expendables: The inputs into the factories which are
not incorporated into SMF products, but are used up by the pro-
duction processes, are called 'expendables'. At this stage of
design, it is extremely difficult to estimate the requirement
for such expendables, such as lubricants for machines and gas
for pneumatic actuators. However, the types of expendables
can be identified, and their required masses are assumed to be
small compared to the material inputs from Earth and Moon.

The principal lunar expendable is oxygen. Some of this
O_2 is injected into the SiO_2 deposition chambers in solar cell
production, to keep the SiO_2 from dissociating to SiO and O_2.
This O_2 input is wasted to space (estimated at roughly 100 tons
per SPS). Lunar oxygen is also used to drive actuators and
pistons (for example, the glass fiber producer). Lunar O_2 can
also be combined with Earth hydrogen to replace cooling fluid
losses, if water is the coolant, in some of the machinery.

Other specific lunar expendables have not been identified.
However, the possibility exists of replacing some Earth ex-
pendables (such as lubricants) with lunar materials (if they
can be used as lubricants). The study group has not investi-
gated this issue. However, any such replacement of earth ex-
pendables should be made with lunar materials either available
directly form the lunar refining processes, or produced at
minimal cost on the Moon. This is because the masses of Earth
expendables (and therefore their transportation costs) are

4.16

expected to be low. Consequently only a minimal increase in lunar production costs is warranted.

Earth expendables consist of a variety of lubricants, cooling fluids, particle suspension gases. Since machines can be designed with long-life lubricants, and cooling and gas-flow systems can be designed with virtually no leakage (as in systems used by the nuclear power industry), the mass of earth expendables is expected to be dwarfed by the mass of earth material inputs (4,900 tons/year).

4.7.2: Refurbishment Parts: Most of the machinery in the SMF is designed for a 20-year lifetime (as per SOW guidelines), and therefore requires roughly 5% of its mass in replacement parts every year. Refurbishment mass totals (and specific estimates of refurbishment mass required for the machine components) appear in Chap. 10, "Line Item Costing". The refurbishment parts come from Earth.

There is also the possibility of manufacturing refurbishment parts at the SMF from lunar materials. One potential example is the baffles used for containment of deposition vapors in the solar cell factory. Due to their fouling by the deposition processes, they are progressively replaced by new baffles from Earth. The possibility exists of making such baffles at the SMF, using woven glass cloth made from lunar materials (the baffles must resist high-temperature vapor; hence the choice of glass rather than a metal). Due to time constrains, the study did not investigate these issues, but later research on these options could reduce SMF costs slightly.

4.17

4.7.3: Consumables: The specific design of habitation and life-support systems is outside the scope of this study, as mentioned in Sec. 2.1. This study therefore used figures from other studies to determine the consumables requirement. Based on data in Refs. 4.6 and 4.7, the consumables needed by one space worker are as follows:

From Earth:
           Freeze-dried food   .7 kg/day
           Hydrogen   .03 kg/day
           Nitrogen   .1 kg/day
From Moon:
           Oxygen   .27 kg/day
                      Total   1.1 kg/day

This assumes a 95% closed water cycle, and a fully closed air cycle (leakage and airlock losses only).

The mass of the habitation section (described in Chap. 8) includes an emergency stock of 30 days of food and air, as-ruming no recycling except wash water. This adds up to 5.05 kg/person day.

The estimated population of the reference SMF is 440 people, assuming production of one 10-GW SPS/year. Therefore the consumables requirement from Earth is 370 kg/day, or 135 tons/year. The lunar oxygen requirement is 43 tons/year. These masses are small compared to the 4,900 tons of required earth material inputs, and the anticipated needs for lunar oxygen from interorbital transportation. The SMF consumables requirement is broken down in Table 4.6. The emergency stockpile in the habitation section masses 67 tons.

TABLE 4.6:   YEARLY SMF CONSUMABLES REQUIREMENT

(for 1 10-GW SPS per year without growth margin)
(SMF population: 440 people)

From Moon:	
Oxygen	43 tons
From Earth:	
Food (freeze-dried)	112 tons
Hydrogen	5 tons
Nitrogen	16 tons

4.7.4: Propellant: Propellant is required by the SMF for sta-
tionkeeping and attitude control. This propellant is lunar
oxygen. The computation of stationkeeping propellant require-
ment is outsi⌐⌐ the scope of this study. At this level of
design, the attitude control requirements are unclear. This
is because many SMF processes can apply forces on the SMF
structure (e.g. by outgassing, or angular momentum transfer
from rotating machinery), and only a detailed   ⌐ical design
can predict these attitude perturbations. The⌐⌐⌐fore the SMF
propellant requirement is not available at this stage. How-
ever, it is expected that this requirement will be dwarfed by
the lunar-oxygen needs of interorbital transportation.

CHAPTER 5

CANDIDATE SMF PROCESSES

5.1: GENERAL DISCUSSION

The required SMF outputs were described in Chap. 3. In general, the SMF must produce the types of outputs listed in Table 5.1.

```
TABLE 5.1:  TYPES OF SMF OUTPUTS
     Solar Cell Arrays
     Structural Members
     End Joints and Joint Clusters
     Busbars
     Electrical Wire and Cables
     Klystron Assemblies
     DC-DC Converter Assemblies
     Waveguides
```

As discussed in Sec. 2.2.2, these SMF products provide the lunar-material components to Solar Power Satellites and to a variety of other satellites and space facilities.

The lunar-material inputs to the SMF were discussed in Chap. 4. As described in Sec. 4.2, the seven majority elements in the lunar regolith (oxygen, silicon, titanium, aluminum, iron, magnesium, and calcium) are assumed available to the SMF, as well as compounds and mixtures of these elements. In addition, natural lunar glass can be extracted by crushing and electrostatic separation of the lunar soil, and is therefore also available as input to the SMF.

A number of assumptions affect these choices of SMF inputs

and outputs. These assumptions are discussed in Chap. 2, specifically in Sec. 2.2, "SMF Scenario Assumptions".

It is the purpose of this study to investigate possible manufacturing processes to convert the lunar-material inputs listed above (together with some Earth inputs) into the products in Table 5.1. The study group considered each type of SMF product in turn, and developed alternative manufacturing schemes to produce these SMF outputs. Sections 5.2 through 5.10 describe these various alternative production and support processes, and discuss their advantages and disadvantages. Each section also identifies the processes chosen for the reference SMF, and the reasons for the choice.

A number of assumptions affect the design and evaluation of the alternative processes and equipment. These general SMF design guidelines and assumptions are described in Chap. 2, Secs. 2.2 and 2.3. In addition, a number of specific assumptions were made in the design of machinery for the alternative processes. These assumptions are described in the discussions which follow.

It is also the purpose of this study to develop a preliminary design and to compute cost estimates for a reference SMF. Based on the choices of processes described in this chapter, operations layouts for the reference SMF are presented in Chap. 6. Production equipment specifications are described

in Chap. 7, support equipment specifications in Chap. 8, and maintenance and repair requirements in Chap. 9. Cost estimates for the reference SMF appear in Chap. 10.

5.2:   SOLAR CELL ARRAY PRODUCTION

5.2.1:   The Solar Cell: Given the assumption of no major SPS redesign beyond lunar-material substitutions (discussed in Sec. 2.2.2), the solar-cell design to be produced by the SMF is shown in Fig. 5.1. The complete solar cell is 177 microns thick, slightly less than twice the thickness of the paper on which this is printed .

Optical Cover 75μ SiO$_2$

50μ Si WAFER (DOPED)

7.7 CM

6.4 CM

1μ AL GRID PATTERN (TOP CONTACT)

2μ AL SHEET (BACK CONTACT)

SUBSTRATE: 50μ SiO$_2$

GRID FINGERS
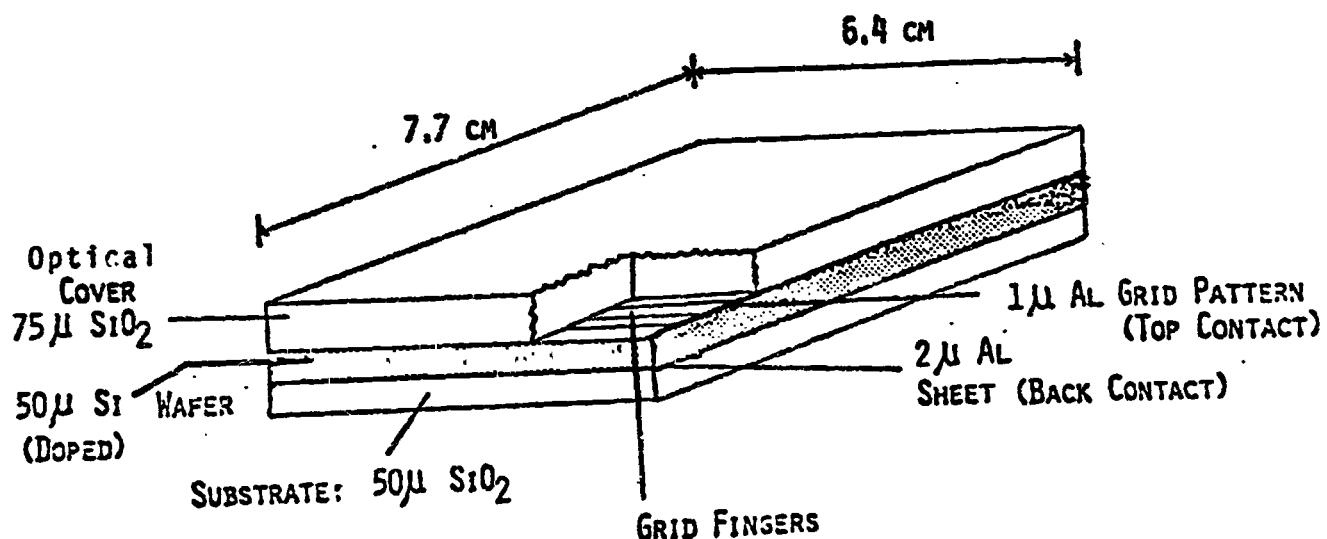
FIGURE 5.1:   BASIC DESIGN OF SMF-PRODUCED SOLAR CELL

From the bottom to the top, the cell consists of five layers:

   1.   The substrate provides partial structural integrity and

5.3

radiation protection to the cell. In a lunar-material solar cell, SiO_2 is a likely material for the substrate.

2. The back contact is a thin sheet of Al. The sheet covers the entire back surface of the silicon wafer.

3. The silicon wafer generates the current from the cell. Made from monocrystalline silicon (or at least polycrystalline silicon with grain size larger than its thickness), the wafer is doped to form a p-n junction. In this particular type of cell, the bottom 45 microns of Si are doped with a p-material (such as Boron). The top 5 microns are doped with n-material (such as Phosphorous). Dopant concentrations are roughly 10^{17} to 10^{18} atoms/cm^3. Exposed to sunlight the cell generates a voltage between its top and bottom surfaces.

4. The top contact is an aluminum 'grid fingers' pattern, designed to cover as little of the top surface as possible (to let maximum sunlight in) while reaching as much of the surface as possible (because there are losses when the current travels through the silicon to reach the electrical contact). The fingers lead the current to a collector bar at one edge of the cell.

5. The top layer of the cell is the optical cover, which must provide some structural integrity, some radiation protection, and a clear sunlight path for the cell. This layer must be transparent to the wavelengths which the cell can use for electrical production. SiO_2 is such a material for silicon solar cells. Since the upper face of the cells faces

the intense radiation of the Sun, the optical cover is thicker than the substrate.

The basic cell design originates from the Boeing-JSC ba.e-line SPS design (Ref. 5.1). The lunar-material substitutions are as suggested by the JSC-GD study (Ref. 5.2).

In most cases, these substitutions have few or no alternatives. The earth-baseline fused silica (SiO_2) substrate needs no substitution, since silica is available from the Moon. The study group considered substituting aluminum for the silica in the substrate, thus reducing the manufacturing complexity by combining substrate and back contact. However, the coefficient of thermal expansion of the substrate must be close · to that of the cell wafer, otherwise the thermal cycling due to SPS eclipse will eventually delaminate the cell. Since the wafer is made of silicon, this eliminates aluminum as an alternative for the substrate material. Late in this study, SiO was also suggested as an alternative substrate material, since it offers advantages in deposition processes, and has apparently been used to coat space hardware. Time pressures did not allow investigation of the radiation-resistance, thermal, and deposition properties of SiO, and the study stayed with the silica substrate. This alternative sho ld be investigated in future research.

The electrical conductivities of the available lunar materials are usually poor, making them unsuitable for electrical conductors. The notable exception is aluminum, which offers

a reduction in mass over earth-baseline copper when used in the cell contacts. The thinness of these contacts (2 microns and 1 micron for the back and top cell contacts, respectively) avoids the differential expansion problem mentioned above.

The silicon wafer in the earth-baseline solar cell needs no substitution, since silicon is available from the moon. The earth-baseline silicon wafers use boron and phosphorus as dopants. Phosphorus is potentially available for the Moon, and Boron could be replaced with lunar aluminum. However, the mass of dopants required is less than a ton per 10-GW SPS, and therefore their source is not si: ʿicant. Since the availability of lunar phosphorus ..a.ted, and aluminum-doped cells have not bec. exper..e ly verified, the study group decided to use bor.n and ,..sphorus from Earth.

The optical cover is made of borosilicate glass in the earth-baseline cells. The JSC-GD study suggests the subs..;tution of fused silica glass, which has properties very similar to boro-silicate glass, and is available from lunar materials. In particular, the coefficient of thermal expansion of SiO_2 is close to that of silicon, thus avoiding cell delamination problem mentioned above. The solar cell produced by this study's reference SMF therefore have fused silica optical covers. As in the substrate, SiO is an alternative optical r r material which should be investigated by future research. Specifically, the transparency of SiO to the solar spectrum must be checked, to determine whether the wavelengths which

can pass through this material can efficiently drive the silicon cell.

In addition to the layers shown in Fig. 5.1, the solar cells also require electrical contacts ("interconnects") between cells to build up the voltage and current outputs of the solar cell arrays to usable levels. The Boeing-JSC baseline design (Ref. 5.1) interconnects the cells to build up voltages of 40.8 kV and 38.7 kV, and a total amperage output of 428,000 amperes in a 10-GW SPS. The alternatives for interconnection are discussed below (see Sec. 5.2.7).

The cells must also be held together structurally to form the arrays. In the Boeing-JSC baseline SPS, the silicon wafers and electrical contacts are positioned in groups of 252 (14 by 18 cells), interconnected, and sandwiched between 1.1m x 1.17m sheets of glass (substrates and optical covers), thus formi "panels". These panels are then electrically and structurally connected together to form arrays. Alternatives for panel buildup are discussed in Sec. 5.2.7.

5.2.2 Basic Processes: The basic processes in the fabrication of a silicon solar cell of the type described above are listed in Table 5.2.

These processes need not occur in the order shown: for example, some fabrication sequences for solar cells start with the production of the substrate, building up the cell in layers; or the individual layers can be separately produced, and then bonded together. However, all the processes listed must occur

TABLE 5.2: BASIC PROCESSES
IN SILICON SOLAR CELL PRODUCTION

Purification of Metallurgical Grade
Silicon to Semiconductor Grade Silicon

Production of Doped Silicon Wafer

Application of Electrical Contacts

Production of Substrate and Optical Cover

Cell Interconnection and Array Buildup

to produce the cell. The following sections describe alternative processes for each of the listed steps.

5.2.3: Purification of Silicon: As discussed in Sec. 4.4.5, examination of the JSC-LPI study reports (Ref. 5.3) and consultation with Dr. Waldron at LPI led to the conclusion by the study group that the silicon received from the Moon is metallurgical grade (99.9% pure). It must therefoe be purified to semiconductor grade (99.999% pure) to serve as material for the wafers in 12.5%-efficient solar cells. Four possible processes for silicon purification are listed in Table 5.3, with their advantages and disadvantages.

Carbon reduction is a technique commonly used to produce metal urgical grade (MG) silicon from silica (Ref. 5.4) through the reduction:

$$SiO_2 + C \rightleftharpoons Si + CO_2$$
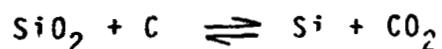
It is possible that this process could produce semiconductor grade (SeG) silicon. However, this can only happen if all the impurities in the input SiO_2 will combine with carbon, forming compounds which can then be easily removed from the silicon.

TABLE 5.3:   PURIFICATION OF SILICON
ALTERNATIVE PROCESSES

| Process	Advantages	Disadvantages
Carbon Reduction	oExisting technology	oNot likely to pro- duce sufficient Si purity oCarbon required from Earth oRequires carbon recovery cycle
Trichlorosilane Distillation	oEstablished tech- nology	oEarth elements re- quired oRequires handling of large amounts of corrosive gases
Silane/ Silicon Process	oExisting technology	oEarth elements re- quired oRelatively complex process
*Zone Refining	oExisting technology oNo Earth inputs re- quired oPotential for high automation	oProcess is slow oSome wastage of input

*Chosen for reference SMF

Since lunar-produced MG Si or SiO_2 would contain undetermined inpurities, it is extremely unlikely that such a process could work.

This process would also require carbon input from Earth, to load the system and to replace carbon losses during operation. To minimize these carbon losses, the process must operate within a pressure container. And the process would require a re- covery cycle to retrieve the carbon from the variety of com- pounds formed   the input impurities.

Trichlorosilane distillation is the method most commonly

used today (Ref. 5.4). It is a three-step process:

1) MG Si is reacted with hydrochloric acid to produce trichlorosilane;

$$Si + 4HCl \rightleftharpoons SiHCl_3 + HCl + H_2 + impurities$$
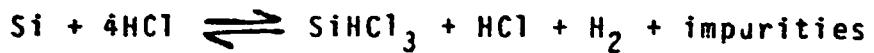
2) The impurities and byproducts are distilled out, leaving 99.999% pure $SiHCl_3$.

3) The trichlorosilane is converted to polycrystalline SeG silicon by thermoelectric decomposition;

$$SiHCl_3 \longrightarrow Si + HCl + Cl_2$$
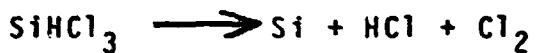
The principal advantage of this process is that it is an established technology. However, it requires a sizable fraction of Earth elements (H, Cl) to load the system and replace losses. To minimize the losses, the process must be contained in pressure vessels.

Another disadvantage of this method is that it requires handling of large volumes of hydrogen, chlorine, and hydrochloric acid. Although the poisonous character of these gases is not a significant problem(since human operators require protection from vacuum anyway), their corrosive aspects add to the complexity of the process equipment.

The silane/silicon process has been developed by Union Carbide Corp.(Refs. 5.5, 5.6). It is a five-step process:

1) MG Si is reacted with hydrogen and silicon tetrachloride to form trichlorosilane;

$$Si + 2H_2 + 3SiCl_4 \rightleftharpoons 4HSiCl_3$$
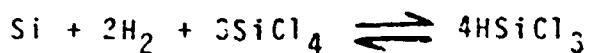
2) The trichlorosilane is then reduced to dichlorosilane

and silicon tetrachloride;

$$4HSiCl_3 \rightleftharpoons 2H_2SiCl_2 + 2SiCl_4$$
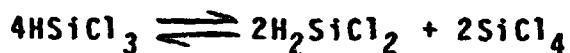
The $SiCl_4$ is input to step (1) above.

3) The dichlorosilane is then reduced to silane and silicon tetrachloride;

$$2H_2SiCl_2 \rightleftharpoons SiH_4 + SiCl_4$$
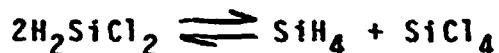
The $SiCl_4$ is input to step (1) above.

4) The SiH_4 is distilled to purify it to semiconductor grade.

5) The SiH_4 is broken into SeG silicon and hydrogen by thermoelectric decomposition;

$$SiH_4 \longrightarrow Si + 2H_2 \qquad (at\ 1050°K)$$
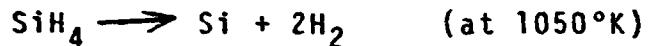
The H_2 serves as input to step (1) above.

This process is existing technology. It requires earth elements (H, Cl) to load the system and replace gas losses, and the process must be contained in pressure vessels. This process is also more sophisticated than other candidates, re-quiring more steps and therefore more complex equipment.

Zone refining uses a different approach than the above-discussed alternatives. The process is described by Fig. 5.2. First, a slab (or rod) of MG silicon is clamped at both ends. The slab is heated near one end to produce a local molten zone. By moving the heat source along the silicon slab, and cooling the slab behind the heat source, the molten zone is 'moved'

Molten Zone

Clamp

Mg Silicon Slab

Discarded end

Discarded
End

SeG Silicon
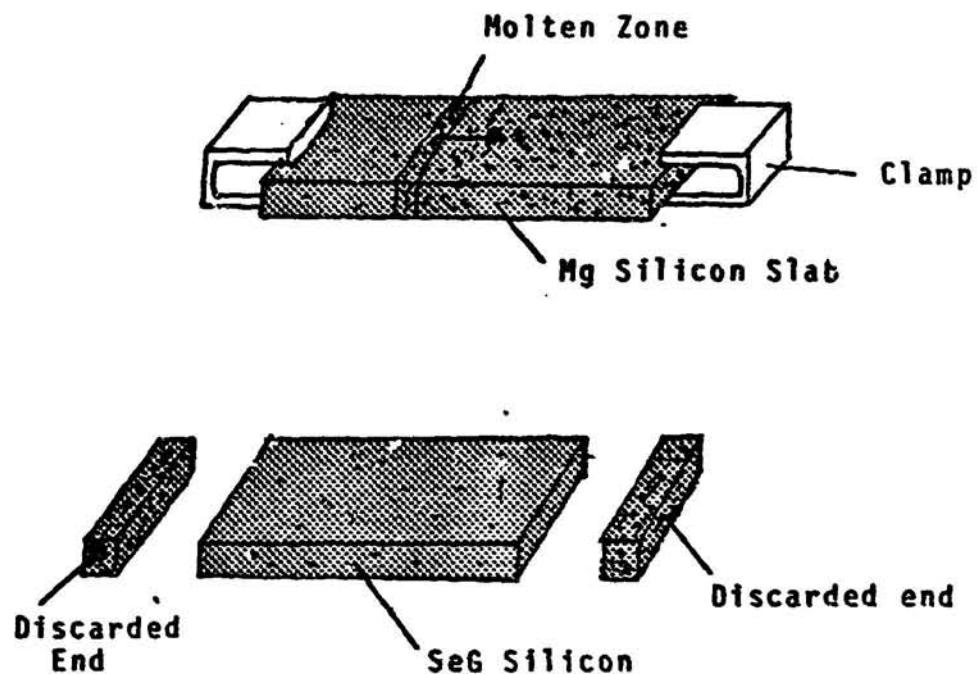
FIGURE 5.2: ZONE REFINING

along the slab. At the rear liquid/solid interface, where
the molten material recrystallizes, the molten Si tends to
crystallize faster than the impurities. Therefore the im-
purities tend to remain in the molten zone, and thus travel
along the slab to the other end. The process is repeated
several times; with each pass of the molten zone along the
bar, more of the impurities are drawn to and solidified near
the end of the slab. Once the body of the slab is semi-
conductor grade, the impure ends are trimmed away and
discarded.

Surface tension forces in the molten zone tend to round
off the corners of a slab during zone refining. However,
this tendency can be counteracted by using induction coils

to shape the molten zone, minimizing the rounding. Therefore, if a slab with square edges is required (as in the reference SMF), use of shaping coils can keep the needed trimming losses to a minimum.

Zone refining is an existing technology. It offers the advantage that it requires no Earth inputs. Also, zero-g may improve the zone-refining process itself by eliminating convection currents in the molten zone (this requires experimental study).

The principal disadvantage of the zone refining process is that it is slow. The process speed is governed by the speed at which the molten zone can travel along the slab, and the number of passes required to purify the rod sufficiently. The molten zone travel rate is set by the rate at which liquid material crosses the liquid/solid interface and becomes solid crystal. The heat balance equation for the planar interface (Ref. 5.7) is:

$$K_s G_s - K_l G_l = P_s H R$$

where:

K_s = thermal conductivity of solid

G_s = temperature gradient of solid at interface

K_l - thermal conductivity of liquid

G_l = temperature gradient of liquid at interface

R = growth velocity

ρ_s = density of solid

H = heat of fusion

For optimum crystal growth -- good quality with maximum speed -- $G_l = 0$ (possibly achievable in space, in the absence of convection).

Therefore:

$$R_{max} = \frac{K_s G_s}{P_s H}$$

From tables of thermal conductivity of silicon at about 1685°K the value of K_s = .215 w/cm°K. Its heat of fusion is 337.0 cal/g and the density is 2.33 g/cm^3. This leaves a value for R:

$$R_{max} = (3.93 \times 10^{-3} \frac{cm^2}{min°K}) G_s$$

where G_s is in °K/cm and R_{max} in cm/min.

Thus, for reasonable growth rates, thermal gradients must be on the order of 1000°K/cm or more. For example, current silicon ribbon growth rates (on the order of 7.5 cm/min) correspond to a temperature gradient of 2000°K/cm. The study group assumed that, by 1990, equipment could be developed to generate temperature gradients of 620°K/cm in slabs (more difficult than in ribbons), leading to a zone travel rate of 2.5 cm/min. However, this temperature gradient requires gas-jet cool ng of the slab behind the molten zone, and the process must therefore be enclosed in a pressure vessel.

Depending on the purity of the input silicon, zone refining can take form 10 to 100 passes of the molten zone (Ref. 5.8). The study group assumed that the MG silicon received from the

Moon would be sufficiently pure that 10 passes would be sufficient.

The slowness of zone refining (which leads to a large number of machines) is mitigated by the potential of the process for high automation. The basic operations are simple: slab handling, repetitious zone travel, end trimming, and slab packaging.

Besides the candidate processes listed above, there are a number of other alternatives mentioned in the literature. For example, Ref. 5.9 mentions sodium reduction of silicon tetrachloride, decomposition of polymerized silicon difluoride, and the silicon halide-alkali metal flame process. Unfortunately, the processes researched to date are all intended for use on earth, and therefore incorporate the advantages and disadvantages of that physical and economic environment. Only zone-refining seems somewhat space-specific, since its thermal gradient may be improved by zero-g, and its large power requirement can be met with cheap solar energy.

It is clear to the MIT study group that much more research must be done in this area to investigate and develop the possible methods of silicon purification. This task may require the design of entirely novel processes, and their verification by pilot plants in space. Fortunately, prototypes of this kind of chemical equipment can usually be small.

For the reference SMF, the study group chose zone refining for the purification of silicon because it is particularly suited to a space environment and because the disadvantages associated with the slowness of the process can be mitigated by automation.

5.2.4: Production of Doped Silicon Wafers: The study group reviewed a number of solar cell wafer production processes as candidates for the SMF. These alternatives are listed in Table 5.4.

The floating substrate method involves pouring molten silicon onto a molten-metal bath (such as tin) to form a sheet of silicon wafer. The principal disadvantage of this process is that it requires gravity (or some kind of directional force field) to control the molten bath.

This problem is common to all bath processes in space. Under zero-g conditions, a liquid will naturally form into a sphere or globule, its surface determined by surface tension and dynamic instabilities (as shown in Skylab experiments, globules can oscillate in shape between configurations such as dumbells and donuts). Theoretically, the surface of a large sphere of molten material could approximate the planar surface of a bath. However, it is difficult to control the position of such a sphere, or to touch it with equipment, without inducing oscillations and distortions in its shape. The molten material also tends to wet anything brought in contact with it,

TABLE 5.4: SILICON WAFER PRODUCTION
ALTERNATIVE PROCESSES

Crystal Growth Processes	Advantages	Disadvantages
Floating Substrate		o Requires gravity or equivalent o Not likely to yield sufficient cell efficiency
Ceramic Plate Dipping		ιuires gravity or ivalent likely to yield ɹfficient cell efficiency
Czochralski Ingot Growth	o High quality crystal o Established technology	o Requires gravity or equivalent o High waste of material o Requires many sawing machines
Dendritic Web	o Low waste of material o High quality crystal	o Requires gravity or equivalent
Zone Refining and Cutting	o High quality crystal o Existing Technology	o High wastage of material o Slow process / many machines
Edge-defined Film-fed Growth	o Existing Technology o Low waste of material o High quality crystal	o Many machines required o Needs pressurized containers
Chemical Vapor Deposition and Recrystallization	o Compatible with some refining processes o Low material waste o May allow deposition of wafer directly onto cell substrate and rear contact	o Requires Earth inputs o Requires pressure vessels and recirculation equipment o Requires additional processes to achieve sufficient crystal quality

(continued)

TABLE 5.4 Continued

Crystal Growth Processes	Advantages	Disadvantages
*Direct Vaporization and Recrystallization	o Conceptually simple o Does not require pressure vessels o Wafer can be directly deposited onto cell substrate and rear contact o Well adapted to space environment	o Little solid data available o Some waste of material o Requires many material sources o Requires additional processes to achieve sufficient crystal quality

Doping Processes		
Diffusion	o Established technology	o Usually requires liquid application o Difficult to control dopants
*Ion Implantation	o Existing technology o Easily automated on a large scale o Good control over dopants	o Induces defects in crystal structure o Requires closed current loop
Co-deposition	o Can reduce time and complexity of solar cell production	o May not be compatible with all silicon wafer production processes o Only applicable to p-dopant in several wafer production processes

*Chosen for reference SMF

and the sphere's material therefore tends to crawl along any solid object touching it. Thermal control is also difficult, since the problems described above restrict the designer to radiative and convective cooling (the convective processes through a gas surrounding the sphere). All of these problems make delicate surface processes on molten spheres (such as the formation of a thin silicon shell) technically difficult, and therefore unlikely.

Another alternative is controlling a bath through centrifugal force. Here the liquid material is whirled around in a container, and coats the walls, forming a stable layer. Although a centrifugal furnace is possible (and several such designs are described later in this chapter), problems arise when materials are layered in such furnaces. The materials must have different densities, since it is the effect of the centrifugal force field on the different densities which forms the layers. However, this leads to different angular momenta of the layers. At the inter·   · between the layers, this tends to create angular momentum transfer, or vortex formation, between the layers; the layers tend to stir themselves together. This effect appeared as a severe problem in the design of colloid-core nuclear rockets (Ref. 5.10), when the layers were made of gases (uranium oxide and hydrogen). In a liquid-liquid interface, the viscous forces resist this interlayer stirring,

but it is difficult to assess under what conditions such layers
would be stable. This problem can be alleviated by the use of
baffles to constrain the motion of the fluids. In this case
the baffles separate the bath into a series of cells, each of
which requires independent input and output systems. The ex-
tension of this case is the separation of the bath into
separate rotating containers; this option is described below.

Another problem with rotating-container baths is the need
for rotating machinery. Although the bearing stresses are
less in zero-g than on Earth, such equipment requires complex
methods to input and output material to and from the container.
Furthermore, it is difficult to stop the container without first
removing or solidifying the contents, since the liquids will then
float free from the container walls, forming globules.

In the case of silicon sheet production by the floating
substrate method, the problems of interlayer stirring could
prehaps be avoided by keeping the rotation speed of the con-
tainer slow, and silicon could be added by an axial feed system.
However, once the layer of silicon had been formed and cooled
into a cylindrical sheet, removing that sheet poses technical
difficulties. Cutting the silicon sheet free of its molten-
metal bath while the container is spinning requires complex
equipment and procedures to prevent release of the molten metal
or contamination of the silicon.

These problems can be alleviated somewhat if the bath pro-
cess is done in a series of containers spinning far from the

rotation axis, as shown in Fig. 5.3. The radius of gyration of each individual bath is large enough that the bath surface is near-planar, and the silicon sheets are of manageable size. However, all input and output must be routed through the central hub, and the equipment requires more structural mass and safety features than a free-floating alternative.

Silicon Sheet Output   Silicon Input

Rotation

Input/Output Tube

Handling Equipment

Molten Metal

Silicon Layer
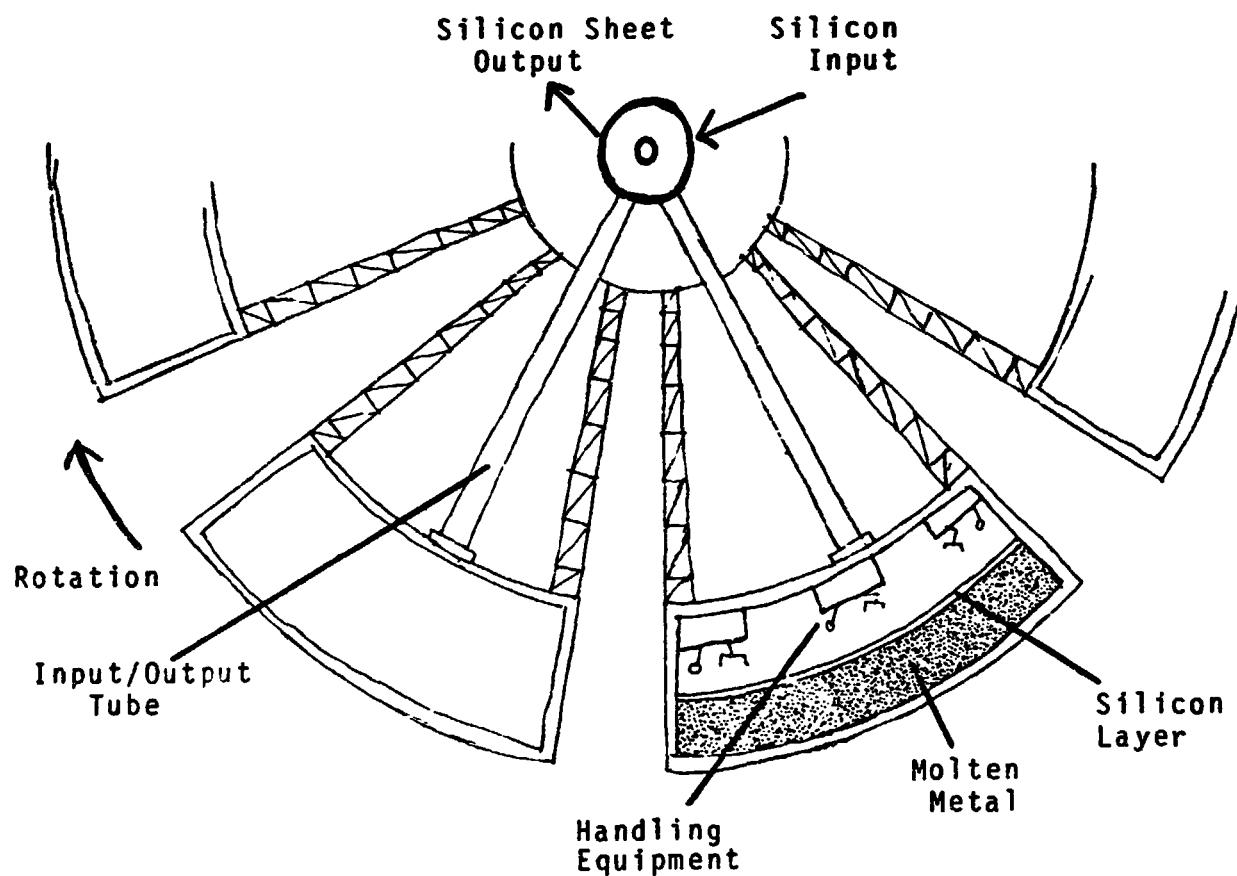
FIGURE 5.3:   POSSIBLE CENTRIFUGAL BATH PROCESS

C - 2

Even if these technical difficulties can be overcome, there is some doubt that the floating substrate method can produce efficient solar cells. On Earth, the floating substrate production of cadmium sulphide cells is being developed by Patscentre International in England. The presently achieved cell efficiency is 4-5% (Ref. 5.11). This process has been considered for silicon solar cell production on Earth, but purity levels and production rates have been too low to merit full scale production on Earth.

Ceramic plate dipping involves dipping a plate into a molten silicon bath, building up a sheet of crystalline silicon. It therefore shares many of the molten-metal-bath problems discussed above. Like the floating substrate process, ceramic plate dipping has output purity and production rate problems, and has therefore never been commercially used on Earth.

Czochralski ingot growth is the most commonly used silicon wafer production technique today (Ref. 5.4). The process is depicted in Fig. 5.4. This method uses a rotating crucible of molten silicon. A counter-rotating seed crystal is slowly lifted up from the molten surface, pulling a silicon ingot up to 10 centimeters in diameter. The ingot grows from the molten silicon as a single crystal. Once the ingot has been formed, it is sawed into thin (~250 microns) wafers.

There are two principal advantages to the Czochralski process. First, it is a well established technology. Second, the crystal produced is highly pure and monocrystalline, the two
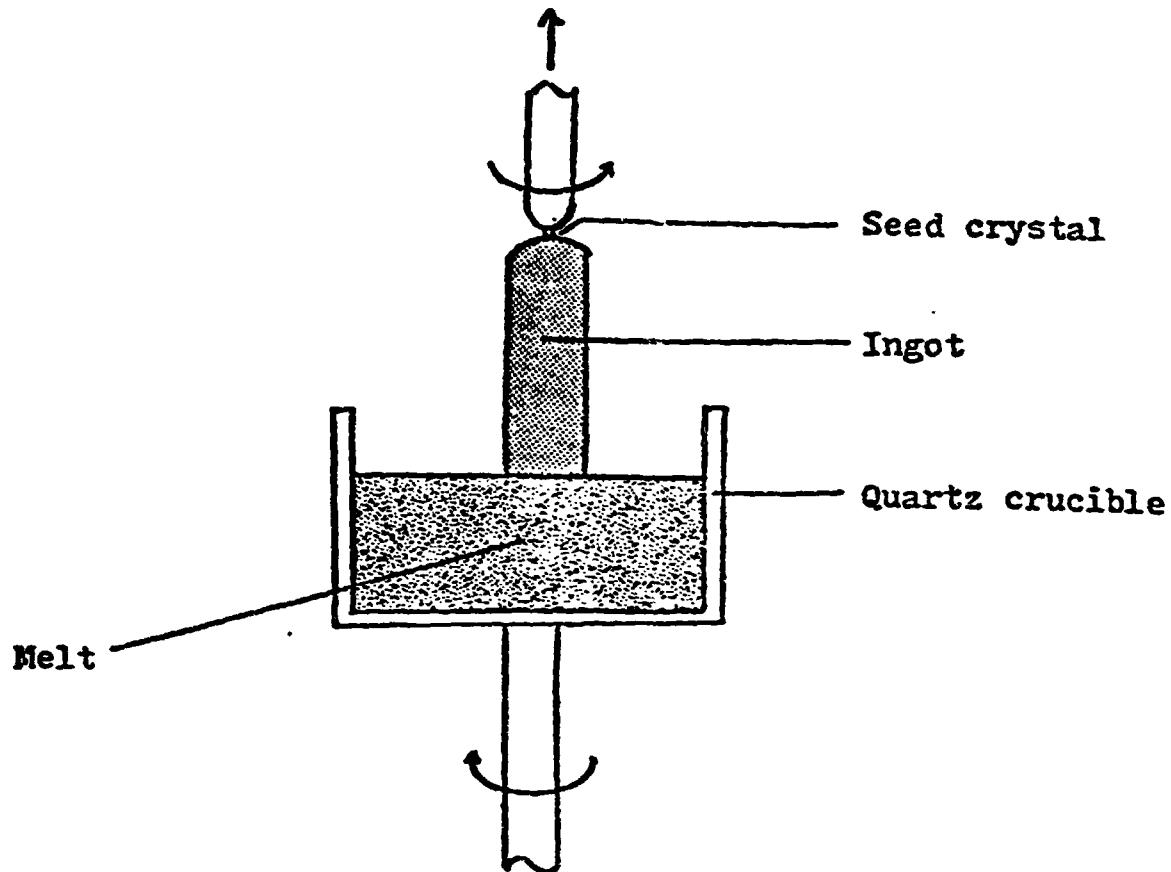
FIGURE 5.4: CZOCHRALSKI INGOT GROWTH

principal requirements for silicon solar cell wafers. A number
of alternative processes (discussed below) require complex pro-
cedures to achieve the needed monocrystalline quality.

Czochralski ingot growth can probably be freed from its
current reliance on gravity to form and control the silicon
bath in the crucible. Rotating facilities (such as those shown
in Fig. 5.3) could contain crucibles and crystal-pulling equip-
ment. An other option is magnetic confinement of the silicon
melt in the crucible. In this technique, induction coils
around the crucible induce eddy currents in the molten silicon,
and electromagnetic coupling between those currents and the

pulsed magnetic field from the coils pushes the silicon into the crucible. The same eddy currents can maintain the temperature of the melt by ohmic heating. There are two disadvantages to this option. First, the magnetic properties of the silicon are such that very powerful fields would be required for the containment of the entire melt. Second, the technique would not only contain the melt, but stir it as well; and this stirring adversely affects the crystal growth by altering the thermal gradient at the liquid-solid interface, thus slowing down the crystallization.

The major disadvantage of the Czochralski method, however, is the subsequent sawing process required to form thin wafers. Slurry sawing is currently the most effective method for sawing silicon ingots. It uses an array of cutting blades lubricated with a slurry of oil and abrasives to slice an ingot into a large number (g.e. 230) of wafers. However, this 230-wafer cut requires 20 hours to go through a 10 centimeter diameter diameter ingot (Ref. 5.12).

Another problem with sawing is the large kerf losses. Since the wafers are rough cut to 250 microns, the kerf losses are larger than the product (Ref. 5.4). Breakage limits cutting time and thickness due to the brittleness of silicon and the saw vibration. The following is a summary of actual current silicon losses:

Ingot Losses by Volume	
Sawing	66%
Lapping	16%
Polishing	4%
Dicing	4.7%
Breakage	1.3%
Total	92%

Improvement in cutting techniques may reduce this waste to 50-70%.

Another current problem with Czochralski ingot growth is contamination of the melt from the crucible. In current operations, each crucible is used once, then replaced by a new one. Although this problem can probably be solved, a new material would have to be developed for the crucible lining.

In the ingot growth process, the crystal growth speed is determined by the same equation which governs the molten zone travel described under zone refining in Sec. 5.2.3. Therefore the crystal growth speed is limited by attainable thermal gradients (7.5 cm/min at 2000°K/cm). For the 20 billion cells required for one SPS, if the wafers are each rough-cut to 250 microns with a 50% kerf loss, the total length of ingot required is 10^7 meters (neglecting breakage losses later in production). If each ingot growth machine produces ingot at 7.5 cm/min, on a 90% duty cycle, 282 machines are required. This requirement is not unreasonable.

However, for the slurry sawing process, if each machine cuts 250 wafers at once in 20 hours, and if the machines work

on a 90% duty cycle, 203,000 machines are required to cut the 20 billion wafers for one 10-GW SPS per year. This large requirement, together with the melt-handling problems discussed above, make Czochralski ingot growth an unlikely alternative for SMF use.

The dendritic web technique draws a ribbon from a molten silicon bath. Two dendrites are dipped into the bath and pulled out, inducing a silicon web between them. The web solidifies into a thin ribbon. This process is depicted in Fig. 5.5 (Ref. 5.4).

The ribbon produced is currently thicker than the needed 50 microns, but it is low in defects. Once the ribbon is solid, wafers can be cut from it with minimal kerf losses; the process is therefore efficient in its use of material.
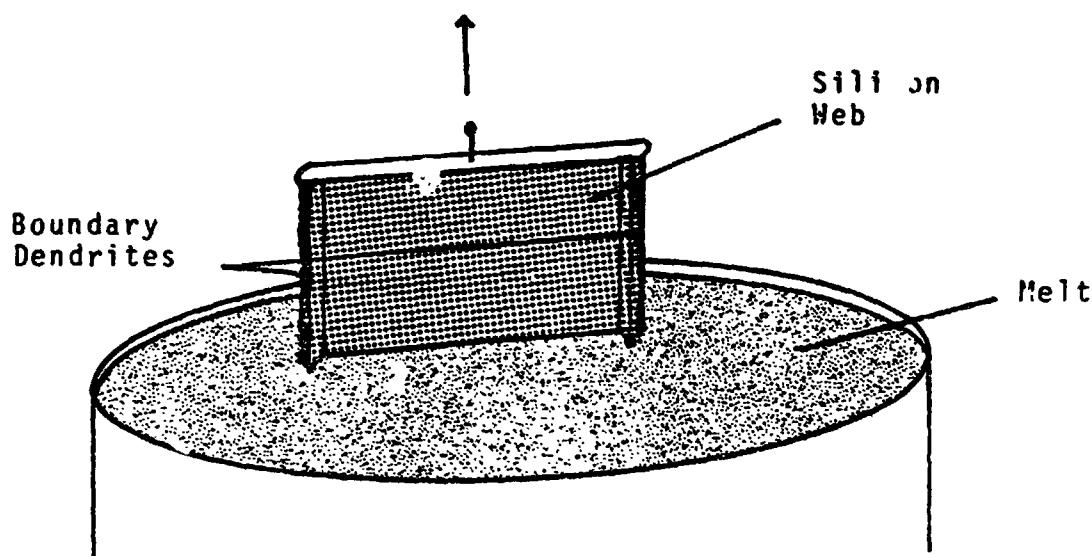

FIGURE 5.5:   DENDRITIC WEB TECHNIQUE

5.26

However, this technique requires pulling silicon from a bath, and therefore has the melt-containment problems discussed above.

Zone refining and cutting starts with the zone refining process described in Sec. 5.2.3. This zone refining in effect replaces the ingot growth in the process described above, producing a pure silicon monocrystal. The rest of the procedure is the same sawing process as in Czochralski ingot growth, to produce the needed silicon wafers. Although the zone refining avoids the difficult technical problems in melt-handling, the sawing process is no faster in this case than in the ingot growth process above. This step would therefore require an estimated 203,000 machines to cut 20 billion wafers for one 10-GW SPS per year. This makes this process an unlikely canditate for the SMF.

Edge-defined film-fed growth (EFG) is a process currently in development by Mobil Tyco (Ref. 5.6). In this process a ribbon of silicon is drawn from a molten silicon bath through a die, as shown in Fig. 5.6.

In this process, the zero-g melt-handling problems described earlier can be avoided by enclosing the molten silicon in a container, so that it can escape only through the dies. Such a design is shown in Fig. 5.7. As shown in the figure, many dies can be fed from the same silicon furnace and reservoir. The solid-silicon feed system shown is a space-specific design which uses magnetic induction coils to heat the silicon and to apply a
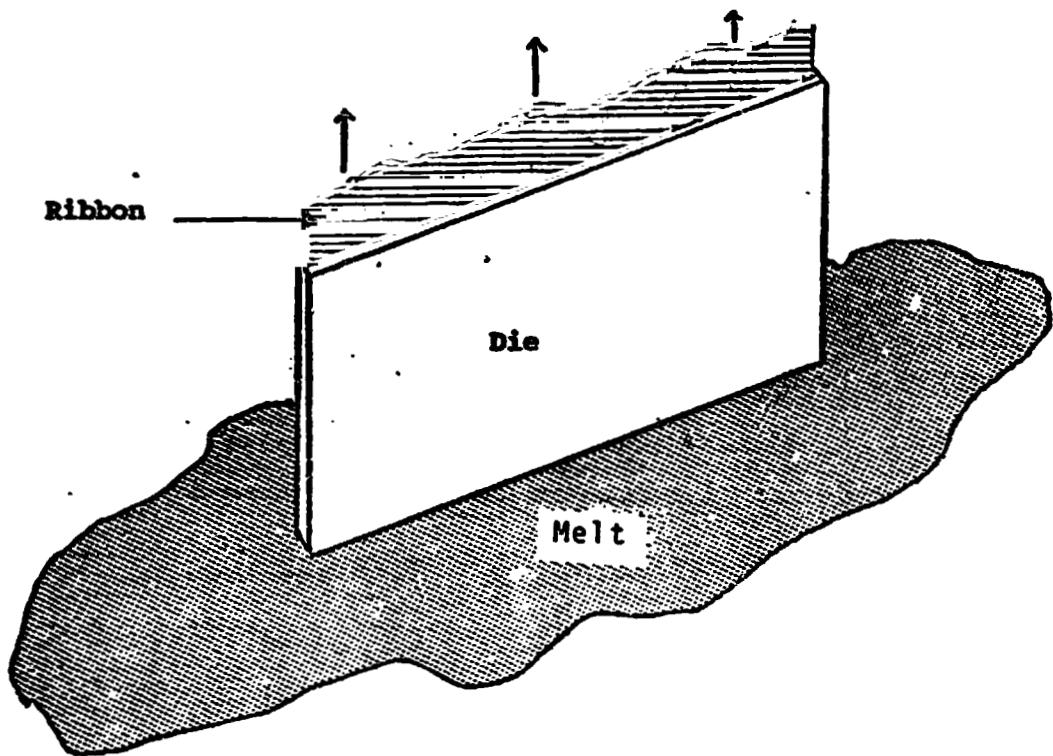
FIGURE 5.6: EDGE-DEFINED FILM-FED GROWTH
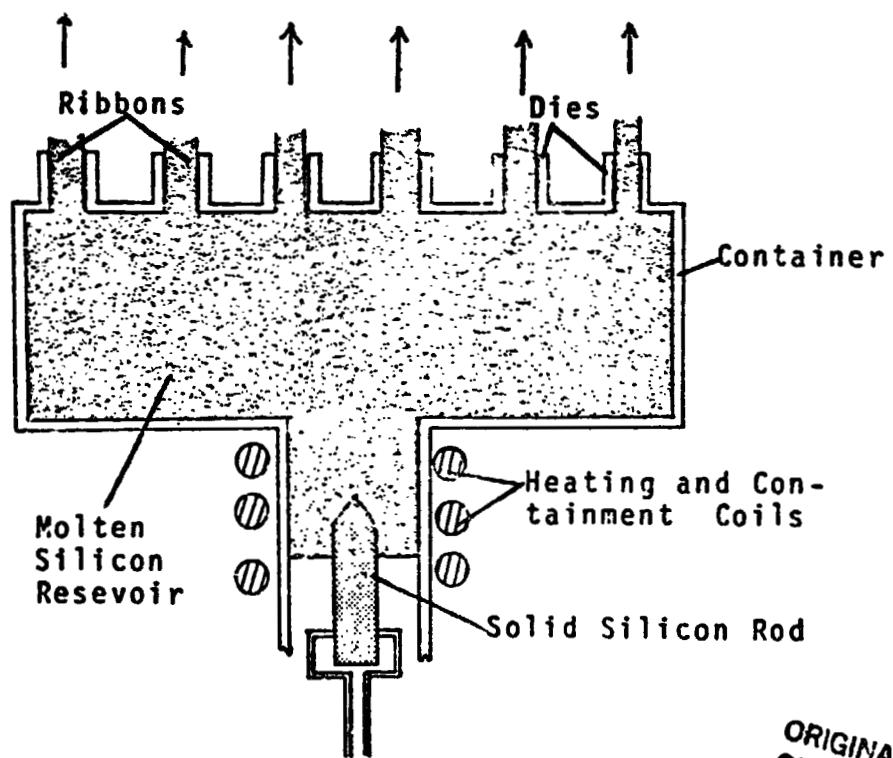
FIGURE 5.7: POSSIBLE EFG RIBBON MACHINE

force on the liquid silicon, into the container. This keeps the molten material from floating out of the heating tube. This design avoids the need for a valve or lock in the feed system.

The magnetic containment force can also be used to pressurize the molten silicon reservoir, making the ribbon-drawing process resemble an extrusion or continuous casting process. This would reduce the structural stresses applied to the ribbon by the drawing process, and may thus allow thin ribbons (50 microns) to be pulled. If such ribbon can be produced, then it can be cut into solar cell wafers with a minimal kerf loss of material.

Current ribbon growth machines draw silicon at a rate of roughly 7.5 cm/min through a rectangular die. The thickness of the ribbon varies for 150 to 250 microns, and the current maximum width of the ribbon is 7.5 cm (Ref. 5.13). The pulling rate is governed by the crystal growth equation described above, and the 7.5 cm/minute speed corresponds to a thermal gradient of 2000°K/cm. The material is cooled by inert gas jets   Given these current parameters and a 90% duty cycle, 41,300 dies would be required to produce 110 km^2 of solar cells for one 10-GW SPS per year (including a 10% assembly wastage allocation). Multi-die machines can therefore offer significant savings over single-die machines.

Graphite dies are currently the most effective for production of high-quality ribbon. These dies are now replaced after producing 10 m of ribbon, because of experimental requirements

and not because of defect in the dies (Ref. 5.14). The effective life of the dies is at present uncertain. However, formation of silicon carbide on their surfaces results in imperfections in the pulled ribbon, causing large drops in solar-cell efficiencies; this requires eventual replacement of the graphite dies. As alternatives to replacement, die refurbishment techniques or alternative die materials can be developed. Currently Energy Materials Corp. is investigating a fused silica die as a possibility. If a die could produce 100 m of ribbon before replacement, the 41,300 dies mentioned above would each need replacement every 22.2 hours, leading to a requirement of 1.5×10^7 dies for on 10-GW SPS per year. Modeling each die as a graphite slab 8 cm wide by 3 cm high by .5 cm thick, the die mass required would be 400 tons per year.

Several lines of reasearch may simplify the equipment and improve production rates. Although current dies produce ribbon 7.5 cm wide, it may be possible to produce wider ribbon, reducing the required number of dies. If the thermal gradient at the silicon's liquid-solid interface can be increased beyond the current 2000°K/cm, ribbon growth rates higher than 7.5 cm/min can be achieved. However, although the space environment does allow greater control over thermal gradients by eliminating convection currents, the current thermal gradients are high and relatively well-controlled, and any improvement in the ribbon growth rate over twice the current speed is unlikely.

There are three principal advantages of the EFG process.

First, the process is existing technology, likely to become a commercial operation in the next few years. Second, assuming that 50-micron-thick ribbon can be produced, cell wafers can be cut with a minimal loss of silicon. Third, the quality of the crystal output is good, although currently produced rib. n is usually annealed (heated below melting point for a time) to improve its efficiency. The annealing process eliminates some of the point defects and grain boundaries in the crystal, improving the monocrystalline quality of the ribbon. Improvements in the EFG equipment may make annealing unnecessary.

The principal disadvantage of the EFG process is that it is slow, and therefore requires many machines. If the 41,300 dies required to produce ribbon for one 10-GW SPS per year are grouped ten to each machine, the production requires 4,130 furnaces and molten silicon reservoirs. Although dies could be grouped in larger numbers, this would increase the size of the reservoirs, possibly leading to thermal control problems. Increase in the ribbon growth rate should likewise reduce the required number of machines, but such improvements are probably limited to a factor of two, as discussed above.

Another disadvantage is that the large thermal gradient at the liquid-solid interface requires cooling of the silicon by inert gas jets. Since such gas is not available from lunar materials, the EFG dies in an SMF must be surrounded by pressure vessels to contain the inert gas. This gas must also be circulated to a radiator for cooling, and returned to the

cooling jets near the dies.

Chemical vapor deposition (CVD) is a process currently used to apply coatings to surfaces. It has also been used experimentally to form silicon sheets for solar cells. In the chemical vapor deposition of silicon, a silicon-bearing gas such as silane (SiH_4) or trichlorosilane ($SiHCl_3$) is applied to a hot deposition surface (at roughtly 1100°K). The gas dissoiates at the surface, leaving a deposited layer of solid silicon. If the gas is silane, the reaction is

$$SiH_4 \longrightarrow Si \text{ (solid)} + SH_2 \text{ (gas)}$$
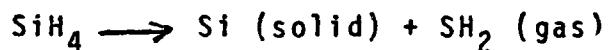
For trichlorosilane, the reaction is

$$SiHCl_3 \longrightarrow Si \text{ (solid)} + HCl \text{ (gas)} + Cl_2 \text{ (gas)}$$

The byproduct gases are then recombined with silicon, to form more silane or trichlorosilane.

The deposition rate is dependent on several factors, specifically the temperature of the surface, the pressure of the silicon-bearing gas, and the efficiency of removal of the byproduct gases (which tend to form a layer on the surface, keeping the silicon-bearing gas away). For silicon, the range of the CVD rate is 1-5 micron/min, with 4 microns/minute as a likely rate for a well-designed process.

The production of one 10-GW SPS per year requires 110 km^2 of 50-micron-thick silicon wafers. If these are grown at 4 microns/min, the growth time of 50-micron silicon sheet is 12.5 minutes. Assuming a 90% duty cycle, 2900 m^2 of silicon wafer

must be deposited every 12.5 minutes to produce the needed
110 km^2 in a year. Therefore the total area of silicon deposition at any time would be 2900 m^2 (roughly 2/3 the area of a football field).

The CVD process offers a number of advantages for SMF use. First, the dissociation reactions for silane and trichlorosilane (listed above) are the final steps in two of the silicon purification alternatives: the silane/silicon process and trichlorosilane distillation (see Sec. 5.2.3). Therefore these purification processes, rather than producing solid SeG silicon (which is then turned into wafers by a separate process), can instead produce semiconductor grade silane or trichlorosilane, which are then used to produce silicon wafers by CVD. This compatibility between these refining and wafer production processes reduces the complexity of these alternatives.

Second, since dissociation of the silicon-bearing gas occurs on hot surfaces, careful thermal control can limit this dissociation to the d position surface (rather than the walls of the dep ition chamber). Also, the undissociated silicon-bearing gas can be recirculated with the byproduct gases, and r turned to the deposition chamber after the byproduct gases have been recombined with silicon. The combination of careful thermal control and gas reuse can thus reduce the loss of materials to minimal leakage losses.

Third, the CVD process can be used to produce a silicon wafer directly onto a previously prepared cell substrate and

rear contact (or rear contact alone), provided that the deposition surface can be heated to the required 1100°K. Although a glass substrate can survive this temperature, the aluminum rear contact suggested for SMF-produced solar cells (see Sec. 5.2.1) melts at 430°K. This would therefore require another conductor for the rear contact, which would have to come from Earth. As a measure of that requirement, production of one 10-GW SPS requires 590 tons of Al for the cell rear contacts.

There are also several disadvantages to CVD. The process involves elements not available on the Moon (such as the hydrogen in silane and the hydrogen and chlorine in trichlorosilane). These elements would therefore have to be brought from Earth to load the system initially, and to replace losses during operation.

Since these Earth inputs should not be wasted, the process also requires the recirculation of byproduct gases and their recombination with silicon. Therefore the entire deposition area (2900 m^2 for production of one 10-GW SPS per year) must be enclosed in pressure vessels. Although the deposition rate appears to increase with the gas presure, most of the gain in deposition rate occurs at low pressures: at roughly 1/100th of an atmoshpere, the CVD rate for silicon reaches 4 microns/min, and above this pressure the rate increases very little. Therefore the pressure forces on the containment vessel would not be severe.

If silane is used, the byproduct gas is hydrogen. If the

CVD process is coupled with the silane/silicon process described in Sec 5.2.3, this hydrogen can be used directly in the purification process, avoiding the need for separate recombination equipment. If trichlorosilane is used, the byproduct gases are chlorine and hydrochloric acid. If this process is coupled with trichlorosilane distillation for refining, the chlorine must be reacted with hydrogen (a byproduct of the trichlorosilane distillation) to make HCl, and the HCl can then be used directly in the refining process. However, a reaction tank for hydrogen and chlorine is part of the trichlorosilane distillation process already, so the use of CVD does not add to that requirement.

Thus the silane and trichlorosilane CVD processes do not require additional recombination equipment if they are coupled with silane/silicon and trichlorosilane distillation refining processes. However, the CVD processes require recirculation equipment. Since the silane CVD process produces only hydrogen, as compared to the chlorine and hydrochloric acid produced by the trichlorosilane CVD process, and since HCl is corrosive and therefore more difficult to handle, the silane CVD process seems better adapted to SMF use. However, the relative merits of silane and trichlorosilane also involve the refining process requirements, and would therefore require more study before a preference could be established.

Another disadvantage of the CVD process is that the quality of the silicon wafer output is insufficient to produce 12.5%

efficient solar cells, because the deposited layer of silicon

tends to pick up the crystal orientation of the deposition

surface; therefore silicon sheet deposited onto a polycrystal-

line surface will be polycrystalline. Polycrystalline cells

are less efficient than monocrystalline cells. A graph of cell

efficiency versus grain size demonstrates this in Fig. 5.8.

Although the position of the curves on the graph is affected

by other factors (thickness of the cell, transparency of optical

coating, direction of grain boundaries), the curves clearly show

that cell efficiency drops sharply with decrease in grain size

(or increase in the number of grain boundaries). Methods for
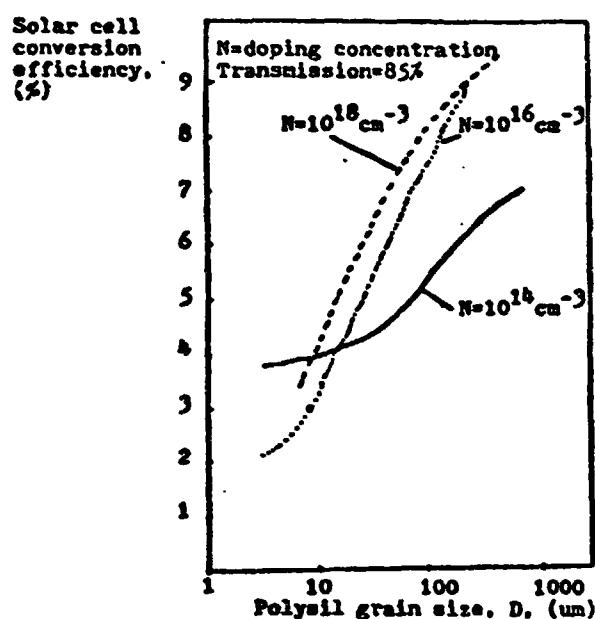
FIGURE 5.8: THEORETICAL VALUES FOR CELL
EFFICIENCY VERSUS GRAIN SIZE

improving the crystalline quality of the output are discussed in the following section on direct vaporization.

Direct vaporization (DV) is currently used to apply coatings to surfaces, and to produce thin sheets of some materials (e.g. aluminum). In this process gaseous particles (molecules or atoms) of material are brought in contact with a thermally controlled surface. The material solidifies onto the surface as a thin coating. No chemical effects are involved. Although the deposition surface temperatures are usually much lower than those for CVD, the deposition surface must carry away the energy of the phase change (from gas to solid) of the deposited material.

The hot particles of material are currently produced by a variety of means. A liquid bath of material can be heated until molecules or atoms boil off from the liquid surface. These particles are then collected as a solid on a deposition surface above the liquid bath. Another option better suit to space applications is to boil off material from a solid piece by impact from a laser or electron beam, or by passing an electric arc over the surface. Such a process is depicted in Fig. 5.9. If the material is not only boiled off but also ionized, then magnetic and electrostatic fields can steer the particles, controlling the geometry of the deposition process; however, this raises the energy requirements considerably.

```
                    ┌──────┐
                    │▨▨▨▨▨│──Silicon Source (solid)
                    │▨▨▨▨▨│
                    └──────┘
                    ╱ .':.  ╲
                  ╱ ⁄ ⁄ │ ╲ ╲
L:ser or        ╱  ⁄ ⁄ │ │ ╲  ╲
F; Gun ────────╱  ⁄ ,' │ │  ╲  ╲
            ┌──┐ ⁄ ⁄  │ │   ╲   ╲   ╱Deposited Coating
            └──┘⁄ ,'  │ │    ╲   ╲ ╱
──────────────────────────────────────────────────
                   ⋁⋋        ╲Deposition Surface
                  Energy
```
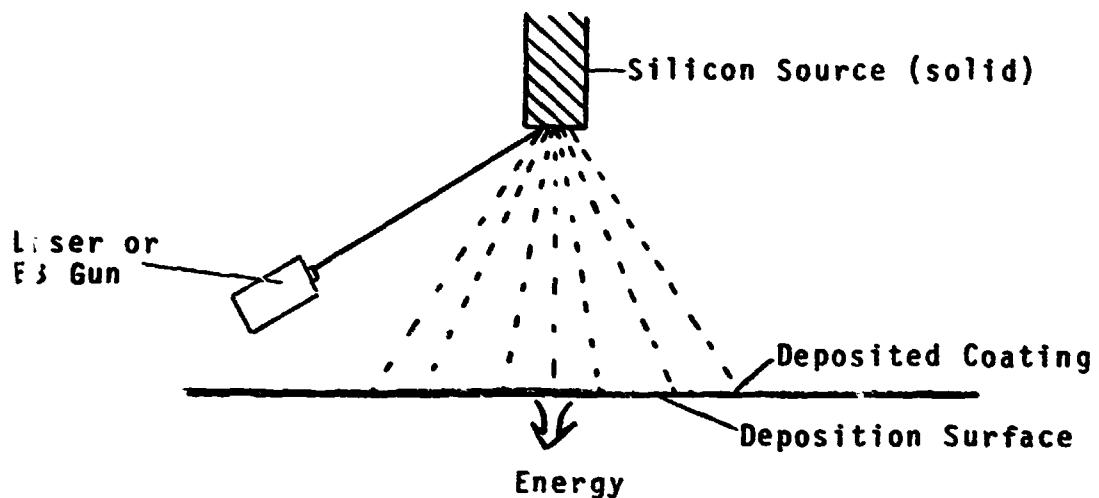
FIGURE 5.9:   DV PROCESS FOR SILICON

The primary requirement of the DV process is a good vacuum
in the deposition area. This is because the boiled-off particles
of material are usually highly reactive. Therefore they will
react either with each other (nucleating flakes of material) or
with any other gas present, before they reach the deposition sur-
face. To ensure that single atoms or molecules of material reach
the surface, these atoms or molecules must behave more as single
particles than as a gas while they travel from the material
source to the deposition surface. In other words, the mean free
path of these particles must be at least the distance from the
source to the surface. Since a gas at 10^{-6} Torr has a mean free
path on the order of 50 cm, this pressure is typical for DV pro-
cesses.

Direct vaporization is expensive on Earth because of its
energy and vacuum requirements. For the DV of silicon, the

5.38

experimental work to date has apparently aimed at the production
of integrated circuit chips and solar cells. Therefore data on
deposition rates is usually proprietary. In general, DV depo-
sition rates range from less than 1 micron/minute to 50 microns/
minute (the latter for aluminum, a commercial process). In
this study the deposition rate for silicon is assumed at
4 microns/minute (the same as for CVD). Given this assumption,
production of one 10-GW SPS per year requires 2900 m^2 of
deposition area.

The DV process offers a number of advantages for SMF use.
First, the process is conceptually simple. It requires no
Earth inputs, chemical reactions, or pseudogravity, and it has
few moving parts. Second, because the DV operating pressure
is on the order of 10^{-6} Torr, the process does not require
complete pressure vessels. To avoid contamination of neighbor-
ing equipment, the deposition areas should be enclosed by
"optical baffles," sheets of material positioned in such a
way that the silicon atom source cannot "see" outside the
deposition volume; the boiled-off silicon atoms, travelling
radially outward from the source, therefore hit either the
deposition surface or a baffle. Some silicon atoms would
escape past the baffles after collisions either with other
silicon atoms or with surfaces, but these losses can be kept
small.

Third, DV can be used to deposit silicon sheet directly
onto the cell substrate and rear contact (or on the rear
contact alone). Since the deposition surface temperature is

low (compared to that for CVD), the aluminum rear contact is not in danger of melting. DV can therefore be used in a layer-by-layer buildup for cell manufacture.

Fourth, DV is well adapted to the in-space environment. On Earth, DV is seldom economically viable because of its requirements for energy and vacuum. In an SMF, both energy and vacuum are readily and cheaply available. DV therefore stands as an example of a process which may be unlikely for Earth use, but may be highly advantageous in the different physical and economical environment of space.

However, the DV process also carries several disadvantages. The principal problem is that little experimental data is available on the application of DV to the manufacture of solar cells. While there is some literature on direct vaporization of various coatings (ref. 5.63), the crystalline quality of these depositions is not described. For example, the power of the energy source, the pressure of the boiled-off silicon, the temperature of the deposition surface, and the thermal conductivity of the deposition surface may all have effects on the deposition rate and quality of the silicon crystal output; these effects have not been assessed. Therefore predictions of the uses of DV carry a technical risk.

Another disadvantage is that the DV process involves some waste of the silicon. As described above, the escape of silicon atoms past the baffles can be kept low. However, the silicon

atoms tend to coat the baffles as well as the deposition surface. One way to avoid this is to keep the baffles at the boiling temperature of silicon; since this temperature is $2603^{\circ}K$, this option is very unlikely. Therefore some silicon will be lost to the baffles. This loss can be minimized by careful design of the process geometry, so that most of the boiled-off particles travel toward the deposition surface rather than the baffles. Given such a design, a deposition efficiency of 67% should be possible (meaning that two-thirds of the boiled-off silicon ends up on the deposition surface, the remainder either on the baffles or out of the deposition volume).

A third disadvantage is that the DV process requires many silicon sources to achieve an even thickness in the deposited sheet. As shown in Fig. 5.9, a single source of silicon atoms tends to produce a gaussian pattern of atoms on the deposition surface, with maximum deposition occurring at the point nearest the silicon source. This problem can be avoided by using many sources of silicon atoms, with overlapping deposition patterns. This option may not require as many lasers or electron beam guns as silicon sources, if each beam can be multiplexed between a number of silicon sources.

Finally, the DV process shares a disadvantage with the CVD process: it produces polycrystalline silicon. As in the CVD process, the silicon deposited by DV picks up the crystal orientation of the deposition surface. As discussed earlier, and as shown in Fig. 5.8, polycrystalline cells are not as efficient as monocrystalline cells.

The reason for this lesser efficiency is that grain boundaries in polycrystalline wafers hamper the motion of charge carriers in the cell. Therefore grain boundaries in the plane of the cell[1] will restrict the motion of current through the cell junction; grain boundaries perpendicular to the plane of the cell will impede the motion of charge carriers across the top surface of the cell to the electrical contact grid fingers.

Therefore cell efficiency can be significantly improved if the cell wafer can be made monocrystalline, or if the polycrystalline grains can be made large enough to extend through the cell and from one grid finger to the next. Extending the grains through the thickness of the cell can be done in two ways: first, if the grains have random shapes, the average grain diameter should be on the order of twice the wafer thickness (or larger); second, columnar grains can be grown through the thickness of the cell. In either case, the grain boundaries no longer hamper carrier motion through the cell, but still impede motion across the cell surface to the top contact grid fingers. If the grain diameters can be made on the order of the distance between grid fingers (usually 1000 microns), then the cell will behave like a monocrystalline cell (Ref. 5.52).

Whether by chemical vapor deposition or direct vaporization, the deposition of monocrystalline silicon at 4 microns/minute

appears impossible, even when depositing on single-crystal silicon. The reason for this involves silicon adatom mobility. Adatoms are silicon atoms which have just been adsorbed by the silicon surface. These atoms must move about the surface to fill in open lattice points to form a perfect crystal. If the deposition rate is too fast the adatoms are buried before they have a chance to settle in and an amorphous deposit results. Deposition rates can be increased by heating the substrate, thus increasing adatom mobility (Ref. 5.53).

However, at intermediate rates, the formation of poly-crystalline silicon wafer is possible. The study group has found a source which reports growth of columnar grains (perpendicular to the deposition surface, and therefore favorable for solar cell manufacture) on aluminum deposition surfaces at 480-520°C. The grain diameters were 4-6 microns and the grain lengths on the order of the thickness of the deposited film. Most important, the deposition rate was 4 microns/minute (Ref. 5.54).

An alternative is to deposit silicon very slowly (rates on the order of 10^{-2} microns/minute). This would require a considerable increase in SMF deposition area. Even though the effect on factory costs of increasing this area is unclear, this option appears unlikely.

Therefore silicon wafers deposited by CVD or DV at 4 microns/minute (or faster) would require further processing

to produce 12.5% efficient solar cells. Two general methods
are suggested to improve the crystal quality of that output:
monocrystalline deposition surfaces, and heat treatment.

The first option deposits the silicon sheet onto a mono-
crystalline surface, so that the silicon wafer will duplicate
that monocrystalline quality as much as possible during
deposition. However, because of the adatom mobility problem
discussed above, the silicon sheet will be polycrystalline.
The extent of this effect has not been sufficiently researched
to predict the quality of the output. Also, there may be
technical difficulties in producing a monocrystalline depo-
sition surface. If this deposition surface is the cell rear
contact on the cell substrate, then the cell rear contact
must be monocrystalline. If the rear contact is vapor-
deposited onto the substrate (a likely possibility, as dis-
cussed later), then the substrate must be monocrystalline.
In general, it is considerably more difficult to produce
monocrystalline sheet than amorphous sheet for substrates.
In particular, the production of monocrystalline silica
(quartz crystal) substrates requires processes essentially
similar to processes for production of monocrystalline
silicon wafers (e.g. Czochralski growth, zone refining, and
cutting). Therefore this option merely shifts the complexity
from making monocrystalline wafers to making monocrystalline
substrates.

It is technically simpler to chemical-vapor-deposit the silicon sheet (or the rear contact and then the sheet) onto a permanent monocrystalline surface. After deposition, the silicon sheet (and rear contact, if included) is peeled from the surface, and the deposition surface is used again. The technical challenge is then in producing the deposition surface, and maintaining its monocrystalline quality in spite of the thermal and handling shocks in its operat'onal use. This limits the design to batch production, since it is unlikely that a continuously moving deposition belt, which must curve around to return to its starting point, could maintain a mono-crystalline surface. Spire Corporation (Ref. 5.55) has used a graphite deposition surface to enhance the growth of columnar grains in the silicon wafer. However, the use of specialized or monocrystalline deposition surfaces can only partially improve the crystalline quality of the output, and it is doubtful that such output could lead to 12.5% efficient cells.

The second general method to improve the quality of the deposited silicon is heat treatment after the deposition is completed. This general method includes three options: annealing, RTR zone refining, and pulsed-beam recrystallization.

The first heat treatment option is annealing. In this process the polycrystalline silicon sheet is heated to just below melting point, and left at that temperature for some time. This eliminates point defects in the crystal structure,

and increases the size of the crystal grains by allowing
migration and disappearance of grain boundaries. However,
grain diameters on the order of 100 microns using conventional
furnace anneals (750 to 950°C, 30 minutes) are doubtful. This
is because a grain field originally characterized by 3-dimen-
sional disorder will not undergo transformation to grains with
mean diameter greater than film thickness (Ref. 5.55). There-
fore melting and slow resolidification seems an inadequate
option. If the deposition process for the silic   afer can
be designed to produce columnar grains through th. cell
thickness, a furnace anneal may increase the diameter of those
grains; however, an end-result diameter of 1000 microns by
this method is also doubtful. One advantage of the furnace
anneal technique, however, is that it can handle large areas
of silicon wafer at once.

The second heat treatment option is ribbon-to-ribbon
(RTR) zone refining, currently being researched by Motorola
(Ref. 5.56) and Spire Corp. (Ref. 5.57). This technique,
depicted in Figure 5.10, uses CO_2 lasers or electron beams
(EB) to create a molten zone within a ribbon of polycrystalline
silicon. The molten zone is then moved along the ribbon,
leaving monocrystalline ribbon behind--a process analogous
to zone refining. Thus wafer production could be a two-step
process: (1) chemical vapor deposition of polycrystalline
silicon in ribbons; (2) laser or EB remelt for refinement.
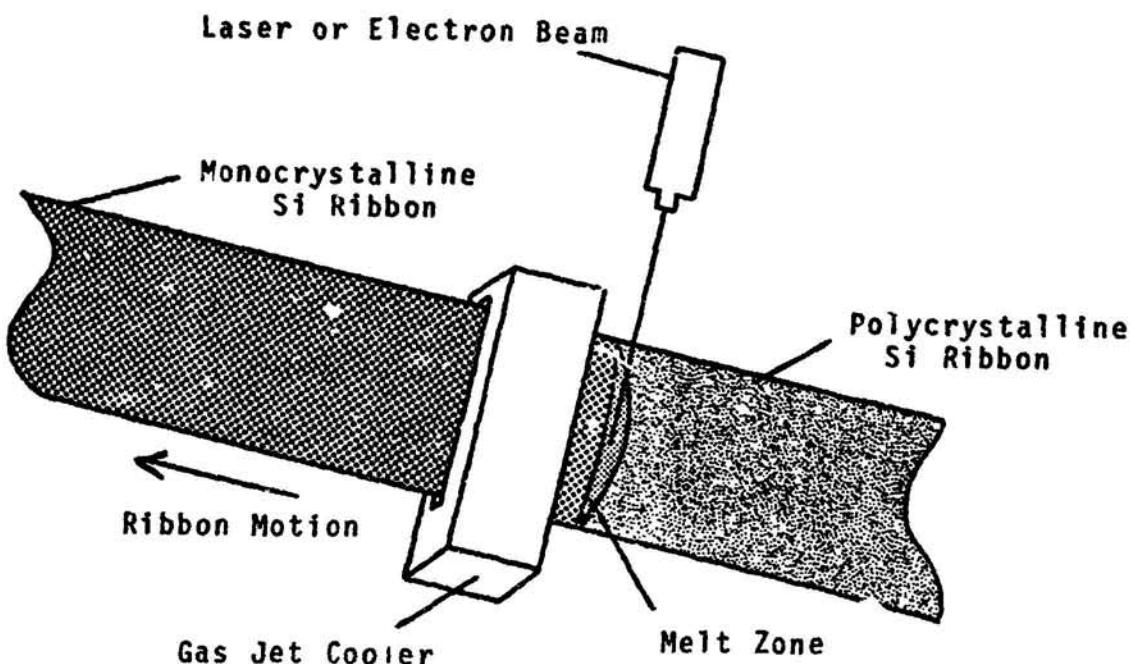
FIGURE 5.10: RTR ZONE REFINING

Motorola reports solar cell efficiencies greater than 10%
using this technique, and projects efficiencies up to 17%
(Ref. 5.56). However, this RTR process is governed by the
crystal growth rate equation explained earlier, and the rate
of this process is therefore limited by the attainable thermal
gradient. If the ribbon is 7.5 cm wide and the thermal gra-
dient is 2000°K/cm, corresponding to a zone travel rate of
7.5 cm/min, the process requires that 41,300 ribbons be re-
fined simultaneously (assuming a 90% duty cycle) for the pro-
duction of one 10-GW SPS per year. This large requirement
can be reduced by using wider ribbons, although the stability
of the molten zone becomes more difficult to maintain for

w:der ribbons. Also, the thermal gradient (and therefore the zone travel rate) could be increased (perhaps by as much as a factor of 2). Even with those improvements, the RTR process would still require much equipment.

The third heat treatment option is pulsed-beam recrystallization, currently under study by Spire Corporation. This research is investigating the effects of short laser or electron beam pulses to melt the silicon locally. The properties of this tuermal condition are not fully understood, but the temperature of the region being processed was calculated to be approximately 7000°C and is even thought of as a high density plasma rather than a melt (Ref. 5.58). These pulsing techniques produce a short-duration burst of low energy electrons or photons. Reported pulsing parameters for electron beams have been a duration of 10^{-7} seconds, a fluence of 0.2 cal/ n^2 and a mean electron energy of 10-20 keV, well below the 125 keV threshold for lattice displacement in silicon (Ref. 5.55). Pulsing parameters for laser annealing varied more widely: pulse durations from 10-60 nanoseconds and photon energies from 0.1-10 J/cm^2. A transient temperature condition is produced in the film, including a steep thermal gradient, conditions ideal for recrystallization. The recrystallization begins and proceeds toward the surface as the thermal condition collapses. The entire region returns to ambient temperature within a few microseconds.

There are several advantages to this technique. First, the thermal gradients created are extremely steep, and there-fore the travel speed of the recrystallization interface is very high. This allows rapid recrystallization of large areas of silicon wafer (when compared to the RTR zone re-fining speed). Second, since no large molten areas are created, the structural integrity of the silicon wafer is not jeopardized.

Third, since the process actually recrystallizes the material, it could operate on low-crystal quality input. Although this has not yet been experimentally achieved, pulsed-beam recrystallization could possibly produce poly-crystalline silicon sheet with large-diameter (e.g. > 100 microns) grains, starting from small-grain (e.g. < 1 micron diameter) polycrystalline material. The best experimental results reported to date are the production of "full-film-thickness columnar crystallites that have a cross-section of at least 30 microns in a polysilicon film deposited on a foreign, noncrystalline substrate " (Ref. 5.65). The re-crystallization sequence used in that experiment by Spire Corp. consists of a pulsed-beam recrystallization, to enhance formation of columnar grains through the silicon wafer, followed by a scan recrystallization, to increase the diameter of the columnar grains. In the scan recrystallization, the beam (electron beam or laser) is tracked rapidly across the

silicon surface. Optimal parameters for this two-step re-crystallization process are being developed experimentally. This two-step sequence is also described in Ref. 5.55.

The pulsed-beam recrystallization process might in fact work best on amorphous silicon sheet, because the recrystallization then benefits from the potential energy released by the atomic structure's conversion from amorphous to crystalline (Ref. 5.64). This would allow high deposition rates for the silicon wafer production, reducing SMF equipment requirements.

In summary, there are two basic approaches to the production of silicon solar cell wafer. The first is the production of high-crystal quality wafer (monocrystalline, or close to it). Processes such as Czochralski ingot growth, dendritic web, zone refining and cutting, edge-defined film-fed growth, and deposition onto monocrystalline surfaces, operate with that goal. In studying these candidates, the study group decided that the production of high-crystal quality wafer is difficult to automate on a large scale.

The second approach is the production of relatively low-crystal-quality (polycrystalline) wafer, followed by further processing to enhance the crystalline quality. Chemical vapor deposition and recrystallization, and direct vapor-ization and recrystallization, are examples of such processes. In studying these options, the study group found that, by

decoupling the tasks of wafer creation and crystal-quality
enhancement into two separate steps, this approach was
better suited for large-scale in-space automation.

For the production of silicon wafer in the reference
SMF, the study group chose direct vaporization of tne silicon,
followed by the two-step (pulsed-beam, then scan-beam) re-
crystallization of the silicon sheet. The study group feels
that this sequence can produce silicon wafers suitable for
the manufacture of 12.5% efficient solar cells. The decision
in favor of DV was made because of the simplicity of the
process, and because of its high degree of adaptation to
the space environment. The recrystallization sequence was
chosen because of the encouraging results of the experiments
by Spire Corp. The study group feels that these processes
can become advantageous in space, given solid research and
development to increase their capabilities well beyond the
current state of the art. However, the study group emphasizes
that these processes are the most advanced technologies pro-
posed, barely in the experimental stage at this time. Their
promise is therefore not guaranteed, and a final choice
cannot yet be made.

To investigate the feasibility and requirements of the
direct vaporization of silicon, the study group ran an ex-
perimental program during the follow-on contract effort.
These experiments and their results are discussed in

Addendum I, "Direct Vaporization Experiments," at the end of this report.

Doping processes are used to mix dopant atoms into the silicon wafers, in concentrations of 10^{17} to 10^{18} atoms/cm^3. The bottom 45 microns of the silicon wafer thickness are doped with a p-material such as boron; the top 5 microns are doped with n-material such as phosphorus. Total requirements for dopants for one 10-GW SPS are less than a ton. There are three candidate doping processes: diffusion, ion implantation, and co-deposition.

Diffusion is done after the production of the silicon wafer. Usually a p-type material is first doped (by diffusion or otherwise) into a blank silicon wafer. Then a layer of n-type material is applied to the top of the silicon wafer, and the silicon is heated: one current diffusion process heats the wafers to 1273°K for one hour (Ref. 5.4). The n-dopant then diffuses into the silicon wafer.

The diffusion process, although used on Earth, poses problems in SMF use. The dopants are usually applied to the wafers in liquid solutions, a difficult task in zero-g. The liquid solutions could be applied with a device similar to a paintbrush, but some of the liquid would be lost to evaporation unless the process were enclosed in a container. Also, the solution would have to wet the surface rather than forming beads. Applying the dopants as solids (by CVD or DV), though

possible, complicates the process considerably. Also, control over diffusion depth and dopant concentration is difficult. Rather than a uniform dopant concentration, the process tends to produce a concentration profile, with the largest dopant concentrations at the surface of the wafer.

Ion implantation takes place both during and after the production of the silicon wafer. In this process dopant material is ionized in an ionization chamber. The dopant ions are then accelerated out of the chamber by a potential difference, and travel with large velocities to the silicon wafer. On impact, the ions penetrate the silicon, implanting themselves in the crystal structure. The velocity of the ions controls the depth of penetration, and the number of ions produced is controlled by the operation of the ionization chamber. Therefore the process provides control over dopant concentrations and profiles. Sometimes the ion deposition process is used with a low ion travel speed to coat the silicon wafer with dopant, prior to diffusion.

Besides this careful control over dopant profiles, ion implantation has several other advantages. It is an established technology. According to one source, ion implantation has "excellent uniformity, reproducibility, and ability to control impurity profile" (Ref. 5.59). Other descriptions in the literature (Ref. 5.15) suggest that the process can be automated on a large scale, an advantage in SMF use.

However, ion implantation carries some complications and disadvantages. One problem is that the maximum depth of penetration of the ions is on the order of a few microns. This is because deeper penetration requires very large ion energies, and the damage to the lattice from the resultant impact can degrade the solar cell quality. Also, at those energies, control over dopant profiles is less accurate. Therefore ion implantation is currently done to depths of 1-2 microns. For the SMF process, the ion implantation of the p-dopant (boron) in the bottom 45 microns of the silicon wafer must be done _during_ the deposition of the silicon. To avoid the mixing of p and n layers during the two-step re-crystallization described above, the n-dopant (phosphorus) should be implanted _after_ the recrystallization. If the baseline junction depth of 5 microns is too large for easy deposition of the phosphorus, the junction depth can possibly be reduced to 2-3 microns; a number of current cells use shallow junctions.

A minor disadvantage of the ion implantation process is that it requires closing the current loop between the ion source and the silicon wafer, since the ion stream carries a flow of electrical charge from one to the other.

Another more significant disadvantage is that the implantation process creates point defects (due to ion impacts) in the crystal lattice. These defects act similarly to grain

boundaries, reducing the efficiency of the cell. However, pulsed lasers and electron beams have been used to anneal ion-implantation damage. Several sources indicate that such a pulsed-beam anneal is superior to a conventional furnace anneal with respect to the performance of the completed device. Sheet resistances obtained have been shown to be identical or lower than with $750^{\circ}C$ or $1000^{\circ}C$ 30-minute furnace anneals (Refs. 5.58, 5.59). Laser anneals can provide complete recovery of electrical activity with little or no degradation of minority carrier diffusion length whereas a thermal anneal of $900^{\circ}C$ and $1100^{\circ}C$ can only partially restore the carrier concentration and reduce the minority carrier diffusion length by a factor of 5 or more (Ref. 5.60). Although there is a redistribution in the doping profile which tends to reduce performance (Refs. 5.58, 5.60) (i.e. the dopants "spread out" slightly) there are indications that this phenomenon is a function of pulsing parameters, and adjusting these parameters may minimize this problem (Ref. 5.58).

If the p-dopant is ion-implanted during the silicon deposition, the subsequent recrystallization of the wafer will eliminate the ion implantation damage. However, the damage caused by the n-dopant application (especially if the dopant is implanted to a depth of 5 microns) would require a pulsed-beam anneal of the n-layer after the implantation.

Co-deposition is a general name for the inclusion of dopants directly in the silicon-wafer production process. As described above, ion implantation is partially a form of co-deposition, since the p-dopant is implanted during Si deposition. The concept of co-deposition can also be applied to other wafer production systems. In floating substrate, ceramic plate dipping, or dendritic web processes, the p-dopant can be mixed into the molten silicon prior to crystal production; the n-dopant must be added later by another method.

In chemical vapor deposition, the dopants can be added during the deposition process either by low-speed ion implantation or by direct vaporization, using many dopant atom sources over the deposition area. Chemical vapor deposition of the dopants (as well as the silicon) may be possible provided that the deposition surface temperature and the pressures of silicon-bearing and dopant-bearing gases can be adjusted to produce deposition of both in the proper concentrations. In the direct vaporization of the silicon wafer, dopants can be co-deposited by ion implantation (as described above), by DV (using separate dopant sources), or by blending the dopants into the solid silicon material sources before the DV of the wafers. However, blending the dopants into the silicon would require ferrying boron and phosphorus to the Moon (or producing them locally), then mixing them into the metallurgical grade silicon output. These dopants would have to be in

sufficient concentrations to yield the required 10^{18} atoms/cm^3 after the zone refining of the silicon at the SMF.

For both CVD and DV processes for silicon wafer production, both p and n dopants could be co-deposited by switching dopants after 45 microns of silicon wafer deposition. However, this would make the later use of recrystallization impossible, since this would blend the p and n layers.

Co-deposition is difficult in Czochralski growth, zone refining and cutting, and EFG processes. This is because all of these processes involve the crystallization of the output from a melt. At the liquid/solid interface, silicon atoms tend to crystallize faster than any other atoms (impurities or dopant), and the dopant therefore tends to be left behind. This tendency might be offset by increasing the concentration of dopant in the melt, so that enough of it will crystallize into the output; however, this has not yet been attempted. In any case, only the p-dopant could be included in this manner, and the n-dopant would have to be added after wafer production.

Despite its possible simplicity, complete co-deposition was not selected for the reference SMF, because of its technical uncertainty (it is not a current technology) and its potential incompatibility with the suggested recrystallization process. The study group chose instead the ion implantation of the p-dopant during the deposition of the silicon wafer, and the later ion implantation of the n-dopant. In between

the two processes is the recrystallization of the silicon wafer, eliminating the p-dopant implantation damage. To repair the damage from the later n-dopant implantation, the study group chose a shallow pulse-beam anneal. This decision was due to the confidence in ion implantation (an existing technology), and to the promise of high efficiencies reachable by annealing the resulting point defects.

5.2.5: Application of Electrical Contacts: As described in Sec. 2.1, the solar cells require rear contacts and top contacts, the rear contact a continuous sheet two-microns thick; the top contact a one-micron thick "grid fingers" pattern. The material for these contacts must be a good conductor, and must make a good electrical contact with the silicon wafer. Among lunar materials aluminum satisfies these requirements. Although alternatives could be brought from Earth (such as silver or copper alloys), this would increase the mass of Earth inputs by at least 1000 tons per 10-GW SPS (the mass of the contacts if made from Al). Since several processes exist to make such contacts from aluminum, alternatives are not justified. Table 5.5 presents three candidate processes for the application of aluminum solar-cell contacts.

Electrostatic bonding involves the separate production of the aluminum contacts as sheets (for the top contact,

TABLE 5.5: APPLICATION OF ELECTRICAL CONTACTS
ALTERNATIVE PROCESSES

Process	Advantages	Disadvantages
Electrostatic Bonding	o Technology exists for thicker sheets	o Requires separate production of contacts o Difficult to handle thin aluminum sheets
Etching Methods	o Established technology	o Require bath processes o Require Earth inputs
*Direct Vaporization	o Existing technology o Conceptually simple o Contacts can be deposited directly onto silicon wafer or substrate	o Requires many material sources o Some waste of material o Requires cleaning of shadow mask Requires sintering of contacts

*Chosen for the reference SMF

patterned sheets), followed by the electrostatic bonding of these

sheets to the surfaces of the silicon wafer. Alternatively, the

contacts can be bonded to the substrate or optical covers, and

the silicon wafer can then be deposited or bonded to the con-

tacts. Although this process has been used to apply thicker

contacts to solar cells, it is unlikely for SMF use for several

reasons. First, it requires separate production of the contacts,

usually by processes such as fine rolling, etching methods, or

direct vaporization. The rolling process can produce five-

micron thick aluminum 'Ref. 5.16). The other processes can

produce one and two micron thick sheets, but in addition can

produce them directly on the solar cell surfaces (as described

below). Therefore separate contact production and bonding

steps add unnecessary complexity to the contact application

process. Second, even if one and two micron thick sheets are produced, handling of these contact during bonding operations is a complicated task requiring delicate equipment (Ref. 5.16).

Etching methods are the most commonly used techniques today. These methods use chemical baths and/or electrolysis baths to apply thin coating of conductor to the solar cell surfaces. The aluminum sheet rear contact can be applied in one step by electrolysis. However, the top contact requires a series of chemical or photochemical steps to produce deposition of aluminum only in the "grid fingers" pattern required. One such "etch-resist" technique uses a contact mask and a chemical bath to alter the surface chemistry of those areas not to be covered by Al grid fingers. These areas then resist the subsequent electrolysis bath which deposits Al on the unaltered surfaces.

Although this is an established solar-cell-contact technology on Earth, in SMF use it carries the severe disadvantage that it requires liquid baths. The problems in dealing with liquid processes in zero-g were discussed in Sec. 5.2.4. In addition. the etching processes require chemicals not available from the Moon, and would therefore require Earth inputs to load the baths and to replace operational losses. These disadvantages make the etching methods unlikely candidates for use in the SMF.

Direct vaporization (DV) has been described in Sec. 5.2.4. The DV of aluminum is an established commerci.l process for the

production of thin sheets of Al (roughly 50 microns thick) and
for the coating of surfaces. DV involves boiling off atoms of
material from a solid material source, using lasers or electron
beams. The boiled-off atoms of material (at a pressure of rough-
ly 10^{-6} Torr) travel to a deposition surface and resolidify,
coating the surface with material. The deposition surface must
be kept cool to encourage the deposition, and the energy released
into the surface by the gaseous-to-solid phase change of the
deposited material must therefore be carried away.

For the deposition of aluminum rear contacts, the process
is simple direct vaporization. For the top contact, a "shadow
mask" is required to produce the "grid fingers" pattern. Placed
between the Al atom source and the deposition surface, the shadow
mask intercepts the atoms travelling to regions to be left un-
coated, and lets through the atoms travelling to those areas de-
stined to be covered by grid fingers. The deposition surfaces
can be either the silicon wafer or the cell substrate or optical
cover, as required by the chosen cell production sequence.

The DV of Al contacts shares a number of advantages with
the DV of silicon wafers (discussed in Sec. 5.2.4). It is an
existing, conceptually simple technology, requiring no Earth in-
puts and no pressure vessels (only baffles to avoid contamination
of equipment and other processes). Contacts can be deposited
directly onto solar cell surfaces, simplifying production. The

process is well adapted to the space environment, in that its principal requirements are vacuum and energy, both cheaply available in an SMF.

The DV of aluminum contacts also shares two disadvantages with the DV of silicon wafers. First, to ensure a uniform thickness of coating, many Al atom sources must be used, with overlapping deposition patterns. Second, since the Al atoms deposit themselves on surfaces other than the desired deposition surface, and because some atoms escape past the baffles to space, some wastage of material is expected. In particular, Al atoms coat the shadow mask used in top contact deposition. This mask must therefore be cleaned before reuse, requiring specialized cleaning equipment. This cleaning equipment can be either a chemical bath (not suited to space use) or a mechanical brushing system (which creates Al flakes, and therefore requires a chip-handling system).

Spire Corporation also reports that a pulsed electron beam sintering of the top electrical contacts is necessary when the contacts are vapor deposited in order to produce good mechanical and electrical behavior (Ref. 5.59). The transient temperature elevation used can be much lower than that used for recrystallization and ion implantation damage anneal. Good results are obtained when the silicon-aluminum eutectic temperature ($578^{\circ}C$) is exceeded, but the pulse is so short that only a shallow interface is created.

Because of the advantages listed above, in particular the high level of adaptation to the space environment, the study

group chose the direct vaporization process for the application of solar-cell electrical contacts, followed by a top contact sintering step.

5.2.6: Production of Substrate and Optical Cover: As described in Sec. 5.2.1, the solar cells include 75-micron-thick optical covers (on the sunward side) and 50-micron-thick substrates (on the shadow side). The function of these layers is to provide structural integrity and radiation protection to the silicon wafer. The materials used must also have coefficients of thermal expansion close to that of silicon, to avoid delamination of the cells due to thermal cycling. In addition, the optical cover must be transparent to those light frequencies in the solar spectrum which operate the solar cell efficiently.

On Earth, materials used for optical covers include tantalum pentoxide, silicon monoxide, silicon oxide-titanium oxide, silicon nitride, and cerium-doped borosilicate glass. Substrate materials include the above, plus composite materials and lower grade 'dirty' glass. As discussed in Sec. 5.2.1, the availability of lunar materials limits the choice of materials for the optical cover to fused silica (SiO_2), or possibly to SiO (this option equires further research). As per the JSC-GD study suggestion (Ref. 5.2), the study group assumed fused silica optical covers. To simplify process requirements and equipment,

the substrates were assumed υ be made of SiO_2 as well.

Research on the production of 50-micron and 75-micron thick SiO_2 layers is difficult, hampered by contradictory opinions by experts and the proprietary character of much research in this area. I. -t of the problem is that these layers have thicknesses seldom produced to date. For example, these glass layers are too thick to be considered 'coatings'. Therefore some coating technologies (e.g. the oxidation of silicon to form a roughly 1-micron thick coating of SiO or SiO_2 on surfaces) cannot produce layers 50 or 75 microns thick. Other coating techniques which use chemical bath dipping are unsuitable for space use because of the problems in handling liquids in zero-g (discussed in Sec. 5.2.4). At the other end of the scale, glass sheet manufacture techniques usually produce sheets with thicknesses 100 microns or more. As a result most of the earlier development in glass layer production is inapplicable to the optical cover and substrate production. Most of the research on 50 to 75 micron thick glass has therefore been for solar-cell applications, and is therefore very recent and/or proprietary.

Nevertheless, several processes are suggested for the production of solar-cell glass layers. These candidates are listed in Table 5.6.

Sheet production and electrostatic bonding involves the separate production of thin glass sheet, followed by its attachment to the solar cell wafer and contacts by electrostatic

TABLE 5.6: PRODUCTION OF SUBSTRATE AND OPTICAL COVER

ALTERNATIVE PROCESSES

Process	Advantages	Disadvantages
Sheet Production and Electrostatic Bonding	oExtension of established technology oCompatible with various production sequence options	oRequires handling of thin sheets oAdds to equipment complexity oMay require Earth inputs ●May require pressure vessels oMay waste some materials
*Direct Deposition Methods	oSimplify processes and equipment	oLittle solid data available oMay waste some material oMay require Earth inputs oMay require pressure vessels

*Chosen for to eference SMF

bonding. The electrostatic bonding of SiO_2 to silicon and aluminum is an existing experimental technique, developed for solar cell applications. The production of thin glass sheet is the more difficult challenge.

A number of techniques are used on Earth: floating substrate, spray-on, DV, CVD. The floating substrate method (analogous to the floating substrate method of silicon wafer production described in Sec. 5.2.4) involves pouring molten glass onto molten metal; this is a commercial process used to make plate glass. Although this technique could possibly be adapted to make 50 to 75 micron thick sheets (much thinner than current output),

the difficulties in handling the molten materials in zero-g (described in Sec. 5.2.4) make this option unlikely for SMF use.

The spray-on technique involves the deposition of small globules of molten glass onto a deposition surface, where the particles form an amorphous layer. Sometimes the glass particles are suspended in an inert gas for transport to the surface. To enhance the formation of an amorphous layer of glass (rather than the production of a white glass powder), the surface must currently be at a temperature of at least 1070°K (Ref.5.17). Therefore the deposition surface must be a refractory material.

The direct vaporization (DV) technique (analogous to the direct vaporization process described in Sec. 5.2.4) is more commonly called 'sputtering' in glass technology. It uses lasers or molecular beams to boil molecules away from a source of solid glass. When these beams hit solid SiO_2, the silica dissociates into SiO and O_2 at roughly 1970°K. These gaseous molecules then travel to the deposition surface and recombine and solidify (Ref. 5.18).The chemistry of the deposition process must be carefully controlled. To enhance deposition of SiO_2 rather than SiO, the process is operated with an excess of O_2 in the deposition chamber. Other factors involved are the temperature and thermal gradient at the surface; DV of SiO_2 currently requires a thermally controlled refractory surface. The effect of deposition surface temperature is at present unclear, and

some sources express concern that the process may produce a white powder rather than an amorphous layer.

Chemical vapor deposition (CVD) can also be used to produce thin glass sheets. CVD (described in Sec. 5.2.4) involves the passage of a material-bearing gas (or gases) over a hot deposition surface. The gas(es) dissociate on the surface, forming the required layer. In the case of SiO_2, one suggested method uses silane (SiH_4) and oxygen as the gases (Ref. 5.19). At a deposition surface temperature of roughly $1000^{\circ}K$, the silane dissociates. Therefore current CVD of SiO_2 requires a thermally controlled refractory surface. Depending on the concentration of O_2 present, the process can form a layer of Si (low O_2), SiO, or SiO_2 (high O_2). Current SiO_2 deposition rates using this method are 2-3 microns/min for thin (2-3 microns) layers.

Of the four glass-sheet production techniques described, three (spray-on, DV, CVD) appear feasible in an SMF. They are compatible with large-scale automated production, and benefit from the cheap energy and vacuum available. Therefore the SMF could produce thin SiO_2 sheets for the cell substrates and optical covers by an extension of current technology. Another advantage of the separate production of glass sheet for substrates and optical covers is the resulting versatility in production sequences. For example it allows deposition of electrical contacts onto the glass surfaces rather than the silicon wafer, followed by bonding of the various layers; or the cells

can be produced in successive deposited layers, starting with either substrate or optical cover.

However, the separate production of glass sheet also carries some disadvantages. First, it requires handling of large areas of thin glass sheets between their production and their bonding to the solar cells. Handling and storage of 50- or 75-micron thick sheets of SiO_2 requires delicate equipment to avoid breakage. Furthermore, the needed production rates (roughly 13,000 m^2/hour for each sheet thickness) require large amounts of handling equipment.

One possible problem is the bonding of the glass sheets to solar cells which do nct have smooth surfaces. While the solar cells themselves are expected to have smooth faces, several likely interconnection options (described in the next section) apply interconnects to the surfaces of the cells. These interconnects therefore protrude above the faces of the solar cell panels. The applied glass sheets would then rest on the protruding interconnects rather than on the cell surfaces. Therefore there would be a layer of vacuum between the optical cover and silicon wafer, leading to partial reflection of the incoming sunlight (from the glass/vacuum and vacuum/silicon interfaces), lessening the efficiency of the cell. Assessing the extent of this degradation would require experimental measurement. It may be possible to bend glass sheets down to the cell surface

between the interconnects; in-house experiments conducted by one of the study group members suggest that a thin glass sheet (roughly 180 microns thick) at room temperature can be bent to a minimum radius of curvature of roughly 15 cm before breakage (Ref. 5.61). Thinner glass sheets at higher temperatures could possibly be bent to tighter radii. However, this possibility would need further experimental research.

The glass sheet production options each have individual problem areas. The CVD option carries the disadvantage that it requires Earth inputs and pressurized containers. The spray-on technique may require the same, if an inert suspension gas is used. The DV process wastes some of its lunar inputs (silica and oxygen) if pressurized containers are not used. However, these problems would also exist if these options were used for direct deposition of glass layers onto silicon wafers and electrical contacts.

Direct deposition onto wafers and contacts is the major alternative to separate glass sheet production and bonding. The critical issues are the achievable deposition rate, and the deposition surface temperature required by the SiO_2 deposition process. If the deposition temperature is above the melting point of the Al contacts ($930^{\circ}K$), direct deposition is highly unlikely. As mentioned above, current spray-on techniques require higher deposition surface temperatures, in the 1000 to $1500^{\circ}K$ range, to produce amorphous glass layers.

Some consultations referenced above (Refs. 5.17, 5.18, 5.19) indicate that the DV and CVD processes, as applied to SiO_2 are so new that predictions about their requirements in 1990 are nearly impossible at this time. However, certain recent consultations suggest that some of the anticipated problems may not be severe. Corning Glass Corporation (Ref. 5.62) indicates that DV of oxides of silicon almost always produces optical quality layers (in contradiction to the fears of producing white powder, discussed earlier). Also, deposition surface temperatures for DV need not be high. The problems encountered by Corning were rather the reverse: excessive heating of the surface by the deposition process, leading to high thermal stresses and separation of the glass layer. This effect, and the suitability of a low-temperature surface (e.g. room temperature) were confirmed by Professor Donald R. Uhlmann of the MIT Dept. of Materials Science and Engineering, who has deposited SiO_2 experimentally. Another source (Ref. 5.64) suggested that possibly the only method to avoid delamination of the glass and silicon layers was to develop a glass with the same coefficient of thermal expansion as silicon. The study group feels that the thermal stress problems can be alleviated by active thermal control of the deposition surface. This decision admittedly includes some technical risk.

The DV and CVD options share some of the advantages and disadvantages of other DV and CVD processes described earlier

(Secs. 5.2.4, 5.2.5, 5.2.6). Direct vaporization is conceptually simple, requiring relatively simple equipment. In the DV of SiO_2, as discussed earlier in this section, dissociation and recombination of SiO_2 takes place, requiring extra oxygen and careful process control. This complicates the equipment required.

DV is well adapted to the space environment, in that its principal requirements are energy and vacuum. Since DV pressures are low, pressurized containers are not required, and can be replaced by baffles.

The principal disadvantage of DV of SiO_2 is the lack of data available on the process. Therefore technical uncertainty. is high. Another disadvantage is that DV requires a large deposition area; therefore many material sources with overlapping deposition patterns are needed to achieve uniform deposition. Also, if pressurized containers are not used, some wastage of the lunar inputs (SiO_2 and O_2) can be expected.

Chemical vapor deposition of SiO_2 offers the advantages of low material waste, since the deposition area is enclosed in pressurized containers. CVD of SiO_2 is also compatible with one candidate silicon refining process, the silane/silicon process (see Sec. 5.2.4). This is because this refining process produces silane (SiH_4) as an intermediate step; silane and oxygen are the material-bearing gases suggested for the CVD of SiO_2.

As in DV of SiO_2, the principal disadvantage to CVD is the lack of solid information on the capabilities and requirements of

the process; technical uncertainty is therefore high. Also, the process requires hydrogen from Earth, to load the sytem and to replace operational losses. To avoid wastage of this hydrogen, the deposition areas must be enclosed in pressurized containers.

The process itself requires careful control to achieve the chemical reactions required on the deposition surface. By-products are H_2, O_2, and H_2O, and these must be controlled as well, since their reactivity creates a risk of explosion. The byproduct water must be broken up into hydrogen and oxygen, and the H_2 and O_2 must be separated. The hydrogen is recirculated to the silane/silicon process, and the oxygen to the SiO_2 CVD.

For the production of solar cell substrates and optical covers, the study group chose direct deposition by DV for the reference SMF. This decision assumes that in 10 years of re-search and development, the technical uncertainties and contra-dictions described earlier can be resolved by experimental work, and that a large-scale automated DV of SiO_2 process can be developed. Should developmental problems occur, there exists the alternative of separate production of glass sheets, followed by electrostatic or laser bonding (Ref. 5.64). The study group feels that the equipment requirements and costs for each option would not be very different. The direct deposition by DV, chosen for the reference SMF, is the simpler option, minimizing mechanical handling operations.

To investigate the feasibility and requirements cf the direct vaporization of silica glass, the study group ran a

set of experiments during the follow-on contract effort. These experiments and their results are described in Addendum I, "Direct Vaporization Experiments," at the end of this report.

5.2.7: Cell Interconnection and Array Buildup: As in the Boeing-JSC baseline SPS, the lunar-material SPS transmits the power output f~om the solar-cell arrays to the transmitting antennas through three busbars. This requires series interconnection of the cells to build up the output voltage to roughly 40 kV, and parallel interconnection to gather power outputs and to provide damage-tolerance to the arrays. A suggested interconnection schematic is shown in Fig. 5.11. Solar cells are
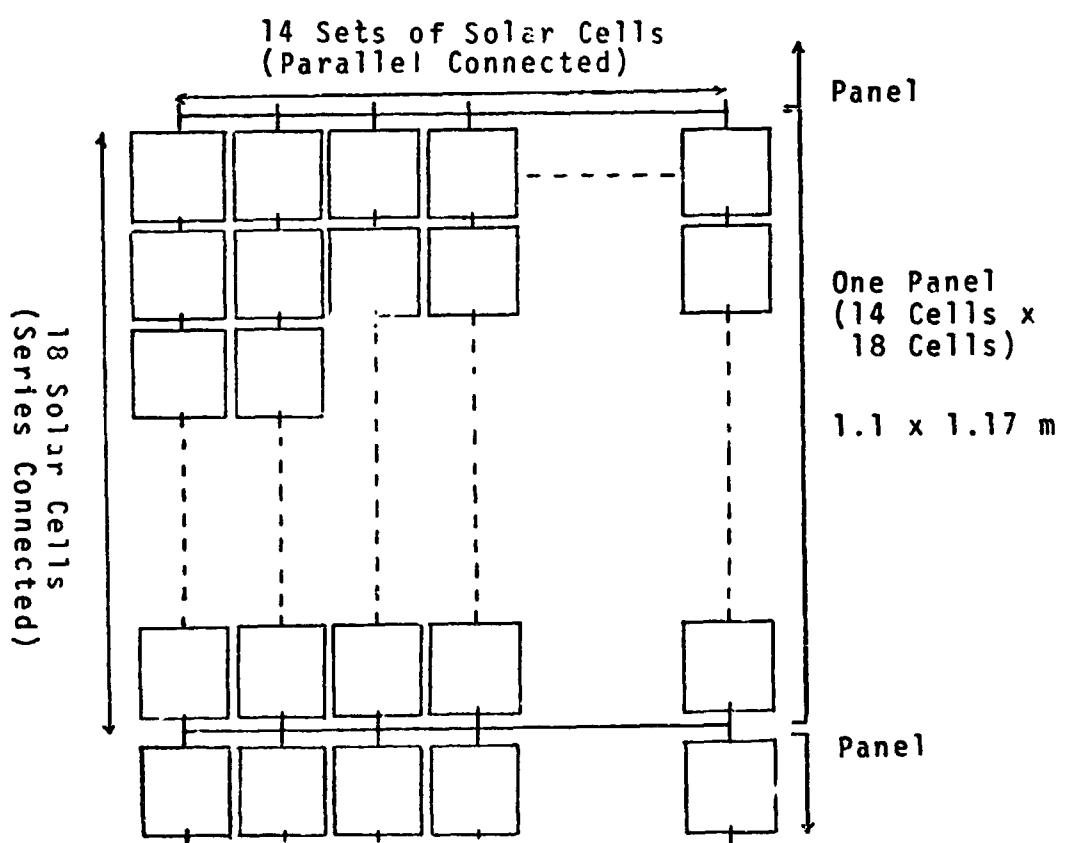
FIGURE 5.11:   SCHEMATIC OF SOLAR-CELL INTERCONNECTION

series-connected in sets of 18 cells (vertical in the figure). The sets are tied in groups of 14, parallel-connected at their ends. Thus each solar cell 'panel' is 18 cells long by 14 cells wide, and behaves electrically like one large solar cell, with the voltage output 18 times that of a single cell, and the power output of 252 cells. The panel is also damage tolerant: if a cell is destroyed (by a handling accident or a micrometeorite) the panel loses 18-cells-worth of power, but the output voltage remains the same.

The solar cell panels are built into damage tolerant arrays by series and parallel connections as well. Since each cell has output voltage .51 volts, roughly 78,000 cells (or 4330 panels) must be connected in series to generate the needed 40 kV. There are roughly 78 million panels in one 10-GW SPS, arranged in 18,000 'strings' of 4340 panels each. The task of the SMF is to produce 'segments' of the SPS arrays, 14 panels wide by 541 panels long (also called 'packages'). The 541 panels in each lengthwise line are series-connected.

The development of large-scale automated interconnection of solar cells is in its infancy. To date fabrication and interconnection of solar arrays has been done by skilled labor; consequently current cells are not designed for ease of automated production. Also, there is virtually no information available on automated interconnection processes, because the

research done to date on such processes is proprietary. The
available references (Revs. 5.6, 5.21) do not go into equipment
details, or they discuss solar cell designs which would be dif-
ficult to produce in an SMF.

There are therefore no well-developed candidate processes
for solar-cell interconnection. Rather, there are several solar-
cell-contact designs, each of which suggests interconnection
techniques. These contact designs are listed in Table 5.7. In
all four options, the basic design of the cell contacts is un-
changed: the rear contact is Al sheet over most or all of the
rear surface of the silicon wafer; the top contact is a pattern
of "grid fingers" leading to a 'collector bar' at one edge of
the cell (both fingers and bar are on the top surface of the
wafer). However, the differences are the methods by which these

TABLE 5.7: SOLAR-CELL CONTACTS
ALTERNATIVE DESIGNS

Contact Type	Advantages	Disadvantages
Wraparound Cell	oEstablished tech- nology	oDifficult to adapt to automated production
Edge Tabs	oEstablighed tech- nology	oDifficult to adapt to automated production
Contact Pegs	oSuitable for large- scale automated production	oNo experimental data oRequires delicate handling of pegs
*Direct Interconnection	oSuitable for large- scale automated production oConceptually simple oProduce structurally sounder panels	oNo experimental data oRequires bonding to fragile wafers

*Chosen for the reference SMF

contacts are made available outside the cell for interconnection.

Wraparound cells have a connection from their top surface collector bar, around the edge of the cell, to a contact on the back of the cell. Thus the back of the cell has the sheet rear contact ov · most of the surface, and the contact from the collector bar on the rest of the surface. This allows interconnections on the backs of the cells only. This type of cell is in common use today. However, it has disadvantages for mass-production. Although the contact can be brought to the back of the substrate, the rear contact is still sandwiched between silicon wafer and substrate. The rear contact must therefore be provided with a connection around the edge of the substrate to a contact on the back of the cell. The study group could not devise a simple method to produce wraparound contacts automatically, on a large scale. This is particularly difficult if the cells are produced in large sheets by deposition methods, then cut into cells; the wraparound contacts would have to be added to the 177-micron thick cell edges, after the cutting. For mass production, this appears overly complicated.

Edge tabs are used in many cells today, and are also used in the Boeing-JSC Earth baseline SPS (Ref. 5.1). The edge tabs project from the edge of the contacts, allowing interconnection either with separate interconnectors or directly between the tabs.

If each solar cell is produced separately, the contacts must be produced with tabs attached, then applied to the other solar-cell layers with the tabs protuding. This is a complicated process; in any case production of 20 billion separate cells per year is unlikely. If the cells are produced in multi-cell sheets and cut a part, the tabs must be attached to the edges of 2-micron-thick contacts, without shorting the contacts together (they are 50 microns apart). The study group could not devise a reliable method to do this. Neither could the group develop a method to vapor-deposit the contacts and tabs together, then free the tabs from the silicon and glass layers.

Because of the unsuitability of wraparound cells and edge tabs for mass-production, the study group devised two alternatives: contact pegs and direct interconnection.

Contact pegs can be used to provide electrical pathways through the glass layers of the cells. The 'pegs' are actually shaped more like coins, .5 mm in diameter by 60 or 90 microns thick. They are electrostatically bonded to the back contact and collector bar, before the deposition of the SiO_2 layers (substrate and optical cover). These glass layers are then deposited, covering the cell surfaces and forming glass bulges over the contact pegs. These bulges are then burned off (or ground off), exposing the outer surface of each peg (hence the 60 and 90 micron dimensions of the pegs, 20% thicker than the glass layers, to guarantee the exposure of peg surface). The

pegs then provide electrical pathways from the top and rear cell contacts to the top and rear surfaces of the cell. Separate interconnects can then be electrostatically welded to the pegs. If the rear contact pegs are positioned at the end of the cell opposite the top collector bar pegs, a short interconnect can be welded from the collector peg of one cell to the rear contact of the next cell to connect the cells in series. The parallel connections at the ends of the panels can be made by aluminum strips welded to the collector pegs of the last row of cells in one panel and the rear contact pegs of the first row of the cells in the next panel. The resulting cell interconnection cross-section is shown in Fig. 5.12.

The principal advantage of this alternative is that it can be automated on a large scale. Many contact pegs can be applied simultaneously by electrostatic welders to sheets of solar cell material, prior to the cutting of these sheets into individual cells.

The principal disadvantage of this option is that, to the best knowledge of the study group, it is an untried concept, and it therefore carries technical uncertainty. Another disadvantage is that it requires handling of the small aluminum pegs (.5 mm in diameter collector bar) and 60 or 90 microns thick). Also, the pegs must be welded to the contacts on the silicon wafers, a delicate process because of the fragility of the wafers. Similarly, the interconnects must be welded to
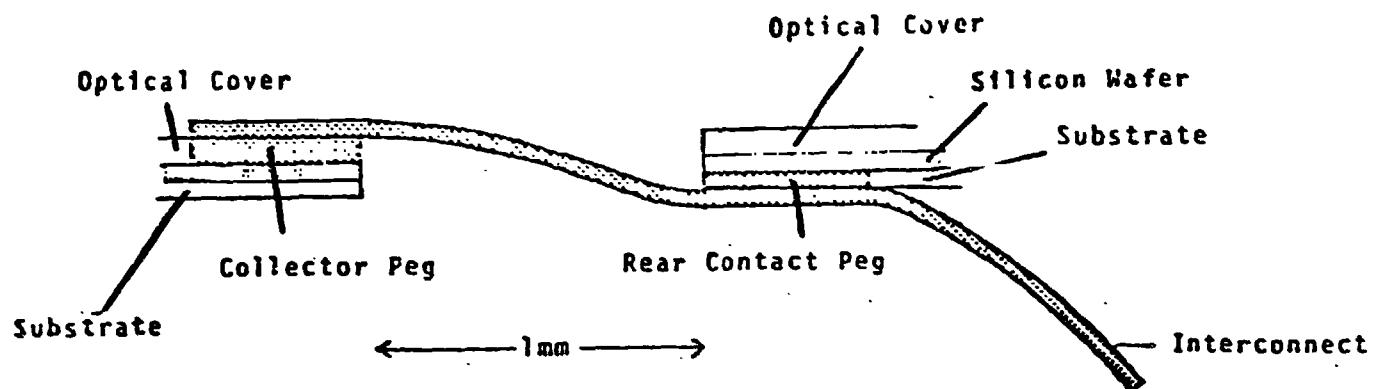
FIGURE 5.12:   CROSS SECTION OF CONTACT PEG
SOLAR CELL INTERCONNECTION

the solar cells; however, the cells benefit structurally from

the glass layers, and this step is therefore less delicate

than the peg application.   Finally, the process requires burning

off the bulges in the SiO_2 layers, a technically uncertain idea.

Determination of the effects of such a process (thermal stresses,

sputtering of glass, oxide layer formation on the pegs) would

require experimental work.

Direct interconnection was devised by the study group to

avoid some of the problems presented by the contact peg method

of interconnection.   In this alternative, the solar cells are

cut from the sheet and interconnected before the deposition

of the glass layers.   The rear contact/silicon wafer/top

contact sandwiches are cut from the produced sheet.   Cell

5.79

interconnects are then electrostatically welded directly to the top collector bars and to the rear contacts.

The optical covers and substrates are then direct-vaporized onto the cell surfaces and the interconnects, in the fashion described in the preceding section. However, the interconnects between panels are masked, so that SiO_2 does not deposit on them. This preserves their flexibility, required for later packaging. The cell interconnection cross-section resulting from this sequence is shown in Fig. 5.13.

Silicon Wafer   Optical Cover

Silicon Wafer

Interconnect

Substrate

← 1mm →

(TO SCALE)
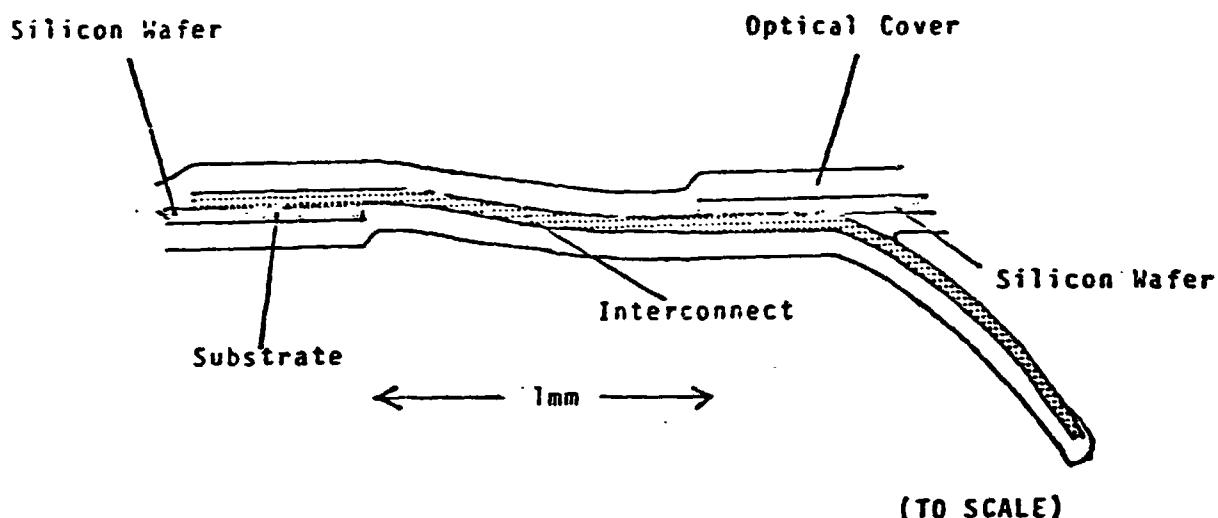
FIGURE 5.13: CROSS-SECTION OF DIRECT
SOLAR CELL INTERCONNECTION

The direct interconnection alternative offers several advantages. It can be automated on a large scale, since many interconnects can be applied simultaneously as the sheets are cut into individual cells. This option is also conceptually

simple. It does not require contact pegs, and the interconnect geometry is relatively simple; the interconnection can be done in one step. This option also does not require the burning off of SiO_2 layers. In fact, the glass layers over the interconnects (shown in Fig. 5.13) serve to reinforce the solar cell panels, improving their structural properties.

Direct interconnection also shares some disadvantages with the contact peg option. It is an untried, technically uncertain concept. It should therefore be experimentally developed. The direct interconnection process also requires the electrostatic bonding of interconnects to the rear contact/silicon wafer/top contact sandwiches. While this is analogous to the welding of pegs to the contacts in the contact peg option, the difficulty is higher in the direct interconnection, because the welding is done to solar cell sections after they have been cut loose from the sheet of solar cell material. Therefore the direct interconnection option requires delicate handling of the fragile silicon wafers, after cutting, during electrostatic bonding.

Because of its conceptual simplicity and advantages for use in mass-production, the study group chose the direct interconnection option for the reference SMF. This assumes that by 1990 an automated system can be developed capable of handling the fragile wafers during interconnection. In this task the design benefits from the zero-g environment, where weight forces and weight-induced friction forces are absent.

The research team also designed an automated system to
build the cell panels into array segments. Preliminary designs
of the cell interconnection and the array buildup equipment
are presented in Chapter 7, "Production Equipment Specifications."

5.3: STRUCTURAL MEMBER PRODUCTION

5.3.1: Structural Member Alternatives: The Boeing-JSC earth
baseline SPS includes structural members made from continuous-
chord tribeams, as shown in Fig. 5.14. In the earth baseline
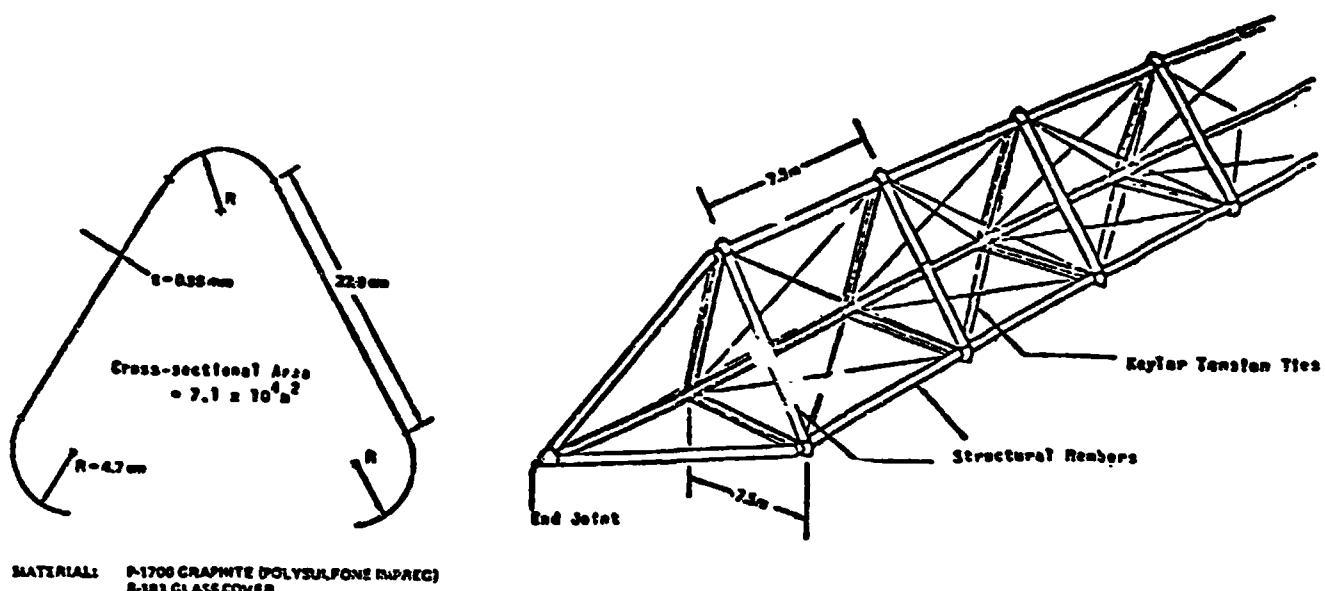
FIGURE 5.14: BOEING-JSC BASELINE STRUCTURAL BEAMS

SPS, these beams are made from graphite/epoxy (G/E) composite
covered with glass fabric. The tribeam longerons are brought
together to a point at the ends of the beams and capped by end
joints. Joint clusters fasten beams together by their end
joints to form the SPS structure. The manufacture of end

joints and joint clusters is discussed in the next section.

Alternatives for structural member materials are listed in Table 5.8. In general, structural member materials fall into two categories: those that expand thermally, such as pure metals, and those that expand very little, such as composites and glassy products. The relative merits of expanding or nonexpanding structure for the SPS are difficult to assess. Although non-expanding structure simplifies the design and lessens the cyclic

TABLE 5.8:   STRUCTURAL MEMBER ALTERNATIVES

Structural Member Material	Advantages	Disadvantages
Foamed Glass	o Low coefficient of thermal expansion o Relatively low-mass structural members o Compatible with SMF waveguide production process	o May require Earth inputs o Structural properties of material uncertain o Requires structural member redesign o Requires dust-handling systems for machining
Composites	o Low coefficient of thermal expansion	o May require Earth inputs o Structural properties of materials uncertain o Requires complex production
*Metal alloys	o Established technology o Versatility of production o Compatible with other SMF processes o Compatible with beam-builder	o High coefficient of thermal expansion o High-mass structural members

*Chosen for the reference SMF

loads on joints and members, the materials needed are more complicated and more expensive in procurement (e.g. composites vs. aluminum). Therefore more research in this area is needed before economics can suggest a clear choice. Such an evaluation, however, is outside the scope of this study.

The study group chose aluminum alloy as the material for the structural members produced by the reference SMF. Assessing the relative advantages of the various candidate materials is complicated, however, and the other alternatives discussed below should be researched further in later studies. Foamed glass is discussed in some detail, since it is the material chosen for waveguide manufacture in the reference SMF (discussed in Sec. 5.9 below).

Foamed glass is the material suggested for lunar-material substitution in the JSC-GD study (Ref. 5.22). The continuous-chord tribeams shown in Fig. 5.12 would be replaced by thin-walled (1 cm) tubes, with diameters 50 cm for primary structural members and 25 cm for secondary structural members (Ref. 5.23). The mass of these members would be 2.0 times the mass of the earth-baseline graphite-epoxy structure. The glass is foamed to resist crack propagation, since pure glass tends to shatter when impacted (either by a handling accident or by a meteorite).

The principal advantage of foamed-glass is its low coefficient of thermal expansion, close to that of glass (2.9×10^{-6} m/m°C). This minimizes structural deformations during SPS

eclipse. Also, the foamed-glass structural members are rela-
tively low-mass when compared to the other alternatives (dis-
cussed below).

Foamed glass is currently produced on Earth by the Pitts-
burgh Corning Corp. (Ref. 5.24), and used primarily for thermal
insulation. The production details are proprietary, but the
principal steps in the making of foamed glass are presented in
Fig. 5.15. Glass (similar to window glass) is first crushed
and ball-milled into powder (5-micron diameter particles). The
glass powder is mixed with small quantities (roughly 1% of the
glass mass) of foaming agents, such as carbon, various sulfates,
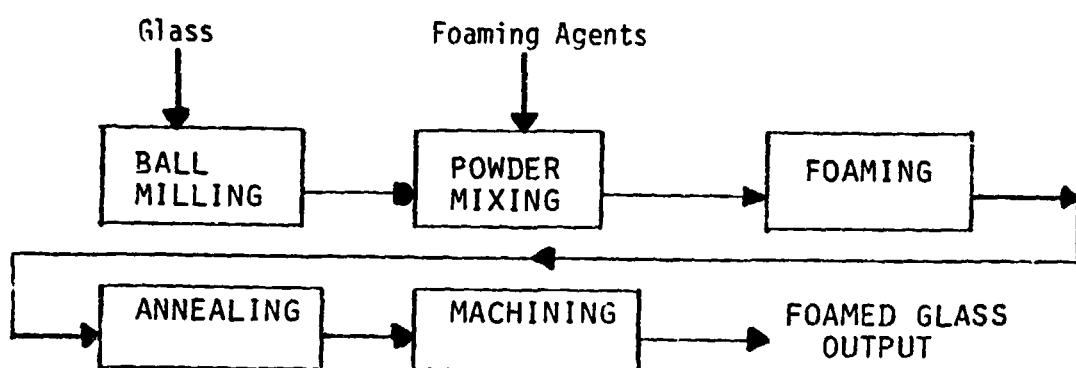
FIGURE 5.15: BASIC STEPS IN FOAMED GLASS PRODUCTION

and water. The mixture is placed in stainless steel molds and
heated in a foaming furnace at 970-1170°K. The glass first
melts, trapping the foaming agents. As the temperature rises,
the carbon reacts with the sulfates and water, releasing

gaseous CO, CO_2, H_2O and H_2S. These gases form bubbles, foaming the glass which expands to fill the molds. The foamed glass is then transferred to an annealing furnace. There the foamed glass is slowly cooled (12-14 hours); this length of time is necessary to avoid shattering due to uneven thermal stresses. Once cooled, the foamed glass is machined to the desired shapes.

A number of variations on this basic production scheme are possible. First, foamed glass can be produced from a variety of glassy materials, such as pumice, volcanic cinders, and obsidian (Ref. 5.25). Therefore natural lunar glass could be used. This glass is available by crushing the fine lunar soil (<90 microns) particles down to 5 microns, then electrostatically separating the glass (Ref. 5.26).

Second, the foaming agents can be varied, both in type and relative percentages. However, the total mass of foaming agents required appears to stay around 1% of the glass mass, and all the options include carbon. Although carbon is available on the Moon in parts-per-million concentrations, there is no guarantee that the proposed lunar refining processes will provide carbon (or the other required foaming agents) as outputs. The study group concluded that foaming agents would have to come from Earth.

Third, variations on the stainless steel molds are possible. British patent No. 1112083 describes an installation to produce sheet foamed glass by floating the glass powder on molten tin

during foaming.   Due to problems in handling molten-metal baths
in zero-g (described in Sec. 5.2.4), this option is unlikely
for SMF use.   Another variation is the shaft furnace (Ref. 5.25)
shown in Fig. 5.16.   This method involves the formation of a
monolithic block by foaming onto a bed of foamed glass in a
shaft furnace.   The shaft furnace acts both as a foaming and an
annealing furnace (the input area being maintained at foaming
temperature, while later in the shaft the glass is subjected
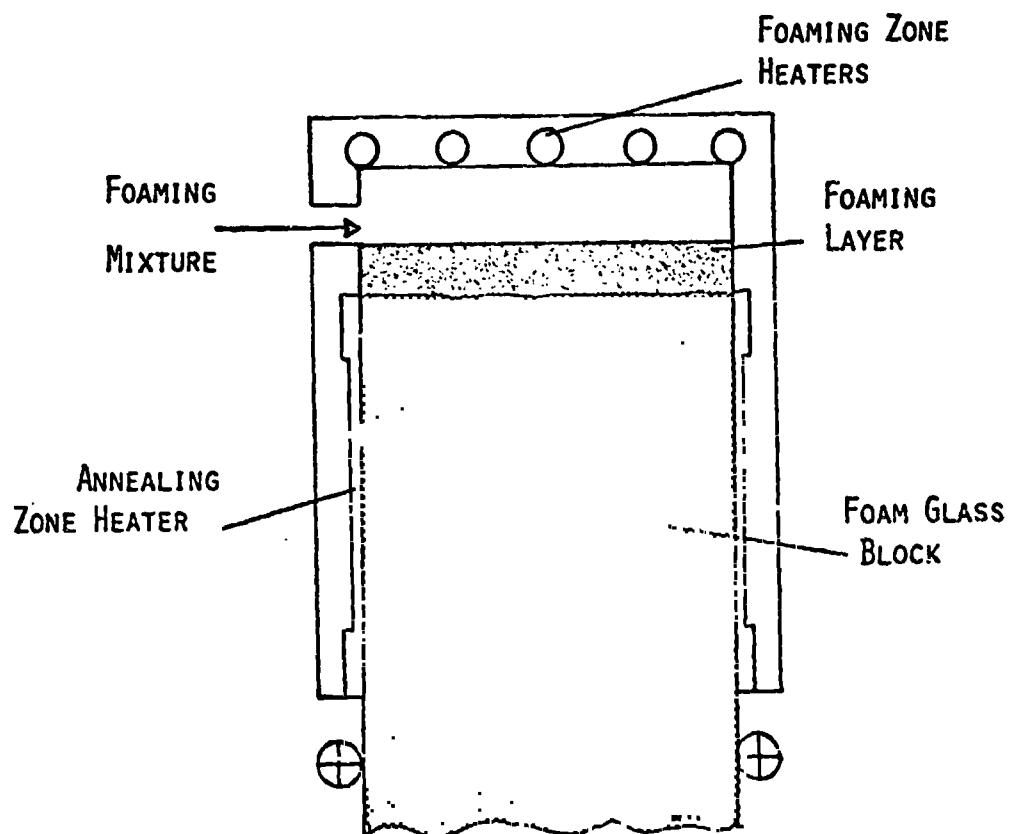
FIGURE 5.16 :   SHAFT FURNACE GLASS FOAMING METHOD

to steadily decreasing temperatures). When necessary the furnace channel cross-section can be re-adjusted to produce foamed glass as complex shapes (i.e., tubes, shells). Such a furnace could conceivably be adapted for use in zero-g by using gas pressure (rather than gravity) to feed the foamed glass along the furnace.

The production of foamed glass is therefore an existing technology, with some options adaptable to space use. Another advantage of the process is that it is a likely candidate for waveguide production (see Sec. 5.9 below), and therefore both productions might share equipment.

Foamed glass has a number of disadvantages, however. First, as mentioned above, the process requires foaming agents wh h include elements not found on the Moon. One suggestion to remedy this problem is the substitution of a stirring process to foam the glass with bubbles of lunar oxygen. But consultations with Dr. David Rostocker of Pittsburgh Coring Corp. indicate that this technique is unlikely to succeed in practice. A viscosity of 10^6 poise would be required in order to prevent oxygen-bubble coalescence, and at this viscosity it would be extremely difficult to stir the glass in order to distribute the bubbles evenly.

Another alternative, suggested by the MSFC COR, is the sintering of beads of natural lunar glass to form a foamed-glass-like material. This would eliminate the foaming stage, removing

the need for foaming agents. This alternative should receive further study.

Second, another disadvantage of foamed glass is the lack of data on the structural properties of the material. Current foamed glass is not used for structural applications, but for insulation instead, and is therefore produced in densities (e.g. 136 kg/m^3) below those required for SPS structural members (e.g. 1250 kg/m^3). The shatter resistance of foamed glass and its response to long periods in space are also issues requiring experimental research.

Third, substitution of foamed-glass members for the earth baseline tribeams also requires a redesign of the structural members, since the foamed glass is in the shape of tubes. The substitution also requires the redesign of the end joints, which must fit onto the tubes rather than onto tribeam longerons.

Finally, the machining of foamed glass produces abrasive dust (Ref. 5.28) and this requires abrasion-resistant cutting tools. This process also requires dust-handling systems, since free-floating dust in zero-g can contaminate and jam equipment.

Composite materials can be used to produce structural members. The elements used in the graphite/epoxy earth-baseline material are not available on the Moon, but a number of partial or total lunar-material substitutions have been suggested by the JSC-GD study (Ref. 5.22). Table 5.9, adapted from Table

3-15 of that study, list; these options and their relevant pro-
perties.

The first lunar-material option (90% Unidirectional S-glass,
25% Resin) is unlikely because it requires 85% of the earth base-
line structural member mass in earth inputs, and therefore does
not offer a significant improvement in transportation cost over
the earth baseline. The other two alternatives (Unidirectional
S-glass in aluminum matrix, or in titanium matrix) require only
lunar materials. The latter option would require the produc-
tion of titanium on the Moon. However, this material is not
required for any other SMF products, and its use in structural
members would therefore add to the complexity of the lunar re-
fining operations. Aluminum, on the other hand, is used in a
wide variety of SMF outputs (e.g. solar cells, DC-DC converters,
radiators, klystrons; see Table 3.3 in Sec. 3.4), and aluminum
production is therefore required on the Moon. The S-glass in
aluminum matrix is therefore the most likely composite candidate
for structural member material.

The principal disadvantage of the proposed composites, how-
ever, is that no experimental work has been done on their struc-
tural behavior or their production. The properties listed in
Table 5.8 are theoretical, and there has been no verification
of the actual behavior of th e materials. Also, the study
group has some doubts that the proposed matrix materials (i.e.
aluminum, titanium) can bond to the S-glass fibers solidly enough

TABLE 5.9: POSSIBLE COMPOSITE
STRUCTURAL MEMBER MATERIALS

Property	Material	Earth Baseline	Possible Lunar Material Substitutions		
		Graphite Polysulfone 120/70$_3$/120	90% Uni S-Glass 25% Resin	Unidirectional S-Glass Aluminum Matrix	Unidirectional S-Glass Titanium Matrix
E_{Axial} (GPa)		143.1	47.3	80.3	94.0
ρ (g/cm^3)		1.766	1.993	2.57	3.31
α_X (μm/m/°C)		-0.380	+4.16	+9.90	+5.90
Equivalent Mass Required					
From Earth		1.00	0.85	0	0
From Moon		0	2.56	2.60	2.85
Total		1.00	3.41	2.60	2.85

E_{Axial} = modulus of elasticity

ρ = density

α_X = axial coefficient of thermal expansion

(Adapted from Table 3-15, Ref. 5.22)

to produce the required properties. A bonding agent may be required between the glass fibers and the matrix material, complicating production and possibly requiring an earth input for the bonding agent.

For composite materials made on Earth, the matrix material is applied as a liquid. As described in Sec. 5.2.4, handling of liquids in zero-g poses problems. This problem could be avoided by producing the composite material on the Moon; however, this increases the transportation cost if any earth inputs are required, complicates the Moon-to-SMF transportation system (which must carry the composites), and requires that the composites survive launch stresses. The composites could also be produced at the SMF by vapor deposition of the matrix, but this option also complicates production.

Metal alloys are a more conventional alternative for structural member materials. Lunar materials available to the SMF are aluminum, titanium, iron, and magnesium; alloys of these metals can all be used in structural members. Alloying the metals does not significantly alter their stiffness properties. The purpose of adding other elements is to improve fracture toughness, to lessen the effect of fatigue and to make the structural members resistant to damage from handling impacts ("ding-proof").

Section 3.2.3 presents a calculation matching the stiffness of the earth-baseline members and aluminum (or Al alloy) replacements. Leaving the cross-section shape and dimensions

the same as those shown in Fig. 5.14, but changing the thickness to match the EI values of the Al and G/E members, the Al thickness required is 1.77 mm, 1.8 times the thickness of G/E. The needed mass of aluminum is 2.2 x 10^4 tons (without wastage allowance), 2.8 times the mass of the earth-baseline structural members. However, as discussed in that section, the study group has doubts about the applicability of the equal-stiffness criterion for material substitution, and feels that the Al mass calculated may be too high.

A similar calculation for titanium or titanium alloys (E = 107 GPa, density = 4.54 tons/m^3) leads to a titanium thickness of 1.14 mm (1.2 times the G/E thickness) and a needed mass of titanium of 2.4 x 10^4 tons (3.04 times the earth-baseline mass). Therefore titanium requires a higher structural member mass than aluminum. In addition, titanium has the disadvantage (discussed above) that it is not required for any other SMF outputs, and would therefore add complexity to the lunar refining operations. Aluminum, on the other hand, must t· produced for a variety of other products. Therefore titanium s little to offer over aluminum except a lower coefficient of thermal expansion (9.5 x 10^{-6} m/m°C for Ti; 25.5 x 10^{-6} m/m°C for Al).

For iron or iron alloys (E = 186 GPa, density = 7.9 tons/m^3) the needed thickness is .66 mm (.7 times the G/E thickness), leading to a required mass of iron of 2.4 x 10^4 tons (3.02 times the earth-baseline mass for structural members). The coefficient

of thermal expansion of iron is 11.7×10^{-6} m/m°C.

As listed in Table 3.3 of Sec. 3.4, iron is required in the SPS for DC-DC converters and klystron parts, and is therefore produced on the Moon. In fact, iron is relatively easily available from lunar materials, since it exists on the surface in very pure form, though in low concentrations. This iron can be magnetically separated from the soil by simple equipment. Iron also occurs in various lunar compounds. In general, iron is more easily refined than Al or Ti, because the free energies of compound formation are usually smaller for iron than for Al or Ti; therefore less energy is required to break the iron compounds. A discussion of the effects of the availability of various lunar materials appears in Chap. 13, "Possible System Tradeoffs".

For magnesium or magnesium alloys (E = 43 GPa, density = 1.7 tons/m^3) the needed thickness is 2.8 mm (3.0 times the G/E thickness) and the required mass is 2.2×10^4 tons (2.8 times the G/E mass). Magnesium is listed in Table 3.3 as a constituent in Al alloy for structural members and joints. It would therefore be produced on the Moon if the structural members used Al of Mg as principal material. However, if Al alloy is used, the expected input of Mg to the SMF (listed in Table 4.5, Sec. 4.6) is 180 tons per 10-GW SPS. If production of Mg on the Moon increases the complexity of the refining, then this requirement could be satisfied from Earth. Magnesium would

have to come from the Moon if structural members were magnesium alloy. The coefficient of thermal expansion of Mg is 25.7 x 10^{-6} m/m°C. Therefore magnesium structural members would mass as much as aluminum structural members, would have approximately the same thermal expansion, but would reduce the system design options by requiring lunar production of Mg.

Thus the leading metal-alloy candidates for structural members are aluminum alloys and iron alloys. the production of metal-alloy structural members has several advantages over the production of foamed glass and composites. First, it is a well established technology. Many processes for metalworking are highly developed, and there is a large body of knowledge on metal manufacture in general. Also, the behavior of the finished products is easier to predict (relative to foamed glass and composites), based on the detailed knowledge of metal usage, particularly in the aerospace industry.

Second, the candidate processes and equipment (described in more detail later) for the production of metal-alloy structural members (e.g. alloying furnaces, vapor depositors, continuous casters, rolling mills, cutters, welders) are versatile: their settings or inputs can be varied to produce different outputs. For example, an alloying furnace can produce a range of alloys, for specialized purposes; vapor depositors produce a variety of sheet thicknesses and alloys; rolling mills can produce many sheet thicknesses of different alloys, for a variety of purposes.

The processes to produce foamed glass and composites are more
limited in their range of output.

Third, the metal-member processes are compatible with other
SMF processes, in that they can share pieces of equipment. For
example, alloying furnaces can also feed die casters to make
complex parts; vapor depositors can also coat waveguides; rolling
mills, cutters, and welders can produce ribbon and sheet for the
production of wires, pipes, and radiators. Thus this structural-
member production equipment can be partially combined with other
SMF processes, reducing equipment complexity and number of
machines, and increasing the equipment utilization rate.

Fourth, the production of metal-alloy structural members
can use beam-builders as the final production stage. Since
such devices are now in development, this reduces technical
uncertainty. Although beam-builders are now being designed to
handle composite materials as well, these are earth-variety
composites (e.g. graphite/epoxy), and these machines would re-
quire modifications to handle lunar composites (e.g. S-glass in
Al matrix). Beam builders are versatile machines, and can pro-
duce tribeams or other shapes in a variety of sizes, by changing
the beam-builder settings. In general, if the SMF produces
metal-alloy ribbon for beam-builders, the ribbon can be formed
into a variety of structural shapes for use in both SPS's and
other satellites. By varying the alloy compositions, electrical
or magnetic properties of metal members can be put to use (e.g.
for communications and radar antennas).

Metal alloys also have several disadvantages. They have a relatively high coefficient of thermal expansion (although Ti and Fe are close to the composite S-glass in Al matrix). As mentioned above, the exact effect of the coefficient of thermal expansion (CTE) of the structure on the cost of the SPS is at present unclear, and the use of thermally variable structure may or may not be a disadvantage. Rather, the relatively high CTE of metal alloys is listed as a disadvantage because it brings in a partial redesign of the SPS, not in its geometry but rather in its thermal behavior.

Another disadvantage is that metal-alloy structural members appear to be more massive than the other alternatives, although the mass calculations based on equal stiffnesses may be overly conservative -- see Sec. 3.2.3). Even if the mass estimates are accurate, the effect of increased structural mass on SPS cost is at present unclear, as discussed Sec. 2.2.1. Therefore, although an increased structural mass in the SPS can be expected to raise program costs, this might not be a significant cost-driver in the lunar-material scenario.

The study group decided that the reference SMF produces metal-alloy structural members, because of the advantages listed above, in particular the versatility of the production equipment and the commonality of that equipment with other SMF processes. The SMF produces rolls of ribbon, to be shipped to beam-builders at the assembly site for SPS's or other satellites.

A more difficult decision was the choice of aluminum over iron as principal metal in the structural member ribbon. One factor in the decision is the advantage in having structural members and joints made of the same material. This is not because of corrosion (galvanic action does not happen in vacuum) or weldability (EB welders can bond dissimilar materials), but because of differential expansion problems due to thermal cycling during SPS eclipse. This cycling would lead to fatigue of the bonds between members and joints. Although there are no clear-cut advantages in aluminum members over iron members, there may be two advantages to aluminum joints. First, they are easier to machine than iron joints, and this simplifies production processes at the SMF. Second, the study group anticipated that the joints would require parts brought from Earth (due to manufacturing complexity), and that Al alloy parts might mass less than steel parts. In fact, since the joints account for only 16 tons of each 10-GW SPS (see Sec. 3.2.10), economics may well dictate that the entire joints come from Earth. However, the masses of Al and steel joints depend on specific joint designs, a task beyond the scope of this study. The differences in mass are not likely to significantly alter the cost of the SPS program.

Therefore the study group could not identify any clear-cut advantages separating Al and Fe for structural members. The deciding factor was the feeling of the study group that if the structural member designs in the SPS were reoptimized for Al alloys and for steels, rather than the earth-baseline G/E, the

structural mass would be less for Al alloys than for steels.
Therefore the study group chose Al alloy as the material for the
structural member ribbon produced by the reference SMF.

5.3.2: Basic Options in Al Structural Member Productio . The
first decision in the development of ribbon production options
is the choice of aluminum alloy. Favorable criteria include
minimum number of different alloying elements, to reduce equip-
ment complexity; alloying elements available on the Moon, to
avoid the need for Earth inputs; high yield strength and hard-
ness, to make the structural members damage-resistant. Two Al
alloys with the desired characteristics and minimum number of
different lunar alloying elements are 5052 (2.5% Mg, 0.25% Cr)
and 6063 (0.7% Mg, 0.4% Si). Consultation with Dr. Robert Waldron
of the Lunar and Planetary Institute indicated that the refining
processes suggested by the JSC-LPI study (Ref. 5.3) could produce
magnesium with minor alterations, but that obtaining chromium
would be more difficult. The study group therefore selected
Al 6063 alloy. There are several basic options for production
of ribbon from this alloy. These alternatives are presented in
Table 5.10.

Lunar alloying and fabrication is possible, since all the
elements required are available on the Moon, and if the Moon-SMF
transportation is provided by rocket, rather than catapult (e.g.
mass-driver), the structural member ribbon could be entirely
fabricated on the Moon. However, this alternative would limit

TABLE 5.10: BASIC OPTIONS IN STRUCTURAL

MEMBER RIBBON PRODUCTION

Option	Advantages	Disadvantages
Lunar Alloying and Lunar Fabrication	o Conceptually simpler	o Limits transportation options o Adds complexity to lunar operations
Lunar Alloying and SMF Fabrication	o Conceptually simpler	o SMF should include alloying equipment anyway o Adds complexity to lunar operations
*Conventional Al Alloy Ribbon Production	o Established technology o Few machines o Compatible with other SMF processes	o Massive equipment
DV of Al Alloy Ribbon	o Existing technology. o Compatible with waveguide production o Well adapted to space environment	o Many material sources required

*Chosen for the reference SMF

the system's options. Therefore the study group decided that the fabrication of structural member ribbon will take place at the SMF, to keep open the possibility of catapult transportation. Note, as discussed in Sec. 4.5 that the physical shapes received by the reference SMF are slabs, rods and bags of powder, assuming rocket transportation. However, the reference SMF could handle catapult payloads instead without extensive modifications; therefore the reference SMF design leaves the catapult option open.

Lunar alloying and SMF fabrication is another option. The aluminum alloy could be alloyed on the Moon prior to shipment, since the needed materials are available there. However, to

preserve the options of switching to other alloying elements
from Earth, and of making other alloys including Earth elements
for other SMF products, the study group decided to include
alloying processes and equipment in the SMF. This also has the
advantage that it lessens the complexity of the lunar operations,
possibly reducing the personnel requirements and the associated
transportation costs to and from the lunar surface.

Therefore the task of the reference SMF is to produce rolls
of .74-meter-wide, 1.77-mm-thick ribbon of Al 6063 alloy, from
solid rods of aluminum, silicon, and magnesium. Two basic
options for this ribbon production are conventional methods
and direct vaporization. The study group chose the conventional
methods of production for the reference SMF. However, the com-
parison between the two alternatives is complicated, and neither
option has a clear-cut advantage over the other. In the early
stages of the study, the research team intended to design first
an SMF using conventional ribbon production, then an SMF using
DV of ribbon, and to compare the two. However, the preliminary
design and costing of the reference SMF indicated that the cost
was driven primarily by the design of the solar-cell production
equipment. Also, preliminary design of the two ribbon pro-
duction options indicated that their difference in cost is
probably not significant. The study group therefore concen-
trated its efforts on solar-cell production design, leaving
the evaluation of the DV of Al alloy ribbon for later studies.

Conventional Al alloy ribbon production uses a string of
processes: melting and alloying of the aluminum; casting

into solid slabs; rolling of the slabs to ribbon thickness; end
trimming and welding to form long ribbon; packaging of the
ribbon. These processes therefore require a melting and
alloying furnace, a slab caster, a rolling mill, an end trimmer
and welder, and a packaging system. Alternative equipment de-
signs are discussed in the following sections.

As discussed in Sec. 4.5, if raw materials are launched
from the Moon by chemical rocket, they can arrive at the SMF
in specialized shapes such as rods and slabs. This suggests
the option of feeding slabs brought from the Moon directly to
the rolling mill, thus avoiding the need for a furnace and slab
caster. However, as mentioned above, the study group decided
to include alloying equipment in the SMF to increase the
versatility of the facility, and to reduce lunar processing
complexity. Given a set of melting and alloying furnaces and
associated slab casters at the SMF, the use of this equipment
to produce pure Al slabs (for other SMF products) as well does
not significantly increase the SMF cost (this equipment, even
when designed small, has a large production capability).

Therefore the inputs required for pure-metal or alloy pro-
ducts (aluminum, iron, magnesium, and some of the silicon)
are shaped as rods sized for input into furnaces. This choice
also preserves the option of launching materials from the Moon
by catapult (e.g. mass-driver), since the rod inputs can be
replaced by pellet inputs with relatively minor modifications
to the equipment. These modifications are described in
Sec. 5.10.

There are three principal advantages in conventional ribbon production. First, the technology is very well established, reducing the technical uncertainty of proposed designs. The design of earth furnaces is strongly affected by the presence of gravity; hence space-specific furnaces must be developed. The availability of vacuum and energy in space makes electron-beam welding a likely substitute for more conventional welding techniques. However, the remaining equipment designs are not very dependent on gravity or atmosphere, and can therefore be adapted to space use without extensive modifications. Even the space-specific furnaces and welders share much of their technology (i.e. refractory coatings   lements, cooling systems) with earth equipment. Therefore m c   the sizable body of knowledge of earth machinery can b applied to ribbon production in space.

Second, the conventional equipment has high throughput rates and therefore requires few machines. Preliminary design indicates that the total structural member ribbon requirement for one 10-GW SPS per year can be produced by one small furnace, one slab caster, one rolling mill, and two end trimmers, welders, and packagers. The required production of 6.5×10^6 meters (23,000 tons) of Al alloy ribbon per year is very small y earth production standards.

Third, the equipment used in ribbon production can be shared with a variety of other SMF processes. As mentioned in

the last section, alloying furnaces can also feed die casters
to make complex parts; rolling mills, trimmers, and welders
can produce ribbon and sheet for wires, pipes, and radiators.
This reduces the complexity and number of machines in the SMF,
and makes more efficient use of the equipment.

The important disadvantage of the conve tional equipment
is that it is more massive (especially the furnaces, caster
and rolling mill) than the equipment for the direct vaporization
alternative. This increases the initial cost of transportation
of the SMF from Earth.

Because of its versatility and compatibility with other
SMF processes, con   onal production of Al alloy ribbon was
chosen for the reference SMF. However, the DV option described
below is also a likely candidate, and both options deserve
further study.

Direct vaporization of Al alloy ribbon is a more tech-
nologically advanced alternative to conventional ribbon pro-
duction. The basic process is similar to the DV processes
described in solar-cell production (see section 5.2). Figure
5.15 shows a simplified DV ribbon production system. EB guns
or lasers boil Al atoms away from a solid source of aluminum.
The atoms travel to a deposition belt and solidify, forming a
sheet. The alloying elements are boiled off in the same manner
and co-deposited with the Al, forming the required alloy;
another option is the ion   implantation of the alloying
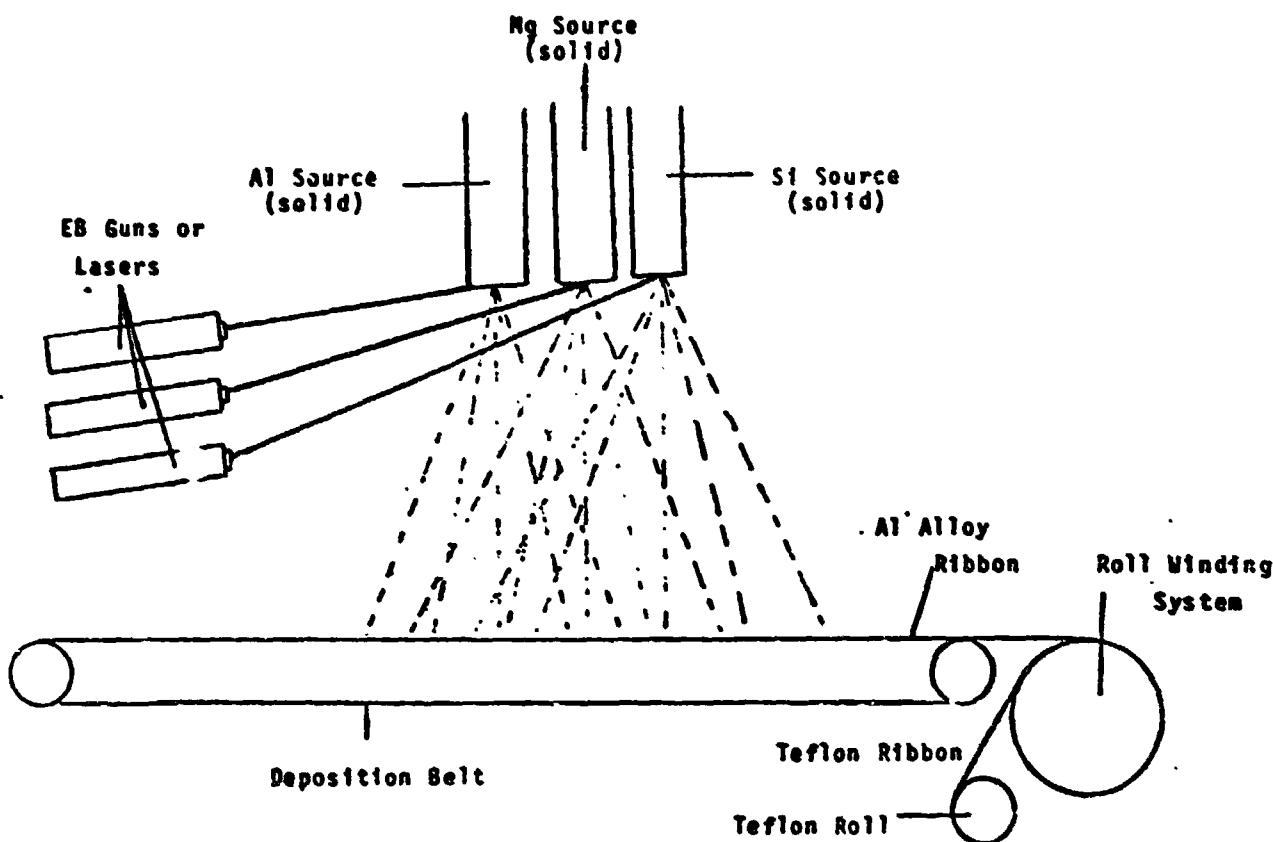
FIGURE 5.17: SIMPLIFIED VIEW OF DV OF AL ALLOY RIBBON

elements (see section 5.2.4). The deposition belt must be de-
signed to remove the thermal energy of the gaseous-to-solid
phase change of the deposited materials. As the belt travels
through the deposition section, the sheet builds up to the
needed thickness. It is then peeled from the belt as a con-
tinuous ribbon and wound onto a roll. To avoid vacuum-welding
of the Al alloy surfaces, teflon film is wound between
successive layers of ribbon. The rolls of ribbon are then
shipped to the assembly site for SPS's or other satellites; the
roll cores and teflon film are later returned to the SMF for
reuse.

The principal requirements of the system are energy and a good vacuum (deposition pressures are on the order of 10^{-6} Torr). One source (Ref. 5.29) suggests that Al can be deposited at rates up to 50 microns/sec by using 1200-kW EB guns. Another source (Ref. 5.30) indicates that deposited metals have mechanical properties similar to those achieved by casting, rolling, and annealing. Therefore the ribbon thickness needed for the structural member ribbon is 1.77 mm (as calculated in section 3.2.3), and the deposition time is 35 seconds. For the production of one 10-GW SPS per year, the required output is 825 meters of ribbon per hour, assuming a 90% duty cycle. If 7 deposition belts travelling at 2m/minute are used, the deposition length of each belt is 1.2 meters.

There are several advantages to DV of ribbon. First, it is existing technology. Commercial DV processes produce metal sheets and coatings, though not yet at the 50 micron/sec rate mentioned above. Some research should be done, however, on possible effects of zero-g on the solidification of the deposited material.

Second, the DV equipment could be shared with part of the waveguide production processes. As described in section 3.2.5, waveguides require a layer of aluminum on their interior surfaces. These could be applied by the DV equipment used in ribbon production. Although solar-cell production processes also require DV of Al, the needed deposition rates are far lower, and the solar-cell handling difficulties suggest using a dedicated production line for solar cell production, rather

than routing solar cell material through DV units shared with ribbon production.

Third, direct vaporization is well adapted to the space environment, because its principal requirements are vacuum and energy. These are cheaply available in an SMF.

The principal disadvantage of DV is that it requires a number of material sources with overlapping deposition patterns to achieve uniform deposition. DV of alloys from separate sources of materials requires a number of alloying element sources interspersed with the Al sources, to achieve uniform alloy composition.

5.3.3: Melting and Alloying: Given the choice of conventional methods of structural member ribbon production, there are a number of alternative designs for alloy-producing furnaces. These candidates are listed in Table 5.11. The study group chose the induction furnace, which requires minimum moving parts and has good control over its contents. The other alternatives described below have specialized uses which may make them useful in certain space applications.

The solar trough collector furnace is shown in Figure 5.18. It is a continuous-flow device for heating materials of various compositions by concentrating solar radiation. The furnace uses a parabolic-cross-section reflector trough to concentrate sunlight into a focal zone with a football-shaped cross-section. This focal zone is surrounded by a pipe covered by a light-absorbent coating. Inside the pipe, particles of lunar material fluidized in a nonreactive gas (such as argon) are heated as

TABLE 5.11: MELTING AND ALLOYING OF AL ALLOY
ALTERNATIVE FURNACES

Type of Furnace	Advantages	Disadvantages
Solar Trough Collector Furnace	o Uses direct solar heat o Low-maintenance device o Accepts varied input shapes	o Not likely for melting material o Requires accurate pointing
Rotating Furnace	o High throughput per furnace o Accepts varied input shapes	o Difficult to control alloying elements o Requires safety systems o Requires maintenance
Solar Paraboloid Furnace	o Uses direct solar heat o High throughput per furnace o Accepts varied input shapes	o Requires accurate pointing o Difficult to control alloying elements o Requires safety systems o Requires maintenance
*Induction Furnace	o Accepts varied input shapes o Almost no moving parts o Good control over contents o High throughput per furnace	o Can only handle certain materials

*Chosen for the reference SMF

they travel down the pipe. This type of furnace can reach temperatures of about $1500^{\circ}K$, a limit imposed by the geometry (Ref. 5.31).

The study group has investigated methods to determine the temperature of particles travelling through the pipe as a function of residence time, density of particles, characteristics of gas and particles, and flow velocity. This is a complex problem involving both radiative and convective heating and variable viscosity of the gas (temperature-dependent). Though
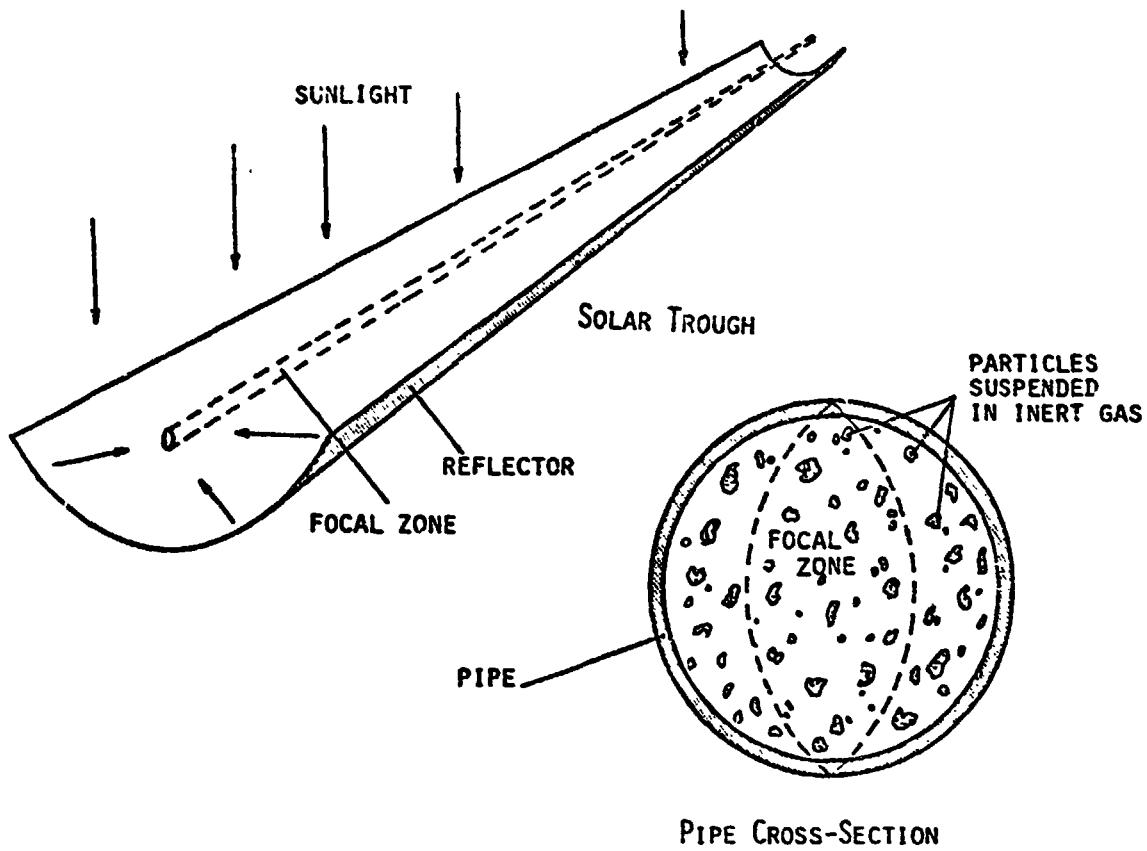
FIGURE 5.18 : SOLAR TROUGH COLLECTOR FURNACE

some simplifying assumptions are possible (treating the gas-
particle mixture as a continuous fluid, for example), the final
design of such a furnace would probably require both ground
and Shuttle prototypes.

The principal advantage of this design is that it uses
direct solar heat, avoiding the need for less efficient energy
conversion systems. This furnace is also a low-maintenance
device, with very few moving parts. Another advantage is that
the furnace can handle various input shapes, such as particles
of material catapulted from the Moon, or rods of material
brought by rocket (provided the rods fit inside the pipe).

However, this design is not likely to be a melting furnace,
due   problems with molten particles sticking in the pipe.
The device could be an efficient, low-maintenance device for
preheating materials, but that option would require an

additional furnace to melt the material. Another disadvantage
is that solar reflector furnaces require accurate pointing
towards the Sun (typically $\pm 1^0$).

A rotating furnace is shown in Figure 5.19. It consists
of a rotating molten-metal container, non-rotating feed and
output systems, and non-rotating heating coils surrounding the
container. During the operation of the furnace, molten material
is spun to the outside of the container. Solid metallic par-
ticles, fluidized in a non-reactive gas (such as argon) are
injected through non-spinning feed pipes and thrown towards the
outside of the spinning container. The argon is pumped back
out through a non-spinning pipe, not shown in the figure. The
particles hit the molten material, stick to the melt, and
mel in turn. Although the feed system shown handles particles,
rod can be fed at an angle through the cover plate, directly
entering the melt.

Since the molten metal is in a centrifugal force field,
it will separate into a layer of dense metal and a layer of
less dense liquid or semiliquid slag, with the slag floating up
toward the rotation axis. In view of the expected high
purities of the inputs (see sec. 4.4), very little slag should
form. The liquid metal is pushed up (toward the rotation axis)
through channels in the container, by means of magnetic pumps
(which can both heat and move the material). The molten metal
leaves the container through an axial, spinning pipe. It
then flows through a rotation bearing and into a non-spinning
pipe which leads it to the next step in its processes. The

FIGURE 5.19: CROSS-SECTION OF ROTATING FURNACE
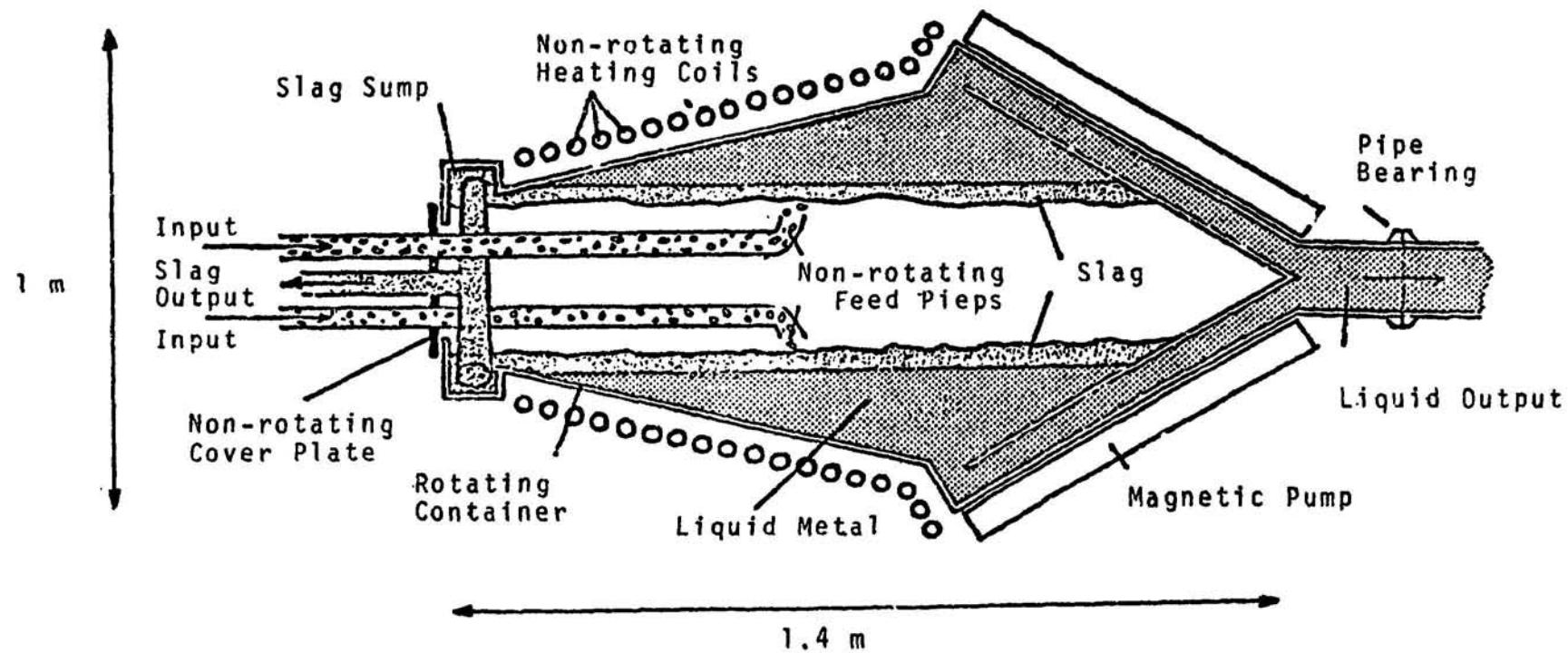
Capacity: .37 m² liquid metal (1000 kg Al)

Estimated Production Rate: .17 m³/hr liquid metal (460 kg/hr Al)

Estimated Mass of Rotating Container (dry): 130 kg

slag flows into a sump, whence it leaves the furnace by being ram-forced up non-rotating tubes and/or by being pushed into the tubes by a pressure differential. The slag then leaves the furnace through an axial pipe through the non-rotating cover plate.

The dimensions and production estimates (Ref. 5.32) listed in the figure indicate that a compact furnace can produce a high throughput of molten Al. Given the listed production rate of 460 kg/hr of Al, one furnace could produce the required 23,000 tons of aluminum for structural member ribbon (for one 10-GW SPS) in 2.1 days. Another advantage of this design is that it can handle inputs in varied shapes (e.g. particles, rods).

Unfortunately, the density gradient which separates liquid metal and slag also tends to separate out the alloying elements if they are added to the melt in the container. This makes control of the alloy composition difficult, unless the alloying elements are mixed with the molten Al after it is pumped out of the rotating furnace. Another disadvantage is that the container is a moving part filled with molten metal, which poses a safety hazard in case of rupture. The furnace also requires maintenance on the moving container and the feed and output systems.

The solar paraboloid furnace (see Figure 5.20) combines the energy efficiency of solar collectors with the liquid-metal handling ability of the rotating furnace. The paraboloid
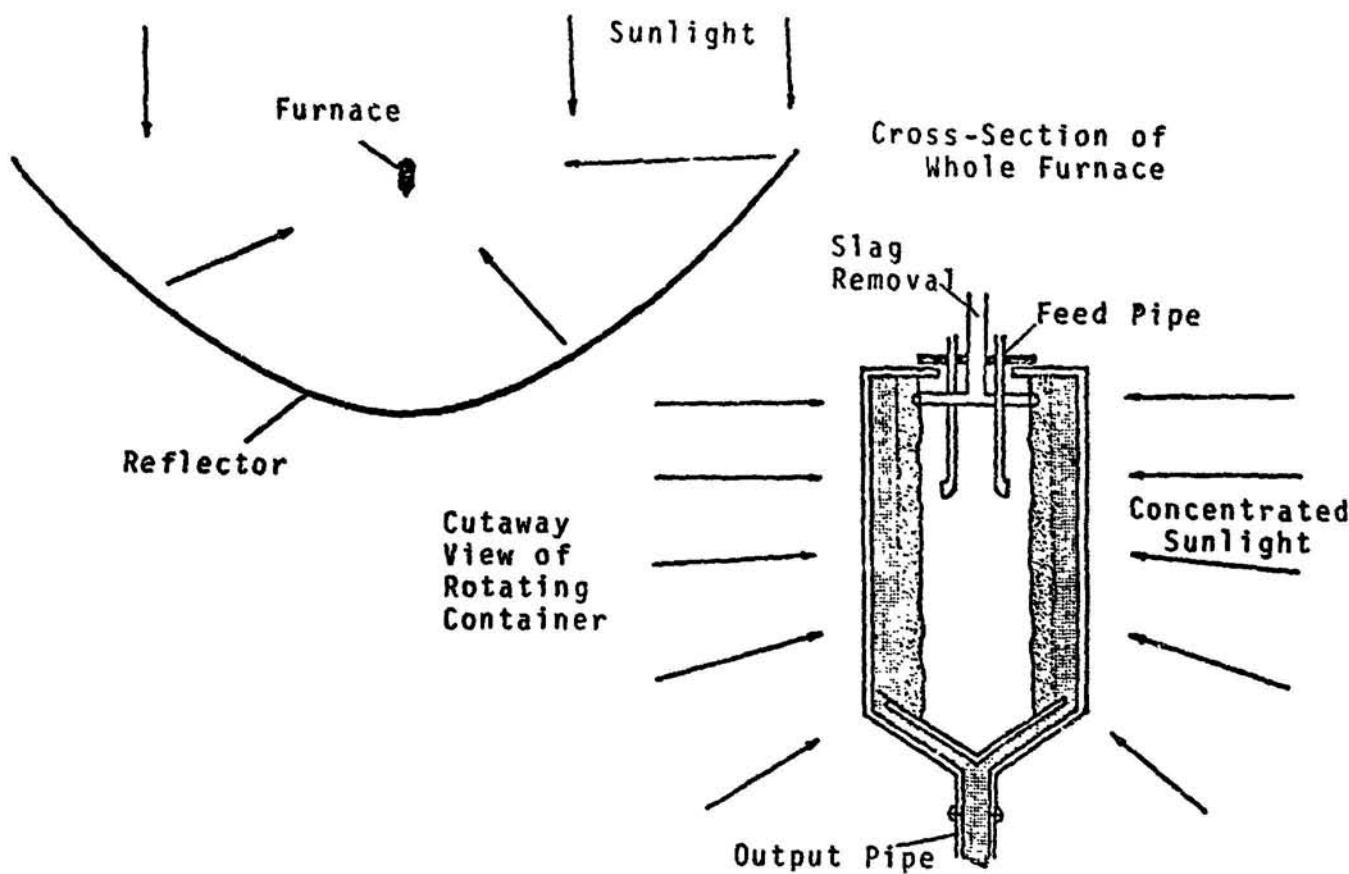
FIGURE 5.20: SOLAR PARABOLOID FURNACE

geometry concentrates the light onto a rotating container. This
more efficient geometry can produce temperatures up to about
$5000^{\circ}K$. The furnace operates in the same fashion as the
rotating furnace, but with sunlight replacing electricity as
the power source. Rotating container, feed and output systems
are conceptually similar to those of the rotating furnace.

Like the solar trough collector, this hybrid design has
the advantage of direct use of solar heat, and the disadvantage
of a roughly $\pm 1^{\circ}$ pointing requirement. Like the rotating furnace,
the solar paraboloid furnace has the advantages of a high
throughput per furnace and the ability to accept inputs in

5.113

varied shapes, and the disadvantages of difficulty in controlling
alloying elements and the requirements for safety systems and
maintenance.

The <u>induction furnace</u> is based on the principle that a
rapidly alternating magnetic field induces currents in metal,
causing resistive heating and melting   that metal. Earth-
based induction furnaces usually consist of a cylindrical coil
surrounding a container of metal. The coil acts as the primary
of a transformer, and the metal charge ˋ   as the secondary.
Ideally, the melt would completely ᵡ   ᴗontainer.

There are compromises between furᵣᵤᴗe capacity, heat loss,
and coupling between coil and metal. Placing insulation between
metal and coil reduces heat loss, but lessens the electrical
coupling and thus results in less efficient heating. There
are tradeoffs between furnace capacity, frequency and power of
electrical current, and output rate. The following examples
(Ref. 5.33) are from current steel-producing technology:

```
  5 kg capacity furnace using   30 kW at 10,000 Hz produces   30 kg/hr
450 kg      "           "      "     350 kW at    960 Hz    "      450 kg/hr
4500 kg     "           "      "    1250 kW at    180 Hz    "     1800 kg/hr
```

As the list above shows, there are economies of scale in
energy consumption. In general, the typical losses in current
induction furnaces (Ref. 5.33) are:

Motor generator loss:	12% of input power		
Capacitor and Conductor loss:	5% "	"	"
I^2R coil loss:	11% "	"	"
Radiation loss:	10% "	"	"
Useful heat in metal and slag:	62% "	"	"

However, by 1990 a well-designed induction furnace can be expected to be 80% efficient.

Magnetic induction can move the material as well as heat it. If the electrical current through the induction coils is not only alternated but pulsed as well, an electromagnetic force is produced on the currents induced in the material. This force pushes on the material, and it can be used to contain or handle the melt. The coil geometry and the pulsing sequence determine the direction and magnitude of the force applied. With careful design, the same coils can heat and handle the melt. Current experimental induction equipment can levitate a lump of material against the force of gravity and melt it while suspended (one such device is in the M.I.T. Dept. of Materials Science and Engineering, in the Induction Laboratory).

The basic design of a space-specific induction furnace is shown in Figure 5.21. This non-rotating furnace consists primarily of a heat-resistant container surrounded by magnetic induction coils. Although magnetic induction coils can be used for containerless melting and movement of materials, in this application magnetic forces are used to build pressure gradients in the melt, and the pressurized melt therefore requires a containment vessel.

The induction coils serve two functions. First, they heat and melt the material in the container. Second, they induce forces and motions in the melt: an overall volumetric force towards the output of the container, which forms a pressure
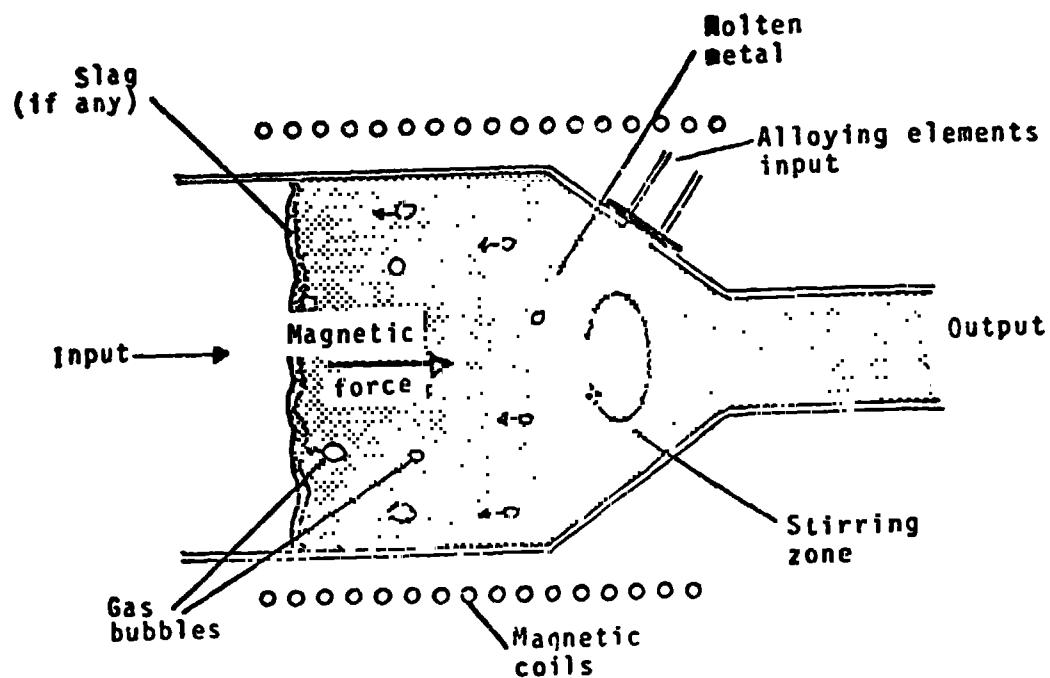
FIGURE 5.21:   MAGNETIC INDUCTION FURNACE

gradient in the melt; and a stirring motion near the output end.
The pressure gradient (increasing from input to output) moves
lighter-density slag and gas bubbles away from the output end
of the container.   The st: 'ng motion blends in alloying ele-
ments let in through a secondary input valve.   Formation of slag
can be enhanced by introducing slagging agents into the furnace.

This furnace design actually allows several heating options.
The container could be heated by resistance coils, leaving the
magnetic coils for melt-handling alone.   Or sunlight could be
directly focussed on the container (with adequate protection
for the magnetic coils) using a paraboloid solar collector.

Magnetic induction furnaces such as the one in Figure 5.21 have several specialized requirements. Since the magnetic field inside the coils heats most metals, container walls and insulation must be made of refractory materials (a mix of 70% MgO and 30% Al_2O_3 is often used on Earth). (Although refractory coatings are required in all furnace containers, they are often supported by a metallic shell in resistance or arc furnaces.) In addition, the container walls and insulation in induction furnaces must allow the magnetic field through them and into the melt. The coils also produce powerful fields outside the furnace, requiring the use of nonmetallic support structure. The coils themselves must be electrically insulated to prevent arcing, and this insulation must be refractory. Finally, the coils generate heat and must be cooled (most earth-based induction furnaces use water-cooled coils).

There are four principal advantages in the use of induction furnaces in an SMF. First, they can accept a variety of input shapes. Particles of input material can be pumped into the furnace suspended in a nonreactive gas such as argon. The particles impact the melt and stick in it, while the argon is pumped out through a filtered outlet. Or rods of material can be fed continuously into the melt by mechanical means. In this option the furnace can operate in vacuum, open to space, since melt containment is magnetic. However, a low pressure in the input section (on the order of 10^{-4} atmospheres) can reduce corrosion and boiloff problems at the liquid-surface/container
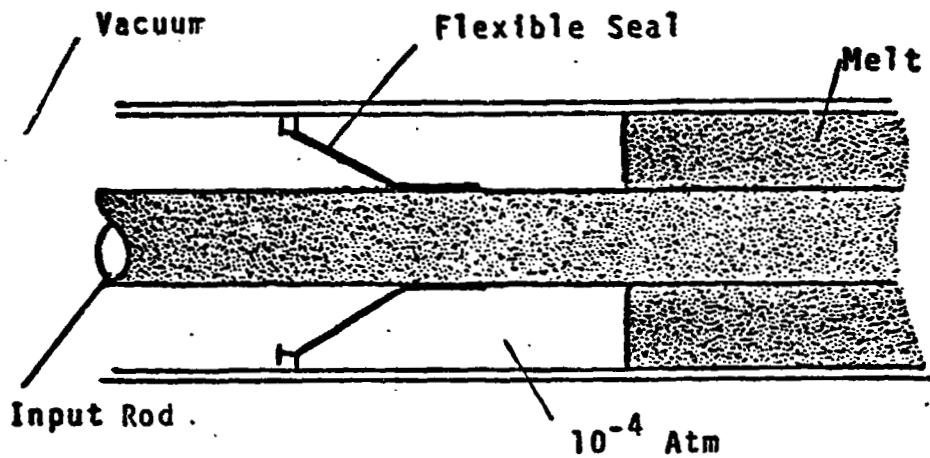
FIGURE 5.22: INDUCTION FURNACE PRESSURE SLEEVE

wall interface. This can be provided by a pressure sleeve, as shown in Figure 5.22. The furnace does not require a pressurized environment outside the sleeve, however.

Second, induction furnaces have almost no moving parts (only feed systems, input valves for alloys, cooling systems for the coils). This reduces wear and simplifies maintenance. As in all container furnaces, the furnace cannot be shut down without first draining it, since solidification of the melt usually destroys the container lining (because of differential contraction of melt and container). However, in an induction furnace coils can be separate from the container, allowing removal and repair of individual coils without shutting down the furnace.

5.118

The third important advantage is the high level of control over the contents of the furnace. The stirring action in the alloying section thoroughly blends the alloy constituents, producing uniform composition. Gas bubbles and impurities are removed by the induced pressure gradient, and the input surface is controlled without recourse to physical containment or centrifugal force. Also, the output molten material can be pressure-fed down a pipeline to the casting devices, pushed by the furnace's magnetic force.

Fourth, induction furnace throughputs are similar to those of the rotating furnaces described above. Therefore a compact induction furnace can easily handle the Al alloy requirement for structural member ribbon.

The principal disadvantage of the induction furnace is that it can operate only on certain materials. Since the magnetic fields must induce currents in the melt, the molten material must be electrically conductive. Furthermore, to heat and control the whole melt, the magnetic fields must penetrate throughout the molten material; therefore materials whose magnetic properties resist this penetration cannot be melted by induction. For example, although the conductivity of molten silicon is sufficiently high, its magnetic properties do not allow deep penetration of the magnetic fields. Therefore, although silicon in thin slabs or rods can be zone refined by induction (see sec. 5.2.3), larger melts of silicon in an induction furnace require very powerful fields, and are therefore

unlikely. Fortunately, the SMF does not require the melting of large loads of silicon. Meta.s such as aluminum, iron, and magnesium, and thin rods of silicon can all be melted by induction.

Based on the advantages and disadvantages of the options described above, the study group chose the induction furnace for the melting and alloying of aluinum for structural member ribbon.

5.3.4: Slab Casting: The most advantageous process identified by the study group for the conversion of molten Al alloy to slabs is continuous casting followed by slab cutting. The continuous caster is shown in Figure 5.23. The caster consists of a
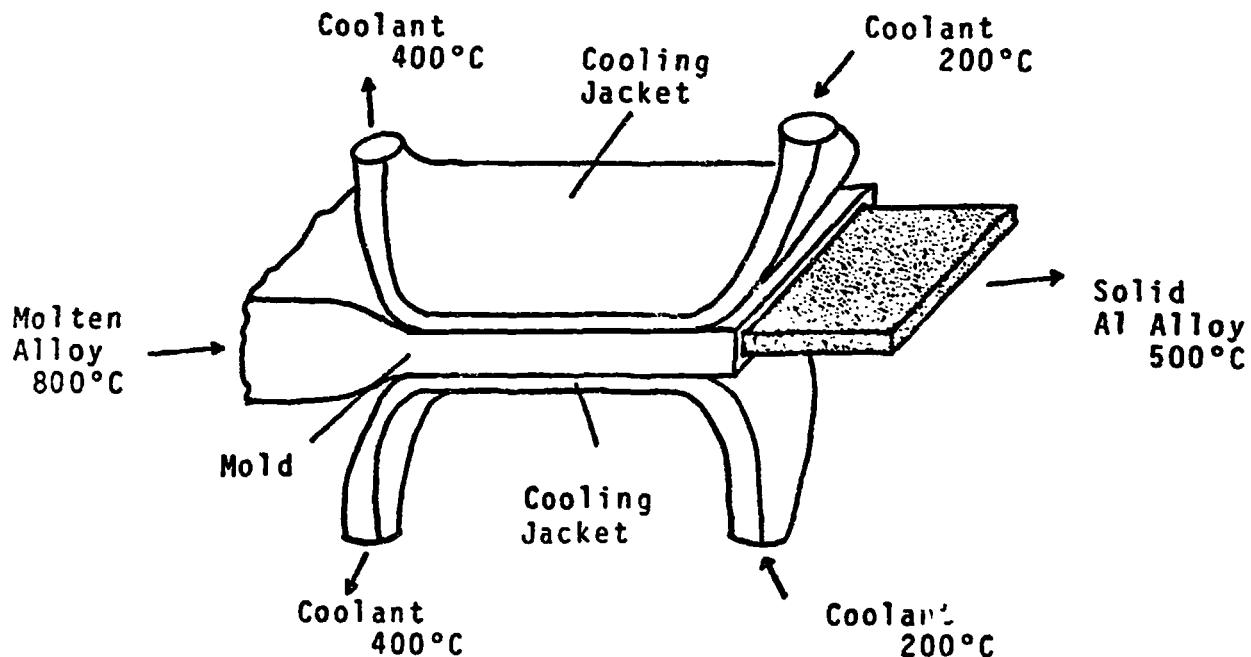
FIGURE 5.23: CONTINUOUS CASTER

rectangular-cross-section mold between two cooling jackets. Aluminum alloy is pressure-fed through the mold. Cooling fluid is fed through the cooling jackets, removing heat through the mold surface from the solidifying alloy. The alloy emerges as a solid continuous slab. For the production of structural members, the slab cross-section is sized at .70 m wide by .02 m thick. The .70 m width expands to the required ribbon width of .735 m during later rolling. The 2-cm thickness is the result of trading off the ease of liquid metal injection and the ease of rolling the resultant slabs.

If the caster is sized for 1 kg/sec production of Al alloy (2.7 cm/sec slab output speed), preliminary design calculations (Ref. 5.34) indicate that if liquid sodium is used as a coolant, a cooling fluid mass flow rate of 2.8 kg/sec is required through the jackets. The length of the mold is estimated at .8 meters. Because of its high conductivity and resistance to corrosion by aluminum, graphite was chosen as the mold material. The hot coolant coming from the caster is routed through radiators for cooling, then reused.

The inlet Al alloy pressure is estimated at 690 kPa (100 psi). This can be provided either by the induction furnaces or by electromagnetic pumps (as shown in Figure 5.24). In such a pump an electric current and a magnetic field are passed through the liquid metal, perpendicular to each other, thus creating a force on the fluid along the pipe. Other options include magnetic induction pumps (similar to the induction
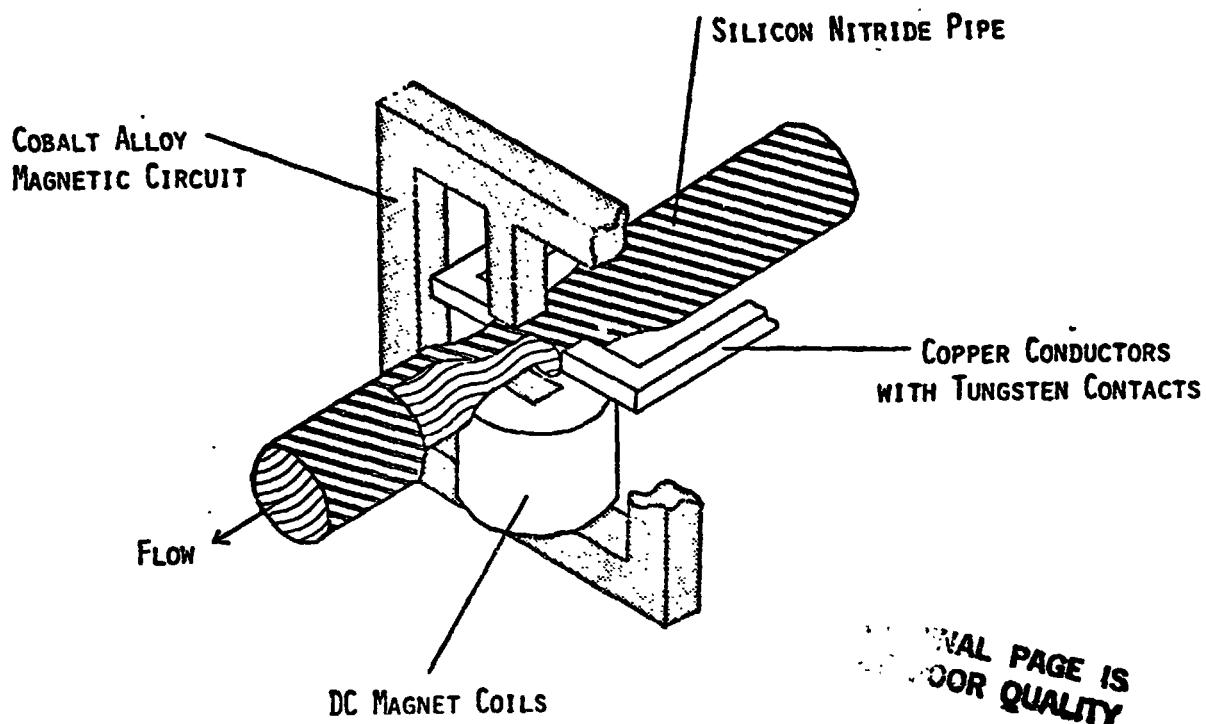
FIGURE 5.24 : ELECTROMAGNETIC PUMP FOR MOLTEN METAL

Labels on figure:
- COBALT ALLOY MAGNETIC CIRCUIT
- SILICON NITRIDE PIPE
- COPPER CONDUCTORS WITH TUNGSTEN CONTACTS
- FLOW
- DC MAGNET COILS

furnaces) which are heavier than electromagnetic pumps, and graphite turbopumps, which require more maintenance and more complicated repair. Electromagnetic pumps are a highly reliable current technology (Ref. 5.35).

The continuous caster is also well-establisned current technology, commonly used in the metals industry to produce slabs and billets. It has a high throughput per machine: at 1 kg/sec, the caster shown above produces the 23,000 tons required for the structural member ribbon in one 10-GW SPS in roughly 300 days (on a 90% duty cycle). Continuous casters are highly reliable devices with duty cycles better than 95%.

Liquid sodium cooling systems are common in the nuclear power industry, and have duty cycles near 100% (Ref. 5.36).

Although a rolling mill could directly receive the output of the continuous caster, this output is cut into slabs for several reasons. First, this decouples the operations of the two machines, allowing one to be maintained while the other operates. Second, some of the slabs are stored as a backlog, to maintain production while the caster is down. Third, this leaves open the option of using a reversing rolling mill (which requires discrete slabs) rather than a continuous rolling mill (which can handle continuous input).

To cut the caster output into slabs, either mechanical or beam cutters can be used. Mechanical cutters (such as shears) were rejected because of the large loads in cutting 2-cm-thick Al alloy, which requires massive equipment. Also, the smoothness of a mechanical cut is poorer than that of a beam cut; a smooth cut eases the rolling mill feed process and leads to smoother edges in the rolling output.

Beam cutters (either electron beams [EB] guns or lasers) work by boiling away a fine slice of the material. Since they must boil this material as well as expose surfaces, their power requirement is higher than for mechanical cutters. However, this is not a serious disadvantage at the SMF, where energy is cheaply available. Beam cutters also benefit from vacuum, which is necessary for EB guns, and useful for lasers (gases tend to defocus laser beams). For the cutting of metals, EB guns were

selected over lasers, because lasers are less efficient and re-
quire more maintenance and repair than EB guns (Ref. 5.37). The
basic components of an EB gun are shown in Figure 5.25 (adapted
from Ref. 5.38).

In an EB gun, electrons are boiled off at a filament
cathode and accelerated by a potential of up to several hundred
thousand volts through a cylindrical anode. The electrons are
focussed by an electromagnetic lens to a point on the workpiece.
Deflection coils provide lateral movement of the focal point.
The "bias" device serves as an on-off switch. EB guns work best
when there is no gas to interfere with the beam or to cause
arcing. Typical current EB gun efficiencies are 50%, meaning
that 50% of the input electrical power goes into the electron
beam (Ref. 5.39). Electron beam guns require a closed current
loop, to return the electrons in the beam to the cathode.
Therefore they can only be used on conductive materials, or the
local buildup of charges at the beam impact point will repel
the electron beam, and the buildup of positive charges in the
cathode will eliminate the potential difference accelerating
the electrons.

EB guns are virtually maintenance-free, requiring only
replacement of the filament cathode. For EB welders, current
filament life is up to 40 hours (Ref. 5.40); the more powerful
EB cutters have far shorter filament life, but the study group
expects that 8 hours will be achievable by 1990. Filaments
mass 1-2 grams and can be replaced automatically by a mechanism
which switches two cartridges, reloading the unused one.

CARTRIDGE WITH
FILAMENT CATHODE

BIAS

ANODE

ELECTROMAGNETIC LENS

DEFLECTION SYSTEM

30 cm
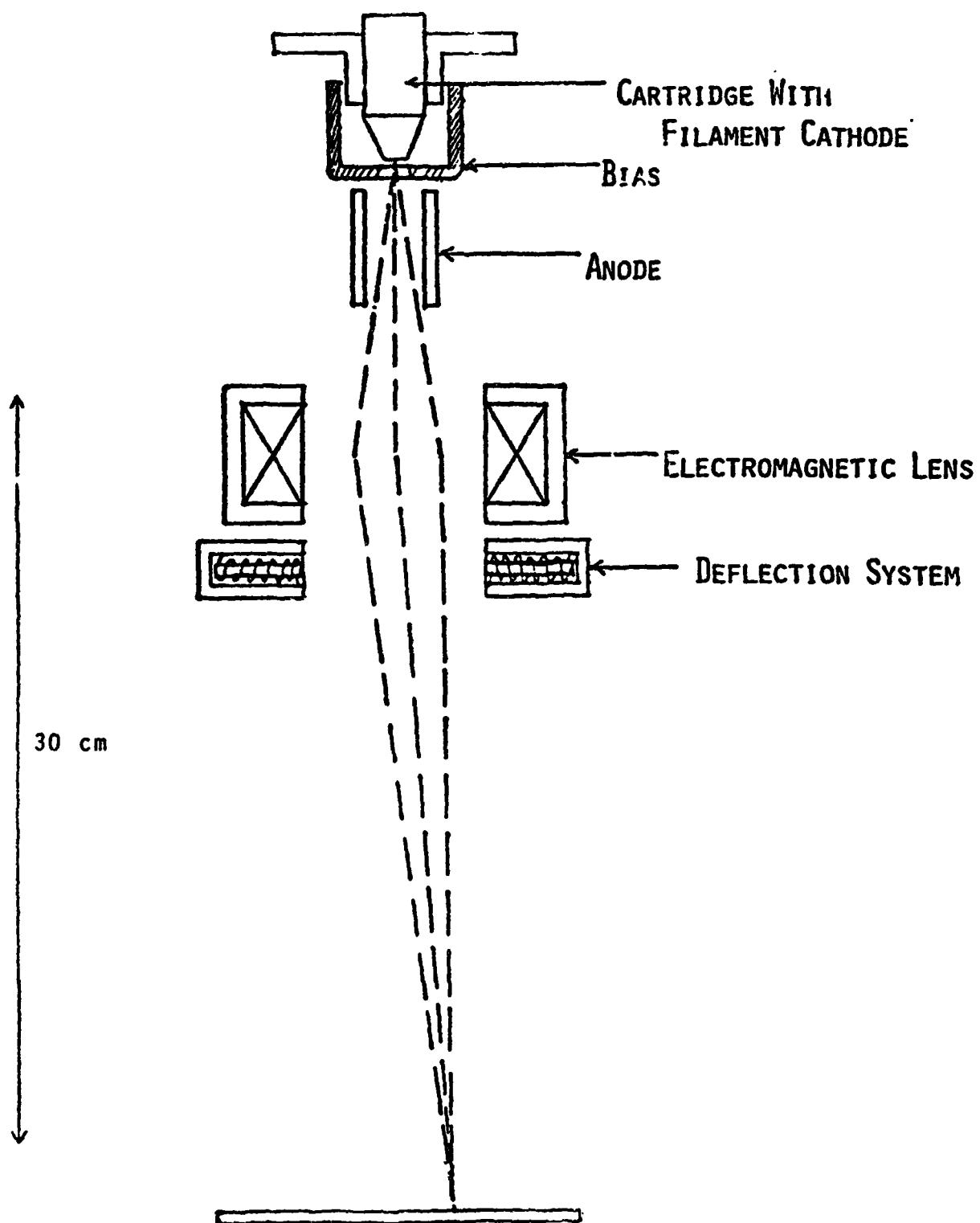
FIGURE 5.25: BASIC COMPONENTS OF ELECTRON BEAM GUN

5.3.5: Rolling: There are two types of rolling mills which can produce ribbon from the Al alloy slabs. A regular rolling mill consists of a series of rolling stands, as shown in Figure 5.26.

INDIVIDUAL ROLLING STAND
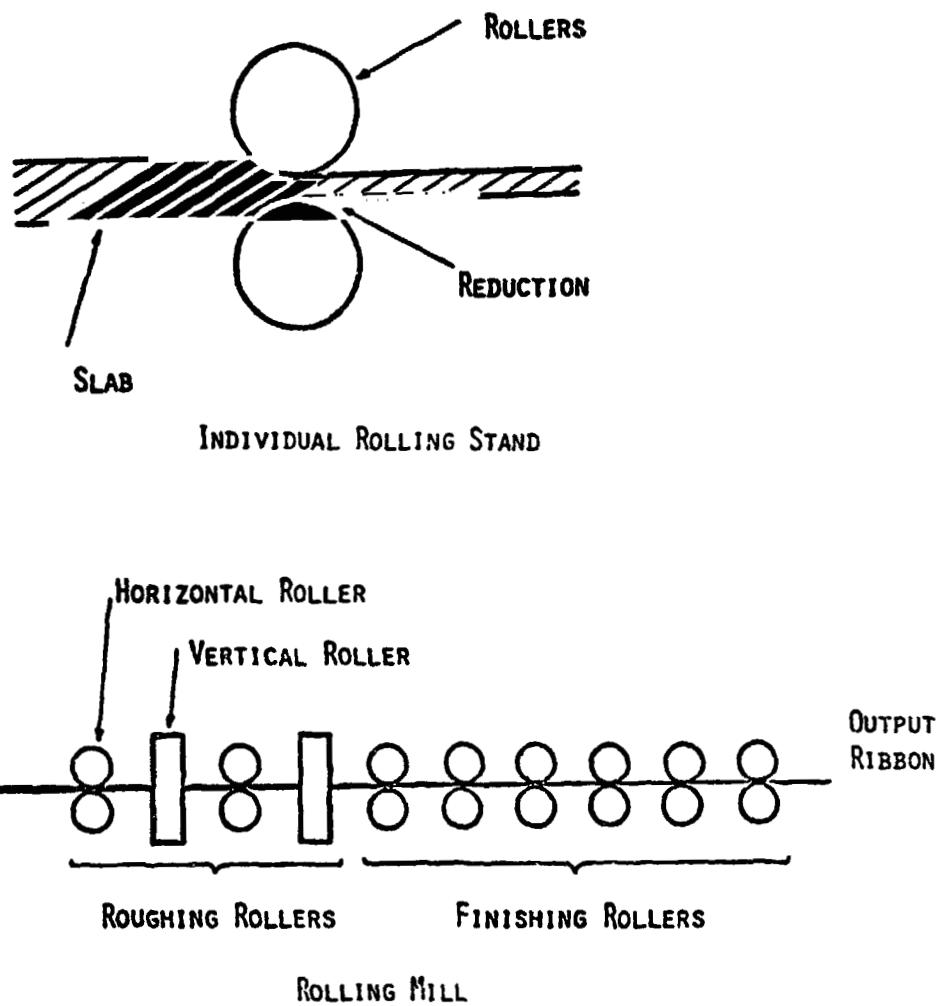
ROLLING MILL

FIGURE 5.26: REGULAR ROLLING MILL

Input slabs travel through one stand after another, and are reduced in thickness by each stand. Each stand rolls the slab only once. Such mills have high production rates.

The other option is the reversing mill, in which slabs are routed back and forth through the same stand several times, and are reduced in thickness by each pass through the stand. This requires a rolling stand with movable rolls, which tighten their gap between passes. Although reversing mills are more complicated than regular rolling mills, they are more versatile and require fewer machines. These mills have lower production rates than the regular rolling mills.

Consultations with industry (Ref. 5.27) indicate that the expected yearly production at the SMF is so low by rolling mill standards that regular rolling mills are not necessary. The lower-mass reversing mills are therefore used in the reference SMF.

Input slabs can also be hot-rolled or cold-rolled. However, if a cold Al alloy slab is rolled to more than 120% of its input length, cracks appear in the material. To avoid this problem, slabs can be annealed between passes or can be rolled hot throughout the process. The final rolling pass should be done cold to improve the structural properties of the output.

The study group chose to hot-roll the input slabs. Slabs therefore travel directly from the continuous caster to the rolling mill, without cooling, or are taken from intermediate storage and preheated before input into the mill. The rolling

mill elongates the input Al alloy slabs by roughly a factor of 11, since it reduces the thickness from 2 cm to 1.77 mm. It also widens the slabs from 70 cm to 73.5 cm, the required width of structural member ribbon. The length of the input slabs is arbitrary, set by handling convenience, although slabs are usuall; at least as long as they are wide. An 80-cm-long slab would then produce roughly 8.8 meters of ribbon.

5.3.6: End Trimming, Welding, and Packaging: To be sent to the SPS assembly site, the structural member ribbon must be packaged for ease of transport and ease of insertion in beam-builders. Since current beam-builders work from rolls of Al alloy, the study group chose rolls as the output shape.

To produce continuous ribbon for this output, the individual pieces of ribbon produced from the slabs must be welded end-to-end. Therefore the ribbon pieces must be end-trimmec to create straight-cut weldable edges (the rolling process produces uneven ends on the ribbon pieces). The side edges of the ribbon are left untouched. As in the cutting of slabs (see section 5.3.4), the cutting options are beam cutters and mechanical shea s. Since the ribbon is thinner than the slabs, a mechanical cutter can produce a clean weldable edge. However, the study group chose EB cutters because they are lighter, more reliable than the other options, and well adapted to the space environment.

The ends of the ribbon pieces are then welded together. Welding options are beam welding (EB or laser), arc welding, and

electrostatic bonding. Welding processes which use fluxes are
not likely for SMF use, since fluxes are usually materials not
available on the Moon. The options listed above require no
fluxes, but may require welding rods made of the material being
welded; such rods could be manufactured at the SMF. Beam welders
work in the same fashion as beam cutters but with less powerful
beams, melting the material rather than boiling it. Both laser
and electron beam welders are used on Earth to produce very high
quality welds (meaning that the welds have nearly the sam-
structural properties as the material).

Arc welding involves applying a large current between the
pieces to be joined and a rod of the same material. An arc is
struck between rod and pieces. The arc melts the material and
the rod is fed into the weld, filling the gap between the pieces
with molten material. On Earth, arc welding rods are commonly
coated with fluxes to prevent contamination of the weld by the
surrounding atmosphere--the flux sets up a gas barrier which
shields the weld zone. In space, the available vacuum prevents
contamination, and flux is unnecessary. However, arc welding
leaves a "bead" of excess material on the weld, which must be
removed to obtain a smooth surface.

Electrostatic bonding is done by applying a voltage between
the two pieces to be welded, then bringing them into contact
along the entire weld surface. A spark jumps across the gap,
fusing the pieces together. This technique is relatively
simple, but it does not produce uniform welds across large

surfaces ` long edges. Also, it requires that the edges be precisely aligned along the entire width of the ribbon at the moment of contact.

Due to their high-quality output and compatibility with the space environment, the study group chose electron beam welders for the production of structural member ribbons. Another factor favoring the choice is that similar (though more powerful) units are used for the end trimming; therefore similar tracking and control equipment can be used. In the actual welding procedure, the ends of the ribbon pieces are first tack-welded together in several places across their width; then the edges are entirely welded. The tack-welds resist the thermal deformations of the edges during welding, keeping the ribbon ends aligned during the process.

After end-to-end welding, the ribbon is wound onto a roller. To avoid vacuum-welding of the Al alloy surfaces to each other, an inert material such as teflon must be inserted between successive layers of structural member ribbon. Other options to stabilize the ribbon surface are oxidation (using jets of oxygen, or running the ribbon through an airlock), and the use of special rolls to keep successive layers of ribbon from touching each other during winding and transportation; these latter options were discarded due to their complexity.

Once the roll of ribbon reaches the diameter used by beam-builders, the last ribbon piece is wound without welding it to the next piece, and the roll is replaced with an empty

roller. After the full roll is loaded into a beam-builder and unwound, the roller and the teflon insert are returned to the SMF for reuse.

5.4: END JOINT AND JOINT CLUSTER PRODUCTION

The requirements for end joints and joint clusters for a 10-GW SPS are estimated at 8 tons of end joints (4000 pieces) and 8 tons of joint clusters (1500 pieces), as listed in Table 3.1. For such low requirements, SMF production can compete economically with import from Earth only if the SMF processes required are minimal. The SMF therefore produces only those parts of the end joints and joint clusters which can be produced by casting alone (since other SMF products require casting also). Any joint parts requiring machining are brought from Earth. This suggests designs for the end joints and joint clusters in which most of the mass is concentrated in a cast "body," with the complicated or precise functions (e.g. snap-locking, angular adjustment) left to lighter parts, brought from Earth and fastened onto the cast pieces. The assembly of the joint pieces can then be done by a machine attached to the beam-builder at the assembly site.

On earth, there are many casting processes used to produce complex shapes (Ref. 5.44). Many of these processes (e.g. sand casting, permanent-mold casting, investment casting, and plaster-mold casting) use gravity to pour the molten material into the mold. Many of these, however, could have the gravity feed replaced by a pressure-feed. Sand casting, however, is

unlikely for SMF use because it would require handling sand in zero-g; handling of powders in space shares most of the problems of handling liquids, as discussed in section 5.2.4. Investment casting requires the production of a pattern for each piece to be cast, and is therefore unsuitable for large-scale production; in addition, the patterns are usually used in a sand-casting process, itself an unlikely option. Plaster mold casting requires production of a mold for every piece cast, and is therefore unsuitable for large-scale production; the molds also require earth materials.

When permanent-mold casting is pressure-fed rather than gravity-fed, it is called die casting. The study group chose this option for the production of complex metal parts at the SMF. The process (as used on Earth) is illustrated in Figure 5.27. Molten metal is poured into a piston chamber. The piston then pushes the metal into the mold (or "die"), pressurizing the molten metal until it solidifies. The pressure reduces the size of any included air bubbles, improving the structure. Once the casting is solid, the mold opens and the part is ejected.

Die casting can be used to make Al or Al alloy parts only in a special variation called cold-chamber die casting. This is because molds are usually made of ferrous alloys, and molten aluminum on hot die surfaces tends to remove some of the ferrous metal. To avoid this, molds are kept cool (relative to the molten metal). The liquid metal therefore solidifies on contact,
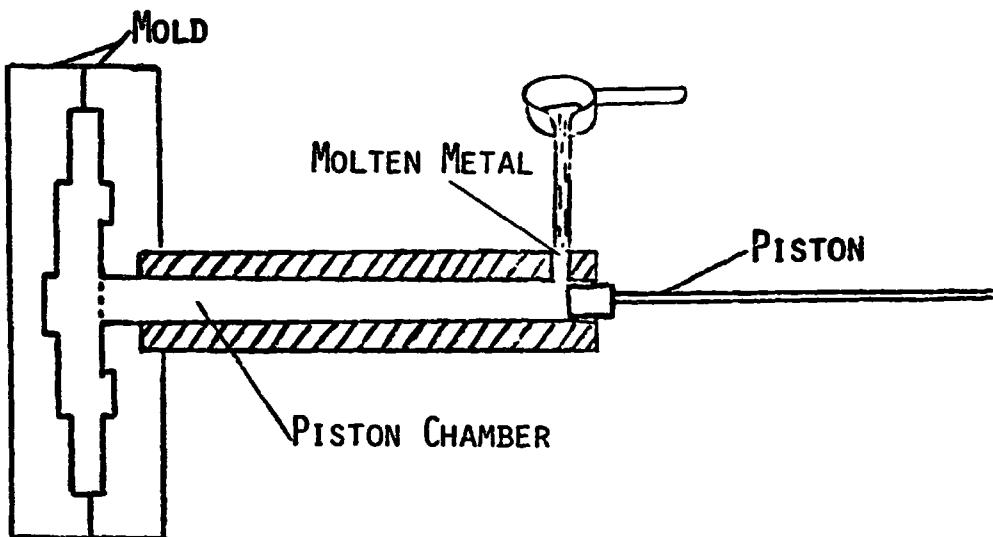
FIGURE 5.27: BASIC DIE CASTING PROCESS

leaving the mold surface intact. The mold therefore requires
active cooling. This technique also requires high feed pressures,
so that the molten metal will flow throughout the die before
solidifying.

Only minor modifications to this process are required for
space use. The molten metal must be pressure-fed from the
pipeline into the piston chamber, using the electr-magnetic
pumps described in section 5.3. The opening from pipeline to
piston chamber must be closable by a valve since the liquid
metal in the pipeline is continually under pressure. The
electromagnetic pumps are limited in their output pressures,
and are therefore not strong enough to feed the mold directly.

The space environment offers two advantages for die casting. First, the molds can be opened to vacuum during each casting cycle, and there is therefore no air or gas to be trapped in the castings during solidification. Second, molds and piston chambers on Earth are sized for gravity as well as pressure forces, and therefore space-specific designs have lower mass.

The present state of knowledge on the effect of zero-g on solidification processes makes a prediction of the output quality of in-space die casting impossible. Zero-g could therefore be an advantage or disadvantage. Experimental research is needed in this area.

Whether on Earth or in space, die casting is a well-established technology, capable of high output (up to 100 pieces per hour), and relatively easy to automate. One piston chamber can feed several molds, either by indexing the molds or by using a set of valves in the feed pipes. The process can produce complex shapes with fine sections.

Die casting also has certain disadvantages. The machinery is massive even in zero-g, because the molds and mold-moving equipment must contain high pressures, on the order of 70 MPa (10,000 psi). The equipment includes complex moving parts such as the piston feed, molten-metal valves, opening and closing systems for the molds, and ejection and handling systems for the castings.

Cold-chamber die casting was chosen for the reference SMF because this process is easy to automate and versatile, and

because its high productivity mitigates the high mass and procurement cost of the equipment.

Another option which should be mentioned is powder metallurgy. Suggested by some researchers as a possible in-space production process, powder metallurgy needs further research to assess its potential. Currently the process requires massive equipment to generate the high pressures requires to fuse the metal powders. Another difficulty is that production of alloy parts requires prior production of alloy powder, adding complexity to the process. Also, the handling and containment of powder is difficult in zero-g. Given a production layout for an SMF which includes furnaces producing molten alloys, casting is the simpler option. However, if the SMF were to receive inputs in powder form, and no furnaces were needed, powder metallurgy could be a favorable option.

5.5 BUSBAR PRODUCTION

As described in section 3.2.6, the busbars in the earth baseline SPS are aluminum sheets 1 mm thick. The Al is as pure as possible, for maximum conductivity. For convenience in manufacturing and handling, the reference SMF manufactures the busbars as strips .74 m wide and 660 meters long (the length of one SPS bay). Therefore 2120 such strips form the required length of 1.4×10^6 meters. The .74 m width is chosen so that busbar strips can be produced using exactly the same equipment as for the structural member ribbon (see section 5.3), although production procedures for these two outputs differ slightly.

For busbar strips, the furnace produces pure (99.6$^+$%) aluminum rather than alloy; the rolling mill flattens the slabs to 1 mm rather than 1.77 mm; and the rolls of busbar strip produced by the roll winder each hold 660 m of strip, rather than whatever length of structural member ribbon is appropriate to the beam-builder.

Therefore the same production equipment can be used for both outputs by alternating materials and production procedures. However, the furnace and continuous caster must be drained before switching from pure Al to Al alloy (or vice versa); since this takes time and involves some loss of material, the furnace and continuous caster should switch input materials only occasionally. If near-continuous production of both is required, intermediate storage of slabs can feed the rolling mill, trimmer, welder, and winder, or two furnaces and two casters can produce both kinds of slabs simultaneously.

5.6 ELECTRICAL WIRE AND CABLE PRODUCTION

5.6.1: Conductor Production: As listed in Table 3.1, 670 tons of wires and cables are produced by the SMF for one 10-GW SPS. This includes 280 tons of insulation on the cables and wires (see section 3.2.8). These wires and cables serve as connectors between strings of panels and as "interbay jumpers" in the SPS. In addition, the klystron solenoids and the DC-DC converters require 2780 tons of insulated wire for coils.

Given the production of 1 mm-thick pure Al ribbon for busbar strips, as discussed in the section above, it is a

relatively simple matter to route this ribbon through a ribbon slicer. This slicer cuts the ribbon lengthwise into 1-mm-wide strips. Each of these strips is therefore 1 mm by 1 mm, and can serve as electrical wire. The square cross-section is an asset in coil-winding, since it leads to greater coil density. As for the wires and cables in the SPS, wire cross-section should not affect performance. If necessary, the width of the strips can be increased, producing wires of rectangular cross-section, with a variety of cross-sectional areas. Or the 1-mm square strips can be bunched together during the insulating process to form cables.

There are two basic options for slicing the Al ribbon into strips: slicing rollers or beam cutters. These options are shown in Figure 5.28. The rollers use a blade-and-slot con-figuration to slice through the ribbon. Slicing rollers offer simplicity, low power requirement, small need for Earth inputs (mostly lubricants). However, the roller system is analogous to a rolling mill, and the equipment is massive. The cut edges are not as sharp as those cut by beams. Also, the slicing rollers must be changed to cut different strip widths.

Beam cutters vaporize a fine strip of material. They are versatile: programming changes can alter the strip widths, or the beam can cut across the ribbon to trim the ends. Beam cutters can also be used as welders, and can share spart parts with beam welders. However, electron beam cutters require periodic filament replacement, and the filaments must come from

Beam Cutters

Ribbon

Slicing
Rollers

SLICING ROLLERS

Ribbon

BEAM CUTTERS
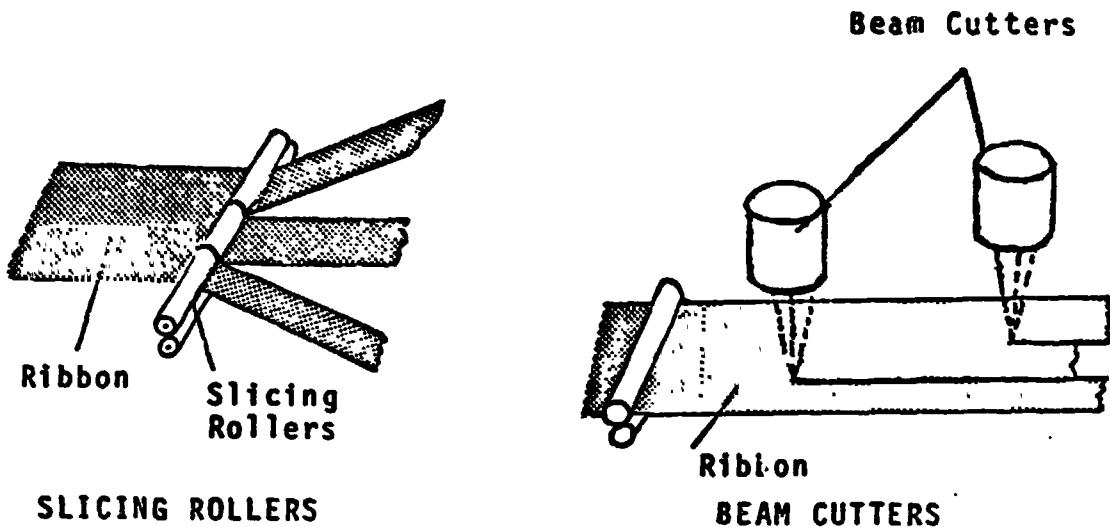
FIGURE 5.28: SLICING OPTIONS

Earth. Also, the vaporized material can be a significant kerf loss, since the strips produced are only 1 mm wide. In addition, this kerf vapor coats surrounding equipment, and may require special containment.

The study group chose slicing rollers because of the relative advantages listed above, and because the high productivity of the equipment mitigates its relatively high mass.

Once sliced, the wire strips are wound on spools and either sent to the insulation winder or to intermediate storage. Although the strip could be directly fed to an insulation winder, this would put the entire production line at the mercy of a breakdown in the slicing operation; also, the insulation winders are high-speed machines, usually faster than ribbon slicers. To avoid vacuum welding of the wire on the spools, the spools are

designed to keep successive windings from touching each other. Another option is to do the slicing and winding in an oxygen-bearing atmosphere which oxidizes (in milliseconds) the surface of the wire, stabilizing it; however, this alternative would require feeding the ribbon to the slicer through an airlock, an excessive complication.

5.6.2: Insulation Production: The choice of lunar materials for electrical insulation is limited. The constituents of the plastics and most cloths used on earth are unavailable on the Moon. The only likely material is glass cloth, woven from drawn S-glass fibers. Only certain types of glass can be drawn into fibers. Silica glass is too brittle, and softens at too-high temperatures. One type of glass suitable for fibers is S-glass, a mixture of 65% SiO_2, 25% Al_2O_3, and 10% MgO. Since SiO_2, Al, Mg, and O are all SMF inputs produced by lunar refining, S-glass can also be produced on the Moon, in 6.4-cm diameter rods. The task of the reference SMF is to convert these rods into glass fibers, then weave those fibers into insulation cloth.

Glass fibers are pulled through dies from a melt of softened glass. One method investigated was the melting of S-glass in a rotating furnace. The molten glass would then be fed to dies and drawn into fibers. Although this method was abandoned in favor of a simpler, more space-specific alternative, it serves to illustrate the technical aspects of melting materials unsuitable for inductive heating, such as S-glass. The rotating furnace is shown in Figure 5.29. Similar in design to the
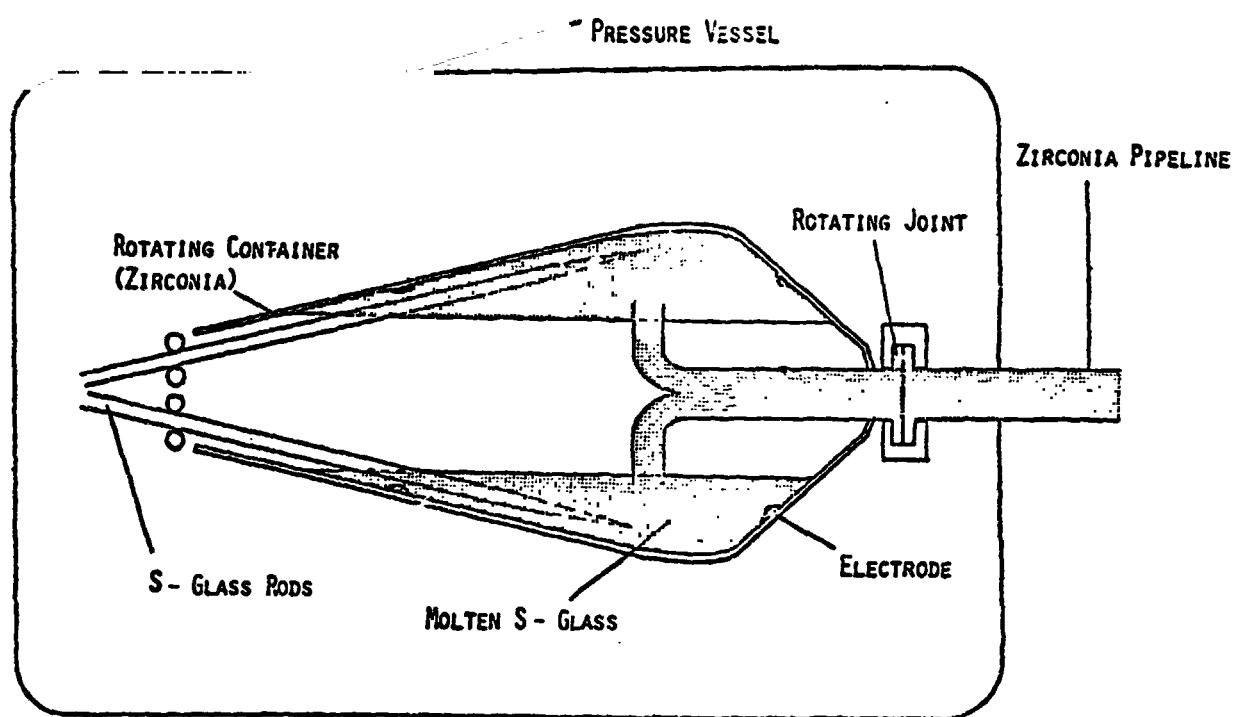
FIGURE 5.29: CENTRIFUGAL FURNACE FOR S-GLASS

rotating furnace for metals (see section 5.3.3), the S-glass

furnace consists of a rotating container and a set of nonrotating

feed and output systems. Solid rods of S-glass are fed into

the spinning melt, and melt in turn by conduction. The melt is

kept at the required temperature either by resistance heating

coils built into the rotating container wall, or by a current

passed through the melt between electrodes (as shown in the

figure). In either option, the power must be fed to the

rotating container through sliprings or brush contacts.

The suggested refractory material for the container wall is stabilized zirconia (ZrO_2). This material is commonly used in industry in a mixture with alumina and silica called ZAS. Zirconia alone is superior to ZAS in abrasion and corrosion resistance, but its unusual thermal expansion properties make it impossible to use in brick form. In space, where the loads on the refractory are less, it should be possible to use thin walled containers and pipes, thus avoiding the thermal expansion problem. However, it is likely that the furnace and pipelines will need to be replaced approximately once every year due to abrasion of the zirconia, and the study group feels more experimental research is needed to find better refractory materials.

Unless the S-glass is melted in an environment with oxygen under pressure, the SiO_2 fraction will decompose and form SiO and O_2. The furnace is therefore surrounded by a container filled with an oxygen-argon atmosphere which keeps the SiO_2 from decomposing. The atmosphere is also used to drive the molten S-glass through to output pipe by pressure differential. The argon reduces the fire risk from the oxygen. However, at high temperatures oxygen corrodes most electrodes (such as graphite) very rapidly. While electrodes are often replaced on Earth, in space this would add to the Earth imports and furnace down-time, and thus adversely affect the cost of the furnace. Platinum-iridium-ruthenium alloys are a possibility, but research is needed to find alloys that can withstand high temperature O_2.

As mentioned above, this rotating furnace was rejected in favor of a simpler, non-rotating system. The key factor allowing

the switch was the relatively low temperature required for fiber-pulling. In the rotating furnace, the S-glass must be heated until its viscosity is low enough for the glass to flow through the output pipe and around the input rods. However, glass fiber pulling should be done from a cooler, far more viscous melt. It is therefore possible to use those viscous forces to keep the soft glass in place, eliminating the need for centrifugal force.

The study group devised such a system for use in the reference SMF. As shown in Fig. 5.30, the glass fiber producer consists of a tube of interior diameter slightly over 6.4 cm. One end of the tube is capped by a multi-hole die. The other end can be opened or closed by a piston. Rods of S-glass are inserted into the tube and heated at the die end by resistance coils in the tube wall. The viscous molten glass fills the end of the tube, and the piston slowly pushes the rod into the
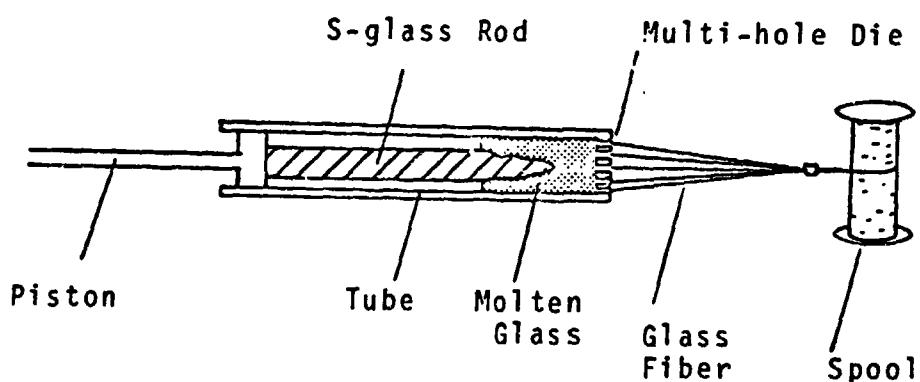
FIGURE 5.30: GLASS FIBER PRODUCER

melt as needed. Glass fibers are drawn through the die and wound onto spools. The entire device is surrounded by vacuum. Because of its simplicity and level of adaptation to the space environment, the study group chose this option for the reference SMF.

The spools of glass fibers and the spools of Al wire are loaded into an insulation winder which weaves glass cloth insulation around wires or cables. This device is similar to tubular-weave cloth-making machines commonly used in industry today. The insulated wire is then respooled for intermediate storage, for use in further processes, or for shipment to assembly sites for SPS's or satellites.

5.7. KLYSTRON ASSEMBLY PRODUCTION

5.7.1: The Klystron Assemblies: Figure 5.31 shows a klystron
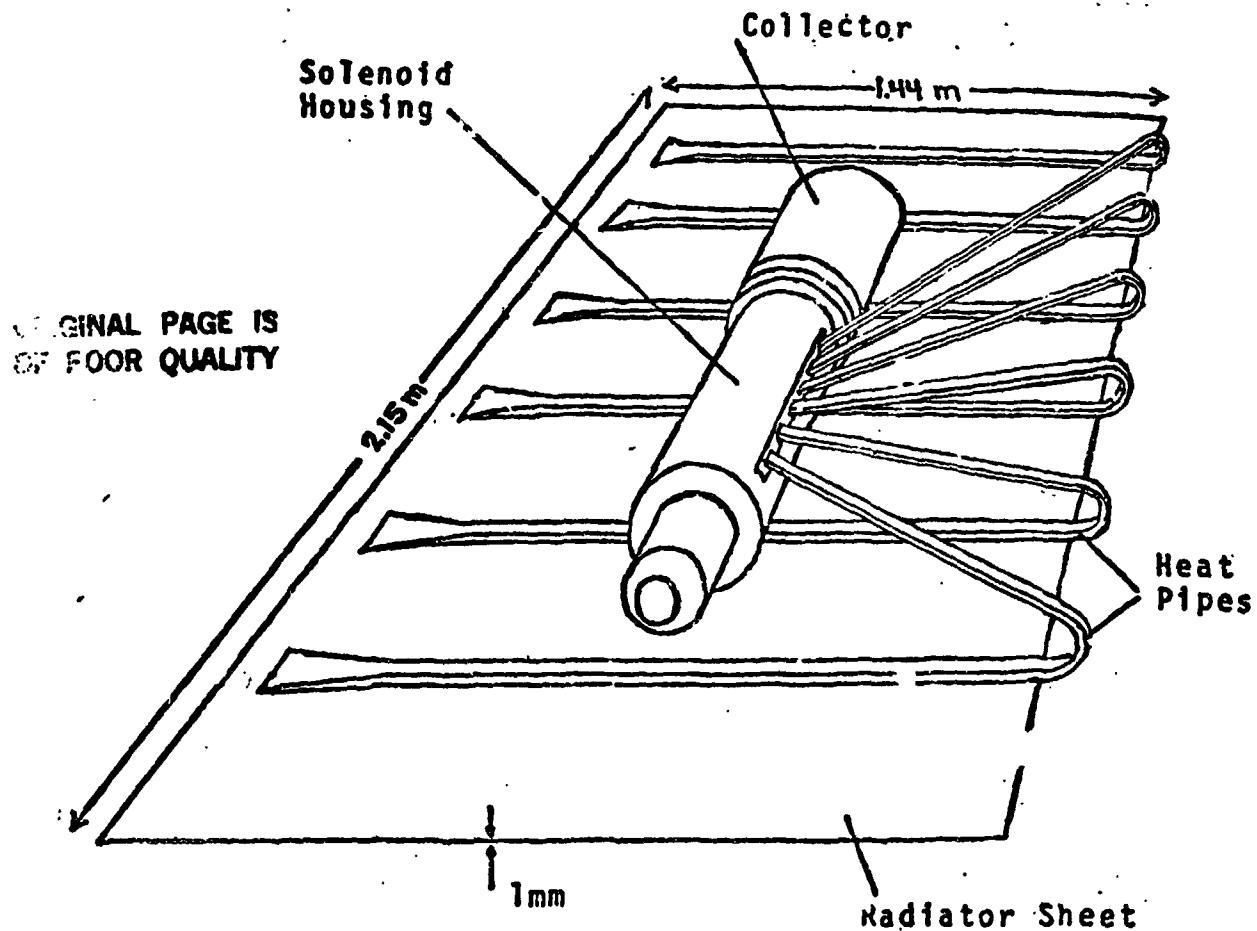
FIGURE 5.31: KLYSTRON ASSEMBLY

5.143

assembly. It consists of a klystron module connected by six
heat pipes to a radiator sheet. The production of one 10-GW
SPS per year requires 2.04×10^5 such assemblies per year, or
roughly 700 assemblies per day on an 80% duty cycle.

The klystron itself is a power amplifier operating in the
microwave frequency range. It receives a reference RF input
(which sets the frequency and phase of the RF output), and DC
power at various voltages up to 40 KV. The klystron tube con-
sists of four principal sections: electron gun, body cavities,
focusing solenoid, and collector. These sections are schematized
in Fig. 5.5L.

A fine beam of electrons is produced by the electron gun
and directed through the body cavities towards the collector
plates (which are at a positive potential with respect to
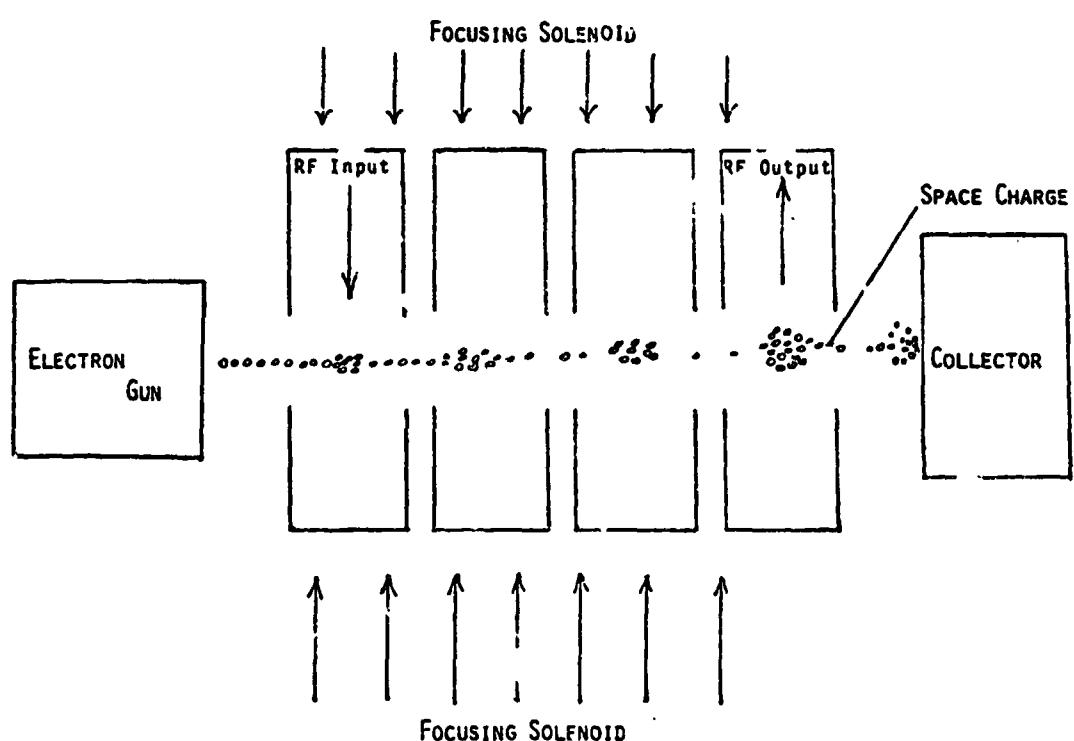
FIGURE 1 -- SIMPLIFIED SCHEMATIC OF KLYSTRON OPERATION

the klystron body). The purpose of the focusing solenoid is to maintain the linearity of the long thin electron beam -- overcoming its natural tendency to scatter. On entering the input (first) cavity, the electrons are subjected to a fluc- tuating electromagnetic field -- supplied by the reference RF source -- at a frequency of 2.45 GHz. The effect of the field is to alternately accelerate and decelerate electrons (depend- ing on which point of the RF cycle an electron is subjected to) resulting in electron bunching. By selecting a suitable geo- metry for subsequent cavities, the tube can be 'tuned' to in- crease the extent of the bunching effects, i.e. to amplify the effect of the weak RF input. At the output cavity the micro- wave energy is extracted from the electron beam. Ideally, at this point, the current modulation of the beam is at a maximum. The spent beam is collected by the collector plates.

In addition to the four sections mentioned above, the kly- stron requires housings surrounding solenoid and collector. These protect the components from contamination and from micro- phonic noise, both of which reduce the klystron efficiency.

Figure 5.33 is a conceptual view of the 70 KW klystron for the earth baseline SPS (Ref. 5.42). However, no detailed de- sign exists for such a tube, and the preliminary design shown is intended for production on Earth, not large-scale production from lunar materials at an SMF. For the klystron produced at the SMF, lunar material substitutions are made as per the sug- gestions in the JSC-GD study (Ref. 5.43). The solenoid cavi- ties and collector and solenoid housing   Al. The

INTERNAL COLLECTOR HEATPIPE/EVAPORATORS

REFOCUSING SOLENOID

CAVITY/SOLENOID HEATPIPE EVAPORATORS

MAIN SOLENOID

RF INPUT FROM SOLID STATE CONTROL DEVICE

COLLECTOR PLATES

MOD. ANODE

HEATER

CATHODE

COLLECTOR HEATPIPE (2) TO RADIATOR

OUTPUT WAVEGUIDE

CAVITY/SOLENOID HEATPIPES (4) TO THERMAL RADIATORS

Inches
cm
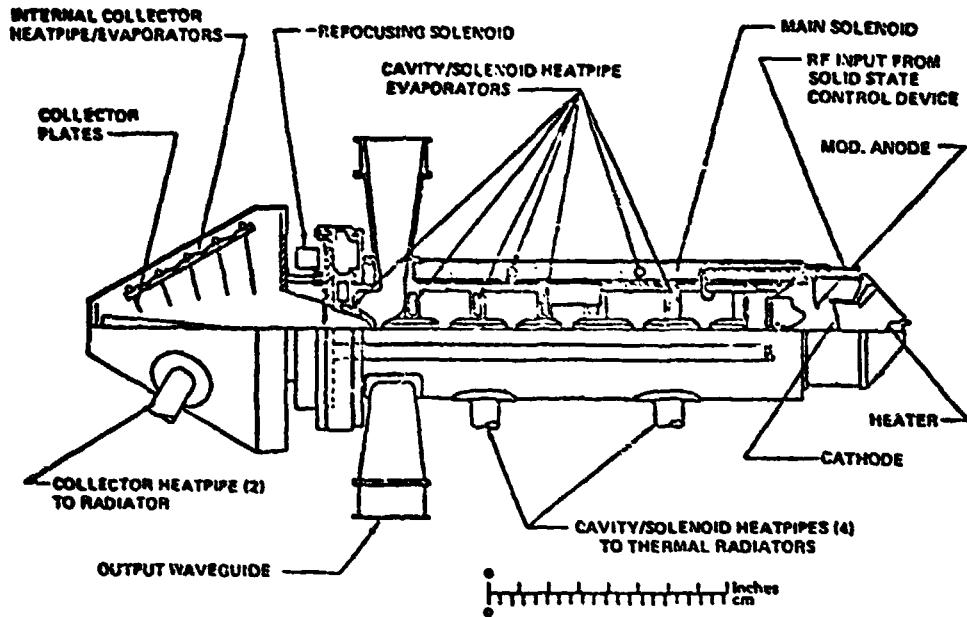
REF: FIG. 4-1, "SOLAR POWER SATELLITE -- SYSTEM DEFINITION STUDY" PART II, VOL. IV, BOEING COMPANY, NASA CONTRACT NAS9-15196

FIGURE 5.33: BASELINE KLYSTRON CONFIGURATION

solenoid poles are pure iron. The solenoid coil windings are Al wire insulated with glass cloth. It is also assumed that where no lunar substitutions for klystron components are made by the JSC-GD study, those parts are brought from Earth (i.e. tungsten collector plates).

Since the klystron is 85% efficient (Ref. 5.1), each 70 KW klystron requires one or more radiators. In the earth baseline design, two radiators (one copper, one aluminum) are used, one

for the cavity and solenoid sections, one for the collector (Ref. 5.43, Figure X-7). For ease of manufacture, the SMF produces one aluminum radiator for both sections. Careful placement of heat pipes on the radiator sheet may make the use of one radiator possible. If two separate radiators are required due to a difference in operating temperatures, the radiator sheet can be cut into two during final assembly of the klystron and radiator. In the earth baseline design, the steel heat pipes from klystron to radiator are filled with mercury. For ease of manufacture, the heat pipes produced by the SMF are made from pure aluminum (rather than the steel suggested by the JSC-GD study). Since mercury strongly corrodes Al, another heat pipe fluid must be substituted. The study group assumed that a suitable heat pipe fluid compatible with aluminum could be developed; there appears to be no current substitute for mercury.

5.7.2: Klystron Production: As mentioned above, no physical design for a 70 KW SPS klystron exists, making the task of manufacturing process definition highly speculative at this time.

The study group approached the problem from two viewpoints. First, in order to obtain some indication of essential production steps, details of the manufacture of a low power, X band, two cavity klystron were studied, and the findings applied, by extrapolation, to the hypothetical 6 cavity tube. Second, the study team consulted industry about the automated manufacture

and assembly of complex machinery. The team then estimated the feasibility, cost, complexity, and productivity levels of an automated power tube assembly operation by these means. A comparison of production methods currently used in the power tube industry (Refs. 5.44, 5.45), and the anticipated requirements for an SMF reveals some important differences.

At present time, power tube manufacture is a largely labor intensive process -- skilled labor being used widely in machining, assembly, and testing operations. Production rates of any given klystron design may be of the order of only 100 to 200 tubes per year. In contrast, the SMF production requires automated units with klystron production rates of about 700 tubes per day. Additionally, manufacturing techniques currently in use are largely based upon the use of copper alloys, and changes or adaptions must be made to allow the use of lunar derived materials in the SMF. Finally, the product of today tends to be of relatively low power output (less than 50 KW) compared to the SPS klystron (70 KW output). Therefore klystron design should be adapted to automated production from lunar materials.

The main klystron solenoid cavity will be die cast from lunar derived Al. The casting will include that of the cavities, which would normally be milled separately on earth. Although die casting can produce components to within .8% of their nominal dimensions, it is anticipated that some final machining of the cavities will be required to come within the tolerance require-

ments. Additionally a polishing process will be necessary,
since surface finish is a contributor to good tube efficiency.

To allow for cooling of the cavities, cooling channels must
be drilled transversely across the webs between the cavities.
The baseline design allowed for the use of a heat pipe cooling
system opeating at 500°C with a mercury coolant fluid. This
would require an additional production step -- the plating of
of the coolant channels with a protective copper coating. Al-
though other liquid metals could be used in the heat pipe, all
have some adverse reaction with aluminum. As mentioned in the
section above, the study group assumed the development of an
alternative heat pipe fluid compatible with aluminum. This
removes the need for plating the coolant channels.

[Note: A modification to the coolant system currently
being suggested by the Boeing Company (Ref. 5.46) is to use a
300°C active cooling system (using   Dowtherm-A coolant) in
the solenoid cavity, and a 500°C active (nitrogen) cooling sys-
tem for the collectors. According to Boeing, in addition to
improved maintainability there is a 33% mass reduction. The
active cooling system shows advantages over a heat pipe system
in a failure analysis. However, the study group decided to
stay close to the baseline SPS design, and therefore kept the
heat pipes.]

In both of the machining stages mentioned above, debris
removal must be done to prevent accumulations from clogging
machinery, and contaminating the workpiece. In a zero-g en-

vironment, any dust or particles left within the cavities will, when the tube is in operation, be attracted by the predominant electrostatic force of the electron gun, significantly reducing the output of the tube. To avoid this potential problem, 'clean room' conditions throughout the manufacturing process are required.

Some machining of the klystron output cavity is anticipated to ease the fitting of a ceramic window, and a close tolerance tube-waveguide interface. The ceramic window serves the functions of a pressure seal for the tube, and as a means of preventing contaminants from entering the cavities via the waveguide. Whether or not the window will be required for in-space operation of tubes is uncertain.

The focusing and refocusing solenoids are coils of insulated wire (produced elsewhere in the SMF, see Sec 5.6). They are wound onto the cavity block by conventional wire-winding equipment.

In order to complete the magnetic circuit, soft iron pole pieces must be flush fitted to the ends of the solenoid and the klystron body. The pole pieces are cast, machined (if necessary) and electron beam welded into position. In the reference SMF, the study group chose to die-cast the solenoid pole pieces. Molten Fe is produced from input rods of lunar iron by an iron furnace. This furnace is also used to produce SENDUST alloy for DC-DC converter cores (see Sec. 5.8). The furnace design

is similar to the aluminum furnace described in Sec. 5.3.3. The molten Fe is pumped through a refractory pipe to a die caster. This die caster produces 448,000 solenoid poles (800 tons total) for one 10-GW SPS. This output is very low by earth-based die-caster standards, and this unit is therefore a small device.

At this point the klystron radiators and heat pipes are attached to the solenoid cavity block. The production of these radiators and heat pipes is discussed in the next section. The design of the interface between the heat pipes and the solenoid cavity block needs further investigation.

Klystron production stages beyond these employ components obtained from Earth. To minimize wastage of earth components, cold testing of the cavities (using an RF probe) is done at this point: the units failing the test are discarded without loss of earth imports. In fact, each production stage is followed by quality control in order to minimize losses.

After the fitting and assembly of a variety of earth components (e.g. high-voltage ceramic seals, modulating anode collector, cathode connector, heater, output waveguides, vacuum ion connector, cavity tuning components, internal cabling, assembly hardware, electron gun, collector), the whole klystron is encased within solenoid and collector housings. These housings are pure aluminum, and they are each die-cast in two parts, so that they can be assembled around the klystron, allowing the passage of heat pipes. Consultations with Mr. Art Kelly of Raytheon Company's Microwave & Power Tube Division in-

dicated that the housing for a power tube needs to be on the order of 1 cm thick to prevent microphonic noise problems; hence castings are used rather than formed sheets.

The completed klystron is conventionally taken through 3 stages of final processing. First, in 'bakeout' the tube is heated to its working temperature in an attempt to liberate any gases which may have been trapped within the metal from which the tube is formed. The purpose of this outgasing is to ensure that no gases are liberated when the tube is in operation which would reduce the internal vacuum level and thus allow breakdown and arcing. The necessity for 'bakeout' in space operations is not clear, since the tube could be operated without a ceramic window, allowing the ambient vacuum to pump away any gases liberated within the tube during operation. This remains a matter for the tube designer, and for some in-space testing.

Second, in processing, the cathode and the collectors are subjected to steadily increasing voltages (up to the working values) in an attempt to 'age' the tube. This stage would probably be necessary in space manufacture as well.

Third, tests on the klystron -- with working voltage applied -- are made in order to verify tuning, operating efficiency, etc. Should it be possible to produce an extremely reliable, highly automated system, it may be acceptable to employ random sampling methods -- in order to avoid the hour-

long testing of every tube. Klystrons meeting the quality con-
trol requirements would be sent to output storage -- ultimately
for dispatch to the SPS construction site. The current tube
wastage rate (due to manufacturing flaws) is around 7%.

In general, the feasibility of the design of a highly auto-
mated klystron production facility looks promising. The tube
itself would have to be specifically designed, though, for ease
of manufacture in space (notably with a reduction in the overall
number of components). Many of the expected operations are
current Earth processes (casting, drilling, machining, winding,
fastening). Conventional welding techniques would be replaced
by the more space-specific (and more accurate) electron beam
welding. Raytheon Co. (Ref. 5.47) has produced an experimental
all-aluminum magnetron using EB welding. The magnetron; though
simpler is design than the klystron, requires assembly techniques
and tolerances on the same order.

5.7.3: Klystron Radiator and Heat Pipe Production: Given the
production of 1-mm-thick pure Al ribbon for busbars (see Sec.
5.5), it is relatively simple to convert pieces of that ribbon
to 1-mm-thick pure Al radiator sheets. The ribbon must first
be end-cut and edge-trimmed to produce straight-edged rectan-
gular sections. These sections are then welded together to
form the radiator sheets.

Earth baseline klystron radiators have a combined (collector
and solenoid radiators) area of 2.57 m^2 (Ref. 5.43, Figure X-7).

They can therefore be replaced by a sheet of Al 2.15 m x 1.44 m
(20% margin added to allow replacement by a single radiator).
Therefore the .74 m wide ribbon coming from the rolling mill
is end-cut into pieces 2.15 m long, and edge-trimmed to width
.72 m. Two such pieces can then be welded edge to edge to
produce the radiator.

As in the structural member ribbon production, to make the
edges straight-cut and smooth for welding, beam cutters are
used on the ribbon (see Sec. 5.3.6). EB welders are also used
to weld the edges of the pieces together, because the high
quality of the weld makes the flow of heat across the seam
easier. As is the structural member ribbon production, the
welders first tackweld the edges together in several places
along their length; then the edges are entirely welded. The
tackwelds resist thermal deformations during welding, keeping
the edges aligned during the process.

The next step is the application of heat pipes to the sur-
face of the radiator sheet. On Earth heat pipes are commonly
sealed tubes, lined with a wick, or striated along their inside
surfaces. The heat pipe fluid boils at the 'hot' end (in this
case the klystron), travels down the tube, and condenses on the
'cold' end (the radiator). The fluid is then returned to the
'hot' end in liquid form by capillary action in the wick or
striations. The heat transfer is accomplished in the phase
changes at the ends of the pipe, and the entire pipe stays at
roughly the same temperature.

Although a wick can be manufactured at the SMF from glass-fiber cloth (glass-fiber cloth is used for electrical insulation -- see Sec. 5.6), this would require two extra production steps, the manufacture of the wick and its insertion into the finished heat pipe. Striations are a simpler alternative, since their production takes one step which can possibly be combined with the pipe-forming process. The problem with striations is that it is very difficult to extend them across a joint in the pipe. The striations on each side of the joint would have to be precisely lined up before joining, to produce uninterrupted capillary paths. This is unlikely in automated production. Special joints can remedy the problem, but these are difficult to manufacture and would therefore have to be brought from Earth.

The study group therefore devised a striated heat pipe configuration with uninterrupted striations from radiator to klystron. To eliminate differential expansion between heat pipe and radiator, the heat pipe material is pure aluminum. The pure Al heat pipe can then be formed from the available 1-mm thick Al ribbon (used for busbars, electrical wires, and radiators).

The principal component of the heat pipe is the 'heat pipe segment,' the striated continuous piece from radiator to klystron. Its production steps are illustrated in Fig. 5.34. First, 1-mm thick, .74 m-wide Al ribbon is sliced into strips

.25 meters wide. This step can be combined with the slicing of electrical wire (see Sec. 5.6), using the same equipment. The strips are end-cut every 3.5 meters, forming 3.5 x .25 x .001 m pieces. These pieces are then striated along their center sections by striating rollers (a design similar to the slicing rollers).

.74 M   .25 M

RIBBON CUTTING   STRIATION

FORM ROLLING

.03 M

.125 M
FINAL CROSS-SECTION
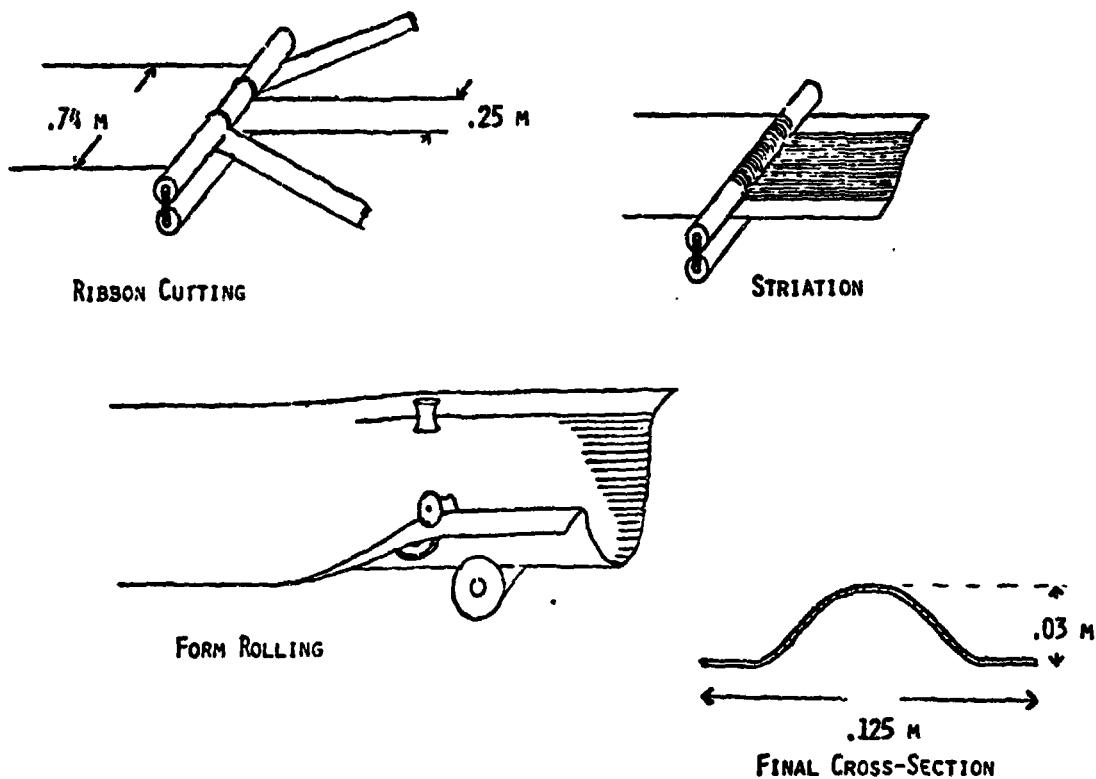
FIGURE 5.34:   BASIC STEPS IN HEAT PIPE SEGMENT PRODUCTION

One end of each piece is left unstriated; this will become the closed end on the surface of the radiator. The pipe segments are then form-rolled to the cross-section shown. The unstriated tip, however, is left unrolled and remains flat.

5.156

The other components of the heat pipe are the radiator sheet
itself and a 'heat pipe ribbon', with dimensions 1.6 x .125 x
.001 meters. The assembled configuration is illustrated in
Fig. 5.35. The radiator end of the heat pipe segment is welded
onto the radiator sheet, closing that end of the pipe. Beyond
the edge of the sheet, the heat pipe segment is bent over, to
reach the expected position of the klystron (relative to the
radiator). The heat pipe segment is then closed (from the edge
of the radiator sheet to the klystron end of the pipe) by welding
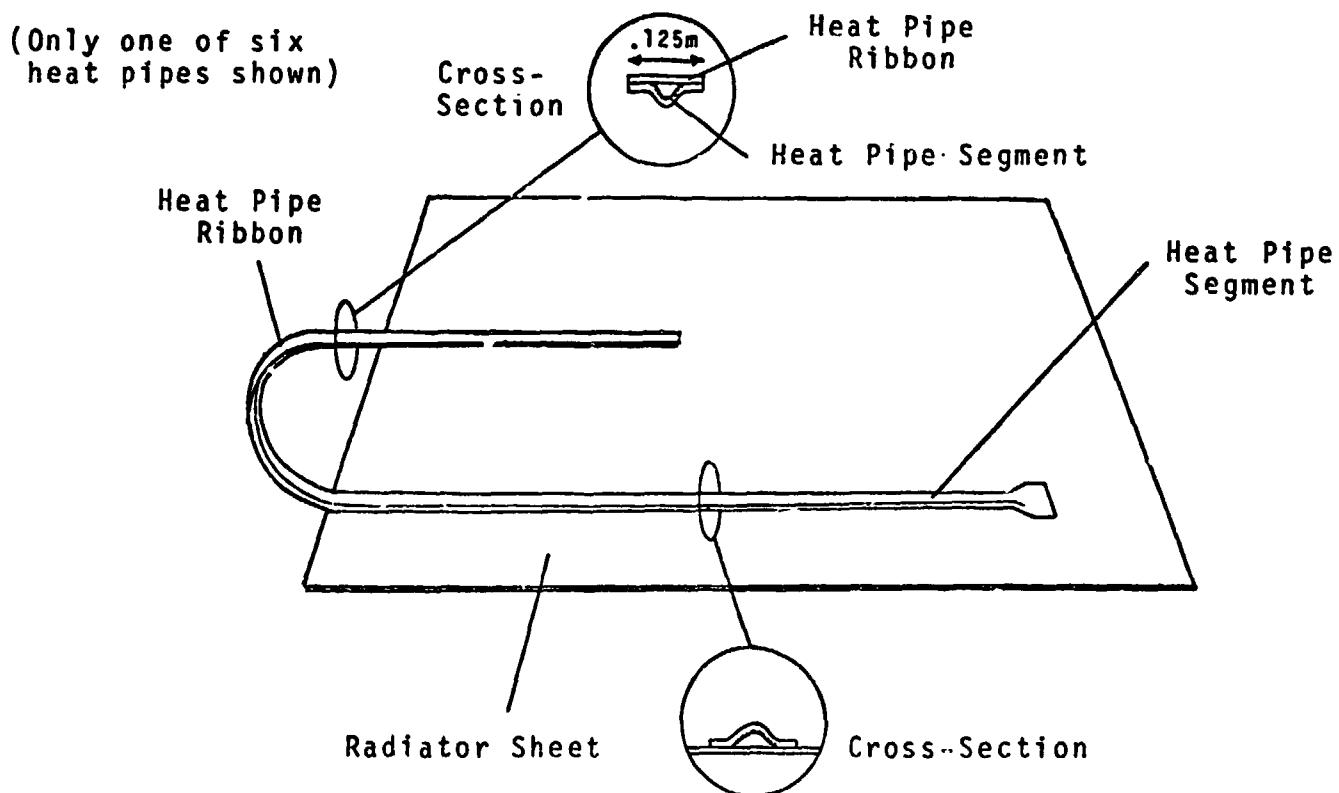
FIGURE 5.35: KLYSTRON HEAT PIPE DESIGN

the edges of the heat pipe ribbon to the heat pipe segment, and the end of the heat pipe ribbon to the edge of the radiator sheet. As in earlier precision welding (see Sec. 5.3.6), electron beam welders are used to assemble the heat pipe.

This heat pipe design offers a number of advantages in manufacture, particularly the use of Al ribbon already available, relatively simple assembly procedure, and the absence of Earth inputs. However, as mentioned above, it requires the development of a cooling fluid with a boiling point close to that of mercury, but which will not corrode aluminum. Also, the heat pipe design, though conceptually similar to striated heat pipes used on Earth, should be tested and refined as needed.

5.8: DC-DC CONVERTER ASSEMBLY PRODUCTION

5.8.1: The DC-DC Converters: The earth baseline and lunar material SPS's both feed DC power from the solar array to the transmitting antennas through power busses operating at roughly 40 KV. This power must be fed to the klystrons at a range of DC voltages from 40 KV down to 30 V (Ref. 5.48, pages 62-67). The system therefore requires DC-DC converters to step down the 40 KV to the necessary voltages. This is done by first changing the input power to AC through a 20 KHz switching circuit using silicon controlled rectifiers or power transistors. The voltage is then stepped down by a transformer. The various outputs are then rectified and filtered back to DC. The conversion efficiency is expected to be on the order of 90-95%, and the DC-DC

converters therefore require radiators to release waste heat. The earth baseline SPS uses aluminum radiators 360 m^2 in area (Ref. 5.48, pages 66-67), with dimensions 9 x 40 meters. Cooling fluid is routed from the DC-DC converter to the radiator through a series of pipes along the surface of the radiator.

Switching circuits, rectifiers, filters, control systems, heat exchangers, and coolant pumps are too complicated for SMF manufacture, and therefore come from Earth. The SMF produces the transformer core and windings, and the DC-DC converter radiator. For the production of each 10-GW SPS, 461 transformers and 461 radiators are required (as listed in Table 3.1).

5.8.2: Transformer Production: The lunar-material substitution . for the earth-baseline transformer core material is SENDUST (85% Fe, 10% Si, 5% Al), as per the suggestion of the JSC-GD study (Ref. 5.43). Consultations with the MIT Electric Power Systems Engineering Laboratory and the MIT Francis Bitter National Magnet Laboratory identified one alternative, a ferrite core made of powdered metal; however, this requires zinc from Earth and a complicated manufacturing process. In general, the used of 20 KHz alternating as transformer input makes conventional core materials unsuitable. For example, pure iron laminated cores cannot be used above 400 Hz because eddy current losses are too great. Adding silicon to the iron and using laminations .25 mm thick decreases the losses, but it is unknown whether it decreases the losses enough to use at 20 KHz. This high frequency was picked for the earth baseline to reduce

transformer mass. However, little data is available on trans-
former materials in this frequency range. No information on
the SENDUST core was available to the study group.

Each transformer core masses 2.2 tons. The low production
rate for one 10-GW SPS per year (461 cores/year or 1.3 cores/day)
allows slow production processes with human operation. The
study group therefore chose to cast the cores in a specialized
transformer core caster. The SENDUST alloy is first produced
in a melting furnace similar to the furnace used to melt and
alloy aluminum (see Sec. 5.3). This iron alloying furnace is
also occasionally used to produce pure iron for the klystron
solenoid pole pieces. The molten SENDUST alloy is fed to the
transformer core caster by electromagnetic pump, through a
pipe made of graphite (to resist corrosion by the liquid iron).
The caster mold has dimensions roughly 1 x 2 x 3 meters, to
hold the entire core.

To accomodate the fluid cooling system, the core must be
pierced by coolant channels. Since it is difficult to produce
large castings with long channels through them, the study group
chose to drill coolant channels through the cores. This re-
quires chip-handling systems.

Transformer coils are then wound onto the core. These are
made from aluminum wires insulated with glass-fiber cloth, pro-
duced at the SMF (see Sec. 5.6). Conventional equipment,
slightly modified for use in space, is adequate for the winding
process.

The final step is the assembly of the DC-DC converter parts brought from Earth to the manufactured transformer. Assembly techniques depend on the design of the parts, but they should not pose any difficulties. The completed DC-DC converters are shipped to the SPS assembly site.

5.8.3: Radiator Production: Due to their large size and mass (roughly 9 x 40 meters and 1.2 tons), the DC-DC converter radiators are shipped separately from the DC-DC converters, and the two components are connected together at the SPS assembly site. Given the production of 2.15 x 1.44 m klystron radiators at the SMF (see Sec. 5.7.3), it is relatively simple to build the DC-DC converter radiators from such Al sheets. Since the total requirement of DC-DC converter radiators for one 10-GW SPS is low (461 pieces massing 550 tons), it is economically necessary to keep dedicated production processes for these radiators to a minimum. Therefore use of klystron radiator production equipment to make sections of DC-DC converter radiator is a significant advantage. Therefore pure Al sheet pieces, with dimensions 2.15 x 1.44 x .001 meters, are laid out in a rectangular array, 7 sheets by 17 sheets, and welded edges-to-edges to form a continuous sheet 10.08 x 36.55 m (area 368 m^2). As in the production of klystron radiators, electron beam welders are used to tack-weld and weld the pieces together. Since the simultaneous welding of 119 sheets together is technically difficult, the radiator is built up in sections.

The radiators also require an array of pipes to channel

cooling fluid across the radiator, as described in Sec. 3.2.9 and shown in Fig. 5.36. The design of the pipes resembles the design of the klystron heat pipes (see Sec. 5.7.3). However, unlike the klystron heat pipes, the radiator pipes are not striated, and they are form-rolled to the cross-section shown in Fig. 5.34 along their entire length, then end-trimmed by an EB cutter for end-to-end welding. Like the klystron heat pipes, the radiator pipes are produced from 1-mm thick, .25-m wide Al ribbon, sliced from the .74-m wide ribbon produced by the rolling mill; and the radiator pipe is form-rolled by the same equipment as the klystron heat pipes.

Once form-rolled and end-trimmed, the radiator pipes are welded end-to-end onto the surface of the radiator sheet, to form nine parallel pipes along the length of the radiator. As in other precision welding process, EB welders are used to attach the pipes to the sheet and to each other.

To join the ends of the pipes together, so that the radiator may receive and return coolant fluid through two pipes, a manifold is attached to the pipes and to the radiator sheet at each end. This manifold is also produced at the SMF by the die caster used for klystron housings, solenoid cores and poles, and end joints and joint clusters (see Sec. 5.4). Each manifold is cast from pure Al, in five parts (to reduce the mold sizes required in the die caster). The manifold parts are welded to the radiator sheet, to the radiator pipes, and to each other with

Manifold

Radiator Pipe

Aluminum Sheet

10.08 m

36.55 m

.001m

.001m

.125 m

DC-DC Converter Radiator:

Aluminum Sheet Mass/radiator
= 995 kg

Total Radiator Mass
= 1220 kg

Radiator Pipe:

Made from .25 x .001 m
Al Ribbon

Total length/radiator
= 310.5 m

Mass/radiator = 210 kg

Manifold:

35 cm

8.12 m

Manifold cast in 5 pieces
from Al .001 m thick
    2 Manifolds/radiator
    Mass/radiator = 15 kg (est.)
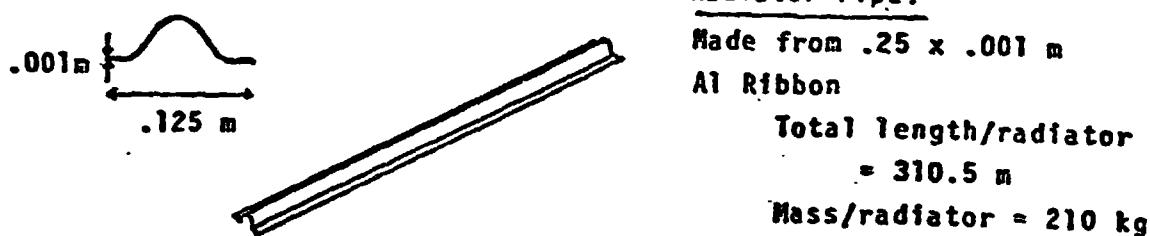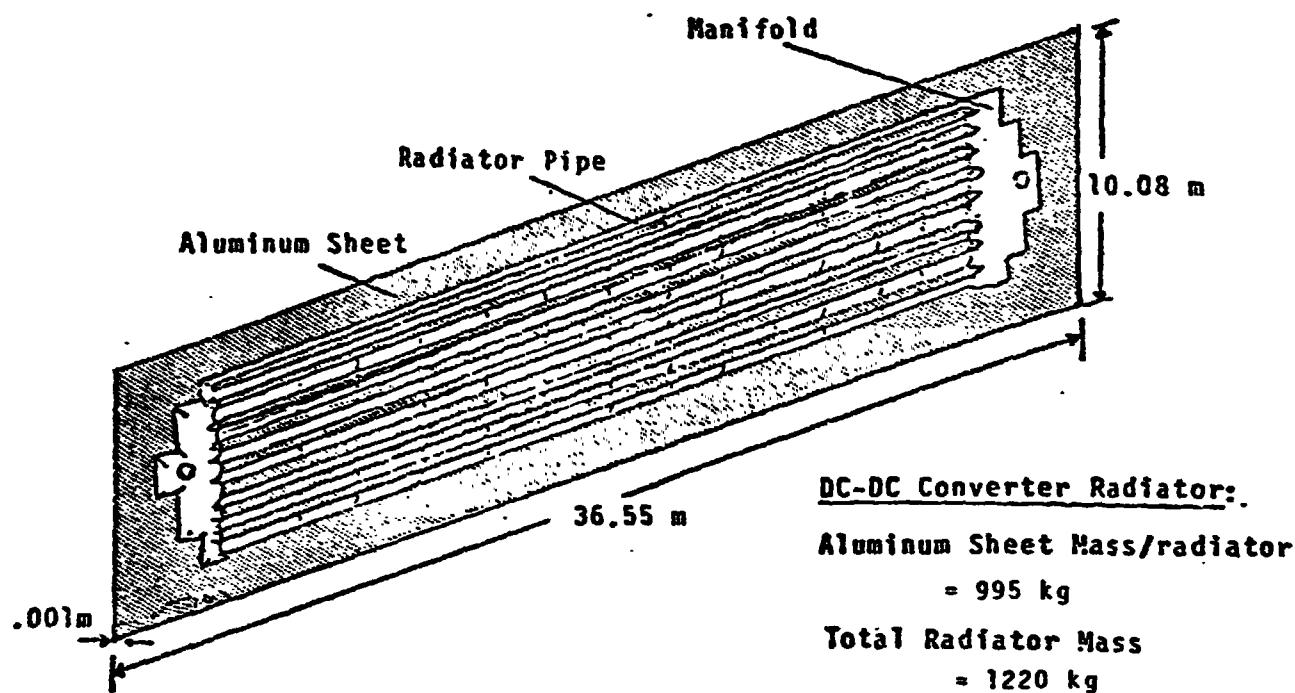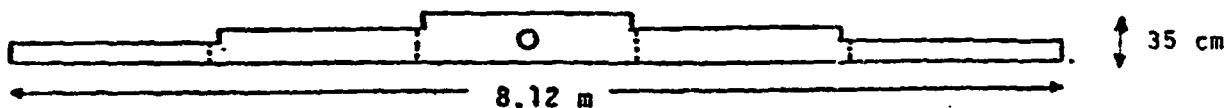
FIGURE 5.36 :   DC-DC CONVERTER RADIATOR DESIGN

5.163

EB welders.

The completed DC-DC converter radiators are shipped to the SPS assembly site. Due to their large size, handling them within the SMF is difficult, suggesting that the assembly station for these radiators should be near the SMF output loading area, to minimize internal transport requirements.

5.9: WAVEGUIDE PRODUCTION

5.9.1: Waveguide Material Alternatives: The earth-baseline waveguides are trapezoidal cross-section boxes made from graphite/epoxy (G/E) composite. The interior surfaces are coated with a layer of conductive aluminum. The trapezoidal cross-section allows stacking of the box sections for transportation. For ease of manufacture, the study group substituted retangular cross-section boxes. The cross-sectional dimensions are .093 x .06 meters and the lengths of the boxes vary according to their location on the transmitting antenna.

As discussed in the JSC-GD study (Ref. 5.43), the important design criterion in waveguides is the close dimensional tolerance required for proper waveguide operation. The waveguides must be able to maintain these tolerances during the thermal cycling due to the transmitting antennas' once-a-day rotation in the sunlight. The JSC-GD study calculates a maximum permissible coefficient of thermal expansion (CTE) of 3.6×10^{-6} m/m-°K for waveguide material, to stay within allowable distortions during thermal cycling.

Given this maximum CTE, the only lunar material with an

5.164

acceptable CTE is silica glass (CTE = 2.9 x 10^{-6} m/m-°K). The
JSC-GD study suggests that waveguides be made of foamed glass,
to avoid shattering of pure glass waveguides due to meteoritic
impact. In foamed glass, the gas bubbles serve as crack-stop-
pers, containing the effects of the impacts.

For the purposes of this study, the research team accepted
the suggestion of the JSC-GD study, and included the production
of foamed glass waveguides in the reference SMF. There are,
however, a number of other promissing material options which
require further study; these options are listed in Table 5.12.

TABLE 5.12: WAVEGUIDE MATERIAL OPTIONS

Waveguide Options	Advantages	Disadvantages
All waveguides brought from Earth	o Can be baseline waveguides	o High transportation costs
Some waveguides from Earth, others from lunar materials	o Can satisfy CTE requirements with simpler SMF operations	o May not be possible Requires earth inputs
Pure glass	o Established technology o Simple manufacture No earth inputs	o Requires extra repair on SPS
Pure glass with woven fiber protection	o Existing technology o Simple manufacture No earth inputs	o May not resist meteorite shattering
Composite with fibers from Earth, matrix from Moon	o Resists Shattering	o Requires earth inputs o Such composite may not be possible o May require complex production
Composite, all lunar	o Resists shattering o No earth inputs	o Such composite may not be possible
*Foamed glass	o Existing technology o Resists shattering	o May require Earth inputs o Some wastage of material o Requires dust-handling systems

*Chosen for the reference SMF

The first option is to bring the waveguides from Earth. They can then be baseline G/E waveguides. As listed in Table 3.2, the waveguides for one 10-GW SPS (without growth margin) mass 4314 tons, or 6% of the SPS mass. In the lunar-material SPS, the expected earth inputs are 8000 tons (see Sec. 3.3). Therefore the additional importation of waveguides from Earth would raise that input by 54%. Since the cost of that increase involves issues of transportation system design and propellant availability, this tradeoff is outside the scope of this study.

Second, it may be possible to use earth-origin waveguides in some sections of the antennas and lunar-material waveguides with higher CTE's in other locations. The calculation of the maximum allowable CTE in the JSC-GD study was done for waveguides near the center of the antenna. However, the thermal histories and dimensions of the waveguides vary according to location on the antenna, and therefore waveguides in other locations may have higher allowable CTE's. If this is the case, some of the materials suggested for structural members (see Table 5.8 and 5.9) may be suitable for some of the waveguides, and their production processes may be simpler than those of other options. One possiblity suggested by Mr. Arthur Yarranton of Raytheon Co. (Ref. 5.49) is the use of ceramic materials such as alumina (CTE = 6.3×10^{-6} m/m-°K). Such waveguides are currently commercially available, and their production is relatively simple. Their resistance to meteoritic shattering is unknown, however. For those antenna sections with low CTE requirements

the waveguides could be brought from Earth. Since the cost of
this concept involves the transportation issues mentioned above
and requires extensive calculations of the thermal character-
istics of the SPS transmitting antenna, evaluation of this op-
tion is beyond the scope of this study.

The third option is the use of pure glass made entirely from
lunar materials. Such glasses can range in quality from pure
silica, to S-glass (65% SiO_2, 25% Al_2O_3, 10% MgO), to natural
lunar glass (separated from lunar soil and sent to the SMF).
The structural requirements on waveguides are low, and therefore
any glasses with acceptable CTE's would probably be suitable.
CTE's for commercial glasses on Earth range from .8 x 10^{-6} m/m-°K
(silica) to 100 x 10^{-6} m/m-°K. S-glass has CTE 2.9 x 10^{-6} m/m-°K.
One advantage cf this option is that production of pure glass
pieces is an established technology. Some production processes
are unlikely for SMF use, such as floating molten glass on
molten metal (see Sec. 5.2.4); but glass sheet can be rolled,
or glass sections can be extruded. Thus manufacture can be re-
latively simple, though achieving the required tolerances would
require careful machining and assembly. Another advantage is
that the process would require no earth inputs, since the com-
ponents of acceptable glasses (e.g. S-glass) are found on the
Moon. The important disadvantage of this option is that wave-
guides made from pure glass will shatter when hit by meteorites.
This would therefore increase the need for replacement of broken
waveguides during SPS operations, requiring production of re-

placement waveguides, and adding to the cost of SPS maintainance. The calculation of that cost increase is outside the scope of this study, however, and time constraints kept the study group from designing a production sequence for pure-glass waveguides.

A fourth option is the production of pure glass waveguides covered with a protective layer of glass cloth. Such cloth is produced at the SMF for electrical insulation (see Sec. 5.6). This option shares the advantage of the pure-glass option above, and in addition may resist meteoritic shattering. However, the principal disadvantage is that this shatter-resistance is not guaranteed. The cloth cannot serve as a crack-stopper, but only as a shield against impacting meteorites. The cloth may indeed stop small particles, but it is possible that these small particles would not cause the glass to shatter anyway. Particles large enough to shatter the glass may do so right through the cloth. Experimental research is needed to assess this possibility.

The fifth material option is a composite material with fibers from Earth and the matrix from the Moon. If the lunar matrix is a high-CTE material, such as aluminum or titanium, then the earth fibers should be graphite (negative CTE) to bring the composite CTE down to the required value. This combination, however, may require so much graphite that it offers no significant savings over bringing complete waveguides from Earth. If the matrix is lunar glass (such as S-glass), then its CTE

is low enough, and the fibers are included for shatter-resistance (crack-stopping) rather than structural or thermal expansion reasons. The fibers can therefore be a low percentage of the waveguide mass. There are three disadvantages to the earth-fiber/lunar-matrix composites. First, they require earth inputs. Second, there is no guarantee that a compatible combination of fiber and matrix can be found. Adhesion between fiber and matrix is necessary if the material is to retain its structural properties, and such adhesion is highly speculative at this time. The third disadvantage is that the conventional process of dipping fibers into a matrix-material bath is unlikely for SMF use (see Sec. 5.2.4). The production of the composite would therefore require a more space-specific process (e.g. vapor deposition), thus complicating fabrication. The issues of fiber-matrix adhesion and space-specific composite production need experimental research. Because of the uncertainties discussed above, the study group discarded this option; however, this alternative deserves further study.

The sixth option is all-lunar composites. Due to the limited variety of materials available, the choices are few. The only materials apparently suitable for fiber production are glasses (such as S-glass) and metals. Metal-metal composites have high CTE's. Although metal-fiber/glass-matrix composites could have adequate CTE's, production seems unlikely since the metal fibers melt at lower temperatures than the glass. This makes the bath process unusable, although it is technically

simple in lunar gravity. It may be possible to vapor deposit glass onto metal fibers without melting them, but this has not been verified. Therefore metal fibers are an unlikely possibility.

If the fibers are made from S-glass, however, they can perhaps be imbedded in metal or glass matrices. However, the S-glass/metal matrices composites suggested for SPS structural members have too-high CTE's (see Table 5.9). The most likely, S-glass in titanium matrix, has a CTE of 5.9 x 10^{-6}m/m°K. Finally, glass fibers could be imbedded in a glass matrix, provided that a process could be devised to apply one to the other without destroying the fibers. Possibly the fibers could be made from a glass with a higher melting point than that of the matrix glass.

The principal disadvantage of all of the lunar-material composites is that they are apparently untried combinations. No data was available to the study group on the likelihood of fiber-matrix adhesion of these various combinations. It may therefore be very difficult to produce an adequate all-lunar composite. Due to this uncertainty, the study group discarded this option. However, should later research answer some of the questions raised above, the all-lunar composites may be a likely alternative for waveguides and other components.

The seventh option (chosen for the reference SMF) is foamed glass. The characteristics of the material and its production

sequence were described in some detail in Sec. 5.3.1. For the production of waveguides, this material shares some of the advantages listed in structural member production: low CTE, existing technology, low mass of waveguides relative to some other options. Foamed glass also resists meteoritic shattering. It also shares some disadvantages: it requires earth-input foaming agents, unless such agents can be produced from lunar materials; and the machining operations produce an abrasive dust which requires dust-handling systems to protect the equipment. In addition, there is some wastage of material, due to kerf losses in cutting operations (described below).

As mentioned above, the waveguides require an interior coating of conductive aluminum. Since pure Al is available at the SMF, no substitution is necessary.

5.9.2: Wave_uide Manufacture: Consultations with Pittsburgh Corning Co. (Ref. 5.50) have confirmed the possibility of manufacturing foamed glass with the required coefficient of thermal expansion. Foamed glass is currently manufactured with CTE's as low as 2.8×10^{-7} m/m-°K. It is also possible to manufacture dense foamed glass suitable for machining to the required tolerances. However, glasses with both properties (CTE and machinability) in combination are still in development. At the present time, information regarding the foaming of these glasses is proprietary. The study group therefore assumed that the basic processes currently used for foamed-glass production (described in Sec. 5.3.1) could be modified to produce waveguide materia'.

The method of waveguide manufacture depends on the shape in which the foamed glass is produced. Several such shapes and methods are illustrated in Fig. 5.57. The simplest method would form the glass around a refractory mold, producing molded channel sections. The channel sections would then be machined to the appropriate tolerances, and coated on the inside with Al. A machined slab of foamed glass, coated with Al, would then be added to complete the waveguide box. However, the molding of foamed glass in such shapes is not in common practice today, primarily because of difficulties in matching the coefficients of thermal expansion of foamed glass and mold. Those mold materials which do have appropriate CTE's tend to bond with the foamed glass during cooling. It may be possible to coat

A) DIRECT MOLDING

MACHINED SLAB

MOLDED CHANNEL

B) CUT SHEET

MACHINED SLAB

C) MILLED BLOCK

MACHINED SLAB

MILLED CHANNEL
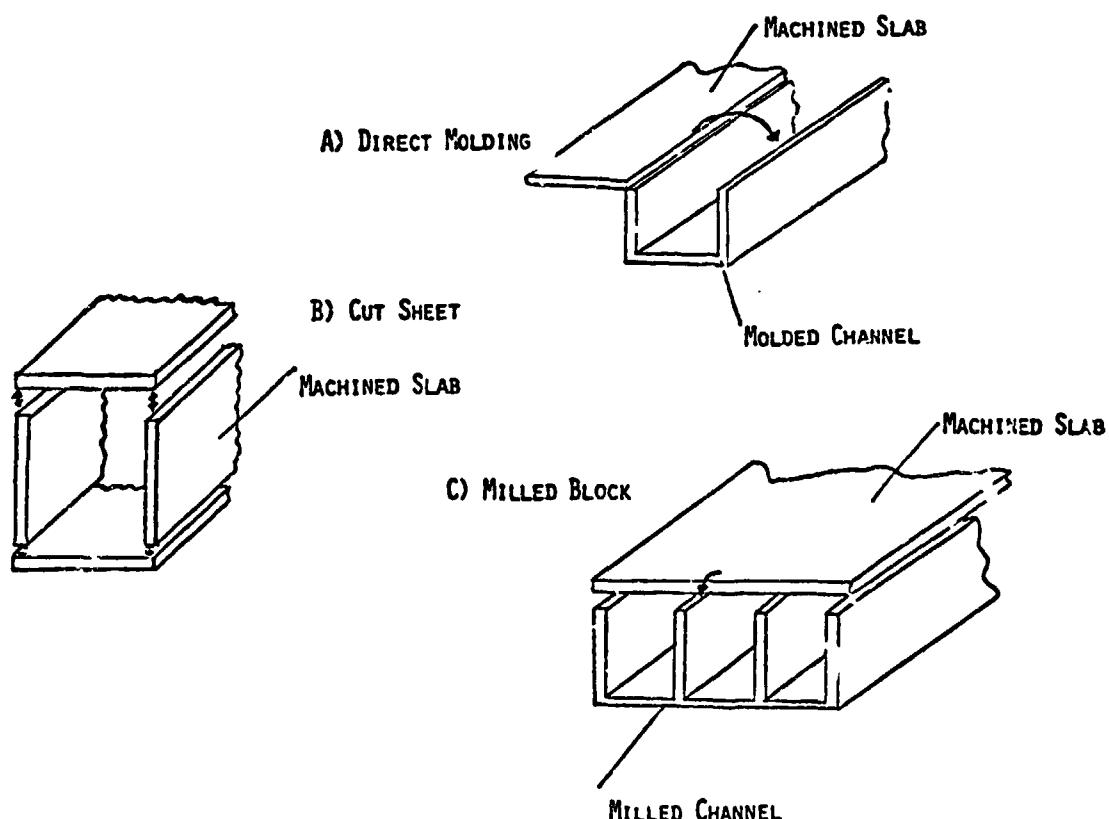
FIGURE 5.37: POSSIBLE FOAMED-GLASS SHAPES FOR WAVEGUIDES

5.172

the molds prior to foaming to alleviate the bonding problem, but such coatings would probably require earth inputs.

The second method is to produce thin sheets of foamed glass, machine the box sides from the sheet, and construct the waveguide from the machined components (after Al-coating). Although the molten-tin-bath method described in Sec. 5.3.1 does produce foamed-glass sheets, these sheets are thicker than required for waveguides. Consultations with Pittsburgh-Corning (Ref. 5.50) indicate that direct production of thin sheets is difficult due to breakage problems during cooling. Sheets of foamed glass are not commercially produced at the present time. Conventionally, foamed glass is produced in blocks from which specific shapes are machined. For the production of this slabs, this leads to wastage during block sawing and during slab machining; this wastage is estimated at 30% of the block material. In addition, to avoid breakage during cutting and handling, the minimum thickness which could be practically produced is estimated to be 2.5 mm (Ref. 5.50). This is roughly 2.8 times the thickness suggested by the JSC-GD study (Ref. 5.43).

The third alternative is to produce large blocks of foamed glass, then mill channels through the blocks. After coating with aluminum, the channels are closed by coated machined slabs. Though conceptually simple, this approach generates a large quantity of waste dust and debris. Due to the difficulties in handling and reprocessing such waste, this option is unlikely for SMF use.

The study group chose the production of foamed glass blocks, followed by the cutting and machining of individual slabs. After coating with aluminum, these 2.5-mm-thick slabs are assembled into waveguide boxes. The study group felt that this more conventional process was more likely to produce foamed glass with the requisite properties and tolerances; since such glasses are still in development, the study group felt that the choice of advanced production processes would stretch the technical uncertainty uncomfortably far.

Currently foamed glass is cut with saws made from hard alloys such as tungsten carbide (Ref. 5.28). This process produces an abrasive kerf dust, which requires special handling systems in zero-g; and sawing is limited in the surface flatness of the output. Despite these drawbacks, the study group chose sawcutting for the reference SMF. The alternative of laser cutting was discarded because of its large mass and power requirement. Electron beam cutters, used in many parts of the SMF, are unsuitable for foamed-glass cutting, since glass is a poor electrical conductor, and the electrons cannot be returned to the EB gun cathode.

As described in Ref. 5.51, waveguides operating at a frequency of 2.45 GHz require an interior coating of aluminum 6.7 microns thick. Although the slow-cut surfaces may be flat enough to meet dimensional requirements, they are not smooth enough for coating, due to the exposed bubbles on the surfaces. There exist several methods to produce foamed-glass blocks with

smooth-glass surfaces (Ref. 5.25). However, these techniques
are applied during the foaming, and are therefore unusable on
cut sheets. Also, the smooth-glass/foamed-glass interface is
subject to stresses during cooling, possibly requiring longer
cooling cycles. The study group therefore decided to use
lasers to smooth the surface by fusing or burning off irregular-
ities.   This concept carries some technical uncertainty, and
the smoothing operation might require addition of glass
to the surface (e.g. by vapor deposition) prior to laser
smoothing. These issues need experimental research, particu-
larly because foamed glass with the needed properties has not
yet been developed, and its properties in a smoothing operation
are therefore difficult to predict.

After the smoothing, the interior aluminum coating is
applied by vapor deposition, a process similar to the direct
vaporization of aluminum contacts in solar cell production
(see Sec. 5.24). The Al is vaporized by electron beams.

The output faces of the waveguides must then be slotted.
In SPS operation, these slots are the output ports of the
waveguides, releasing the microwaves to space. The slots
require close tolerances in dimensions and position. There-
fore those slabs destined to be output faces are slotted by
laser. Holes are also laser-cut through the waveguide input
faces. Feeder waveguides from the klystrons are connected to
these input holes at the SPS assembly site. The coated sheets
are then assembled into waveguide boxes by automated machinery

The sheets are fused together with lasers, avoiding the need for adhesives from Earth. The finished waveguides are packaged and shipped to the SPS assembly site.

5.10 MODIFICATIONS REQUIRED FOR PELLET INPUTS

As discussed in Sec. 4.5, the reference SM designed in this study assumes that raw materials are launched from the Moon by chemical rocket, and can therefore arrive at the SMF in shapes convenient for input into the factories (i.e. rods, slabs, bagged powder). These shapes would not be available, however, if the lunar launch were done by catapult (e.g. mass-driver).

The lunar materials input shapes to the reference SMF are listed in Table 5.13 (repeated from Table 4.4). Replacing these shapes by pellet inputs requires relatively simple modifications of the input sections of the SMF.

In the reference SMF, aluminum and iron rods (6.4 cm diameter) are fed into induction furnaces of the type described in section 5.3.3 (see Figs. 5.21 and 5.22). To replace these rods by pellets, two options are possible. In the first option the pellets could be loaded into 6.4 cm-diameter tubes; the tubes would then be crimped at both ends. These tubes could then be fed into the furnaces in the same fashion as the rods, though slightly faster to account for their lesser density. The tubes would be manufactured at the SMF from Al or Al alloy

TABLE 5.13: PHYSICAL SHAPES OF
LUNAR MATERIAL INPUTS TO THE REFERENCE SMF

Type of Input	Shape and Dimensions
Lunar Inputs	
Aluminum:	
For Al and Al alloy products	Rod, 6.4 cm diameter 10 m length
For SENDUST alloy	Rod, 2.5 cm diameter 3 m length
Silica:	Slab, 1 m x 1 m x .04 m
Silicon:	
for solar cell production	Slab, 1.2 m x .42 m x .04 m
Fo furnaces	Rod, 3.5 cm diameter 3 m length
Natural Lunar Glass:	∠5 micron powder, bagged
Iron:	Rod, 6.4 cm diameter 10 m length
S-Glass:	Rod, 6.4 cm diameter 8 m length
Magnesium:	Rod, 1.7 cm diameter 3 m length

ribbon (already available) or from Fe ribbon, produced by
routing molten iron from the furnace through a continuous
caster and the existing rolling mill. This option would there-
fore require the addition of a continuous caster for iron
slabs, a form rolling and welding unit to produce the tubes,
and a tube-filling system. This tube-filling system could be
either mechanical or pneumatic. In the pneumatic case, the
pellets would be fluidized in an inert gas (e.g. argon) and
pumped through the tube. The pellets would be stopped by a
mesh grating. When the tube would be filled, the argon would
be pumped out, the grating retracted, and the tube crimped at
both ends.

In the second option, the pellets could be fluidized in an inert gas and pumped directly into the furnace. The pellets would enter the furnace with enough velocity to splash into the melt. The inert gas would be pumped out through a filtered outlet. This option requires sealing the furnace to avoid loss of gas, and providing a pellet fluidization system.

The production of Al 6063 alloy requires input of silicon and magnesium. The silicon could be piped in from a silicon furnace (described below). Or the silicon pellets could be sealed in tubes made of Al 6063 alloy, and fed to the furnaces as rods. This latter option could be used for magnesium pellets also. Finally, a small magnesium furnace could be added, which would receive pellets fluidized in inert gas, and would feed molten Mg to the Al alloy furnace.

For the production of SENDUST alloy, the iron furnace could receive liquid aluminum and silicon from the aluminum and silicon furnaces, or Al and Si pellets could be loaded into tubes. The tubes could be made of Al, Si, Fe, or SENDUST alloy.

Silica and silicon have magnetic properties which make them unsuitable for melting in induction furnaces. To produce the slabs used in solar cell production, the raw material pellets would therefore be fed to a rotating furnace such as those shown in Figs. 5.19 and 5.29. The furnace in Fig. 5.19 is designed for pellet inputs. The output of the silica and silicon furnaces would be cast into slabs, either by continuous casters or die casters. In addition, the silicon furnace would feed

5.178

molten silicon to the Al and Fe alloying furnaces. This option would therefore require the addition to the SMF of silicon and silica rotating furnaces, and slab casters for each material.

Since a lunar catapult could launch small bags of natural lunar glass powder, no changes to the natural lunar glass input are necessary.

In the reference SMF, S-glass rods are fed into glass fiber producers (see Fig. 5.30). Since these devices are piston-fed tubes, they could be loaded with pellets prior to the piston's travel down the tube. The loading could be done mechanically or pneumatically. In the pneumatic option, the tubes would require an inlet door for the pellets and a filtered outlet for the inert gas. After loading of pellets and evacuation of the gas, the piston would begin its travel. Another option would be the loading of S-glass pellets into a tubular-woven "sock" of S-glass fibers. This filled sock would then replace the rods in the reference design. These socks could be manufactured by the existing insulation weavers.

Thus the replacement of the reference lunar inputs by pellet inputs would not entail major modifications to the reference SMF. The study group feels that these modifications would not have a significant impact on the cost of the SMF.

CHAPTER 6

SMF LAYOUTS

6.1: OVERALL OPERATIONS LAYOUTS OF REFERENCE SMF

6.1.1 Overall Layout: Figure 6.1 presents the overall layout of the reference SMF. The figure is an expanded version of Fig. 1.3 describing the Space Manufacturing Facility concept.

The SMF consists of five major operations sections. The input/output station includes docking facilities and loading and unloading equipment. It receives all inputs to the SMF and dispatches all outputs, and acts as a temporary warehousing facility.

The factories receive raw materials and expendables from the input/output station and manufacture the required SMF products. Personnel are required for supervision, maintenance, and repair.

The habitation section provides the SMF personnel with radiation-shielded living quarters. These quarters include facilities for exercise and recreation, and life-support.

The power plant produces and conditions electrical power from solar energy. This power operates equipment in all sections of the SMF.

The production control section is an operations section rather than an actual facility. It controls all the operations of the SMF, maintaining inventory, adjusting production levels, allocating the available resources as required by the production schedules.
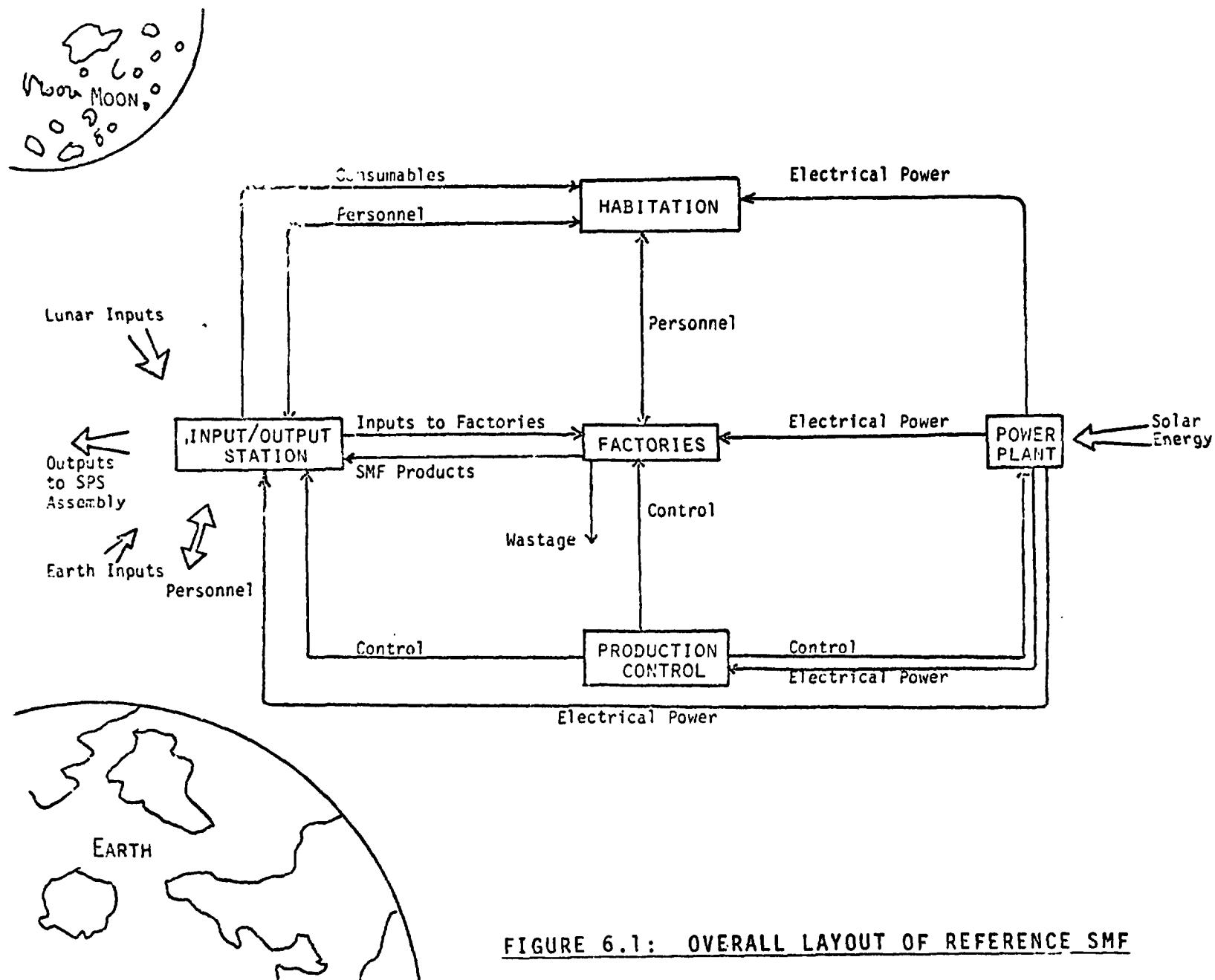
FIGURE 6.1: OVERALL LAYOUT OF REFERENCE SMF

Although Fig. 6.1 is labeled as an overall layout of the reference SMF, other SMF designs would probably share most of these features. Other designs might separate input and output stations, couple the outputs directly to the SPS assembly (if the SMF and SPS assembly were both done by the same facility), or use nuclear rather than solar power. But the functions of the basic components in the figure, and the interactions between the sections, are fundamental to the SMF concept.

More detailed layouts for the factories, including mass-flows between processes, are described in this chapter. Section 6.6 discusses layouts for the support equipment, including the input/output station and power plant.

6.1.2: Factories Layout: Figure 6.2 presents a layout of the major operations within the factories (the input/output station is included for clarity). Unlike Fig. 6.1, this layout is specific to the reference SMF designed by this study. Alternative processes (such as those discussed in Chap. 5) would lead to different layouts.

The operations layout in Fig. 6.2 traces the paths of the SMF material inputs listed in Table 4.5 (see Chap. 4, "SMF Inputs") as they are manufactured into the outputs listed in Table 3.1 (see Chap. 3, "Specifications of SMF Outputs"). The SMF output products are underlined in the layout.

Examination of Fig. 6.2 leads to several observations. First, this reference SMF layout is simple: there are few Earth factories whose major operations layout fit on one page.

6.3
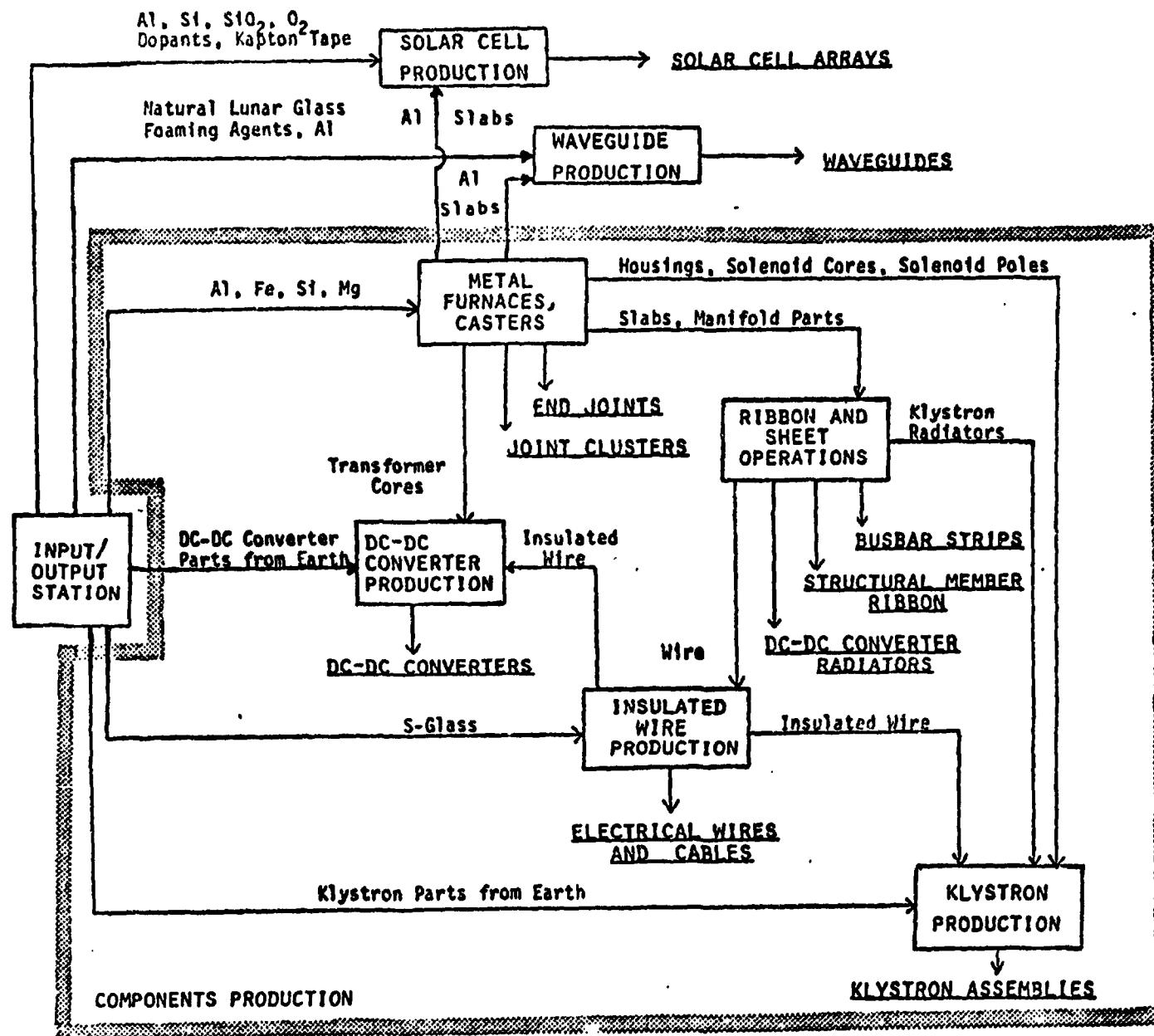
FIGURE 6.2: MAJOR OPERATIONS LAYOUT OF REFERENCE SMF

There are two principal reasons for this simplicity. The
first is the small number of different types of SMF outputs.
Although the SPS contains a large variety of components, much
of this variety is in low-mass components. These components
can therefore be economically brought from Earth, leaving a
small number of types of products for SMF manufacture. The
SMF products, however, account for roughly 90% of the SPS mass.

The second reason is that the SPS components manufactured
by the SMF are relatively simple. Although the SPS does con-
tain some high'·· sophisticated components (such as switching
circuitry, attitude control systems, and klystron components),
that complexity is also concentrated in the low-mass components ·
which are brought from Earth rather than manufactured at the
SMF.

The exception to this simplicity is the production of
solar cells. As will be shown by a later detailed layout,
this production is a complex undertaking. However, at this
level of scrutiny (considering only the major factory opera-
tions), the solar cell production operations may be con-
sidered as one major operation.

Thus, much of the manufacturing variety and complexity can
be left on Earth, in the production of complex low-mass com-
ponents. These components are then brought either to the SMF
for assembly processes or to the SPS final assembly site.

Another observation from Fig. 6.2 is that the reference
SMF operations layout can be conceptually split into three
sections: solar cell production, waveguide production, and

the rest of the operations (collectively called "components production"). In general each of these 'factories' receives one set of inputs from the input/output station and applies manufacturing processes to these inputs, without requiring intermediate inputs from the other 'factories' in the SMF. The exception is the use in the solar cell production and waveguide production of aluminum slabs manufactured by the 'components production' section. However, these slabs could also be brought from the Moon; manufacturing them at the SMF reduces the complexity of the lunar casting processes.

Each factory also returns a particular set of products to the input/output station. Thus the solar cell factory produces only solar cell arrays; the waveguide factory only waveguides; and the components factory produces the remaining SMF products.

This conceptual splitting of SMF operations is possible because the various factories do not share processes. In the design of the reference SMF, every effort was made to combine processes into single pieces of equipment; for example, several production sequences in the components factory share the rolling mills in the 'ribbon and sheet operations'. However, after all such combinations were done, the processes in the three factories remained separate from each other, even when the materials being used were the same. For example, the aluminum contacts in the solar cells are too thin to be produced on the rolling mills in the components factory; they are therefore vapor-deposited. In general, the inputs to any one factory differ from the inputs to the others. For example,

6.6

although all three factories need some type of glass, the solar
cell factory requires optical-quality silica; the waveguide
factory can use natural lunar glass (thus reducing refining
requirements); and the components factory requires S-glass
for production of glass fibers.

Detailed layouts of the major operation in the reference
SMF are shown in Secs. 6.3, 6.4, and 6.5. These layouts in-
clude massflows of materials through the various processes.
Section 6.2 discusses some general considerations in computing
massflows. Explanations of the specific massflows appear in
the detailed layout sections.

6.2: ESTIMATION OF MSSFLOWS

6.2.1: Wastage in the Reference SMF: The massflows in the
detailed layouts in the following section are all based on
the production of one 10-GW SFS (without growth margin).
Therefore the materials breakdown of the SMF outputs (as
listed in Table 3.3) is the starting point for the computation
of the material massflows in the reference SMF layouts. The
types of material inputs needed are the same as the types of
materials required in the SMF outputs. If there were no
wastage in the production processes, the quantities of mate-
rial inputs would also be the same as the output quantities
listed in Table 3.3. However, some wastage occurs in every
production process, the inputs and the internal massflows
must therefore include allowances for this wastage.

Two types of wastage come into play. 'Process wastage'
is the loss of material inputs in the proper functioning

of the process. For example, sawing operations waste kerf from the cuts; milling operations produce chips; and vapor deposition processes lose vapor to space or to containment surfaces other than the deposition surface. These losses apply to every piece produced by the process, and can be predicted from the equipment designs.

The second kind of wastage is 'spoilage', the loss of pieces of product due to failure in the manufacturing process. For example, a machine control system malfunctions, and the output is rejected by quality control systems; or a machine indexing error occurs, ruining the workpiece within it. This type of wastage applies only to occasional pieces. It is unexpected, but statistically predictable from the equipment designs. Salvaging may in some cases be possible but in a highly automated process may not always be cost effective.

The reference SMF designed by this study was therefore used to estimate wastage and to calculate massflows in the layouts. The losses in the processes were first calculated by estimating wastage at each step in the processes, and computing massflows between each step accordingly. These calculations led to two observations.

First, for the products of the components factory in the reference SMF (i.e. structrual member ribbon, klystron assemblies, busbar strips, DC-DC converters, electrical wires and cables, DC-DC converter radiators, end joints, and joint clusters), the total process waste and spoilage estimates from

material inputs to finished outputs ranges from 1% to 10%. In other words, the process with the highest waste (that of the klystron assemblies) loses 10% of those SMF material inputs destined to become part of the final assemblies.

Second, these wastage estimates are no more significant than the uncertainties in the SMF output quantities. As described in Chap. 3, these output quantities were calculated from lunar-material substitutions into the Boeing-JSC baseline SPS design. Since both the baseline SPS design and the lunar-material substitutions carry uncertainties, often 10% or larger, the 1-10% wastage estimates do not significantly alter the accuracy of the input quantities for the products mentioned above. Moreover, the uncertainties in the wastage estimates are dwarfed by the uncertainties in the product quantities. A careful determination of process wastage and spoilage is therefore unnecessary.

These two observations do not apply to the solar cell array and waveguide production. In both cases, the process wastage is significantly higher than in the components production. In solar cell production, the vapor deposition processes have an estimated deposition efficiency of 67%, with the other 33% of the input material lost to space or deposited on containment surfaces other than the deposition surface. In waveguide production, kerf losses in cutting and slotting foamed-glass sheets are estimated to waste 30% of the foamed glass. Both solar cell production and waveguide

6.9

production also have spoilage losses, beyond the process was-
tage.

These observations led to allowable simplifications in the
computations of the massflows in the layouts as discussed in
Sec. 6.3.7. The rationale for the specific massflows is ex-
plained in the detailed layout sections.

6.2.2: Waste Disposal: In the early stages of this study,
when preliminary estimates of wastage were made, the predicted
figures were so low that the addition of specialized repro-
cessing equipment to the SMF design seemed a needlessly costly
complication, for several reasons. First, some of the waste
is unrecoverable: vapor escaping from deposition processes
is lost to free space, and substandard or broken solar cells
can be reduced to their component materials only with complex
separation and purification techniques. Second, returning
metallic wastes (chips, trim, broken pieces) to the melts re-
quires packaging of the waste for furnace insertion, or modi-
fication of the furnace designs to accept loose material as
inputs. Third, the anticipated waste contains only traces of
earth materials, and therefore its loss adds only to the re-
latively lower cost of lunar material transportation. Fourth,
the solid waste can serve as radiation shielding after only
a bagging operation, avoiding any need for reprocessing.

As the design of the reference SMF evolved, the processes
changed, and their wastage estimates became more accurate --
and higher. The reference SMF design presented in this

report wastes 50,000 tons of every 150,000 tons of material inputs (or 33% of the input mass). Of the 50,000 tons, an estimated 36,000 tons are wasted in solar-cell production, and another 6,500 tons are wasted in waveguide production.

In view of the high waste mass, particularly in solar-cell production, modifications to the reference SMF should be considered, either to reduce the wastage, or to reprocess the waste. A discussion of these issues appears in Chap. 13, "Possible System Tradeoffs".

6.3: COMPONENTS PRODUCTION OPERATIONS LAYOUTS

6.3.1: Section Organization: The major operations layout of the reference SMF factories is shown in Fig. 6.2 above. The lower section of that layout presents the major operations of the components factory, which produces structural member ribbon, klystron assemblies, busbar strips, DC-DC converters, electrical wires and cables, DC-DC converter radiators, end joints, and joint clusters. Each of the major operations of the components factory (shown as boxes in Fig. 6) will now be expanded into a detailed layout. The layouts e accompanied by explanations of the sequences of processes. (Note: The singular form is used for simplicity when referring to a particular type of equipment [e.g. 'the furnace'] although there may be several such pieces of equipment in the SMF.) The circles on some of the arrows in the layouts indicate internal storage devices (described in Sec. 6.6.2). The mass figures listed in the layouts are the total massflows (inclu-

ding wastage allowances) required for the production of one
10-GW SPS. Section 6.3.7 presents the rationale behind these
massflows. Since the reference SMF is sized to produce one
10-GW SPS per year, the figures in the layouts are yearly mass-
flows through the machinery. The equipment designs are pre-
sented in Chap. 7, "Production Equipment Specifications".

6.3.2: Metals Furnaces and Casters Layout: The box labeled
'Metals Furnaces and Casters' in Fig. 6.2 is expanded into a
detailed layout in Fig. 6.3. At the upper left-hand corner
of the detailed layout, iron rods (from the input/output
station) are fed into a melting and alloying furnace, which
alternately feeds two die casters. In the first case, the
furnace feeds molten iron to a die caster producing solenoid
poles for klystrons. These solenoid poles are then sent to
the klystron production section.

In the second case, aluminum and silicon rods are also
fed into the furnace to produce SENDUST alloy. The alloy is
fed to a die caster to produce SENDUST transformer cores for
DC-DC converters. The cores are then sent to the DC-DC con-
verter production section.

Lower down in Fig. 6.3, aluminum rods (from the input/out-
put station) are fed into a melting and alloying furnace. This
furnace produces four output streams. In the first case, mag-
nesium and silicon rods are fed into the furnace as well, to
produce Al 6063 alloy. This molten alloy is fed to a con-
tinuous caster, which produces 6063 alloy slabs. These slabs
are th   sent to the ribbon and sheet operations section.

6.12

Al Rods
55 tons

Si Rods
110 tons

Fe Rods
1700 tons

IRON
MELTING/ALLOYING
FURNACE

Molten Fe
800 tons

DIE CASTER

SOLENOID POLES
800 tons

Molten SENDUST Alloy*
1100 tons

TRANSFORMER
CORE CASTER

TRANSFORMER CORES
1100 tons

Mg Rods
180 tons

Si Rods
100 tons

Al Rods
44000 tons

ALUMINUM
MELTING/ALLOYING
FURNACE

Molten Al 6063 Alloy**
25000 tons

Molten Al
14700 tons

CONTINUOUS
CASTER

SLAB
CUTTER

AL 6063 ALLOY SLABS
25000 tons

AL SLABS
14700 tons

Molten Al
4100 tons

Molten Al 6063 Alloy**
18 tons

DIE
CASTER

SOLENOID CORES
1100 tons
KLYSTRON HOUSINGS
3000 tons
MANIFOLD PARTS
8 tons

END JOINTS
9 TONS
(After 10% wastage: 8 tons)

JOINT CLUSTERS
9 TONS
(After 10% wastage: 8 tons)

O Indicates an Internal Storage Device

* SENDUST Alloy is 85%Fe, 10%Si, 5%Al.

** Al 6063 Alloy is 98.9%Al,
   0.7%Mg, 0.4%Si.

6.13

FIGURE 6.3:   METAL FURNACES AND CASTERS: DETAILED LAYOUT

In the second case, pure molten aluminum is fed to the continuous caster to produce aluminum slabs. These slabs are sent to three destinations: 3,050 tons to the solar cell factory, 165 tons to the waveguide factory, and 11,500 tons to the ribbon and sheet operations section of the components factory.

In the third case, molten aluminum is fed to a die caster with a number of different molds. This caster produces solenoid cores (one part), klystron housings (collector and solenoid housings, two parts each), and manifold parts (five parts per manifold). The solenoid cores and klystron housings go to the klystron production section. The manifold parts are sent to the ribbon and sheet operations section.

In the fourth case, molten Al 6063 alloy goes to the die caster. The caster produces end joints (one part) and joint clusters (several shapes). These end joints and joint clusters are SMF outputs; they are sent to the input/output station.

6.3.3: Ribbon and Sheet Operations Layout: Figure 6.4 expands the box labeled 'Ribbon and Sheet Operations' in Fig. 6.2 into a detailed operations layout. At the left-hand end of the detailed layout, Al 6063 alloy slabs (from the metals furnaces and casters section) are fed into a rolling mill. This rolling mill reduces the slab thickness, producing 1.77 mm thick Al 6063 ribbon (.74 m wide). The pieces of ribbon are then end-trimmed and welded into long structural member ribbon which is then wound onto rolls for shipment. During the roll winding, a teflon sheet is sandwiched between successive

6.14
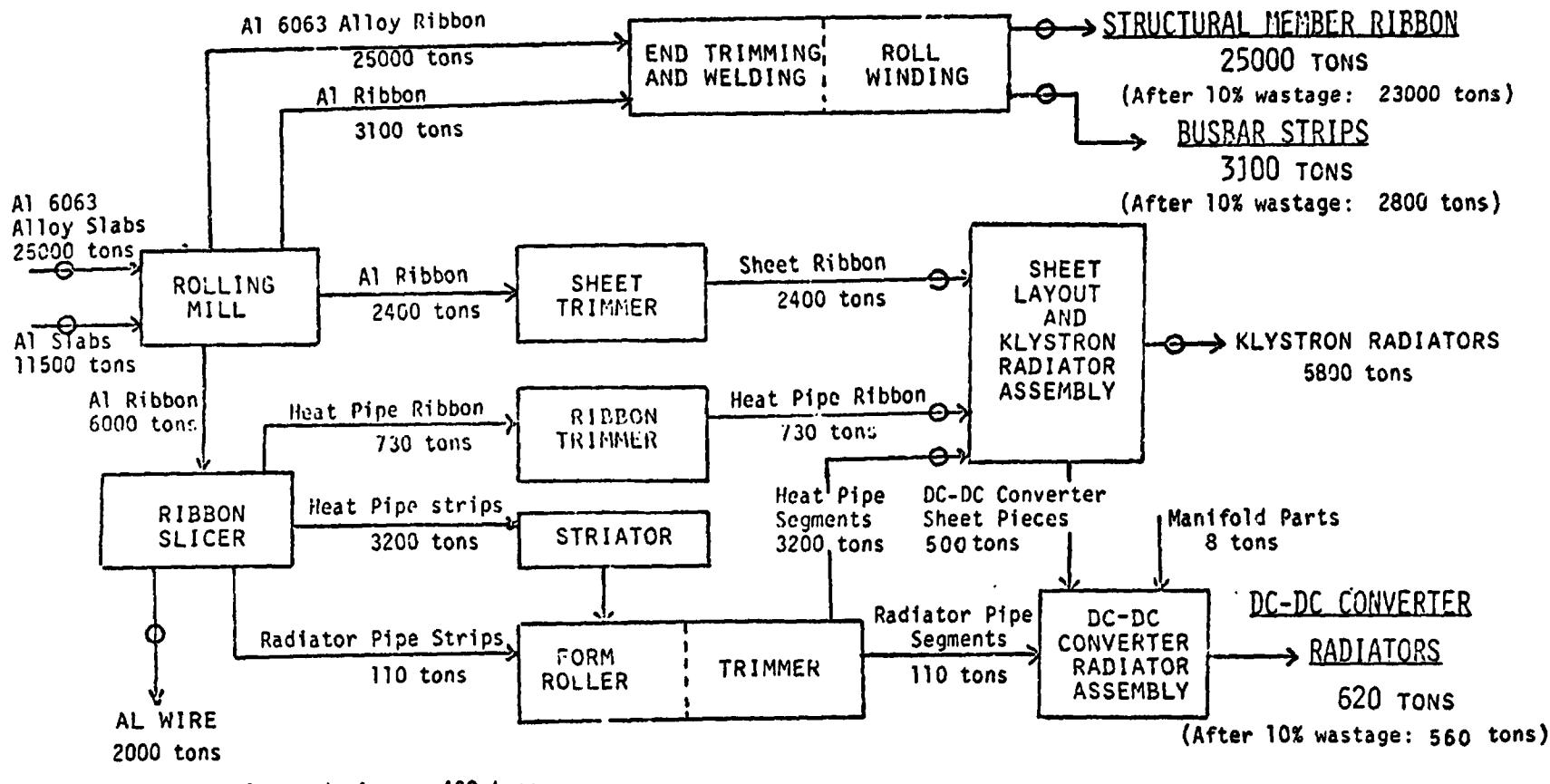
FIGURE 6.4: RIBBON AND SHEET OPERATIONS: DETAILED LAYOUT

layers of Al alloy ribbon, to prevent ribbon surfaces from vacuum-welding together. The rolled-up structural member ribbon is SMF output; it is sent to the input/output station.

The rolling mill also receives pure (99.6+%) aluminum slabs from the metals furnaces and casters section. From these slabs the rolling mill feeds three output streams. In all three cases, the rolling mill produces 1 mm thick Al ribbon (.74 m wide). In the first case, the ribbon is end-trimmed and welded into long busbar strips, which are then wound on rolls. As with the structural member ribbon above, teflon sheet is inserted into the busbar strip roll to keep ribbon surfaces from vacuum-welding.

In the second case, the Al ribbon goes to a sheet trimmer, which cuts the ribbon and trims its edges to form pieces of sheet ribbon (.72 m x 2.15 m). These are sent to sheet layout and klystron radiator assembly (discussed later).

In the third case, the rolling mill feeds the Al ribbon to a ribbon slicer. The ribbon slicer cuts the .74 m wide ribbon into strips ranging in width from .25 m down to 1.0 mm. These strips feed four output streams from the ribbon slicer.

First, heat pipe ribbon .125 m wide is sent through a ribbon trimmer, which cuts the ribbon into 1.6 m lengths. These lengths of heat pipe ribbon are sent to the sheet layout and klystron radiator assembly.

Second, heat pipe strips .25 m wide and 3.5 m long are passed through a striator which scores one side of the strips with fine grooves. These grooves will eventually serve as capillary return paths for fluid in a heat pipe. The striated

heat pipe strips are then form rolled to produce heat pipe segments. These segments are sent (without trimming) to the sheet layout and radiator assembly operation.

Third, radiator pipe strips .25 m wide and 3.5 m long are form rolled to the same cross-section as the heat pipe segments mentioned above (see Fig. 3.6 for cross-section). These strips are trimmed to 3.45 m length, and sent to the DC-DC converter radiator assembly (discussed later).

Fourth, the ribbon slicer produces a range of widths of aluminum wire, as small as 1.0 mm x 1.0 mm. This wire is sent to the insulated wire production section.

The sheet layout and klystron radiator assembly receives pieces of sheet ribbon, heat pipe ribbon, and heat pipe segments from other parts of the components factory, and produces two output streams. For the first output, pieces of sheet ribbon are welded together into sheet pieces 1.44 m x 2.15 m x .001 m. These pieces are sent to the DC-DC converter radiator assembly.

For the second output, sheet pieces are produced as described above, but heat pipe segments and pieces of heat pipe ribbon are welded to the sheet pieces, forming six heat pipes extending from one surface of the sheet pieces. The sheet pieces with the heat pipes are the klystron radiators, and they are sent to the klystron production section.

The DC-DC converter radiator assembly receives sheet pieces, radiator pipe segments, and manifold parts from other parts of the components factory, and assembles the sheet

6.17

pieces into radiator sheets 36.55 m x 10.08 m x .001 m. The radiator pipe segments and manifold parts are welded to one surface of the sheets, forming a network of pipes for cooling fluid. The completed DC-DC converter radiators are SMF outputs; they go to the input/output station. Since the radiators are too large for the SMF internal transport system, this assembly facility is located near the input/output station, and the DC-DC converter radiators are moved by the loading/unloading manipulators.

6.3.4: Insulated Wire Production Layout: The 'Insulated Wire Production' box in Fig. 6.2 is expanded into a detailed operations layout in Fig. 6.5. Rods of S-glass (65% SiO_2, 25% Al_2O_3, 10% MgO) from the input/output station are fed into a heated pipe, and when molten, are drawn through a multi-hole die to produce glass fibers, which are wound on spools.

The spools of glass fibers and aluminum wire (from the ribbon and sheet operations section) are loaded into a wire wrapper, which produces three output streams.

The first output is spools of insulated wire for DC-DC converter coils, which is sent to the DC-DC converter production section. The second output is spools of insulated wire for klystron coils, which is sent to the klystron production section. The third output is electrical wires and cables (on spools); this is an SMF output, and is sent to the input/output station.

6.18

Glass Rods
1500 tons

Al Wire
2000 tons

GLASS
FIBER
PRODUCTION

Glass Fiber
or Spools

1500 tons

WIRE
WRAPPING

INSULATED WIRE:
FOR DC-DC CONVERTER COILS
480 tons
FOR KLYSTRON COILS
2300 tons

ELECTRICAL WIRES
AND CABLES

740 TONS

(After 10% wastage: 670 tons)
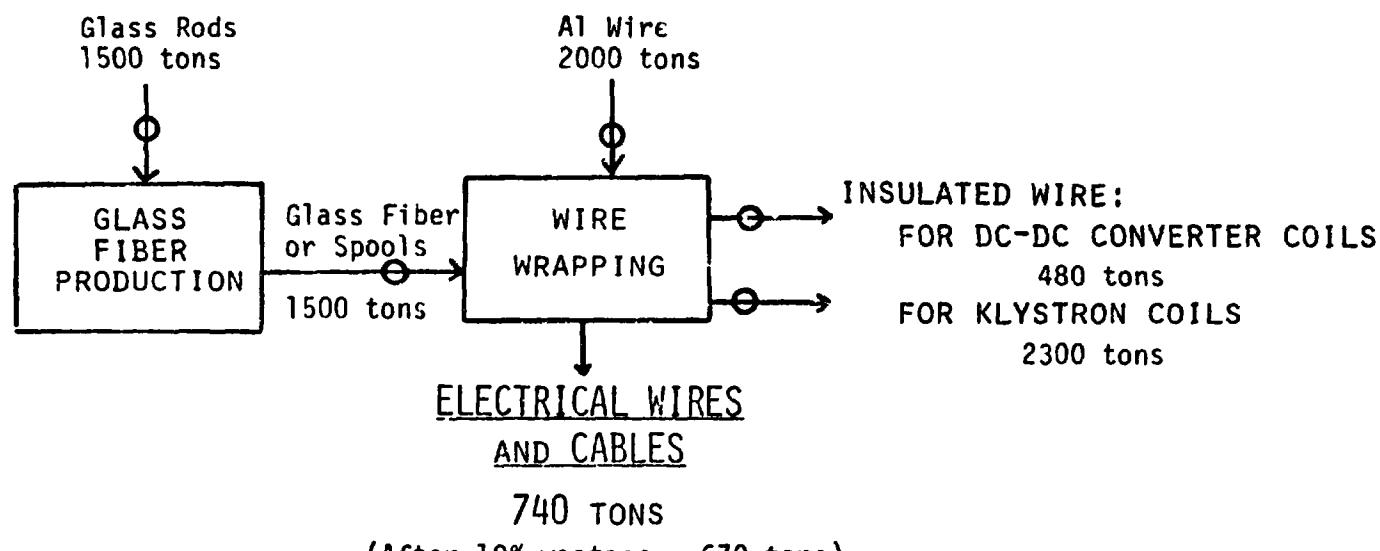
O Indicates an Internal Storage Device

FIGURE 6.5: INSULATED WIRE PRODUCTIOi: DETAIL5D LAYOUT

6.3.5: DC-DC Converter Production Layout: Figure 6.6 expands the 'DC-DC Converter Production' box in Fig. 6.2 into a detailed operations layout. Transformer cores (from the metals furnaces and casters section) are drilled to provide core coolant channels. Next, insulated wire (from the insulated wire production section) is wound into coils around the transformer cores. Finally, DC-DC converter parts from Earth (from the input/output station) are added to the transformer to complete the DC-DC converters. These converters are SMF outputs; they go to the input/output station.

Transformer Cores   Insulated Wire   DC-DC Converter Parts
1100 tons   480 tons   from Earth
                                                        700 tons

┌───────────────┐   ┌───────────────┐   ┌───────────────┐
│ DRILLING OF │   │   COIL   │   │   │
│   COOLANT   │ ───> │   │ ───> │   ASSEMBLY   │
│   CHANNELS   │   │   WINDING   │   │   │
└───────────────┘   └───────────────┘   └───────────────┘
                                                      │
                                                      ▼

                                             DC-DC CONVERTERS
                                                2300 TONS

◯Indicates an Internal Storage Device   (After 10% wastage: 210ᵤ tons)
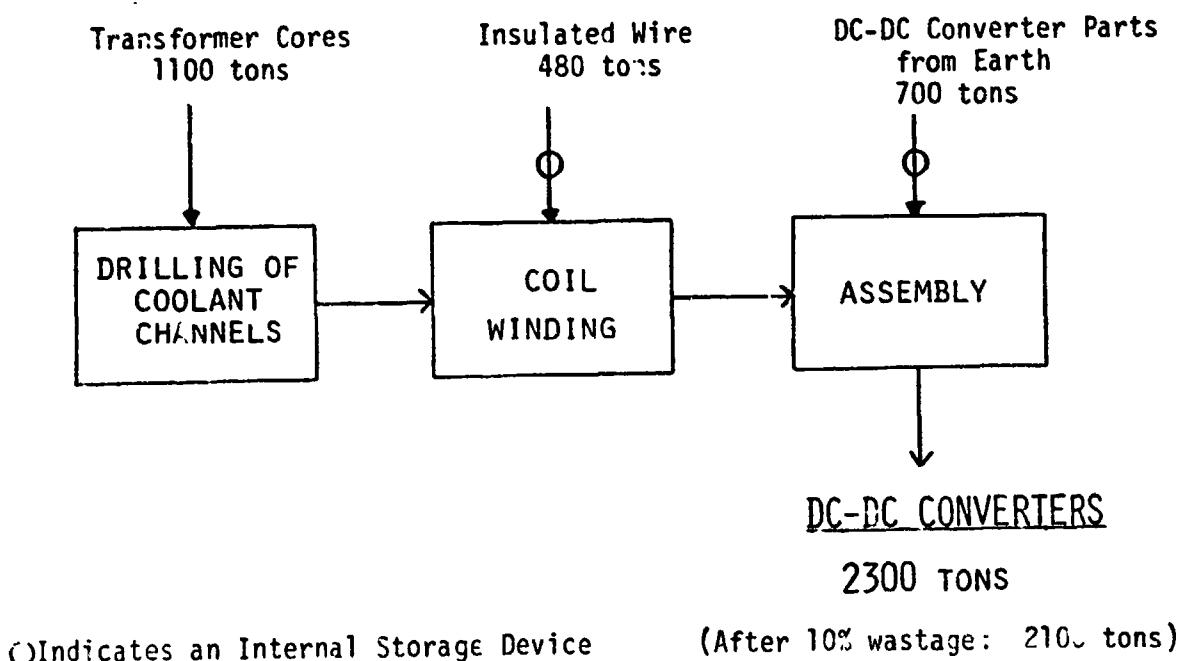
FIGURE 6.6:   DC-DC CONVERTER PRODUCTION: DETAILED LAYOUT

6.20

6.3.6: Klystron Production Layout: The box labeled 'Klystron Production' in Fig. 6.2 is expanded into a detailed operations layout in Fig. 6.7. Solenoid cores (from the metals furnaces and caster section) are first machined and polished to obtain adequate cavity dimensions and surface finish. Next, transverse coolant channels are drilled through the solenoid cores. The cores are tested for proper cavity operation.

Ceramic windows are part of the klystron parts from Earth (from the input/output station); they are fitted into the output cavities. Next, the solenoid cores are wound with insulated wire (from the insulated wire production section).

Solenoid poles (from the metals furnaces and casters section) are welded in place, and the assemblies a old tested for proper function. Next, the solenoid cores are attached to the radiators (from the ribbon and sheet operations sections).

The klystron units now go into final assembly, where components from Earth (collectors and other components, from the input/output station) and collector and solenoid housings (from the metals furnaces and casters section) are assembled to the solenoid cores, completing the klystron assemblies. The assemblies are then baked out and processed, a "running-in" process to outgas and age the tube, and tested to verify proper function of the klystron. The klystron assemblies are SMF outputs; they are sent to the input/output station. Note: All the sections of all the SMF factories include quality control procedures. However, they are not shown in the

Solenoid Cores
1,100 tons

Ceramic Windows*

Insulated Wire
2,300 tons

MACHINING AND POLISHING → DRILLING OF COOLANT CHANNELS → TESTING → FITTING OF OUT CAVITIES → SOLENOID WINDINGS

WELDING OF POLE PIECES → COLD TESTING → RADIATOR ATTACHMENT → FINAL ASSEMBLY → BAKEOUT AND PROCESSING → TESTING

Solenoid Poles
800 tons

Radiators
5300 tons

Solenoid Housings and Collector Housings
3000 tons

Collectors*
Other Components*

(*Total mass of ceramic windows, collectors, and 'other components' : 3500 tons.)

○ Indicates an Internal Storage Device

KLYSTRON ASSEMBLIES
16,500 TONS

(After 10% wastage: 15,000 tons)

FIGURE 6.7:   KLYSTRON PRODUCTION: DETAILED LAYOUT

operations layouts. Only the klystron production layout includes testing, because the tests required are particularly sophisticated and significantly increase the complexity of production.

6.3.7: Components Production Massflows: As described in Sec. 6.2.1, examination of the process and equipment designs in the components factory yielded total process waste and spoilage estimates between 1% and 10% for each output product. And the uncertainties in the wastage estimates are dwarfed by the uncertainties in the product quantities. Taking these considerations into account, the study group simplified the problem with two decisions.

First, for the 1%-10%-wastage products (structural member ribbon, klystron assemblies, busbar strips, DC-DC converters, electrical wires and cables, DC-DC converter radiators, end joints, and joint clusters), the study group assumed a conservative 10% total wastage (combined process wastage and spoilage) from material inputs to finished products.

Second, for each of these products, rather than allocating a fractio of the 10% wastage to each of the production steps, the study group made the simpler, conservative decision to size each production step for maximum wastage.

In other words, the throughputs through all components production steps are first calculated as if there were no wastage whatsoever (based on one 10-GW SPS without growth margin). Then all the massflows were set 10% higher. It is

6.23

these higher massflows which appear in the operations layouts. The components factory equipment is also sized for these mass-flows. These two decisions greatly simplify the bookkeeping of massflows, without significant loss of accuracy. The SMF material inputs masses in the components production layouts match those listed in Table 4.2. The SMF output masses in parentheses (after the assumed 10% wastage) match those listed in Table 3.1.

6.4: SOLAR CELL PRODUCTION OPERATIONS LAYOUTS

6.4.1: Operations Layout: Figure 6.8 presents a detailed operations layout of the solar cell factory in the reference SMF. The following discussion traces the growth of the solar cells through the layout. Specific descriptions of production equipment appear in Chap. 7.

Starting in the upper left-hand corner of the layout, aluminum (from slabs from the metals furnaces and casters section) is deposited by direct vaporization (DV) to form rear contacts (2 microns thick) for the solar cells. At the same time, metallurgical grade (MG) silicon (from the input/output station) is zone refined to semiconductor grade (SeG). This SeG silicon is then direct vaporized onto the rear aluminum contacts, to a depth of 50 microns. Simultaneously, the p-dopant (boron) is ion-implanted into the bottom 45 microns of the silicon. The silicon layer is then recrystallized to improve the crystalline quality of the deposition. A pulsed-beam recrystallization fosters the growth of columnar grains, and a scan recrystallization widens the diameter of these grains.

6.24

MG Si 26,500 Tons → ZONE REFINING → Process Waste 5,600 Tons

Al 975 Tons
SeG Si 21,000 Tons
Boron <1 Ton
Phosphorus <1 Ton

DV OF AL REAR CONTACT

DV OF SILICON AND P-DOPANT IMPLANTATION

PULSE RECRYSTALLIZATION | SCAN RECRYSTALLIZATION

N-DOPANT IMPLANTATION

ANNEAL

Process Waste 325 Tons

Process Waste 7,000 Tons

Al 975 Tons
SiO₂ 30,000 Tons
SiO₂ 19,500 Tons

DV OF AL FRONT CONTACT

FRONT CONTACT SINTERING

CELL CROSSCUT

CELL INTERCONNECTION

DV OF SiO₂ OPTICAL COVER

DV OF SiO₂ SUBSTRATE

Process Waste 325 Tons

Cell Interconnects

Process Waste 10,000 Tons

Process Waste 6500 Tons

MASK CLEANUP → Process Waste 600 Tons

Al 1100 Tons
DV OF INTERCONNECTS → Process Waste 360 Tons

Panel Interconnects

Kapton Tape 420 Tons

PANEL ALIGNMENT AND SPARE PANEL INSERTION

PANEL INTERCONNECTION

LONGITUDINAL CUT

KAPTON TAPE APPLICATION

ARRAY SEGMENT FOLDING AND PACKAGING

SOLAR CELL ARRAYS
48,900 Tons
(After 10% Wastage:
44,000 Tons)

6.25

FIGURE 6.8: SOLAR CELL PRODUCTION: DETAILED LAYOUT

Next, the n-dopant (phosophorus) is applied by ion-implantation to the top 5 microns of the silicon layer. After the n-dopant application, an annealing step heals the resulting point defects in the crystal lattice.

Aluminum (from the metals furnaces and casters section) is then deposited by DV to a depth of 1 micron to form the front contacts. This deposition is done through shadow masks, in two steps: the first deposition mask forms the fingers of the grid fingers pattern; the second mask forms the collector bar, completing the pattern on the cells. Once used, the masks are coated with aluminum, and must be cleaned before being returned to the DV process. Following the deposition of the aluminum, the top contacts are sintered by a low-power beam scan over the grid fingers pattern.

The sheets of solar cells are then cut into sections ('crosscut'). Cell interconnects are inserted between the sections of cells and electrostatically bonded to the collector bars and rear contacts. Every 18 strips, the interconnect is omitted. This forms panels of 18 sections each, with panel dimensions 1.17 m x 1.1 m. The interconnects are produced by a separate machine which direct-vaporizes aluminum (from the metals furnaces and casters section) to form a sheet of Al; this sheet is then cut into interconnects.

After the cell interconnection, a 75-micron thick optical cover of SiO_2 (from the input/output station) is direct-vaporized onto the top surface of the cell panels, covering the silicon wafers, top contacts, and interconnects. Next, a

50-microns thick layer of SiO_2 is direct-vaporized onto the bottom of the cell panels, covering the rear contacts and inter-connects. This layer is the glass substrate for the cells.

Panels are then aligned to form larger arrays. At this stage defective panels can be removed and spare panels can be inserted (to maintain the proper output rate of solar cell arrays). Panel interconnects (made by the same equipment as the cell interconnects) are then inserted between panels and electrostatically bonded to the collector bars and rear con-tacts of the cell strips at the panel edges (these collector bars and rear contacts were masked during SiO_2 deposition).

The panels are then cut across the solar cell sections ('longitudinal cut'), separating each section into 14 solar cells an the panel into 252 interconnected cells. Kapton tape (from the input/output station) is then applied to the rear surface of the cells, covering the edges of the panels. This tape serves as structural backing to the solar cell arrays.

The array segments (each 14 panels wide and 541 panels long) are then accordion-folded and packaged into a cushioned box for transport out of the solar cell factory, to the input/output station for final delivery to the SPS assembly site.

6.4.2: Solar Cell Production Massflows: The massflows in the layout in Fig. 6.9 are estimated from the process and equipment designs, based on the production of one 10-GW SPS (without grow margin). As mentioned in Sec. 6.2.1, process waste in sc r cell production is significantly higher than

6.27

in components production. This is due to an estimated deposition efficiency of 67% in the direct vaporization processes (2/3 deposited, 1/3 wasted), and estimated loss of 21% of the input silicon during zone refining, and the wastage of 600 tons of aluminum on the from contact shadow masks. Besides the process waste, a spoilage rate of 10% was assumed, due to the fragility of the cells and the precision required in process control.

Rather than estimating fractions of the total spoilage rate for each production step, the 10% spoilage rate was conservatively applied to the entire set of massflows. In other word the throughputs were calculated (including the process waste) as if there were no spoilage. All the massflows were then increased by 10%. It is these massflows that appear on the operations layout. The material inputs masses match those in Table 4.2. The SMF output mass in parentheses (after the assumed 10% spoilage) matches that listed in Table 3.1. Subtracting the material outputs masses (from Table 3.3) from the material inputs masses (from Table 4.2) yields the wastage for each type of material. Dividing that wastage by the input mass for any material gives the wastage percentage listed in Table 4.2.

6.5: WAVEGUIDE PRODUCTION OPERATIONS LAYOUT

6.5.1: Operations Layout: A detailed operations layout of the waveguide factory in the reference SMF appears in Fig. 6.9.
   ..   tions of the equipment are presented in Chap. 7.

Natural   Foaming
Lunar   Agents
Glass 18,000 tons   240tons

```
┌──────────┐  Mixed    ┌──────────────────┐  Foamed Glass   ┌────────┐  Foamed Glass
│ POWDER   │  Powder   │ FOAMING/ANNEALING│    Blocks       │ CUTTER │    Sheets
│ MIXER    │ ────────> │    FURNACE       │ ──────────────> │        │ ─────────────┐
└──────────┘           └──────────────────┘                 └────────┘              │
                                                                 │                  │
                                                                 ▼                  │
                                                          Process Waste            │
                                                    Nat'l Lunar Glass 5300tons      │
                                                    Foaming Agents      70tons      │
                                                                                    │
┌───────────────────────────────────────────────────────────────────────────────── │
│
│              Al  165tons
│                   │
│                   ▼
│  ┌──────────┐  Foamed Glass  ┌──────────┐   ┌────────────┐   ┌──────────┐   ┌───────────┐
└─>│ SMOOTHER │    Sheets      │ DV OF AL │   │SHEET CUTTER│   │ ASSEMBLY │   │ PACKAGING │
   │          │ ─────────────> │ INTERIOR │──>│ AND SLOTTER│──>│          │──>│           │
   └──────────┘                │ COATING  │   └────────────┘   └──────────┘   └───────────┘
                               └──────────┘                                         │
                                    │                                               ▼
                                    ▼
                              Process Waste                                    WAVEGUIDES
                                55tons                                         13,000tons
                                                                          (After 10% wastage:
                                                                               12,000tons)
```

6.29

FIGURE 6.9: WAVEGUIDE PRODUCTION: DETAILED LAYOUT

Natural lunar glass (brought from the Moon as 5-micron powder, bagged) and foaming agents (brought from Earth as powder) are moved from the input/output station to the powder mixer, where they are thouroughly mixed. The mixed powder is loaded into a mold, heated into foamed glass, and cooled over 12 hours. The blocks are then cut into thin sheets (2.5 mm thickness) by multiple saws. The sheet faces which will form the interior of the waveguide are then smoothed by a scanning laser, to produce a surface suitable for coating with aluminum. This aluminum (from the metals furnaces and casters section) is direct-vaporized onto those surfaces, to a depth of 6.7 microns.

Following the Al deposition, the sheets are sliced into strips sized to become sides of the waveguides. Those strips which are output faces are laser-slotted, and those which are input faces are laser-holed. During the SPS assembly, input feeds from the klystrons will be connected to those input holes. The strips are then assembled into waveguide "sticks" by laser-fusing the corners together. The completed sticks are packaged and sent to the input/output station.

6.5.2: Waveguide Production Massflows: Based on production of one 10-GW SPS (without growth margin), massflows in the layout in Fig. 6.9 are estimated from the process and equipment designs. As mentioned in Sec. 6.2.1, process waste is significantly higher in waveguide production than in compo-

nents production. The estimated process waste from cutting
and slotting the foamed glass is 30% of the material. Also,
the estimated efficiency of Al direct vaporization is 67%
(2/3 deposited, 1/3 wasted). In addition to the process
waste, a spoilage rate of 10% was assumed, in view of the
fragility of the waveguides.

Rather than estimating fractions of the total spoilage
rate for each production step, the 10% spoilage rate was con-
servatively applied to the entire set of massflows. In other
words, the throughputs were calculated (including the pro-
cess waste) as if there were no spoilage. Then all the mass-
flows were increased by 10%. It is these massflows that are
on the operations layout. The material inputs masses match
those in Table 4.2. The SMF output mass in parentheses
(after the assumed 10% spoilage) matches the one listed in
Table 3.1. Subtracting material outputs masses (from Table
3.3) from the material inputs masses (from Table 4.2) yields
the wastage for each type of material. Dividing that wastage
by the input mass for any material gives the wastage per-
centage listed in Table 4.2.

6.6: SUPPORT OPERATIONS LAYOUTS

6.6.1: Input/Output Station Layout: Figure 6.10 presents
a detailed layout of the box labeled 'Input/Output Station'
in Fig. 6.2. The equipment designs are presented in Chap. 8,
"Support Equipment Specifications".

The large unpiloted cargo modules (from LEO, Moon, or SPS
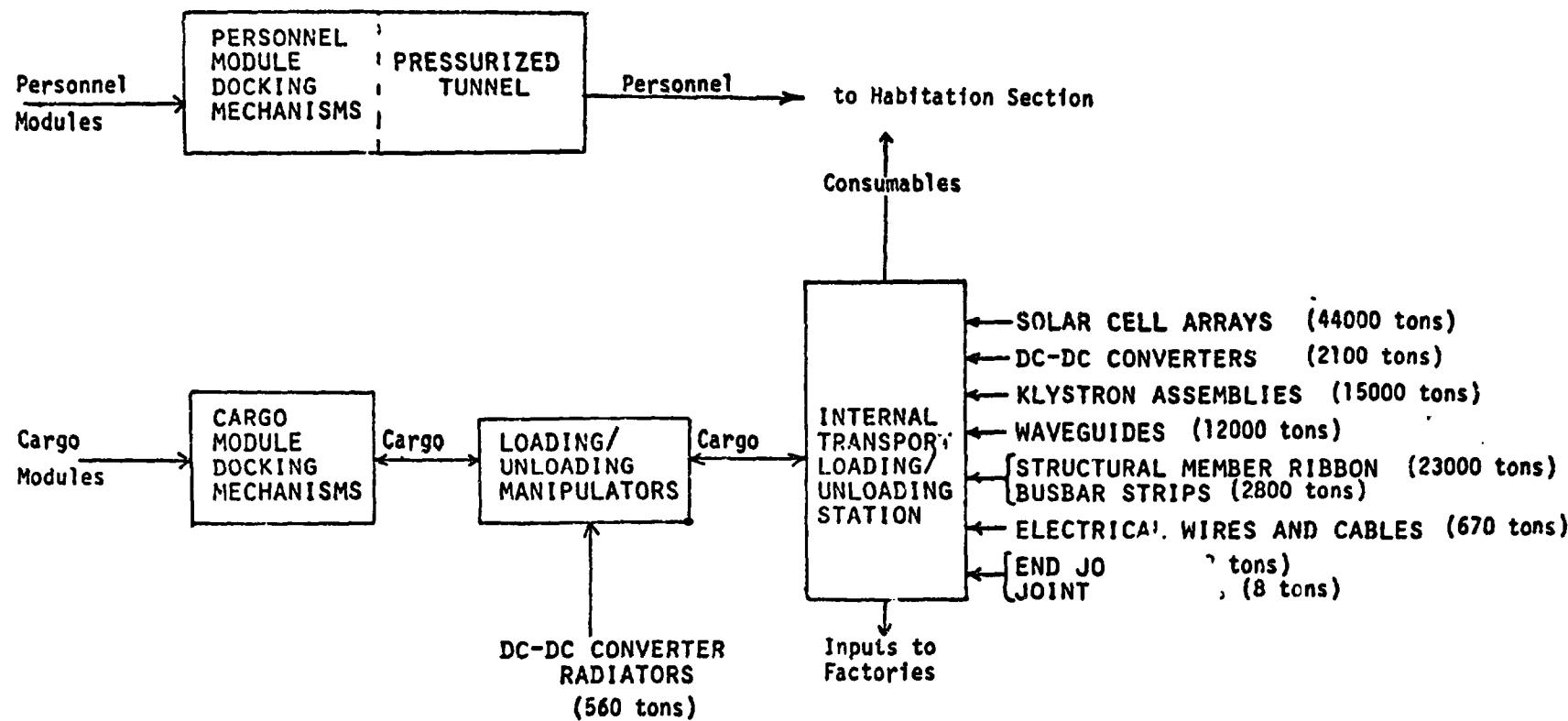
FIGURE 6.10: INPUT/OUTPUT STATION: DETAILED LAYOUT

assembly site) are docked by the loading/unloading manipulators to large retention latches. While they are docked to the SMF, these cargo modules serve as storage areas for inputs waiting to enter the SMF, and for SMF outputs awaiting shipment to the SPS assembly site.

Inputs (i.e. material inputs to factories, expendables, refurbishment parts, propellant, consumables) are unloaded from the containers by the manipulators and transferred to the internal transport loading/unloading station. This station is merely a transfer point between the manipulators and the magnetic-cart internal transport system. Once in the magnetic carts, the SMF inputs are routed to the appropriate destinations.

Most of the SMF outputs reach the input/output station via the internal transport system. They are picked up by the loading/unloading manipulators at the internal transport station, and loaded into cargo modules. The exception is the DC-DC converter radiators, which are too large to fit in the internal transport system. These are picked up by the manipulators directly from their production area, which is located within reach of the input/output station.

Personnel modules (smaller than the cargo modules) are docked by their pilots to standard androgyn docking mechanisms. Personnel can then transfer through the pressurized docking ring to a pressurized tunnel leading to the habitation section. The reverse process brings personnel from the SMF into the personnel modules for departure.

6.33

The output masses shown in the layout are those required for the production of one 10-GW SPS (without growth margin). They match the masses listed in Table 3.1,"SMF Outputs".

6.6.2: Internal Transport and Storage Layouts: An operations layout for the internal transport system would carry little information: the operations of the transport system are to load, carry, and unload. Instead, Fig. 6.11 presents a very simplified schematic of the system.

The internal transport system links three principal sections of the SMF: the input/output station, the habitation section, and the factories. Not shown on the schematic are internal storage devices within the factories, or the complex network of tracks carrying inputs to individual machine, intermediate products between machines, and outputs out of the factories. Equipment descriptions appear in Chap. 8.

To guarantee that production is not slowed by the unavailability of transport carts during peak demand periods, a number of extra carts are available to the system. These are kept in cart storage are.. '⸱ several locations around the SMF. Routing control (more an operations section then an actual facility) maintains a map and cargo manifest of the entire system, including the locations of all carts. It receives information on cart location from the entire system, and updates its location map continuously. Based on this data, routing control optimizes the traffic pattern and issues appropriate stop-and-go or switching commands to the
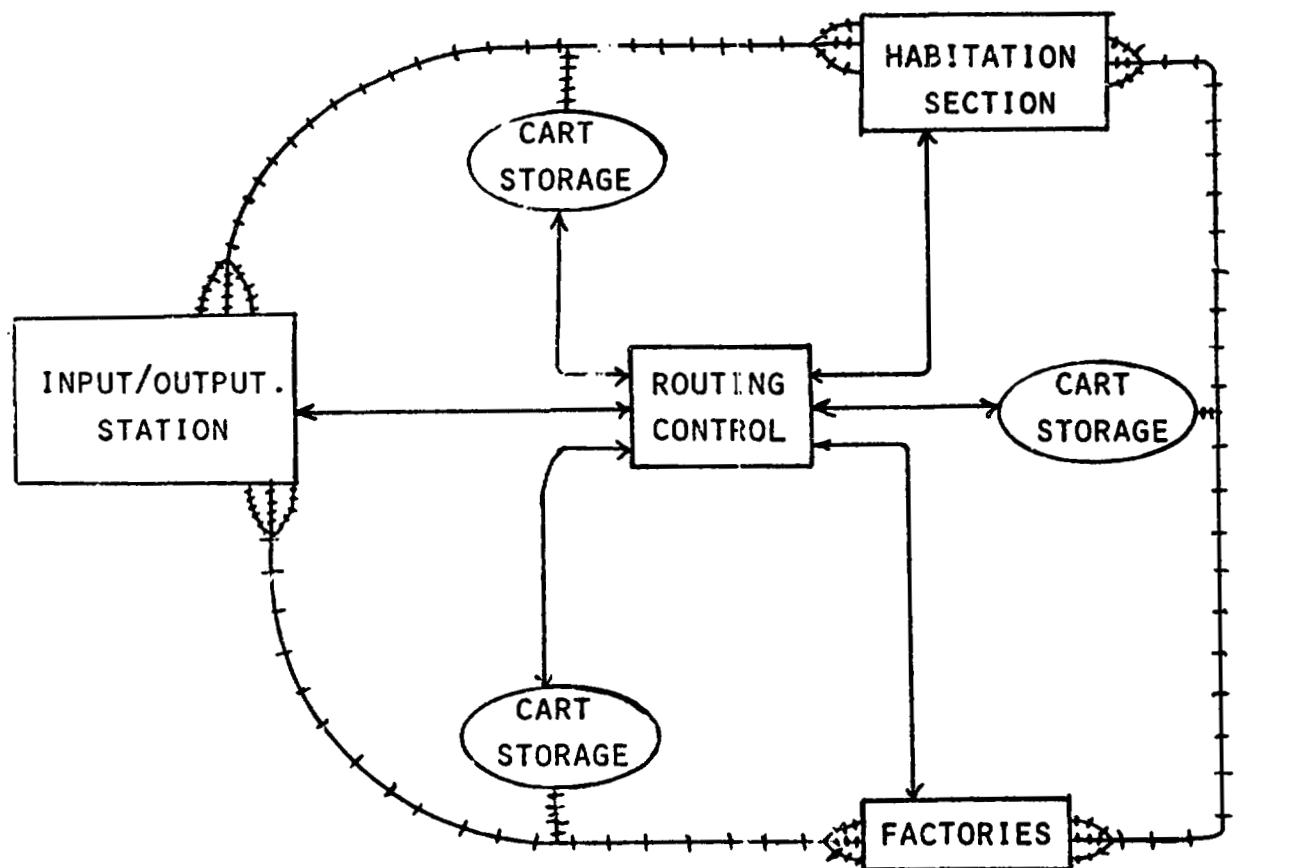
Double-headed arrows represent
information going to Routing
Control and commands going to
SMF Sections and cart storage
locations

╌╂╌╂╌╂► TRANSPORT TRACKS

FIGURE 6.11:   INTERNAL TRANSPORT SCHEMATIC

system. Carts can be individually routed and controlled by this system.

There are three types of internal storage in the reference SMF. The first is the bulk storage at the input/output station. The cargo modules, once docked, serve as storage for input materials ready to enter the SMF and for SMF outputs ready for shipment. When a cargo module's input materials have been entirely replaced by SMF outputs, the module is released and shipped to the SPS assembly site.

The second type of internal storage is within the factories. When a machine requires small pieces as inputs, an internal transport cart can hold many such pieces and serve as internal storage. The cart is parked on a sidetrack next to the input of the machine, which slowly empties the cart as needed. When emptied, the cart moves away, and a full cart replaces it. Similarly, machines which produce small outputs can slowly fill a cart, which moves away when full.

The third type of internal storage (also within the factories) is an 'internal storage device'. Such devices are intermediate warehouses to hold machine inputs and intermediate products of the production lines. They serve as local supply depots to sections of the factories. Figure 6.12 shows a possible operations layout including such devices. Inputs (either from other machines or from the input/output station) are brought by the internal transport system to internal storage devices. The inputs are off-loaded from the transport

6.36

C - 4(

Process
Input
From
Internal
Transport

INTERNAL
STORAGE
DEVICE

Process Input

PROCESS
MACHINERY

Process
Output

Process
Input
From
Internal
Transport

INTERNAL
STORAGE
DEVICE
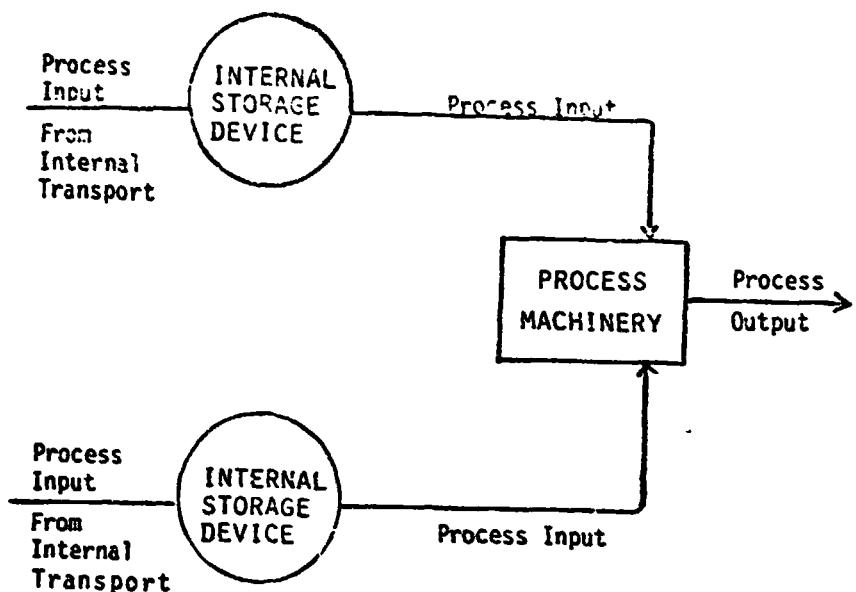
Process Input

FIGURE 6.12: POSSIBLE INTERNAL STORAGE OPERATIONS LAYOUT

system into the storage devices, adding to the process machinery's input reserves. Meanwhile, the machinery draws on stored inputs as needed. This system allows uninterrupted production despite irregular flows of inputs to the internal storage devices.

6.6.3: Power Plant Layout: Figure 6.13 presents an operations layout of the SMF power plant. Descriptions of the equipment appear in Chap. 8.

Sunlight falls on a solar array, generating DC power. This power is fed by busbars to two power conditioning systems. The first system consists of DC-DC converters and switching systems, which produce high-voltage AC power at 300 Hertz, for use in the induction furnaces in the components factory.

The second power conditioning system consists of DC-DC converters and switching systems, which produce DC power at
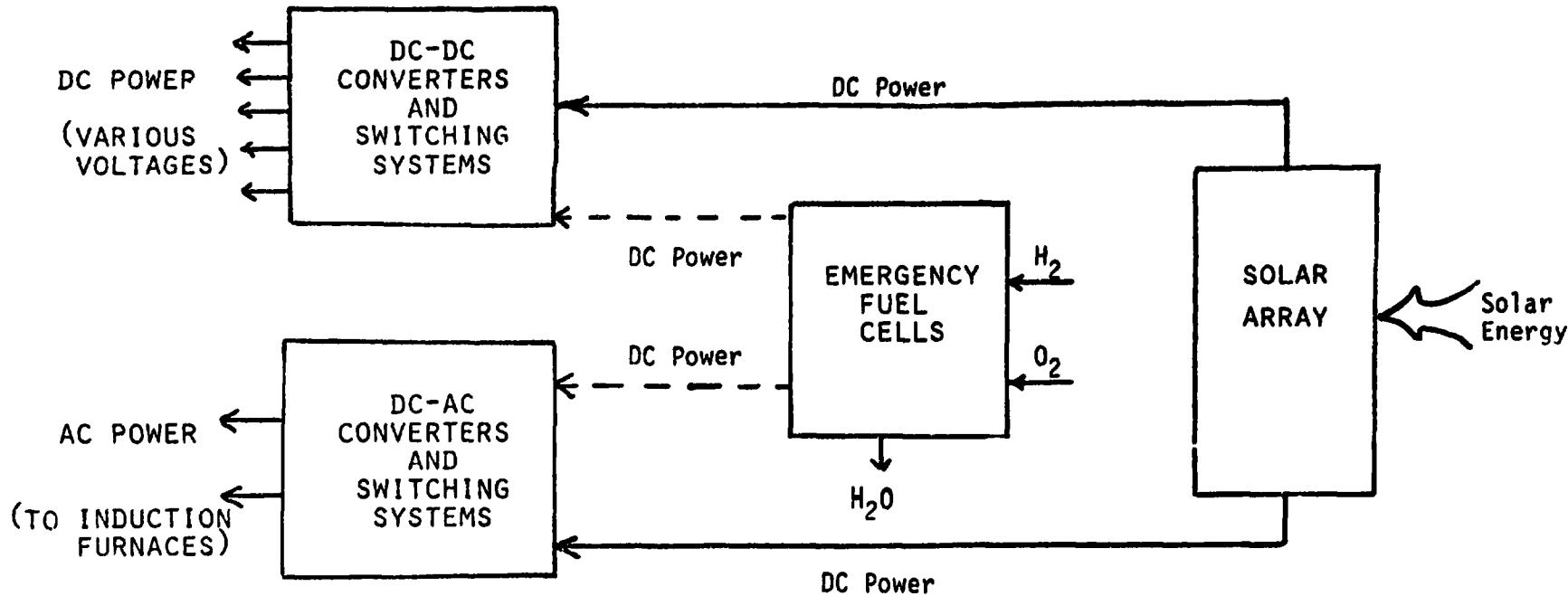
FIGURE 6.13: POWER PLANT OPERATIONS: DETAILED LAYOUT

various voltages. These power outputs supply all of the pro-
duction equipment in the factories, repair shops, support equip-
ment (including control centers), habitation section, internal
storage devices, and the input/output station.

In case of solar eclipse, or malfunction of the solar-array
pointing system, power can be produced by emergency fuel cells,
which feed DC power to the power conditioning system. During
primary power failure, these fuel cells produce enough power
to avoid damage to equipment and danger to personnel while the
production equipment shuts down; to keep essential support
services (e.g. docking, internal transport, life-support, re-
pair) working until primary power returns; and to keep the
life-support systems of the habitation section operating.

The fuel cells are actually operated at low output at
all times, to keep them in operating condition, and to pro-
duce power to handle peak loads (the solar array produces
mainly baseload power). The cells are fueled with lunar oxy-
gen and earth hydrogen; their water output makes up the water
losses in the food and water cycles.

Power requirements for individual process machines and
support machines are listed in Chaps. 7 and 8, respectively.
The total power requirement and component requirements are
listed in Chap. 10.

6.6.4: Production Control and Management Layout: The opera-
tions in production control and management are schematized in
Fig. 6.14. The system includes three levels of control: fac-

SMF Outputs

INPUT/
OUTPUT
STATION

FACTORY

Inputs to Factories

Input and
Output
Inventories

Internal
Inventory
Information

Factory
Operations
Commands

Machine
Adjustment
or Shutdown

Maintenance
and Repair
Work

MAINTENANCE
AND
REPAIR

Shipment
Schedules

Loading Commands

Maintenance
and Repair
Commands

PRODUCTION
MANAGEMENT

Resources
Status

FACTORY
RESOURCES
MANAGEMENT

Factory
Status

FACTORY
MONITORING

Long-range
Planning

Production
Objectives

Reprogram

Machine
Operation
and Quality
Control
Information

FIGURE 6.14:   PRODUCTION CONTROL AND MANAGEMENT

DETAILED LAYOUT

tory monitoring, factory resources management, and production management.

The lowest level is factory monitoring, which continuously receives information on machine operation and output quality. If product quality is substandard, the factory monitoring section sends commands to the factory to adjust the appropriate equipment settings.

If the substandard output persists, or if a machine breakdown occurs, the factory monitoring section sends commands to the factory to shut down the affected equipment, and sends commands to the maintenance and repair section to fix the problem. Similarly, the factory monitoring section monitors the need for maintenance of the factory equipment, and sends commands to the maintenance and repair section to do that maintenance. The options, strategies, and equipment for maintenance and repair are discussed in Chap. 9.

Factory monitoring is decentralized, i.e. spread throughout the factory. It matches the functions of the human machine operator on Earth (it could also be a human operator in space). The human operator on Earth adjusts the machine to maintain output quality, shuts it down if necessary, and calls for maintenance or repair services as needed.

The next level in SMF production control and management is the factory resources management section. This section receives information from several sources. From the factory monitoring section, it receives continuous information on the status of

the factory, i.e. which machines are working, which are shut down, which are approaching scheduled maintenance. From the factory itself, the factory resources management section receives information on the contents of internal storage systems. From the input/output station, it receives information on the input and output inventories in the cargo modules.

From all this information, the factory resources management section builds and continuously updates a picture of the resources available for production: status of machinery, size and location of material inventories. Based on this picture, this section models and predicts factory throughput. It then optimizes factory operations in the predictive model.

To implement the optimum model, the factory resources management section issues commands to the input/output station and to the factory, and reprograms the factory monitoring section. The commands start and stop equipment, and control the routing of internal transport systems (the commands are fed to the 'routing control' described in Sec. 5.6.2). The reprogramming of the factory monitoring section can change the quality control criteria and/or alter the response to machine breakdown.

For example, should the factory resources management section be faced with the problem of producing a large number of a given component quickly, but with reduced quality requirements, it can do the following: 1) command the input/output station to load the necessary inputs into the factory as quickly as possible; 2) command the internal transport routing control to give priority to those inputs; 3) command the factory equipment

to produce as much of the needed product as possible; 4) repro-
gram the factory monitoring section to reduce quality control
criteria (thus reducing the quantity of rejected product); 5)
reprogram the response to machine breakdown, so that the factory
monitoring section will send more repair workers to fix any
failures in the needed equipment; 6) reprogram the factory moni-
toring section to delay maintenance on the necessary machinery.

The earth analogy to the factory resources management is
the shop foreman who knows the status of the shop's equipment,
the availability of the shop personnel, the contents of the
stock racks and the storage room, and the output expected from
the shop. The shop foreman allocates the available resources to
maximize the output required.

The factory resources management section of the SMF in-
cludes several such personnel to oversee the operations of the
complex SMF factories. The large volumes of information required
are processed by computers.

The upper level of production control and management is
production management. The SMF production manager receives
information from within the SMF and from other sectors of the
space industrialization scenario. From the factory resources
management section, production management receives updates on
the resources available to the SMF. From the Moon and the SPS
assembly site, the SMF production manager receives information
on shipment schedules for both expected input shipments and
required output shipments. These facts are then evaluated to-

gether with long-range planning goals to determine the near-term objectives of SMF production. Production management then gives these objectives to the factory resources management section for implementation. Following the example above, the decisions to produce as much of the needed product as possible, and to lessen the quality control criteria, would be the SMF production manager's.

6.6.5: Habitation: An operations layout of the habitation is outside the scope of this study. A number of studies on habitat design are available in the literature (Refs. 6.1, 6.2, 6.3). A description of the habitation section design used in this study appears in Chap. 8.

6.6.6: Stationkeeping: The stationkeeping system has three functions: to maintain the SMF in the desired orbit; to provide general attitude control to keep the structure shaded by its solar array; and to provide fine attitude control to keep the shape of the SMF within structural tolerances. In general, the stationkeeping system requires navigational sensors, relative position sensors for the various sections of the SMF, and thrusters. Descriptions of this equipment appear in Chap. 8; definition of their quantitative requirements is not part of this study.

REFERENCES

(1.1) **Lunar Resources Utilization for Space Construction**, General Dynamics Convair Div., NASA contract NAS9-15560, Progress Report 1, pp. 3-6 to 3-14.

(2.1) **Lunar Resources Utilization for Space Construction**, General Dynamics Convair Div., NASA contract NAS9-15560, Progress Report 1, pp. 3-18 to 3-20.

(2.2) **Recommended Preliminary Baseline Concept**, SPS Concept Evaluation Program, NASA JSC, January 25, 1978.

(2.3) **Lunar Resources Utilization for Space Construction**, General Dynamics Convair Div., NASA contract NAS9-15560, Progress Report 2, pp. 3-21 to 3-58 and App. X.

(2.4) **Extraterrestrial Materials Processing and Construction**, Lunar and Planetary Institute, NASA contract NAS 09-051-001, Third Quarterly Report and Final Report.

(3.1) **Recommended Preliminary Baseline Concept**, SPS Concept Evaluation Program, NASA JSC, January 25, 1978.

(3.2) **Lunar Resources Utilization for Space Construction**, General Dynamics Convair Div., NASA contract NAS9-15560, Progress Report 2, pp. 3-21 to 3-58 and App. X.

(3.3) **Solar Power Satellite System Definition Study**, Boeing Corp., NASA contract NAS9-15196, Part III, Final Report, March 7, 1978.

(3.4) **Lunar Resources Utilization for Space Construction**, General Dynamics Convair Div., NASA contract NAS9-15560, Progress Report 7.

(4.1) Phinney, W.C., Criswell, D., Drexler, K.E., and Garmirian, J., "Lunar Resources and their Utilization," Third Princeton/AIAA Conference on Space Manufacturing Facilities, Princeton 1977, AIAA Paper 77-537.

(4.2) **Extraterrestrial Materials Processing and Construction**, Lunar and Planetary Institute, NASA contract NAS 09-051-001, Third Quarterly Report and Final Report.

(4.3) **Lunar Resources Utilization for Space Construction**, General Dynamics Convair Div., NASA contract NAS9-15560, Progress Report 7, p. 4.7-10.

(4.4) Strange, David, "Future Geophysical Techniques for Probing Beneath the Regolith--Prospecting Objective, **Eleventh Lunar Science Conference**, Pergamon Press, 1976.

(4.5)   Lunar Resources Utilization for Space Construction, General Dynamics
        Convair Div., NASA contract NAS9-15560, Progress Report 4, p. 4.6-26.

(4.6)   TRW Space Data, TRW Systems Group, J.B. Kendrick (ed.), Third Edition.
        1967.

(4.7)   Lunar Resources Utilization for Space Construction, General Dynamics
        Convair Div., NASA contract NAS9-15560, Progress Report 4, p. 4.5-36.

(5.1)   Recommended Preliminary Baseline Concept, SPS Concept Evaluation
        Program, NASA JSC, January 25, 1978.

(5.2)   Lunar Resources Utilization for Space Construction, General Dynamics
        Convair Div., NASA contract NAS9-15560, Progress Report 2, pp. 3-21
        through 3.29.

(5.3)   Extraterrestrial Materials Processing and Construction, Lunar and
        Planetary Institute, NASA contract NAS 09-051-001, Third Quarterly
        Report and Final Report.

(5.4)   Initial Technical, Environmental, and Economic Evaluation of Space
        Solar Power Concepts, vol. 2, NASA TMX-74310, August 31, 1976.

(5.5)   Lunar Resources Utilization for Space Construction, General Dynamics
        Convair Div., NASA contract NAS9-15560, Progress Report 6, pp. 4-132,
        4-133.

(5.6)   Proceedings of the 9th Project Integration Meeting, Low-Cost Solar
        Array Project, Report 5101-67, April 11-12, 1978, p. 3-19.

(5.7)   Flemings, Merton C., Solidification Processing, McGraw-Hill, New
        York, 1974, pp. 3, 4.

(5.8)   Gatos, Prof. Harry C., MIT Dept. of Materials Science and Engineering,
        personal communication.

(5.9)   Lunar Resources Utilization for Space Construction, General Dynamics
        Convair Div., NASA contract NAS9-15560, Progress Report 6, p. 4-109.

(5.10) Lewellen, W.S., A Review of Confined Vortex Flows, MIT Space Pro-
        pulsion Laboratory, NASA-CR-1772, Sept. 1970.

(5.11) Edge, Dr. Gordon M., Director, Patscentre International, Cambridge
        Div., Melbourn, Royston, UK, personal correspondence.

(5.12) Holden, S.C., Slicing of Silicon into Sheet Material, Silicon Sheet
        Growth Development, for the Large Area Silicon Sheet Task, of the
        Low Cost Silicon Solar Array Project, Varian Associates, Lexington,
        MA, September 27, 1976.

(5.13) Mollock, I., Low Cost Silicon Solar Array Project, Quarterly Report,
        Jet Propulsion Laboratory, June 1977.

(5.14) Ravi, Dr. K. V., Mobil Tyco, personal communication.

(5.15) Duchynski, R.J.. "Ion Implartation for Semiconductor Devices," Solid State Technology, vol. 20, No. II, November 1977.

(5.16) Drexler, K.E., personal communication, based on research in Design of a High-Performance Solar Sail System, SM Thesis, MIT Space Systems Laboratory, May 1979 (in progress).

(5.17) Bowen, Prof. H.K., MIT Dept. of Materials Science and Engineering, personal communication.

(5.18) Coble, Prof. R.L., MIT Dept. of Materials Science and Engineering, personal communication.

(5.19) Haggerty, Dr. J., MIT Energy Laboratory, personal communication.

(5.20) No reference.

(5.21) Carbajel, B.G., Automated Array Assembly Task (Phase I), Annual Report, Texas Instruments Inc., NASA CR-153909. March 1977.

(5.22) Lunar Resources Utilization for Space Construction, General Dynamics Convair Div., NASA contract NAS9-15560, Progress Report 2, pp. 3-29 through 3-36.

(5.23) Lunar Resources Utilization for Space Construction, General Dynamics Convair Div., NASA contract NAS9-15560, Progress Report 6, p. 4-122.

(5.24) Foamglas, Cellular Glass Insulation, Bulletin of the Pittsburgh Corning Corporation, May 1977.

(5.25) Demidovich, B.K., "Manufacture and Use of Foamed Glass," Army Foreign Science and Technology Center, Charlottesville, VA, October 25, 1974.

(5.26) Lunar Resources Utilization for Space Construction, General Dynamics Convair Div., NASA contract NAS9-15560, Progress Report 7, p. 4.7-10, and Hurlich, Abraham, General Dynamics Convair Div., personal communication.

(5.27) Jeffrey, P., Aluminum Corp. of Canada, personal communication.

(5.28) Visit to Eastern Refracting Co., Belmont, MA.

(5.29) Schlier, S., and Jaesch, G., "Deposition by Electron Beam Evaporation with Rates of up to 50 Microns/sec," paper presented at the Third Conference on Metallurgical Coatings, San Francisco, April 3-7, 1978.

(5.30) Bunshah, R.F., "Structure/Property Relationships in Evaporated Thick Films and Bulk Coatings," J. Vacuum Science Technology, vol. II, 1974, p. 633.

(5.31) Extraterrestrial Processing and Manufacturing of Large Space Systems, MIT Space Systems Laboratory, NASA contract NAS8-32925, Progress Report I, (SSL ɔ. 7-78), Appendix B.

(5.32)   Extraterrestrial Processing and Manufacturing of Large Space
         Systems, MIT Space Systems Laboratory, NASA contract NAS8-32925,
         Progress Report 2, (SSL No.   8-78), Appendix B.

(5.33)   Electric Furnace Steelmaking, vol. I, C.E. Sims (ed), American
         Institute of Mining, Metallurgical and Petroleum Engineers, 1967
         (Second Revised Printing).

(5.34)   Extraterrestrial Processing and Manufacturing of Large Space
         Systems, MIT Space Systems Laboratory, NASA contract NAS8-32925,
         Progress Report 5, (SSL No. 11-78), Appendix B, and Progress Report
         7, (SSL No. 1-79), Viewgraph E4.

(5.35)   Verkamp, J.P., Electromagnetic Alkali Metal Pump Research Program,
         NAS-3-25-43, May 22, 1964.

(5.36)   Howard, Dr. P., Argonne National Laboratory, personal communication.

(5.37)   Ezekiel, Prof. S., MIT Laser Systems Laboratory, and Hubbard, T.,
         Raytheon Industrial Laser Group, personal communications.

(5.38)   Electron Beam Technique, Steigerwald/Strahltechnik, pamphlet
         distributed by Farrel Co., Ansonia, CT.

(5.39)   Class, W., Mgr., Electron Beam Section, Farrel Co., personal
         communication.

(5.40)   Roblin, M., Electron Beam Welding Inc., Los Angeles, CA., personal
         communication.

(5.41)   Materials and Processes in Manufacturing, E.P. DeGarmo (ed), Third
         Edition, MacMillan Co., New York, 1969.

(5.42)   Solar Power Satellite System Definition Study, Boeing Corp.,
         NASA contract NAS9-15196, Part II, vol. IV, from Fig. 4-1.

(5.43)   Lunar Resources Utilization for Space Construction, General
         Dynamics Convair Div., NASA contract NAS9-15560, Progress Report
         2, pp 3-21 to 3-58 and App. X.

(5.44)   Visit to Raytheon Co., Microwave and Power Tube Division,
         Waltham, MA.

(5.45)   The Klystron as a Microwave Power Source in the SPS Application,
         Varian Associates Inc., Palo Alto Microwave Tube Div.,
         November 1977 (report prepared for Boeing Co.)

(5.46)   Denman, O., Boeing Corp., personal communication.

(5.47)   Zawada, F.A., Raytheon Co., Microwave and Power Tube Div.,
         Waltham, MA, personal communication.

(5.48)   Solar Power Satellite System Definition Study, Boeing Corp.,
         NASA contract NAS9-15196, Part III, Preferred Concept System
         Definition, March 1978.

(5.49) Yarranton, A., Special Microwave Devices Operation, Ferrite Devices, Raytheon Co., Waltham, MA, personal communication.

(5.50) Rostocker, Dr. D., Pittsburgh Corning Co., Pittsburgh, PA, numerous personal communications.

(5.51) Solar Power Satellite System Definition Study, Boeing Corp., NASA contract NAS9-15196, Part II, vol. IV, Microwave Power Transmission Systems, December 1977, pp. 171-177.

(5.52) Kirkpatrick, A.R., Spire Corp., personal communications, June, 1979.

(5.53) Ephrath, L. M., "Growth of Polycrystalline Silicon Films on Metal Substrates", Ph D thesis, Dept. of Physics, Boston College, 1974.

(5.54) Fang, P. H., Ephrath, L. M. and Nowak, W. B., "Polycrystalline Silicon Films on Aluminum Sheets for Solar Cell Application", from "Applied Physics Letters", Vol. 25, No. 10, November 15, 1974.

(5.55) Kirkpatrick, A. R., Soloman, S. J., Oren, M., Shaugnessy, T. P., Silas, V., Younger, P. R. and Greenwald, A. C., "A Nonconventional Approach to Thin Film Fabrication", from 13 IEEE Photovoltaic Specialist Conference, 1978.

(5.56) Gurther, R. W., Laser Zone Growth in a Ribbon to Ribbon (RTR) Process, Silicon Sheet Growth Development for the Large Area Silicon Sheet, Annual Report, Motorola, Inc., September, 1977.

(5.57) Robinson, A. L., "Laser Annealing: Processing Semiconductors Without a Furnace," Science, July 28, 1978, p. 333.

(5.58) Muller, J. C., Grob, A. and J. J., Stuck R., Siffert, P., "Low Cost Ion Implantation Procedure for the Realization of Silicon Solar Cells in a Continuous Way", from 13th IEEE Photovoltaic Specialist Conference, 1978.

(5.59) Kirkpatrick, A. R., Minnucci, J. A. and Greenwald, A. C., "Silicon Solar Cells by High-Speed Low-Temperature Processing", from IEEE Transactions on Electron Devices, Vol. ED-24, No. 4, April, 1977.

(5.60) Young, P. T., White, C. W., Narayan, J., Westbrook, R. D., Wood, R. F., Christie, W. H., "Solar Cells from Laser-Annealed Ion-Implanted Silicon", from 13th IEEE Photovoltaic Specialist Conference, 1978.

(5.61) Lurio, Charles A., "The Bending and Twisting Behavior of Thin Glass Sheets", Final Report for Course 16.62, Department of Aeronautics and Astronautics, MIT, May 14, 1979.

(5.62) Young, Peter, Corning Glass Corp., Research Division , personal communication, July, 1979.

(5.63) Physical Vapor Deposition. Airco Tennescai, R. S. Hill, ed., Airco, Inc., 1976.

(5.64) Little, R. G., Spire Corp., personal communication, July, 1979.

(5.65) Solomon, S. J., Development of Recrystallization and Thin-film Solar Cell Processes, Final Report (draft), Spire Corporation, May, 1979, for DOE Contract #EG-77-C-01-4106.

(6.1) Lunar Resources Utilization for Space Construction, General Dynamics Convair Div., NASA contract NAS9-15560, Progress Report 4, pp. 4.5-18 through 4.5-53.

(6.2) Vajk, J.P., Engel, J.H., Shettler, J.A., "Habitat and Logistic Support Requirements for the initiation of a Space Manufacturing Enterprise," 1977 NASA Ames/OAST Summer Study on Space Settlements and Industrialization.

(6.3) A Systems Design for a Prototype Space Colony, D.B.S. Smith (ed), Dept. of Aeronautics and Astronautics, MIT, published by the William F. Marlar Memorial Foundation Inc., 1977.